JPRS L/9639

2 April 1981

Translation

STUDY OF HYDRODYNAMIC INSTABILITY BY NUMERICAL METHODS

Ed. by

A.A. Samarskiy

FBIS FOREIGN BROADCAST INFORMATION SERVICE

NOTE

JPRS publications contain information primarily from foreign newspapers, periodicals and books, but also from news agency transmissions and broadcasts. Materials from foreign-language sources are translated; those from English-language sources are transcribed or reprinted, with the original phrasing and other characteristics retained.

Headlines, editorial reports, and material enclosed in brackets [] are supplied by JPRS. Processing indicators such as [Text] or [Excerpt] in the first line of each item, or following the last line of a brief, indicate how the original information was processed. Where no processing indicator is given, the information was summarized or extracted.

Unfamiliar names rendered phonetically or transliterated are enclosed in parentheses. Words or names preceded by a question mark and enclosed in parentheses were not clear in the original but have been supplied as appropriate in context. Other unattributed parenthetical notes within the body of an item originate with the source. Times within items are as given by source.

The contents or this publication in no way represent the policies, views or attitudes of the U.S. Government.

APPROVED FOR RELEASE: 2007/02/08: CIA-RDP82-00850R000300100002-5

JPRS L/9639

2 April 1981

STUDY OF HYDRODYNAMIC INSTABILITY BY NUMERICAL METHODS

Moscow IZUCHENIYE GIDRODINAMICHESKOY NEUSTOYCHIVOSTI CHISLENNYMI METODAMI in Russian 1980 signed to press 26 Dec 79 pp 1-227

[Translation of the collection of scientific articles "Study of Hydrodynamic Instability of Numerical Methods", edited by A.A. Samarskiy, Institut prikladnoy matematiki AN SSSR, 400 copies, 227 pages]

CONTENTS

[Text] Editor's Foreword

Numerical simulation based on finite-difference methods oriented toward computer applications is acquiring greater and greater significance in the investigation of physical phenomena. The nonlinearity of the processes and the corresponding equations makes the computer experiment a powerful, and in a number of cases, the only possible means of efficient solution of complex applied and theoretical problems.

This publication is one of the thematic collections on the urgent problems of applied mathematics published by the Institute of Applied Mathematics imeni M. V. Keldysh.

Stability problems play an important role in the investigation of a number of problems of modern physics and in a number of cases they play the defining role.

Solution of the problems connected with studying the development of instabilities of various types imposes rigid requirements on the numerical methods and algorithms. Therefore a number of articles in the collection are devoted to a discussion of the computer aspects connected with solving stability problems. These are the paper by B. D. Moiseyenko, L. V. Fryazinov, in which a prospective algorithm for numerical simulation of the motion of an incompressible medium is discussed, and the paper by V. M. Goloviznin, T. K. Korshiy, A. A. Samarskiy, V. F. Tishkin and A. P. Favorskiy which contains a generalization of the variation approach to constructing completely conservative magnetohydrodynamic systems to the case of three spatial measurements.

The remaining articles contain examples of a numerical solution and theoretical study of instabilities in a medium.

In a paper by a group of authors, a brief survey is given of previously obtained results pertaining to the numerical simulation of the Rayleigh-Taylor instability in experimental glass shells investigated at the Physics Institute of the USSR Academy of Sciences.

APPROVED FOR RELEASE: 2007/02/08: CIA-RDP82-00850R000300100002-5

A study is made of the results of the numerical simulation of the occurrence of tornadoes as a result of gas dynamic instability performed by N. M. Zuyeva, V. V. Paleychik and L. S. Solov'yev.

It is known that the hydrodynamic approach turns out to be highly effective in many problems with respect to physical meaning. Accordingly, the collection contains a survey by L. M.Degtyarev and V. V. Krylov of the algorithms and results of numerical simulation of the self-focusing of light in nonlinear media obtained using the hydrodynamic analogy for the Schroedinger type equation.

Recently the interest in studying the general laws of the development of instability in a continuous medium in the nonlinear stage has intensified noticeably. This has served as the basis for inclusion of new interesting results obtained by S. P. Kurdyumov, N. V. Zmitrenko, A. P. Mikhaylov, et al., in the collection pertaining to the formation and interaction of nonlinear structures in the peaking mode. The conclusions contained here have a very broad range of theoretical and practical applications.

A. A. Samarskiy

HEAT INERTIA AND DISSIPATIVE STRUCTURES

[G. G. Yelenin, N. V. Zmitrenko, S. P. Kurdyumov, A. P. Mikhaylov, A. A. Samarskiy, pp 5-27]

1. Introduction

In this paper a study is made of the phenomena of heat inertia accompanied by the localization of heat and thermonuclear combustion in a dense plasma during the development of processes in it in the peaking mode.

Analytical and multidimensional numerical solutions to the problems are presented in partial derivatives, explaining a number of the peculiarities of development of superheated and other types of instabilities in such a plasma.

It is demonstrated that heat inertia can lead to the metastable existence of instabilities having paradoxical form of the region of localization ("thermal crystals"). The conditions of the excitation of the combustion of a medium in the peaking mode are formulated, leading to localization of the combustion in individual sections in the form of structures of different types. It is demonstrated that the resonance conditions of their excitation are determined by the eigenfunctions of the nonlinear self-similar problem. Estimates are presented of the region of occurrence of these phenomena during the processes of heating the plasma by shaped laser radiation and during initiation of combustion in laser targets. The relation of the described phenomena to the fundamental laws of the occurrence and complication of organization in nonlinear media is indicated.

2. Metastable Localization of Heat

The process of the propagation of heat in a stationary medium with nonlinear thermal conductivity in the simplest one-dimensional case is described by the equation:

$$\frac{\partial T}{\partial t} = \frac{\partial}{\partial r}\left(\kappa(T)\frac{\partial T}{\partial r}\right), \qquad (1)$$

where $T(r, t)$ is the temperature, t is the time, $0 \leq r < +\infty$ is the coordinate, $k = k(T) = k_0 T^{\sigma}$, $\sigma > 0$ is the coefficient of thermal conductivity.

Let at the boundary of the unheated medium

$$T(r, t_0) = 0 \qquad (2)$$

the temperature increase by the law

$$T(0,t) = T_0 (t_f - t)^n, \quad n < 0, \quad T_0 = const > 0. \tag{3}$$

On variation of time in the interval $t_0 \leq t < t_f$ the law (3) simulates the temperature buildup in the peaking mode with focusing time (the temperature going to infinity $t = t_f$.

For $t_0 = -\infty$ the problem (1)-(3) is self-similar. The actual process, of course, begins with a finite point in time $t = t_0 \neq -\infty$. If the initial data for $t = t_0$ are self-similar (for example, zero -- (2)), then a time is required for establishment of the process and manifestation of its laws.

It has been established [1a, 1c, 4] that a defined class of boundary conditions with peaking (3) leads to the appearance of the effect of metastable localization of heat consisting in the following. For the initial data (2), the region in which the temperature is nonzero does not change its dimensions during a finite time interval ($t_0 \leq t < t_f$), although the temperature and the quantity of heat inside this region of localization can increase to values as large as one might like. The effective depth of heating of the substance by a heat wave (for example, halfwidth) remains constant (the so-called S-mode) or it decreases with time (LS-mode). For the initial data differing from (2) the indicated properties are maintained in the effective sense (the temperature in the region of localization is as many times the background as one might like).
The boundary conditions localizing the heat are characterized by the following.

For $n < -1/\sigma$ localization is absent. The heat is propagated to the medium in the form of a wave with growing halfwidth; for the initial conditions (2) the wave front moves with finite velocity (HS regime). The external characteristic of the HS-regime is convexity of the profile $T^{\sigma/2}$.

For $\eta = -1/\sigma$, $t_0 = -\infty$, the problem (1)-(3) has an exact solution in the form of the stopped heat wave (S-mode).

$$T(r,t) = \begin{cases} T_0 (t_f - t)^{-1/\sigma} (1 - r/r_\phi)^{2/\sigma}, & r \leq r_\phi, \\ 0, & r > r_\phi, \end{cases} \tag{4}$$

where $r_\phi = \sqrt{2k_0 T_0^\sigma (\sigma+2)/\sigma}$ is the depth of heating determined by the properties of the medium (K_0, σ) and the intensity of the boundary conditions (T_0). In the S-mode the heat wave front is stationary, the profile of the value of $T^{\sigma/2}$ is linear; on approximation of t to the time t_f, the temperature and the quantity of heat in the region $0 \leq r \leq r_\phi$ approach infinity.

In the case of $n > -1/\sigma$ the heat is propagated in the LS-mode. In Figure 1 the temperature profiles are presented at different points in time which were obtained as a result of the numerical solution of the problem (1)-(3). The x's denote the halfwidth; after establishment of the mode (reaching self-similarity) it is contracted. The profile of the value of $T^{\sigma/2}$ in the LS-mode is concave.

As was demonstrated in [4], the phenomenon of metastable localization of the heat is retained also for assignment of a heat flux at the boundary which varies in the peaking mode (the secondary boundary problem), both with consideration of the disturbances in the boundary mode and with consideration of the more complex nonexponential dependence of the coefficient of thermal conductivity k(T) on the temperature. The conditions of establishment of the S and the LS-modes were discovered for deviation of the initial data from the self-similar and in the presence of a nonzero temperature background. In both cases, for establishment of all of the peculiarities of the localization of the heat, it is sufficient that the temperature at the boundary, varying in the mode (3), exceed by an order the maximum value in the initial distribution (boundary or background).

The property defining the localization is the "convexity" or "concavity" of the profile. In reference [4, 1a] this is illustrated in the example of the Cauchy problem for (1).

Let at the time $t=t_0$ for $-\infty<r<+\infty$ the following initial distribution be given:

$$T(r,t_0)=\begin{cases} T_m\left(1-|r|/r_0\right)^{2/\sigma}, & |r|\le r_0, \\ 0, & |r|>r_0. \end{cases} \tag{5}$$

In [4], on the basis of the comparison theorem it was demonstrated that the solution of the Cauchy problem (1) and (5) is majorized by the solution of (4) (for $r<0$ in (4), $-r$ is used instead of r), and, consequently, it is localized in the region $-r_0<r<r_0$ in the time interval no less than

$$t_* = r_0^2\sigma/\left(2k_0(\sigma+2)T_m^{\sigma}\right) \tag{6}$$

that is, $T(r,t)\equiv 0$ for $|r|\ge r_0$ for $t_0\le t\le t_0+t_*$. The same thing is true also for any initial distribution having fronts that coincide with (5) and not exceeding (5) anywhere. The lower bound of the localization time is estimated by (6).

The formulated statement strictly defines the class of "concave" temperature profiles for the given medium (that is, for the given value of σ). Their localization time depends on the properties of the medium (k_0, σ), and also on the characteristics of the initial temperature distribution r_0 and T_m.

For a hydrogen-like plasma with particle density n ($n=n_i+n_a$, where n_i is the ion density, n_a is the density of the neutral atoms, $n_e=n_i$ is the electron density) and n-type thermal conductivity the localization time for various physical conditions is as follows:

Table 1

Target	n_e (cm^{-3})	n_a (cm^{-3})	T_m (ev)	r_0 (cm)	t_* (sec)
DT-plasma	$5\cdot10^{20}$	0	10^3	$8\cdot10^{-3}$	10^{-11}
H-plasma	10^{15}	0	1	10	$2\cdot10^{-3}$
Solar photosphere	$3\cdot10^{13}$	10^{17}	0.5	$2\cdot10^8$=2000 km	$5\cdot10^{14}$=10^7 years
Intrastellar gas	10^{-3}	10	10^{-2}	$3\cdot10^{19}$= 100 parsec	$6\cdot10^{25}$= 10^{18} years

3. Development of Thermal Structures

The peaking modes can exist in a medium with nonlinear thermal conductivity and in the absence of boundary conditions, as a result of the effect of nonlinear volumetric heat sources [1b-g, 2, 5].

The Cauchy problem in the region $-\infty<r<+\infty$ for the equation

$$\frac{\partial T}{\partial t}=\frac{\partial}{\partial r}\left(k_0 T^{\sigma}\frac{\partial T}{\partial r}\right)+q_0 T^{\beta},\quad q_0>0, \tag{7}$$

has a self-similar solution of the following type when $\beta>1$ for times $t\geq t_0$:

$$\begin{aligned} &T(r,t)=q_0^{n}(t_f-t)^{n}f(\xi),\\ &\xi=r\left(\sqrt{k_0 q_0^{n\sigma}}(t_f-t)^{m}\right)^{-1},\\ &n=(1-\beta)^{-1},\quad m=\frac{1}{2}(1+n\sigma)=\frac{1+\sigma-\beta}{2(1-\beta)}, \end{aligned} \tag{8}$$

if the initial data $T(r, t_0)$ have the form of (8). Here

$$t_f=t_0+f^{\beta-1}(0)\left[q_0 T^{\beta-1}(0,t_0)\right]^{-1} \tag{9}$$

Here $f(\xi)$ is the solution of the equation

$$\begin{aligned} &-nf+m\xi f'=(f^{\sigma}f')'+f^{\beta},\\ &f^{\sigma}f'=f=0 \text{ for } \xi=\pm\infty. \end{aligned} \tag{10}$$

The solution of problem (7) for the initial data of another special type $T(r, t_0)=T(t_0)=\text{const}$ also leads to peaking conditions. This solution (homothermal combustion) has the form:

$$T(r,t)=T(t)=\left[(\beta-1)q_0(t_f-t)\right]^{n} \tag{11}$$

where t_f is defined with respect to (9) with $f(0)=(\beta-1)^{n}\equiv f_0$.

The study of the stability of the solution (11) with respect to small values of $\delta T=A(t)\exp(-2\pi i r\lambda^{-1})$ indicates that for $\beta<\sigma+1$ it is stable for disturbances of all wave lengths, and for $\beta>\sigma+1$ it is unstable for disturbances of any wave length; here the disturbances increase by the law $\sim(t_f-t)^{\beta n}$. The homothermal combustion for $\beta=\sigma+1$ is unstable for disturbances with wave lengths greater than critical $\lambda>\lambda_c=2\pi\sqrt{k_0/(q_0(\sigma+1))}$; here the disturbances increase by the law $\sim(t_f-t)^{n_1}$, $n_1=\beta r[1-(\lambda_c/\lambda)^2]$.

The study of the Cauchy problem for (7) led to establishment of three combustion modes of the medium [1, 2, 5]:

For HS-mode ($1<\beta<\sigma+1$) the heat is propagated to the cold medium in the form of a heat wave with finite front, and for $t\to t_f$ the combustion encompasses the entire space.

For the S-mode ($\beta+\sigma+1$) the solution $T(r, t)$ is nonzero in a finite interval of $-r_\phi \leq r \leq r_\phi$, but r_ϕ, in contrast to the HS-mode does not depend on the time, and remains constant. At the same time the heat is not propagated to the cold medium, although in the combustion zone the temperature reaches infinite values for $t \to t_f$.

For the LS-mode ($\beta \geq \sigma+1$) the heat wave front is at infinity, and the effective width of the combustion zone (for example, the halfwidth) is contracted. Here the temperature at the central point goes to infinity for $t \to t_f$.

The study of the temperature profile is based on investigation of equation (10) which is converted by the substitution $x=f^{\sigma+1}$ to the equation of motion of a particle in the force field

$$x'' = m\xi x^{-\frac{\sigma}{\sigma+1}} x' - (\sigma+1)\left(n x^{\frac{1}{\sigma+1}} + x^{\frac{\beta}{\sigma+1}}\right) \tag{12}$$

In the case of the S-mode ($m=0$, the force field is conservative) (12) is easily integrated

$$f(\xi) = x^{\frac{1}{\sigma+1}}(\xi) = \left[\frac{2(\sigma+1)}{\sigma(2+\sigma)} \sin^2\left(\frac{\pi\xi}{\Delta\xi_T} + \pi\theta\right)\right]^{1/\sigma}, \tag{13}$$

where θ is the integration constant, and

$$L_T = \sqrt{\frac{k_0}{q_0}}\,\Delta\xi_T = \frac{2\pi\sqrt{\sigma+1}}{\sigma}\sqrt{\frac{k_0}{q_0}}, \tag{14}$$

is the so-called fundamental length. For the nonlinearity of the stage of development of the instability of homothermal combustion, the dimensions of the combustion regions are a spectrum of lengths $\lambda_0 \leq \Delta r \leq L_T$, where on approaching the focusing time this spectrum degenerates into one boundary of the length: L_T.

As the calculations show, independently of the conditions $\Delta r_0 < L_T$ and $\Delta r_0 > L_T$, where Δr_0 is the region of finiteness of the initial temperature disturbance, the solution of the Cauchy problem for (7) asymptotically arrives at one period (14) of the solution (13). In this sense L_T is the "fundamental thermal length" of the S-mode. The establishment of combustion in the region of dimension L_T is illustrated in Figure 2 (here $k_0=1$, $q_0=1$, $\sigma=2$, $\beta=3$). For $\Delta r_0 < L_T$ first the heat spreads, the region of combustion grows until its diameter reaches a value L_T. For subsequent values of the time, the combustion rate increases by several orders, a type of heat release flash occurs which is analogous to the phenomenon of a chain reaction, but only for the case of a nonlinear medium.

The investigation of equation (12) in the case of LS-mode ($m>0$, negative friction) led [1d, 5] to the detection of a set of combustion eigenfunctions satisfying the condition $f^\sigma f' = 0$ and $f=0$ for $\xi \to \infty$. The number N of the eigenfunctions is determined by the parameters of the medium σ and β by the formula

$$N = \left[\alpha - \left[\frac{\alpha}{\alpha}\right]\right] + 1, \quad \alpha = \frac{\beta - 1}{\beta - \sigma - 1}. \tag{15}$$

The first eigenfunction has one central peak; the high-order eigenfunctions contain a number of peaks that increases with the number of the function. Figure 3 shows the first four functions for the case $\sigma=2$, $\beta=3.18$. Here $f=f/f_0$ and $\xi=\xi f_0^{0.5(\beta-\sigma-1)}$ are plotted on the axes. The total number of functions for this case N=13.

The self-similar solutions of the LS-mode are self-focusing -- in the peaking time all of the isolated points of the self-similar solution, for example, the local temperature peaks, "converge" at the center of symmetry. The maximum temperature distribution (for $t \to t_f$) has the form

$$\lim_{t \to t_f} T(r,t) = C r^{-\frac{2}{\beta-\sigma-1}}, \quad \beta > \sigma + 1, \tag{16}$$

where the constant C is special to each of the eigenfunctions (its value increases with an increase in the number of the functions). This behavior of the solution indicates localization of combustion and "cutting off" of the "tails" of the self-similar solution. On assignment of finite initial data for the Cauchy problem (7) in the case of the LS-mode, as the calculations show, the profile T(r,t) inside the region of combustion is close to self-similar and essentially distorts at the boundaries of the region where T(r,t) vanishes, and infinite "tails" of the self-similar solution are not realized. The study of [1b-g, 5] permits indication of the value of L_T^* of the resonance length of the excitation of combustion in the LS-mode analogous to the value of L_T from (14).

$$L_T^* = \pi \sqrt{\frac{2(\beta+\sigma+1)}{\sigma(\beta-1)}} \sqrt{\frac{k_0}{q_0}} T_{0m}^{\frac{\sigma+1-\beta}{2}}. \tag{17}$$

The size of the localization region in the LS-mode depends not only on the properties of the medium, but also on the maximum temperature T_{0m} at the initial disturbance. Figure 4 gives the numerical solution in the case of the LS-mode ($\beta=5$, $\sigma=2$, $k_0=1$, $q_0=1$) demonstrating the propagation of the region of combustion with respect to the dimensions L_T^* and the heat release flash at this dimension with the appearance of the characteristic features of LS-mode. The dependence of L_T^* on T_{0m} is illustrated in Figures 5 and 6 for the same values of the parameters β, σ, k_0 and q_0 as for Figure 4. The small ($T_{0m}=1$) value of T_{0m} led to a large value of L_T^* and merging of the local disturbances; a large value ($T_{0m}=3$) led to a small value of L_T^* ($L_T^* < \Delta r_0$) and individualization of the development of local disturbances.

4. Multidimensional Effects in the Heat Localization Phenomenon

In contrast to the one-dimensional case, in the multidimensional case the region of localization of the heat can have a different shape (in the one-dimensional

case, the region of space included between two parallel planes). In the three-dimensional configuration the region of localization can be a closed part of space of finite volume.

In the case of a medium without volumetric sources for special assignment of the boundary with the initial conditions the region of localization is separated from the cold space by thermal "faces" which are not deformed during a finite time.

For example, in the three-dimensional case with special assignment of the initial temperature distribution the region of localization can be an octahedron. The four tetrahedral pyramids made up of the bases are the simplest (analytically) obtained region of metastable localization of heat (the "thermal crystal"). During the localization time inside the octahedron the temperature is nonzero (the maximum temperature in the center), and it vanishes on its "faces." The value of the localization time is estimated by the same formula as for the one-dimensional case (6), where r_0 is the characteristic linear dimension of the "thermal crystal" (see Figure 7).

In the case of the presence of a volumetric source, the multidimensional interaction of the regions of local excitation of combustion was studied in [6]. Depending on the degree of overlap of the regions of the initial temperature disturbances, these structures either continue to burn individually[1] or they merge into one structure. In the last case this merging can take place both symmetrically[2] and asymmetrically[3] depending on the degree of symmetry of the initial data (in the overlap of the initial combustion regions).

5. Localization of Heat in a Plasma with n-Type Thermal Conductivity

The boundary conditions leading to localization of the heat permits theoretical concentration of any amount of energy in a fixed region of space and holding of it for a finite time interval. Therefore it is of interest to estimate the plasma parameters reached as a result of heating the plasma by a powerful laser pulse in the mode with peaking, generating localization, for example, in the S-mode [1a, 1g, 4].

Let the completely ionized DT-plasma ($\sigma=2.5$) be heated by a laser pulse, and let the laser emission be absorbed at the boundary. For the estimates we shall neglect the gas dynamic motion, the characteristic radiation of the plasma and other processes. We shall consider that at the time $t_0=0$, the flat layer of material bounding the vacuum with an area $s=r_\phi^2$ begins to be heated.

Under the assumption that has been made, it is possible to make some estimate based on the analytical solution of (4).

---

[1] See Figure 8.

[2] See Figure 9.

[3] See Figure 10.

The establishment of the S-mode for $\sigma=2.5$ is guaranteed on satisfaction of the condition $t_{f/c}\geq 10^3$ where t_f is the focusing time, t_{f-c} is the time of completion of the laser pulse effect. Here c is the time the temperature $T_M=T(0, t_{f-c})$ is maintained which is reached at the time $t=t_{f-c}$. For $t_{f/c}\cong 10^3$ the ratio of the maximum flux $W_M=W(0, t_{f-c})$ to the initial $W_0=W(0, 0)$ is equal to $W_M/W_0\cong 10^4$ to 10^5, and half the pulse energy is contributed in time $5c\cong t_f/200$.

The effect of the gas dynamics is estimated by the ratio $r_\phi/r_{T\Delta}$, where $r_{T\Delta}$ is the depth of penetration of the rarefaction wave calculated by the speed of sound at the boundary.

The table of estimates is presented for the DT-plasma with density $2\cdot 10^{-3}$ g/cm^3 and $t_{f/c}\cong 10^3$.

Table 2

(1) №	(2) T_M(кэв)	(3) W_M(вт/см^2)	(4) r_ϕ(см)	(5) ε (нсек)	(6) E_0(дж)
1	1	10^{14}	$8\cdot 10^{-3}$	$5\cdot 10^{-3}$	10^{-1}
2	3	10^{15}	$3{,}4\cdot 10^{-2}$	$6\cdot 10^{-3}$	10
3	8	10^{16}	$1{,}1\cdot 10^{-1}$	$5{,}2\cdot 10^{-3}$	10^3

Key:
1. No
2. T_M(kev)
3. W_M(watts/cm^2)
4. r_ϕ(cm)
5. ε(nanoseconds)
6. E_0(joules)

Here E_0 is the total energy input by the laser pulse.

As the calculations with consideration of the gas dynamic motion indicate [4], it is not a theoretical obstacle for the manifestation of the localization of heat on the basis of its inertia by comparison with the thermal process where the latter develop in the peaking mode. It is demonstrated that for $r_\phi/r_{T\Delta}>1$ to 2 the gas dynamics in general are insignificant. For the estimates 1 to 3 of Table 2 $r_\phi/r_{T\Delta}<1$, where the maximum value of $r_\phi/r_{T\Delta}$ is reached in the first example. The numerical solutions considering the gas dynamic motion [4] indicate that for the given example the gas dynamics improve the localization -- the temperature and localization time increase, the temperature profile becomes more concave (a smaller mass is efficiently heated than in the stationary medium).

After the end of the pulse, the gas dissipates and is cooled. The shock wave formed as a result of the fact that the heat wave "goes over" the density peak and beginning to move after rearrangement of the temperature profile to "convex" goes from the substance to the vacuum. This powerful shock wave can serve as the sign of localization when it is detected experimentally, for in the case of the effect of nonpeaking conditions on the plasma (for example, the laser radiation power increases linearly with time) such a wave does not occur.

6. Localization of Thermonuclear Combustion in a Plasma with n-Type Electrical Conductivity

As was demonstrated in reference [1e], the value of the resonance length (17) can be used to formulate the thermonuclear flash conditions. Thus, the combustion in a mixture of equal composition of D and T takes place under peaking conditions if the size of the temperature disturbance $\Delta r_0 > \Delta r_я$. The value of $\Delta r_я$ is defined by the following arguments.

Let it be possible to neglect the combustion of the DT-material and the processes of radiation transport and consider the plasma as a single-temperature, ideal and stationary medium. Then for the temperature range of $1 \lesssim T \lesssim 30$ kev the ignition process is described by the equation

$$\frac{\partial T}{\partial t} = \kappa_0 \frac{\partial}{\partial r}\left(T^{\sigma}\frac{\partial T}{\partial r}\right) + \frac{q_0 T^{\beta}}{1+BT^{b}}, \qquad (18)$$

where $k_0=8.1\cdot10^3\ \rho^{-1}\ cm^2 sec^{-1} kev^{-2.5}$, $\sigma=2.5$, $q_0=4.7\cdot10^5 \rho sec^{-1} kev^{-4.5}$, $\beta=5.2$, $B=2.4\cdot10^2\ kev^{-3.6}$, $b=3.6$; $\rho(g/cm^3)$ is the density of the DT-mixture.

In the temperature range of 1-3 kev the source in (18) is close to the expression $q_0 T^{\beta}$. Since $\beta=5.2>3.5=\sigma+1$, this source can, in accordance with [1b-1g. 2] lead to localization of combustion on a defined length. For large temperatures consideration of the term BT^B in the denominator of the expression for q(T) in (18) leads to a change in the effective value of β_{eff} in the notation $q(T)=q_{eff}T^{\beta eff}$. Thus, for T=5 kev, $q(T)\approx q_S T^{\sigma+1}$ with $q_S\approx5.1\cdot10^6\rho sec^{-1}kev^{-2.5}$. For $T\gtrsim5$ kev, $\beta_{eff}<\sigma+1$. Using these approximations and formula (17) the following characteristics of thermonuclear combustion are obtained in the range of 1-10 kev if it is excited by a disturbance of $\Delta r_0 > \Delta r_я = L_T^*$. The size of the region of localization of combustion $\Delta r_я$ is given by (17) by the formula: $\Delta r_я \approx 0.5/\rho T_{0m}^{0.85}$ cm (on variation of the initial amplitude in the range of 1-3 kev). The combustion is localized during the time $\Delta t_я \approx 10^{-6}/\rho T_{0m}^{4.3}$ sec. When the temperatures $T\approx5$ kev are reached in the combustion process, the size and the localization time of the combustion region are determined by the S-mode: $\Delta r_я^{(s)}\approx0.2/\rho$ cm, $\Delta t_я^{(s)}\approx8\cdot10^{-8}/\rho T_{0m}^{2.5}$ sec. With further increase in the temperature, its profile inside the localization region begins to be rearranged to convex, and for T>10 kev an increase in the combustion region begins.

As was shown in [1e], the scales reached $\Delta t_я$ and $\Delta r_я$ are such that for $T\lesssim7$ kev it is actually valid to neglect the two-temperature nature and burnup, to consider the absorption of the α-particles local. and not to consider the neutron contribution.

Consideration of the volumetric radiation turns out to be necessary for reasonable temperature ranges (no less than 1 kev) and density ranges (compression no greater than by 10^4 times). De-excitation is equivalent to the addition of the discharge $g(T)=g_0T^{0.5}$ to (18), where $g_0=2.2\cdot10^8\ sec^{-1}\ kev^{0.5}$.

For $T\gtrsim3.7$ kev, we set $g(T)<q(T)$. If the structure of the thermonuclear combustion begins to be formed at temperatures of no less than 4 kev, then the volumetric radiation cannot extinguish it. In Figure 11 results are presented from the

calculation considering the losses to volumetric radiation. The initial disturbance amplitude ~4 kev, $\Delta r_0 \sim 0.1$ cm, $\rho=20$ g/cm^3/

On the other hand, there is a density range for which the hot region is optically dense, and the radiant thermal conductivity is small by comparison with the n-type conductivity. For T≤7 kev, this corresponds to compressions of ~10^6 times with respect to the ratio to the density of DT-ice. In this case there is no volumetric de-excitation.

As was shown in [1e], the gas dynamic motion can be neglected if $T_{0m} \geq 3$ kev. If at the beginning of the flash the gas dynamic motion of the DT-plasma to the center (compression) continues, it can compensate for the losses to volumetric radiation in an optically transparent plasma for T<4 kev.

BIBLIOGRAPHY

1. Samarskiy, A. A.; Kurdyumov, S. P., et al.

a) "Effect of Metastable Localization of Heat in a Medium with Nonlinear Thermal Conductivity," DAN [Reports of the USSR Academy of Sciences], Vol 223, No 6, 1975, p 1344.

b) "Thermal Structure and Fundamental Length in a Medium with Nonlinear Thermal Conductivity and Volumetric Heat Sources," DAN, Vol 227, No 2, 1976, p 321.

c) "Nonlinear Processes in a Dense Plasma," In technical document TECHNOLOGY OF INERTIAL CONFINEMENT EXPERIMENTS, IAEA-200, Vienna, 1977, p 185.

d) "Combustion of a Nonlinear Medium in the Form of Complex Structures," DAN, Vol 237, No 6, 1977, p 1330.

e) "Localization of Thermonuclear Combustion in a Plasma with n-Type Thermal Conductivity," PIS'MA V ZHETF [Letters to the Journal of Experimental and Theoretical Physics], Vol 26, No 9, 1977, p 620.

f) "Occurrence of Structures in Nonlinear Media and Nonsteady-state Thermodynamics of Peaking Conditions," PREPRINT IPM [Preprint of the Institute of Applied Mathematics], No 74, 1976.

g) "Nonlinear Processes in a Dense Plasma and the Peculiarities of the Thermodynamics of the Peaking Modes," PREPRINT IPM, No 109, 1976.

2. Zmitrenko, N. V.; Kurdyumov, S. P. " [sic] and [sic]-Modes of Self-Similar Compression of a Finite Mass of Plasma and the Peculiarities of the Conditions 'with Peaking,'" PMTF [Applied Mechanical-Thermal Physics], No 1, 1977, p 3.

3. Kurdyumov, S. P.; Mikhaylov, A. P.; Plokhotnikov, K. E. "Localization of Heat in Multidimensional Problems of Nonlinear Thermal Conductivity. Thermal Crystal," PREPRINT IPM, No 22, 1977.

4. Zmitrenko, N. V.; Kurdyumov, S. P.; Mikhaylov, A. P.; Samarskiy, A. A. "Metastable Localization of Heat in a Medium with Nonlinear Thermal Conductivity under the Conditions of Its Manifestation in an Experiment," PREPRINT IPM, No 103, 1977.

5. Yelenin, G. G.; Kurdyumov, S. P. "Conditions of Complication of the Organization of Nonlinear Dissipative Media," PREPRINT IPM, No 106, 1977.

6. Kurdyumov, S. P.; Malinetskiy, G. G.; Poveshchenko, Yu. A.; Popov, Yu. P.; Samarskiy, A. A. "Interaction of Thermal Structures," PREPRINT IPM, No 77, 1978.

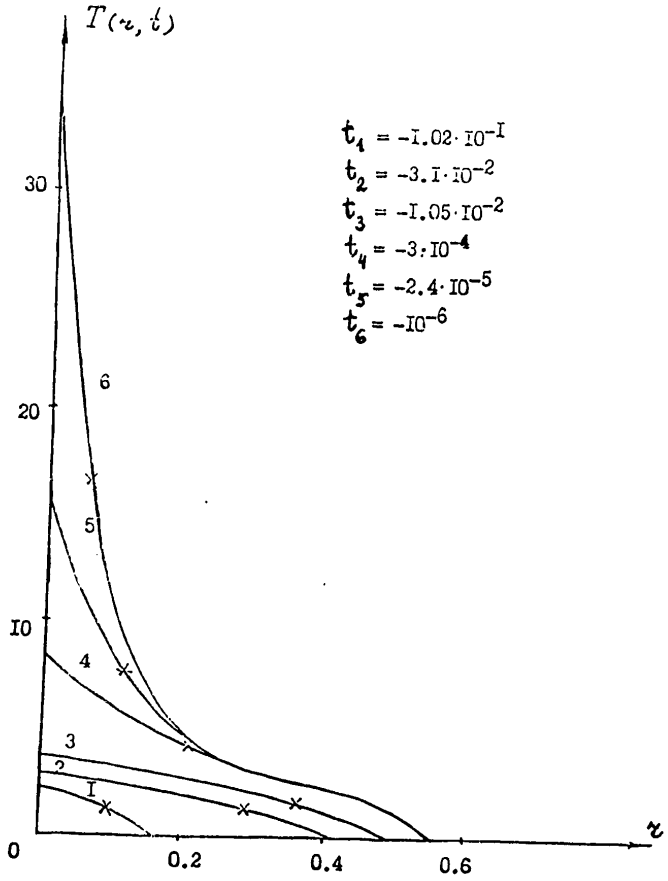

Figure 1

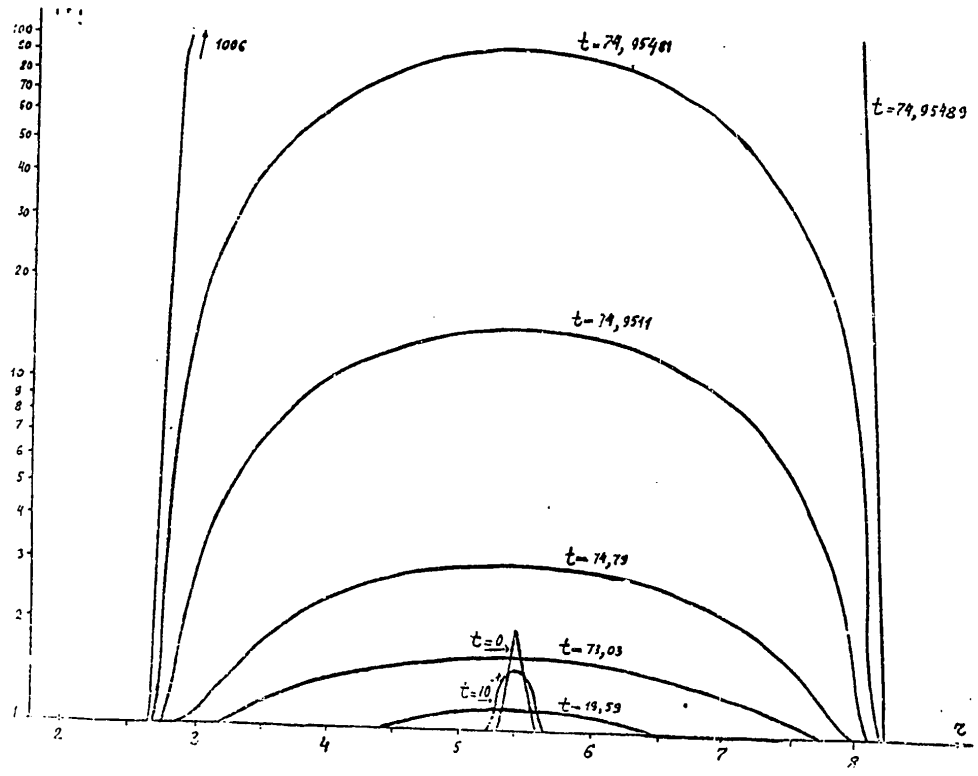

Figure 2

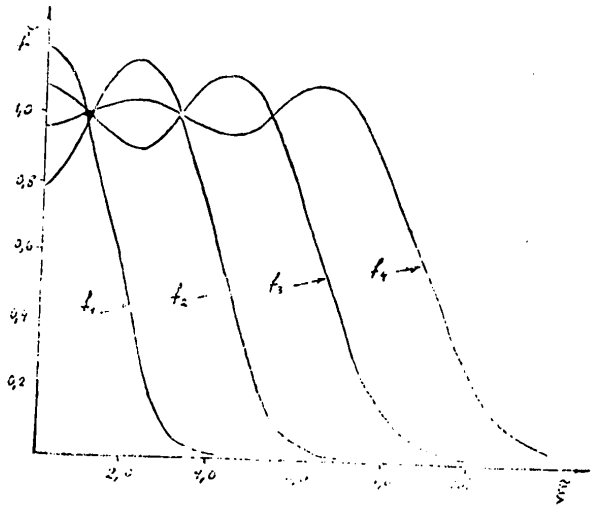

Figure 3

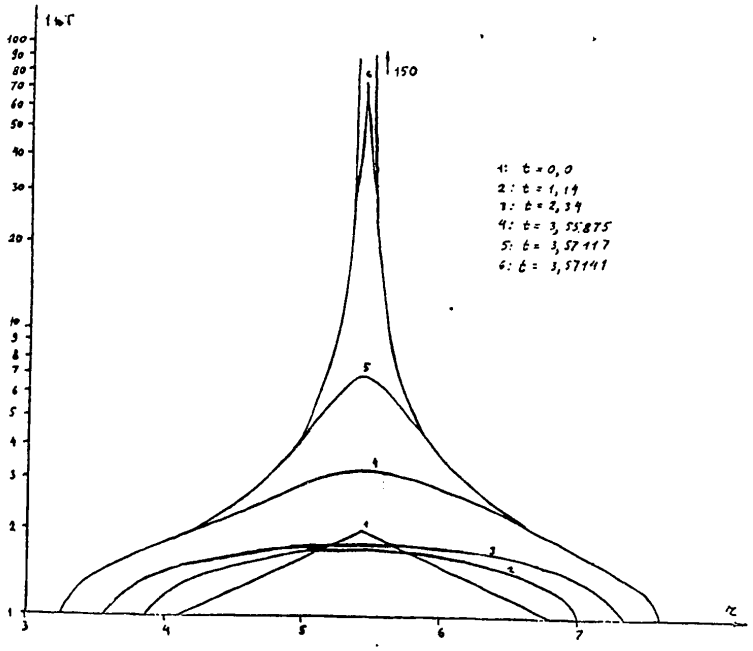

Figure 4

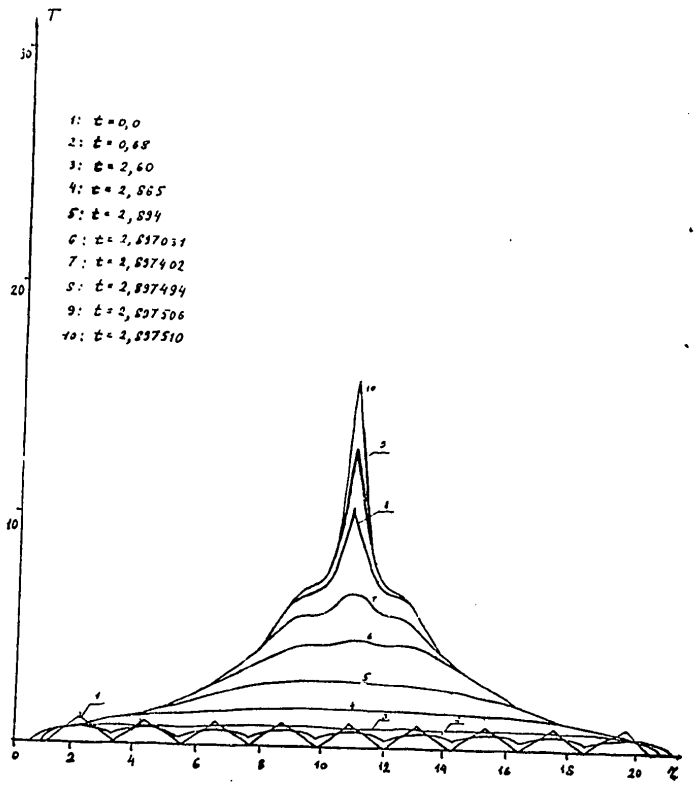

Figure 5

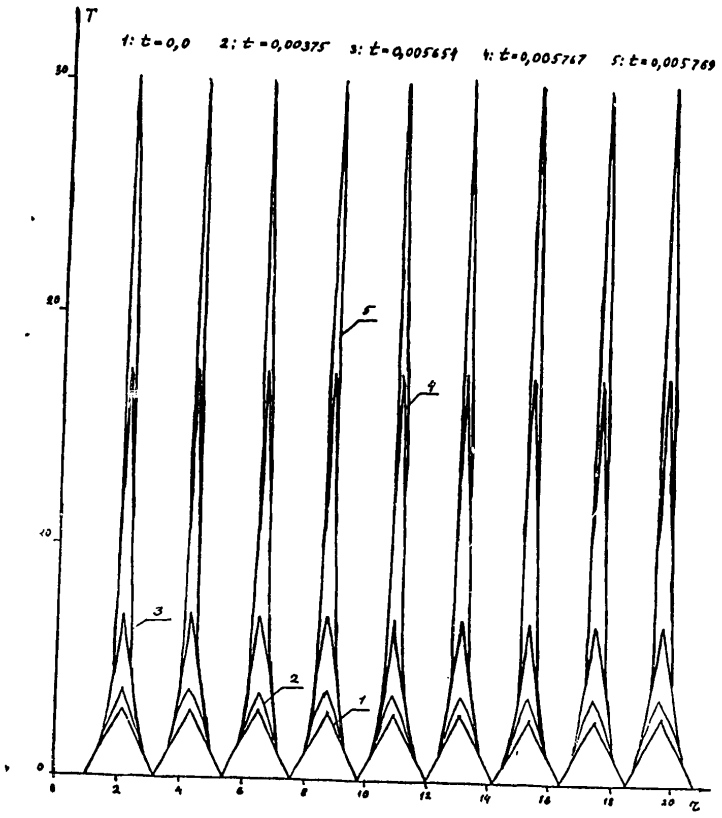

Figure 6

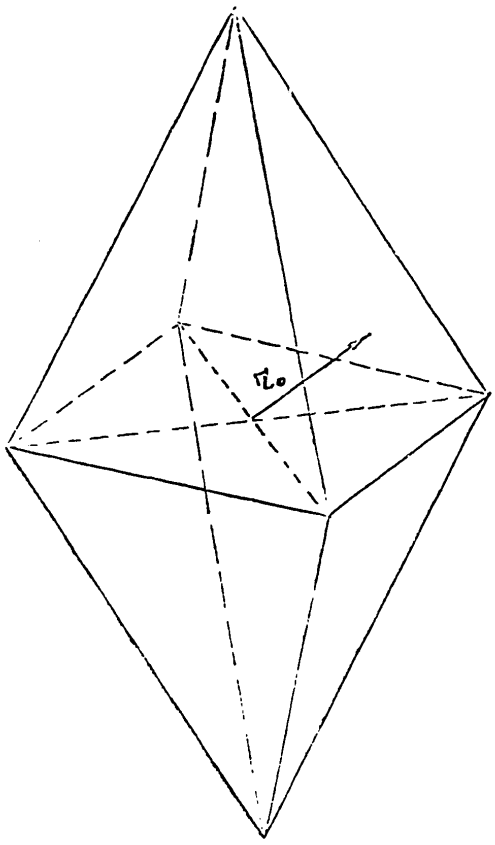

Figure 7

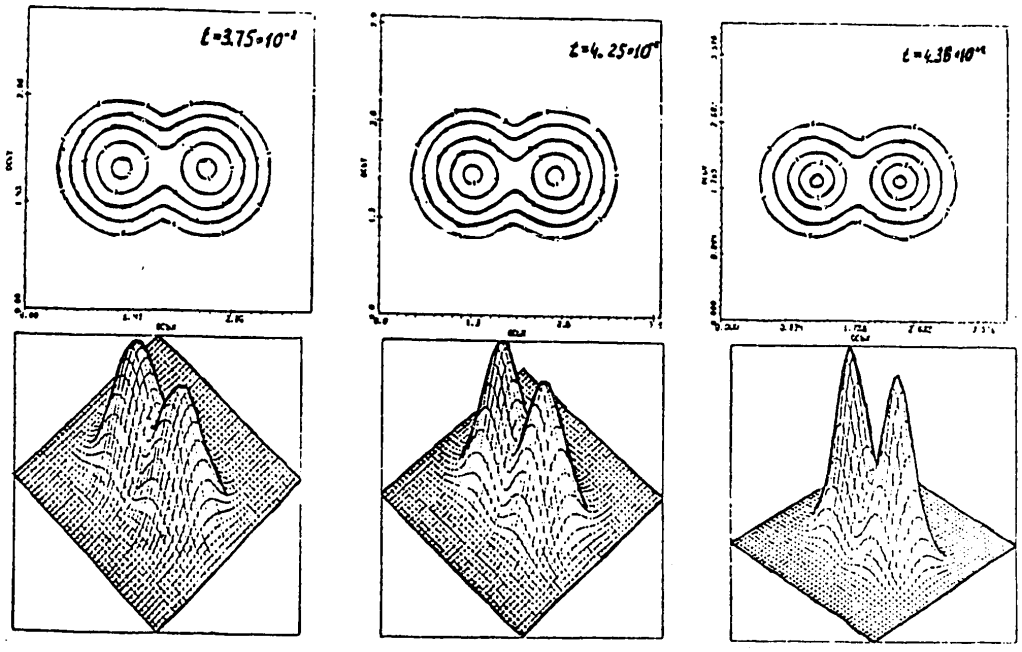

Figure 8

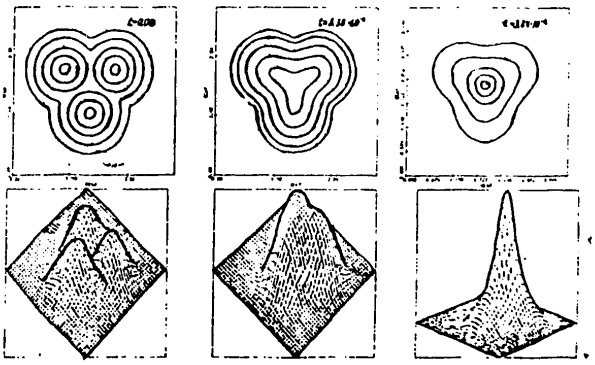

Figure 9

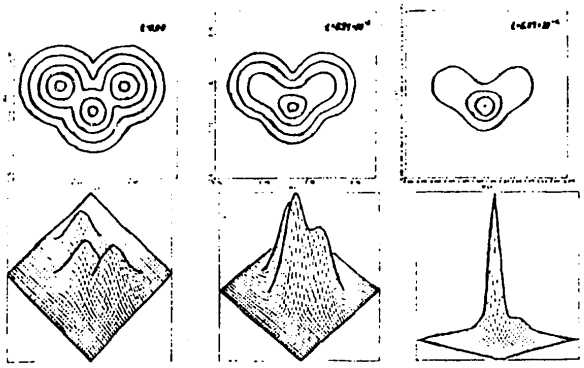

Figure 10

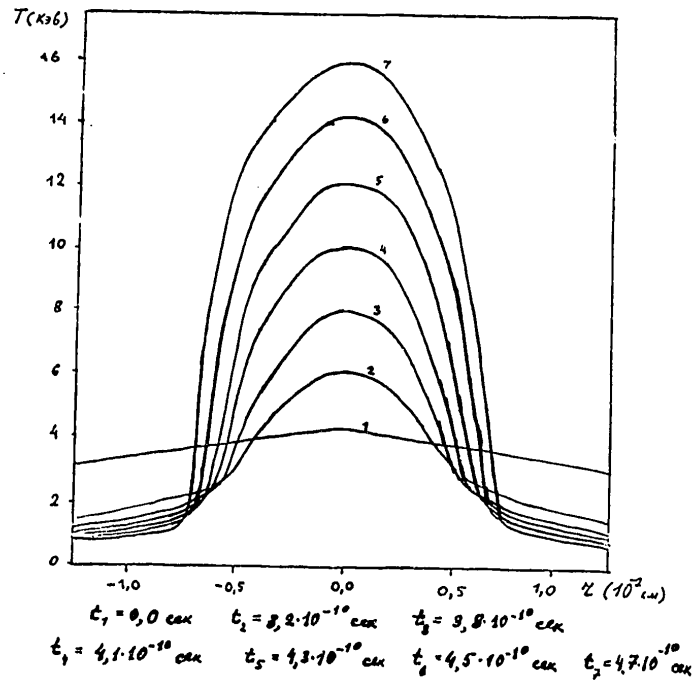

Figure 11

STUDY OF THE STABILITY OF THE COMPRESSION PROCESS OF THIN GLASS SHELLS

[Ye. G. Gamaliy, V. A. Gasilov, V. B. Rozanov, A. A. Samarskiy, V. F. Tishkin, N. N. Tyurina, A. P. Favorskiy, M. Yu. Shashkov, pp 28-64]

Introduction

In this paper a study is made of the stability of the process of compression of thin glass shells which are considered in [1], [2] and are being studied at the present time both theoretically and experimentally [3], [4], [5], [6].

It is known that high density of the material during hydraulic compression can be achieved only if the initial nonuniformities do not increase during the compression process to values that significantly disturb the spherical symmetry. At the present time there are a number of theoretical-calculation papers in which the stability problem has been considered [7], [8], [9], [10], [36].

This paper is devoted to the mathematical simulation of the effect of disturbances of the various types on the process of compression of glass shells with parameters taken from [6]. The basis for the procedure used in solving the equations is the completely conservative difference systems described in reference [37]. The use of moving curvilinear finite-differences in the calculations permits the development of the instability to be traced to the stage where the defining effect comes from the nonlinear effects. On making the transition to the nonlinear conditions, the growth rate of the disturbances decreases, which, in turn, is felt in the high-frequency disturbances for which the nonlinear effects appear comparatively early.

The results of the performed calculations permit determination of the number of the harmonic which has the highest growth rate and initial amplitude of the disturbances for which the effect of the instability begins to be felt noticeably in the parameters of the compressed plasma.

§1. General Statement of the Problem

1. The possibility of heating and compressing a substance to high temperatures has been investigated in a number of papers by Soviet and foreign authors [11], [12], [13], [14], [15], [16], [17], [18], [19]. In references [1] and [2] it was demonstrated that the prospective area here is the use of shells with high aspect ratio. The simplest configurations of this type are a thin glass shell filled with a low-density gas (see Figure 1 borrowed from [7]).

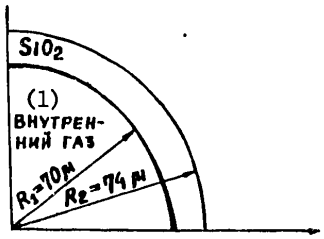

Figure 1

Key:
1. Internal gas

The parameters of the shells studied in the given paper were selected close to the parameters of experimental targets [6]. In Figure 2 we have the energy flux incident on the target taken from [7].

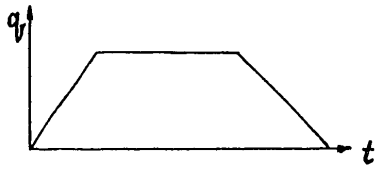

Figure 2

2. For a description of the process of compressing the shell with the reduced parameters, the hydrodynamic approximation is used. The n-type thermal conductivity, the phenomenon of the temperature discontinuity and ion-electron relaxation were taken into account. All the physical properties of the plasma were calculated under the assumption of complete ionization. The corresponding system of equations has the form:

$$\frac{d\rho}{dt} + \rho \operatorname{div} \vec{v} = 0 \tag{1.1}$$

$$\rho \frac{d\vec{v}}{dt} = -\operatorname{grad} P \tag{1.2}$$

$$\rho \frac{d\varepsilon_e}{dt} = -P_e \operatorname{div} \vec{v} + \operatorname{div} \vec{w_e} + \operatorname{div} \vec{q_r} - Q \tag{1.3}$$

$$\rho \frac{d\varepsilon_i}{dt} = -P_i \operatorname{div} \vec{v} + Q \tag{1.4}$$

$$P = P_e + P_i \; ; \; P_e = P_e(\rho, T_e), \; P_i = P_i(\rho, T_i) \tag{1.5}$$

$$\varepsilon_e = \varepsilon_e(\rho, T_e) \; , \; \varepsilon_i = \varepsilon_i(\rho, T_i) \tag{1.6}$$

$$\left(\frac{\vec{q}}{|q|}, \nabla\right)\vec{q} = K(\rho, T_e)\vec{q} \tag{1.7}$$

$$\vec{W_e} = \varkappa(\rho, T_e)\,\mathrm{grad}\,T_e \tag{1.8}$$

$$Q = Q_0 \rho^2 \frac{T_e - T_i}{T_e^{3/2}} \tag{1.9}$$

Here ρ is the density of the substance,

$\vec{v}$ is the hydrodynamic velocity,

P_e, P_i, P are the electron, ion and total pressures,

T_e, T_i are the electron and ion temperatures,

ε_e, ε_i are the electron and ion specific internal energies.
The system (1.1)-(1.9) was solved in the approximation of axial symmetry.

As follows from the experimental papers [6], [3] for the investigated energy flux density the number of epithermal electrons is small, and it has no influence on the compression. Therefore the heating by the fast electrons was not taken into account, and the thermal conductivity was considered to be classical.

Thus, the investigated approximation quite completely gives a qualitatively and quantitatively correct description of the processes.

§2. Nature of the Occurrence of Instability

1. There are two stages of the process where the motion is hydrodynamically unstable. The first stage is acceleration of the heavy unevaporated part of the shell by a hot, low-density ablation layer. The second stage comes when the pressure in the compressed nucleus increases to a degree such that it begins to brake the denser shell. These stages are separated in time by the region of stable flow with approximately constant velocity [see [4]).

2. In a number of simplest cases, the estimate for the rate of development of disturbances can be obtained analytically. Thus, for example, the analytical solutions are obtained in the case where the disturbance wave length is large by comparison with the characteristic dimensions of the investigated subject [20], [21], [22]. There are also a number of papers devoted to the study of the behavior of an incompressible liquid in a constant gravitational force field [23], [24], [25], [26], [27], [28], [29], [38].

3. In contrast to the classical situation, on compression of the shells, the development of the instability takes place against an essentially nonstationary background which is formed as a result of interaction of the nonlinear thermal

and hydrodynamic processes. The investigation of the instability in the first stage near the ablation boundary is also complicated by the fact that the evaporated substance flows through the instability zone with high velocity, and the zone itself moves through the mass deep into the shell.

The noted facts complicate the application of analytical methods and make numerical simulation in practice the only method permitting successful solution of the stated problem.

§3. Test Calculations. Choice of the Finite Difference

1. When investigating the dynamics of the development of the disturbances by numerical methods, the question arises of to what degree the correctly used procedure transmits the quantitative and qualitative nature of the growth of the disturbances. In order to explain this question, a number of test calculations were made including comparison with the known analytical solutions and calculations on series of finite-differences becoming denser. The calculations demonstrated that the numerical solution quantitatively and qualitatively correctly reproduces the dynamics of the development of the disturbances.

2. As one of the model problems, a study was made of the problem of the stability of a thin layer of incompressible liquid under the effect of gravity [20]. The gravitational acceleration is directed opposite to the y-axis (see Figure 3).

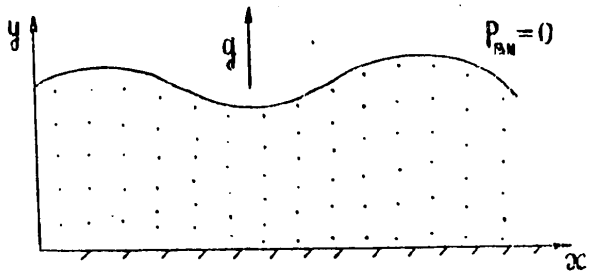

Figure 3

On the lower boundary of the layer of liquid, the condition of nonpenetration was given. The upper boundary was assumed to be free.

At the initial point in time the height of the free boundary of the liquid was disturbed by the law

$$h = h_0(1 + \alpha \cos \kappa x) \qquad (3.1)$$

here h_0 is the height of the undisturbed layer,

α is the amplitude of the disturbance,

$k=2\pi/\lambda$ is the wave number,

λ is the disturbance wave length.
The speed of the liquid at the initial point in time is assumed to be

$$u = -\alpha\sqrt{g h_0}\sin(\kappa x) \tag{3.2}$$

$$v = \alpha\kappa y\sqrt{g h_0}\cos(\kappa x) \tag{3.3}$$

For numerical solution of this problem, entirely satisfactory agreement was obtained between the numerical and the analytical solutions in the different stages of development of the instability.

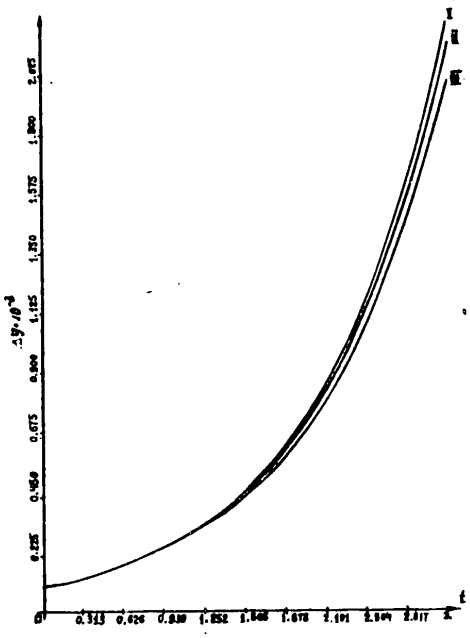

Figure 4

In the initial period of movement, the behavior of the liquid is described well by the linear approximation, according to which the disturbances must increase as $\exp(k\sqrt{gh_0}t)$. In Figure 4 comparative graphs are presented for the growth of the disturbance amplitude calculated by the linear theory and by the data from the numerical calculation.

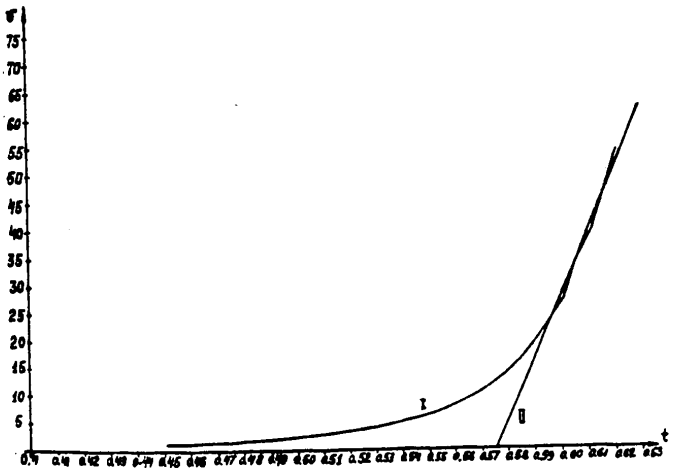

Figure 5

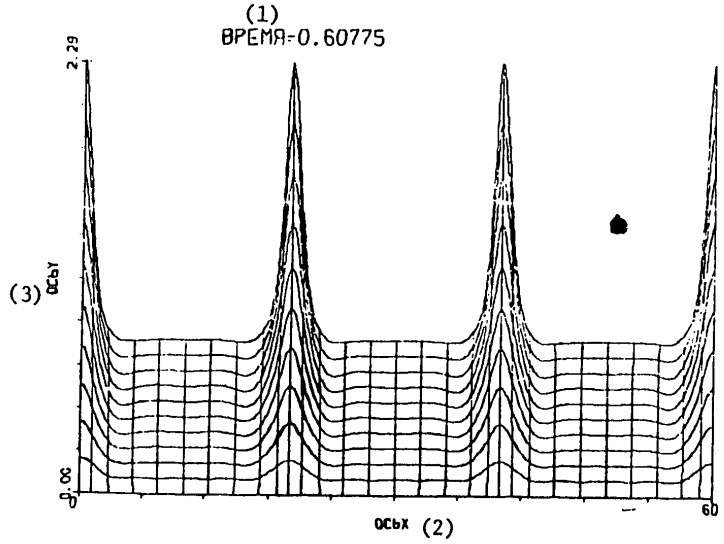

Figure 6

Key:
1. time; 2. x-axis; 3. y-axis

In the later stage, the linear approximation loses its correctness, but for the nonlinear problem the asymptotic regime exists [25], [26], [27], [38], for which the solution "peaks" directed upward move with acceleration close to the gravitational acceleration. Figure 5 shows the arrival of the numerical solution at this regime. In conclusion, Figure 6 gives the shape of the liquid boundary at the time close to the time of reaching the asymptotic motion regime.

3. Satisfactory agreement was also obtained on numerical simulation of the problem of Rayleigh-Taylor instability of a fine strand of thread (see [21]). The thread was simulated by a layer of incompressible liquid, the thickness of which was appreciably less than the wave length and the amplitude of the initial disturbance (see Figure 7).

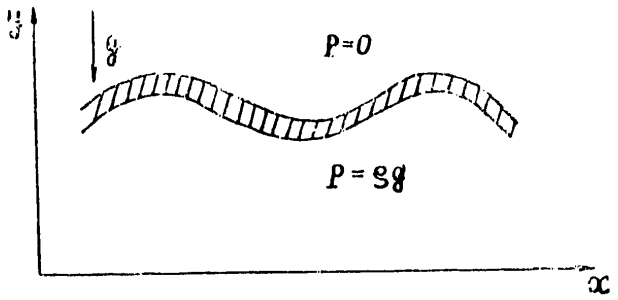

Figure 7

The gravitational acceleration was directed down along the y-axis. At the upper and lower bounds of the layer the pressure was given: P=0 at the upper bound and P=ρg at the lower bound, ρ is the linear density of the undisturbed layer. The thread coordinates were disturbed by the formulas

$$x = x_0 + a \sin(k x_0) \tag{3.4}$$

$$y = a \cos(k x_0) \tag{3.5}$$

x_0 is the coordinate of the undisturbed thread. The velocities were assumed equal to zero at the initial point in time.

If the thickness of the layer is sufficiently small, then the equations of motion have analytical solution of the type [see [21]):

$$x = x_0 + a \sin(k x_0) \tag{3.6}$$

$$y = a \cos(k x_0) \tag{3.7}$$

Here they acquire the shape of a cycloid. This solution will be valid until t^*: $ka\cos ht^*=1$ when the cycloid forms a self-intersection.

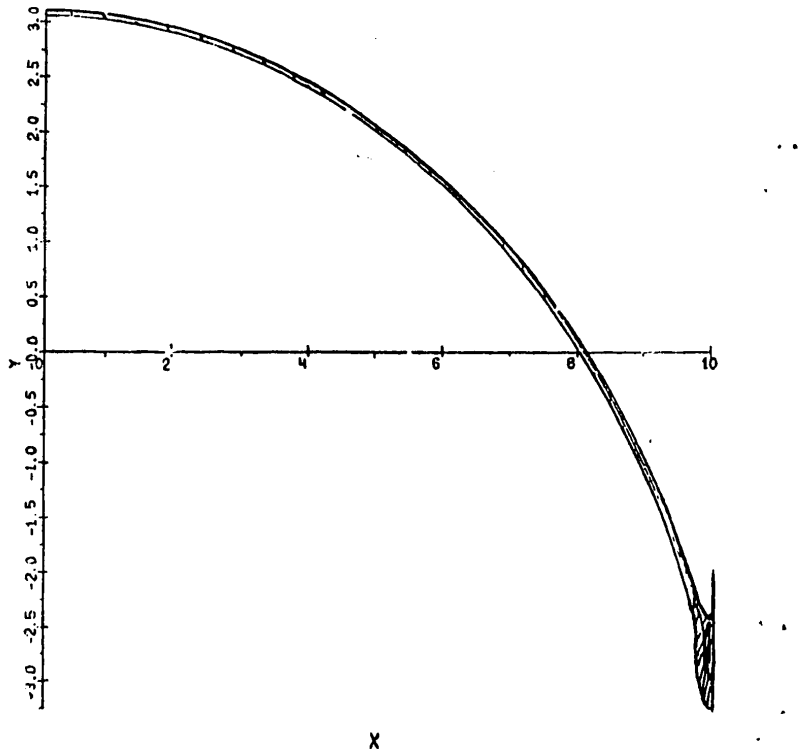

Figure 8

The results of the numerical calculation satisfactorily reproduce the solutions of (3.6)-(3.7) to the time t^* when the layer thickness increases, and cumulative jets are formed (see Figure 8). The divergence of the numerical and the analytical solutions was 0.5%. Let us note that the appearance of cumulative jets was predicted in [21].

4. For numerical simulation, the problem of the choice of the number of finite-difference nodes is important. The use of dense finite-difference nets unjustifiably increases the solution time of the problem, and when using a small number of nodes, significant deviations from the correct value can occur. In order to determine the optimal number of nodes, several calculations were made of the compression of a glass shell described in §1, where disturbances were introduced into the initial shape by the following laws:

$$R=R_0\left(1+\alpha\frac{\Delta}{R_0}\sin n\theta\right) \qquad (3.8)$$

n is the harmonic number,

Δ is the shell thickness,

α is the amplitude of the disturbance.

The disturbance amplitude α was taken equal to 0.01, and the number of the harmonic, n=10.

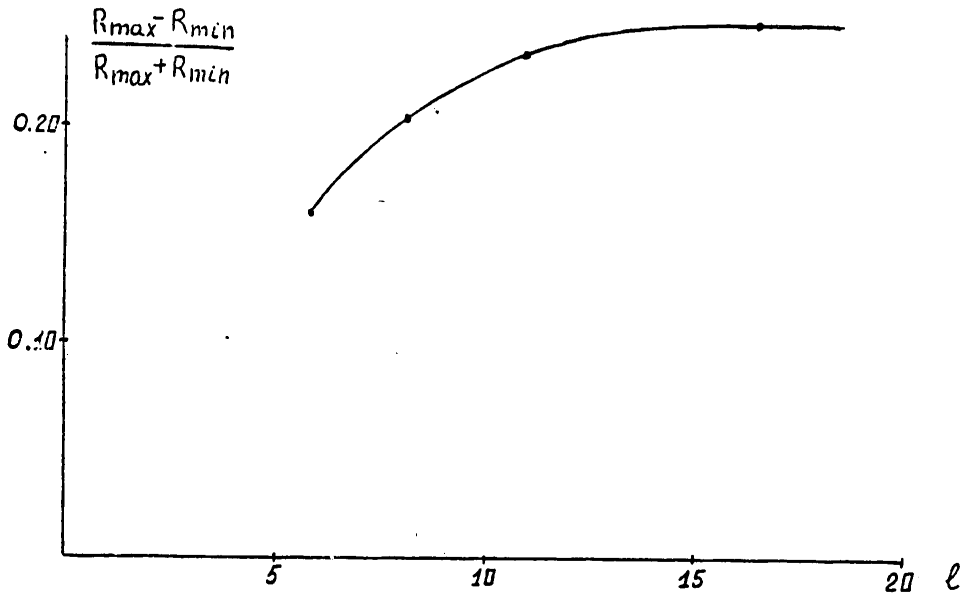

Figure 9

The calculations demonstrated that with an increase in the number of finite-difference nodes, the disturbance growth increases, but for a number of nodes per disturbance wave length $\ell \geq 10$ to 15, saturation of the growth rate takes place (see Figure 9). Let us note that approximately the same criterion was obtained in reference [31]. In the calculations described below, the number of finite-difference nodes was selected beginning with this criterion.

5. The study of high harmonic numbers ($n \geq 20$) is possible when performing the calculations in the sector with angular dimensions less than $\pi/2$ under the condition that the angular overflow of plasma during compression is much less than the dimensions of the sector. On the lateral boundaries of the sector, the equality of the normal velocity component to 0 was given. In order to check whether this influences the nature of the growth of disturbances, the harmonic was calculated with n=20 in the sector with its aperture angle $\pi/2$ and aperture angle $\pi/10$ (see Figures 10, 11). A comparison shows that the qualitative and quantitative nature of the development of the instability did not change.

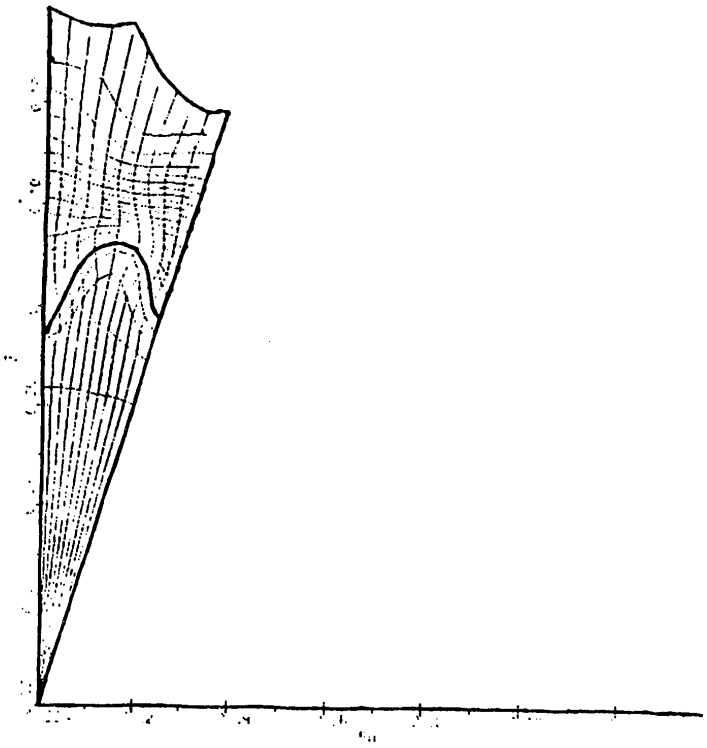

Figure 10

§4. Analysis of the Instability in a "Corona"

1. When studying two instability zones of the process of compressing glass shells, the study of the instability near the evaporation boundary is of independent interest, for the development of the disturbances in this zone can lead to disturbance of the shell in the initial stage compression. The development of disturbances on the inside boundary of the shell takes place at a time close to the time of maximum compression, but in this case the growth of the disturbances can lead to significant worsening of the plasma parameters.

2. When studying an instability near the evaporation front of the shell material, the region of subsonic flow of the gas is of the greatest interest, for the disturbances hitting the supersonic flow are carried away and cannot influence the compression. The distribution of the plasma parameters with respect to space near the evaporation boundary is formed as a result of the effect of a rarefaction wave occurring behind the front of the shock wave going to the center and

the thermal wave. The characteristic density distribution, velocity, temperature and pressure distributions of the plasma in the "corona" obtained from one-dimensional calculations are presented in Figure 12. It is obvious that the evaporation boundary and the maximum density gradient are located in the region of subsonic flow of the plasma moving toward the center.

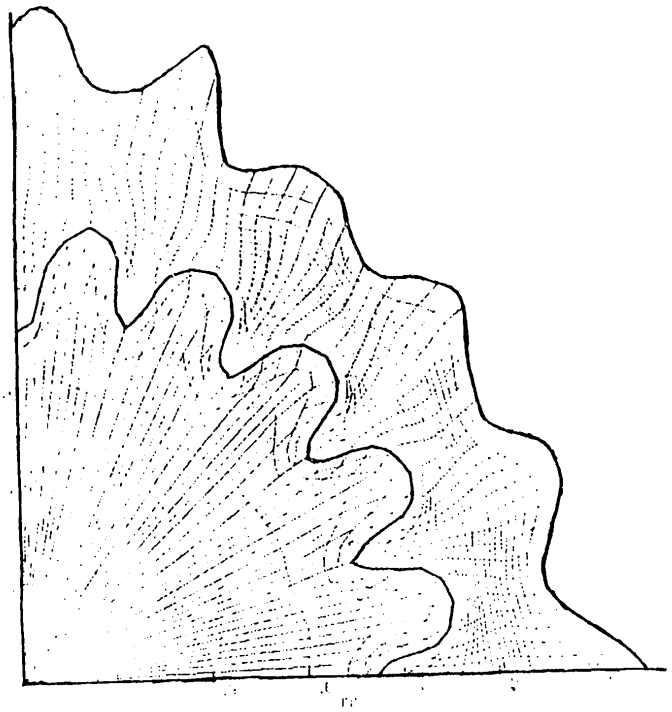

Figure 11

3. In order to explain the problem of stability near the evaporation boundary it is useful to call on the stability criteria obtained in the linearized problem both for incompressible liquid [5] and adiabatic and isothermal motion of a compressible liquid [4]. According to these criteria, the flow is unstable if the pressure and density gradients are directed opposite to each other, that is,

$$(\nabla \rho, \nabla P) < 0 \qquad (4.1)$$

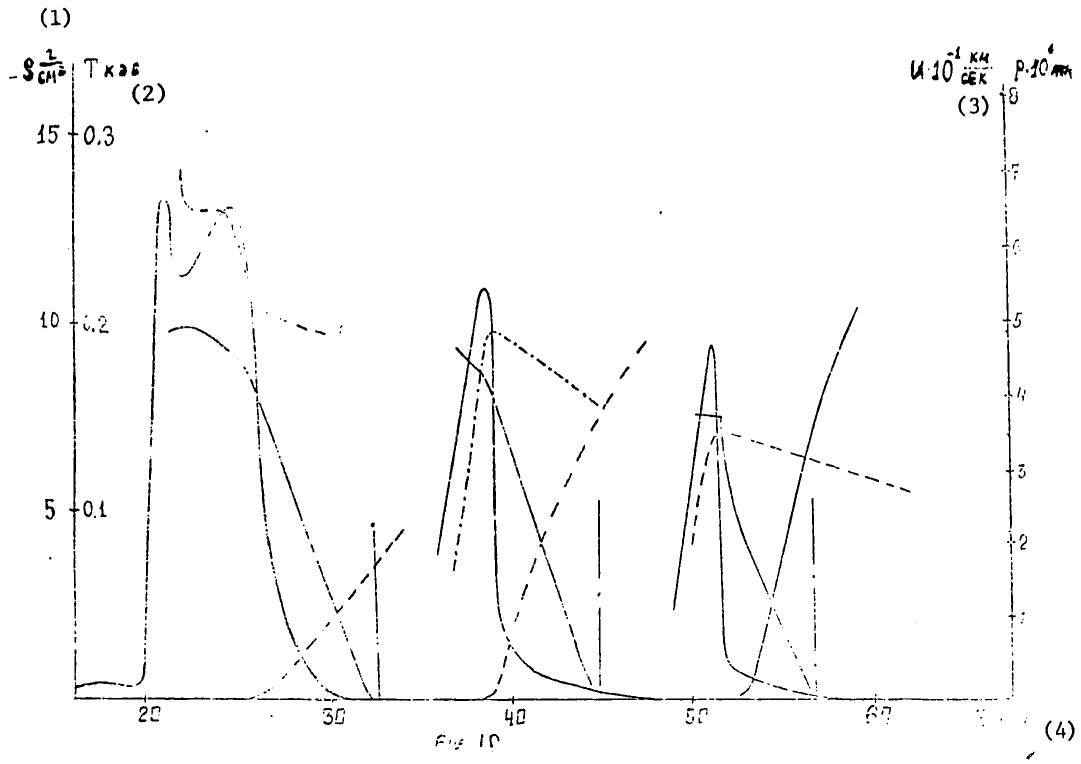

Figure 12

Key:
1. ρ, g/cm^3
2. T, kev
3. km/sec
4. R, microns

An indirect confirmation of the correctness of this criterion for a broader class of flows is the solution of the problem of stability of a plane stationary "corona" for identically directed pressure and density gradients. As the results of the numerical calculations for the linearized system of equations show , the initial disturbances damp in this case [see [32]).

Using the indicated conditions, it is easy to see from Figure 12 that the instability zone lies between the maximum pressures and densities and is very narrow ~0.2 to 0.3 micron. Beginning with the time when the outside boundary stops evaporating, the situation in the "corona" becomes stable.

4. The effect of the dissipation and evaporation of the substance is most strongly felt in the development of low-frequency disturbances, for which the growth rate of the Taylor modes is low. The stabilizing effect of the evaporation can be seen if we trace the development of the disturbance in the isolated

Lagrange layer which initially moved toward the center, and then was captured by the thermal wave. Figure 13 shows the trajectory of motion of this layer (averaged with respect to the angle 0) and the relative amplitude of the disturbance upon it $(R_{max}-R_{min})/(R_{max}+R_{min})$ as a function of time. In this calculation, disturbances were introduced into the shape of the target by formula (3.8), $\alpha=0.01$, $n=10$. From Figure 13 it is obvious that until the particle moves with the cold shell its motion is stable. As the thermal wave captures the particle, the speed of motion toward the center decreases. From the time of the beginning of deceleration, the growth rate of the disturbances increases sharply, the maximum of which is reached at the time of halting of the particle. Then, as the transition is made to supersonic flow, the growth rate of the disturbance decreases. Let us note that in this version the disturbances are concentrated on the outside of the cold part of the shell and are almost unpropagated inward, in spite of the fact that the disturbance wave length is much greater than the shell thickness. This means that the high-amplitude disturbances

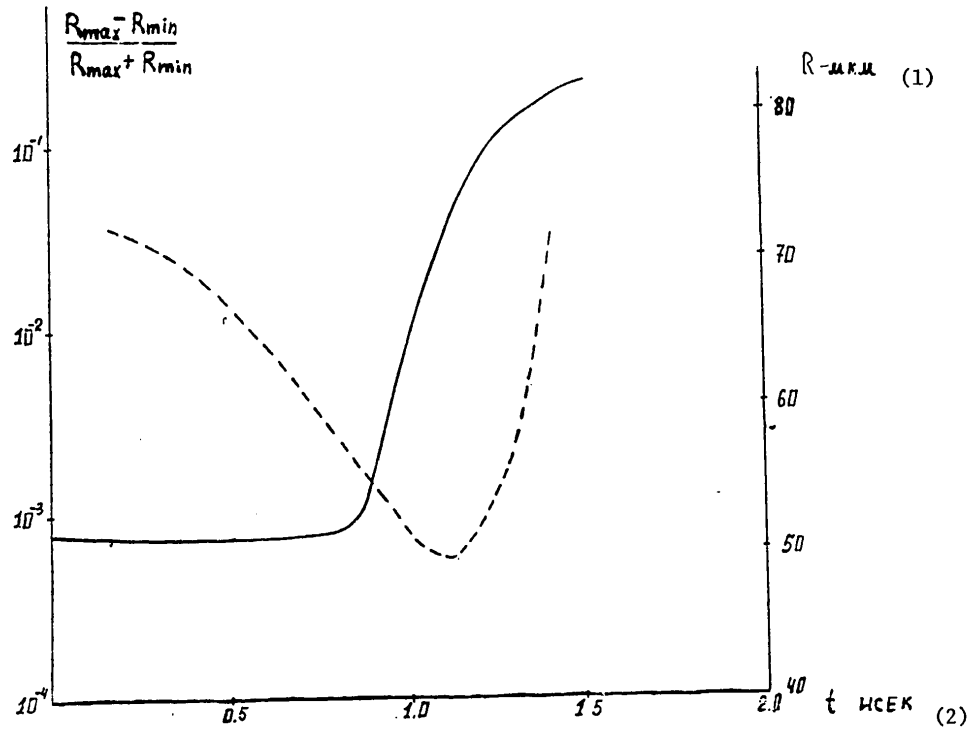

Figure 13

Key:
1. R, microns
2. t, nanoseconds

do not succeed in being propagated from the outer boundary to the inner boundary as a result of the stabilizing role of evaporation, for all the new particles of the outer boundary where the maximum disturbances are concentrated are entrained by the thermal wave and are carried away without having significant influence on the state of the shell.

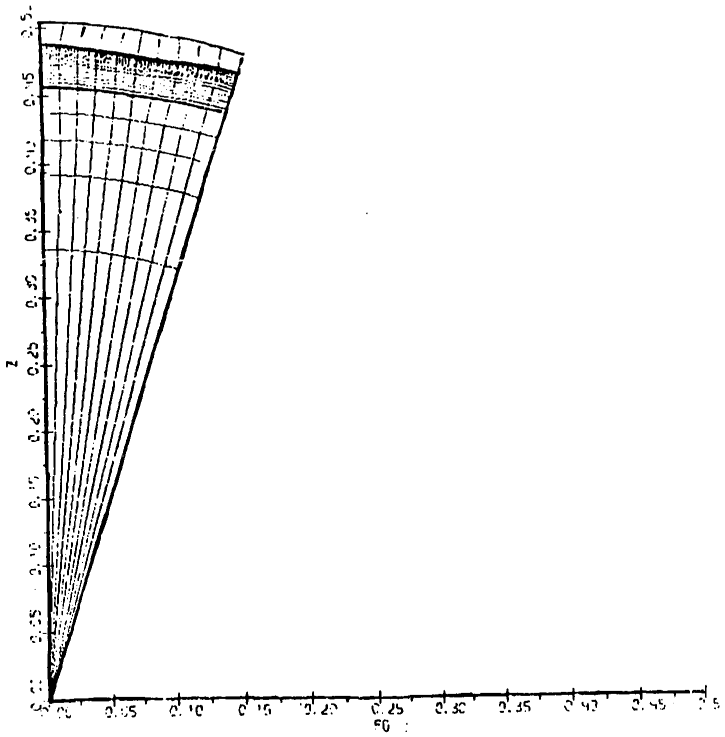

Figure 14

5. In order to discover the effect of short-wave disturbances, calculations were made with the shaped disturbances by the formula (3.8), $\alpha=0.01$, in this case the number of the harmonic was varied: n=20, 40, 60 (see Figures 14, 15, 16). For the harmonic numbers with $n\geq 20$, the increment of the growth of the disturbances is quite large, and the disturbances penetrate deep into the shell. The outside surface of the shell bends, which, in turn, causes bending of the adjacent cold layers. However, the disturbances inside are less than on the outer boundary, which is seen well by the distortion of the Lagrange lines in Figures 14, 15, and 16. Here, the disturbances damp with departure into the shell more strongly the higher the number of the harmonic, which agrees qualitatively with the data from the linear theory.

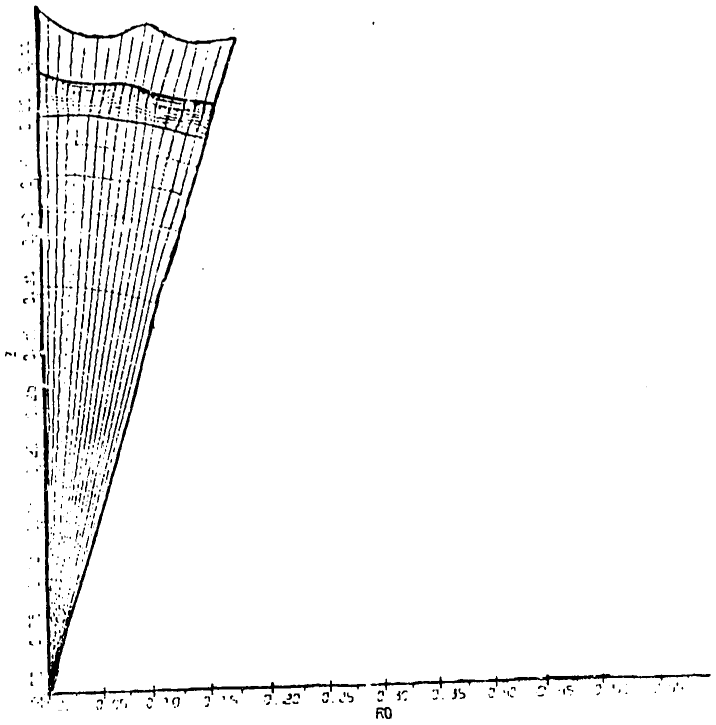

Figure 15

6. In order to study the interaction of different harmonic numbers, let us perform the calculation where disturbances of harmonic 24 and 60 were introduced into the shape simultaneously (see Figure 17). From the figure it is obvious that the disturbances of harmonic 24 only reached the outer boundary. Let us note that in the calculation with disturbances of only harmonic 24 or harmonic 60, the disturbance amplitude at the outer boundary was much less, which indicates the effect of the nonlinear interaction between the disturbances with different wave length.

From Figure 17 it is also obvious that the amplitude of the disturbances of both harmonic 24 and harmonic 60 is approximately identical, although in the linear theory the increment of harmonic 60 is higher. This is connected with the fact that the development of the disturbances takes place in the nonlinear mode, which occurs when the disturbance amplitude increases so much that

$$K\Delta \gg 1 \qquad (4.2)$$

Δ is the disturbance amplitude,

K is the wave number.

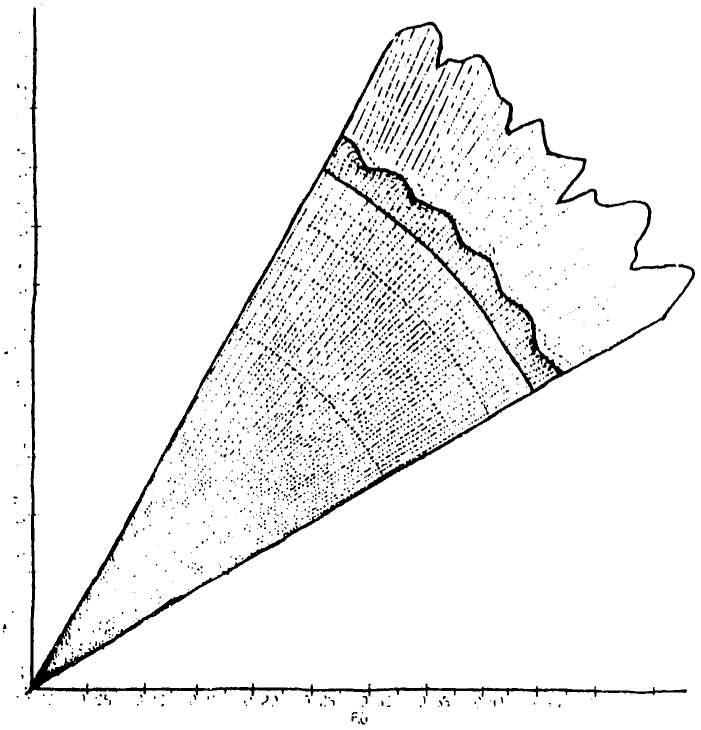

Figure 16

For this mode the growth rate of the disturbances is saturated, and it is approximately identical for all numbers of harmonics.

7. On the whole the instability in the corona is the standard Rayleigh-Taylor instability. The amplitude of the disturbance increases by more than 100 times. The effect of the evaporation and dissipation leads to the fact that the increments of the growth of the disturbances turn out to be somewhat less than the Taylor modes. This is especially felt in the long-wave disturbances which cannot be propagated even to the shell.

The short-wave disturbances penetrate to the cold part of the shell, but the depth of penetration decreases rapidly with an increase in the harmonic number. The harmonics with $n \approx 15$ to 20 can have the strongest influence.

§5. Free Flight Stage

1. In the free flight stage (before the beginning of braking of the shell), almost periodic fluctuations of the inside boundary of the shell occur, the phase of which depends on the time, and the amplitude increases insignificantly (see [9], [33]). The indicated results of the numerical calculation are in

good agreement with the results of the analytical solution of the linearized problem of instability of the spherical boundary of a gas bubble in an incompressible liquid [33]. These fluctuations occur as a result of adiabatic contraction of the surface of the bubble on compression

$$\Delta = \Delta_0 \left(\frac{R}{R_0}\right)^{1/4} \cos(\varphi - \varphi_0)\cos(n\theta) \tag{5.1}$$

From (5.1) it follows that at the time determined from the equation

$$(2K+1)\frac{\tilde{\jmath}i}{2} = \left(\frac{3}{2}\right)^{1/2} n \ln \frac{R_0}{R(t)} \tag{5.2}$$

the inside boundary will be spherical. A comparison of the result of (1)-(2) with the data from the numerical calculation (Figure 18) reveals qualitative agreement.

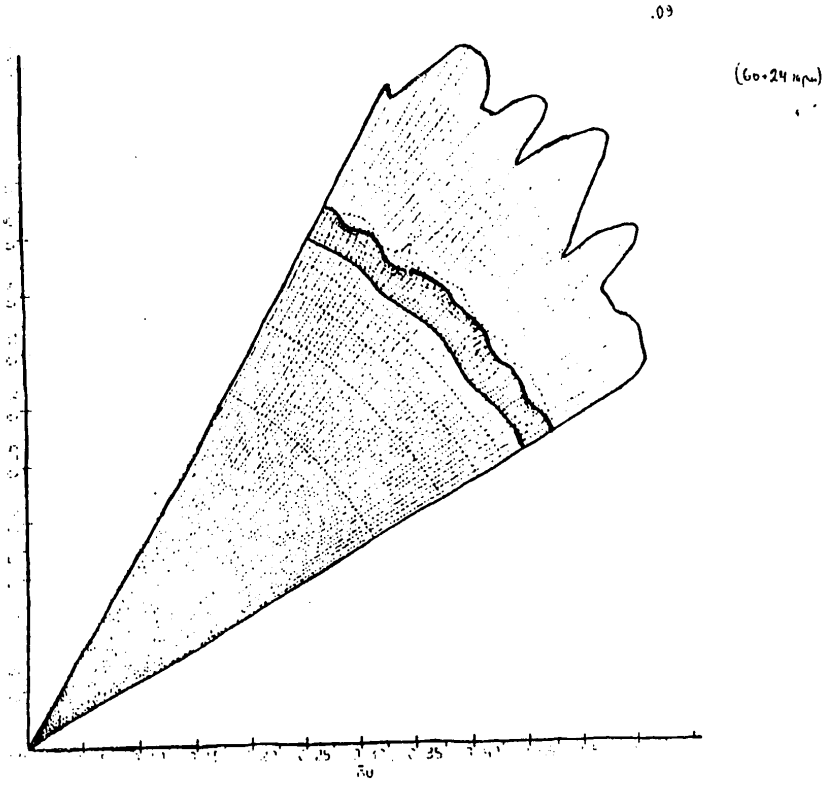

Figure 17

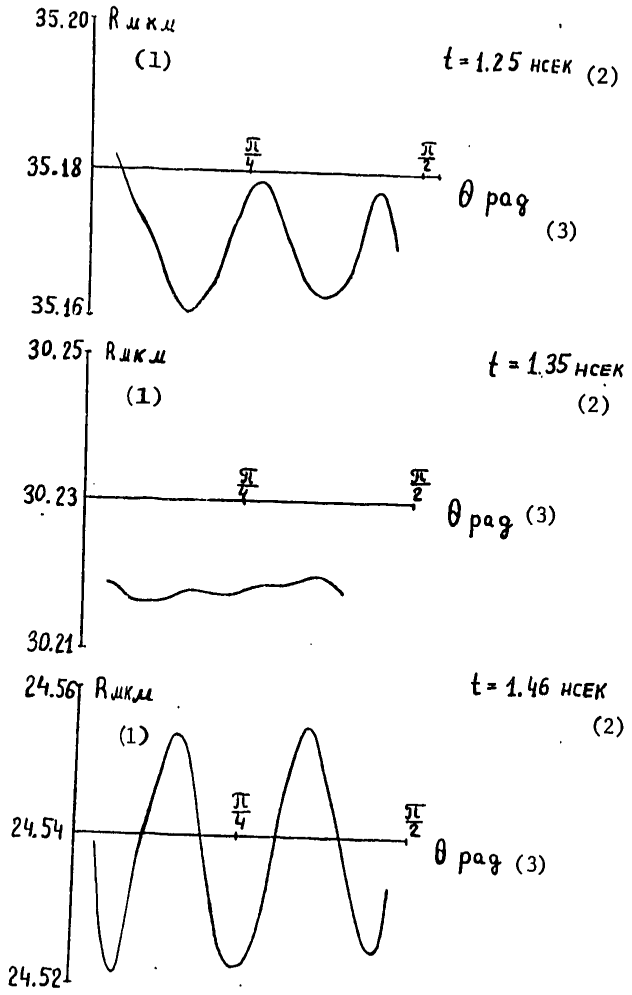

Figure 18

Key:
1. R, microns
2. nanoseconds
3. radians

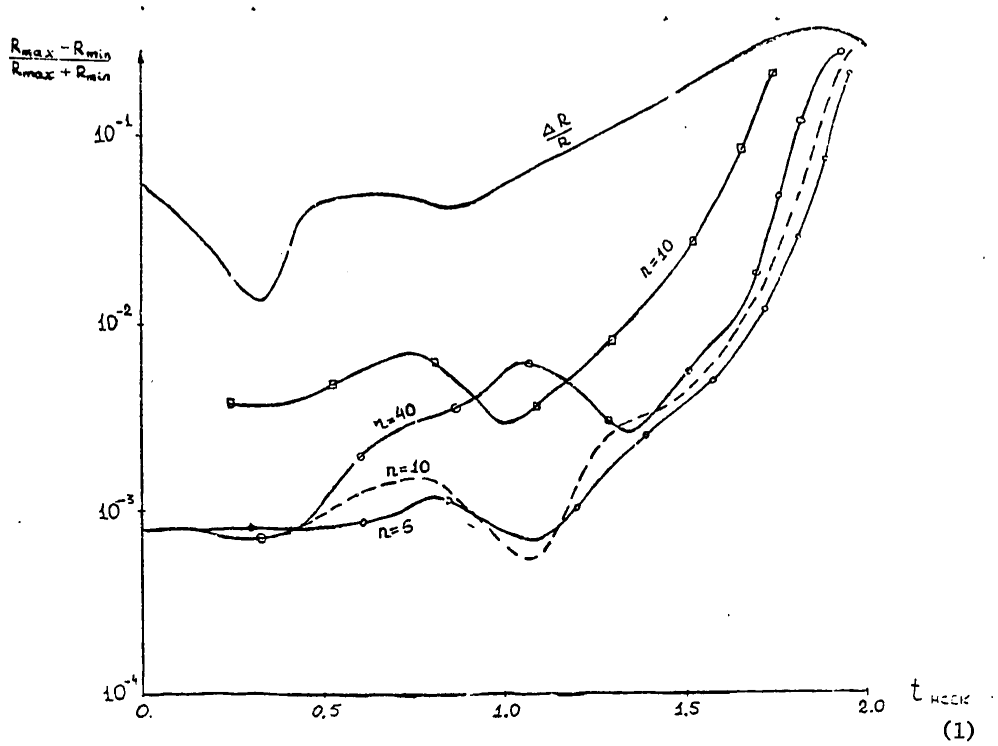

Figure 19

Key:
1. nanoseconds

§6. Instability of the Inside Boundary of the Shell

1. Instability of the inside boundary of the shell occurs when the gas included inside begins to brake the shell. The relative amplitude of the disturbance as a function of time for different harmonic numbers is presented in Figure 19. A comparison with the value calculated by the formula (see [4])

$$\Delta_n = \Delta_{n0} \cdot exp\left\{ \int \frac{n}{4\sqrt{R}} \frac{du}{dt} dt \right\}^{1/2} \qquad (6.1)$$

shows that the low harmonics $n \lesssim 10$ increase approximately with the same rate. For $n>12$ the growth rate becomes less than the Taylor modes, and the harmonics with $n=20$, 40 develop completely in the linear mode. The effect of the "nonlinear saturation" of the disturbance growth rate is especially clearly obvious if the relative amplitude of the disturbance is represented as a function of the harmonic number, taking time as the parameter (Figure 20).

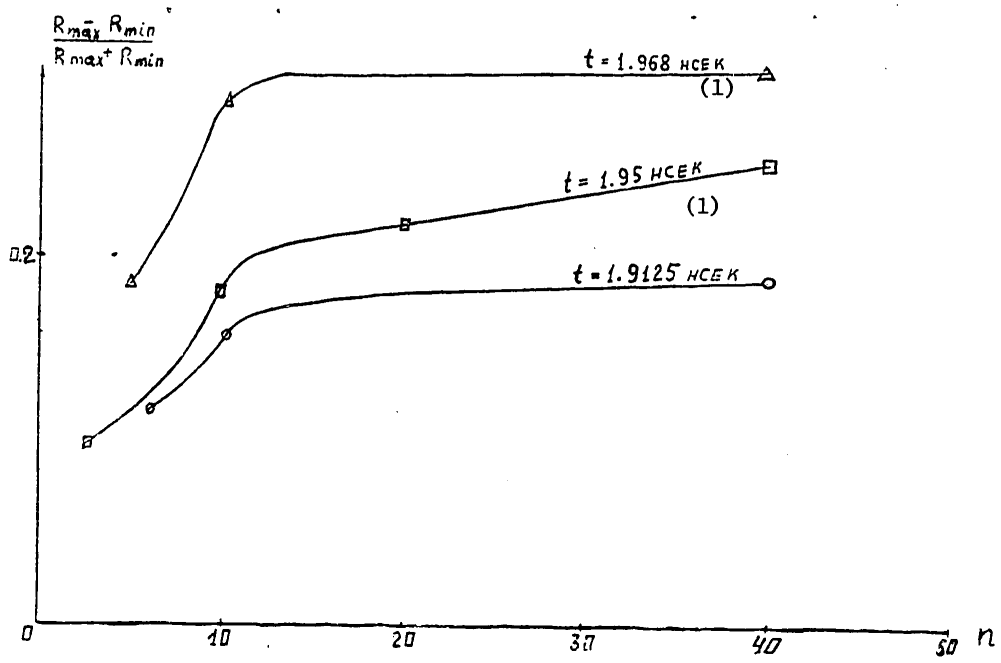

Figure 20

Key:
1. nanoseconds

2. From Figures 19, 20 it is obvious that for harmonic 10 the deviation from linearity occurs only at the last points in time, and for harmonics 20 and 40, the nonlinear mode comes in the earlier stages of motion. Let us note that the exponential growth of the disturbances in the linear mode takes place while

$$\Delta \cdot K \ll 1 \qquad (6.2)$$

Δ is the amplitude of the disturbance,

K is the wave number.

The results of the calculations show that for the initial amplitude of the disturbance $\alpha=0.01$ this condition is violated already for n=10 by the time of maximum compression. Consequently, the saturation of the increment with growth of the wave number is due to the nonlinear effect.

Figure 21

Thus, for the investigated shells with aspect ratio of 20, the maximum disturbance growth rate is achieved for 15-20. The presence of short-wave components in the spectrum of the initial disturbances is not dangerous for the investigated shells.

3. In order to study the effect of the disturbances of the intensity of the energy flux, a calculation was made of a number of versions where disturbances were introduced into the energy flux by the formula

$$q_r = q_0(t)(1 + \alpha \cos n\theta)$$

The disturbance amplitudes α and the harmonic numbers n were varied within various versions.

These calculations demonstrated that the disturbances of the energy flux lead to smaller distortions of the inside boundary than the shape asymmetry. An obvious symmetrizing factor here is the heat conducting equalization in the "corona." Thus, a comparison of the maximum disturbance amplitude on the inside boundary for 1% amplitude of the initial disturbance and the same wave length indicates

that the shaped disturbances lead to amplitudes that are twice as high as the nonuniformity of the fluxes (Figures 21, 22).

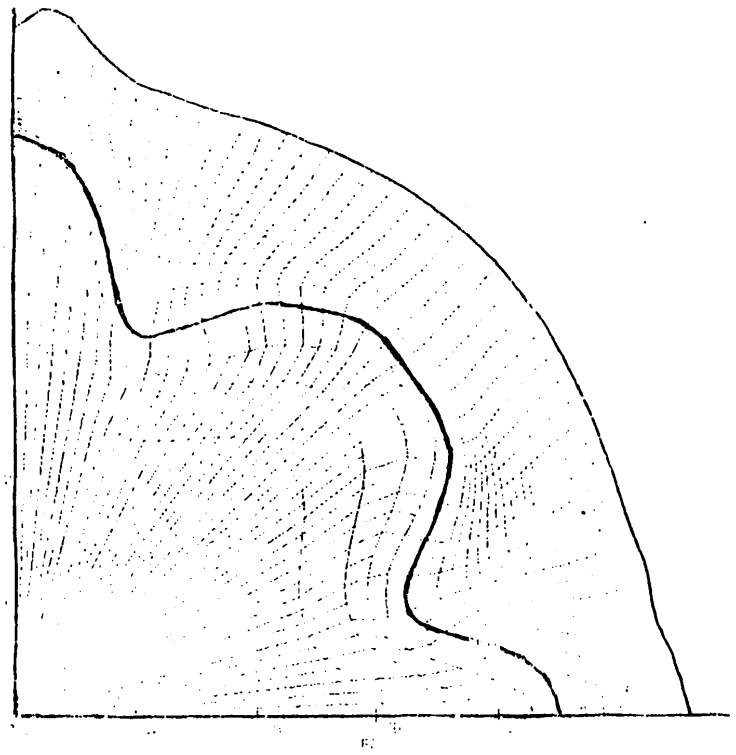

Figure 22

4. Let us discuss what changes in the state of the shell and the gas the instability effect leads to. The relative thickness of the shell in the axisymmetric case increases by approximately 8 times by the time of maximum compression. However, at this time the disturbance amplitude (with initial disturbance amplitude of 1% of the shell thickness) becomes comparable to the thickness. However, this fact still does not mean rupture of the shell. Indeed, from the state of the shell at the time close to the time of maximum compression it is obvious that the Lagrange lines corresponding to the inside boundary of the shell are more strongly distorted than the outside lines (see Figure 10). Thus, a significant magnitude of the disturbance on the inside boundary of the shell indicates that part of the shell material has reached the inner cavity. Let us note that the average density and temperature of the inside gas with respect to the nonspherical volume differ slightly from the corresponding values in the spherical case (Figures 23, 24). However, it is not necessary to attach great significance to this fact, for the penetration of the shell material into the nucleus obviously leads to mixing of the nonperipheral layers of the gas with the shell material and to a decrease in the partial density of the internal gas.

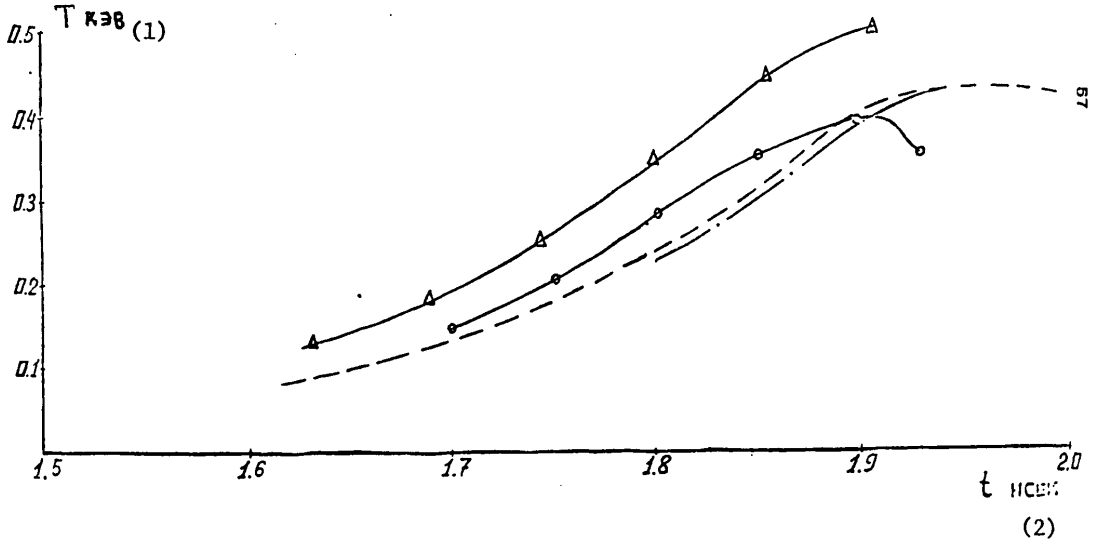

Figure 23

Key:
1. T, kev
2. nanoseconds

In order to estimate the role of the instabilities it is useful to compare the energy of turbulent motion with the kinetic energy of the plasma in the given calculations. The energy dissipated in the turbulent motion per unit time can be estimated (see [34]) as

$$\frac{dE_T}{dt} \approx \frac{\rho v_T^3}{l_T} \tag{6.3}$$

here

$v_T=\gamma l_T$ is the characteristic turbulent velocity (see [35]),

l_T is the characteristic scale of the turbulence (in the given case, the maximum amplitude of the disturbances),

γ is the buildup increment of the disturbances.

If the kinetic energy of the plasma

$$E_{кин}^{(1)} = \frac{1}{2}\rho v^2 \tag{6.4}$$

Key: 1. kin

v is the hydrodynamic velocity,

ρ is the gas density,

then

$$\frac{E_T}{E_{KИН}} \underset{(1)}{\sim} \frac{\gamma^3 l_T t_0}{v^2} \qquad (6.5)$$

Key: 1. kin

t_0 is the instability development time.

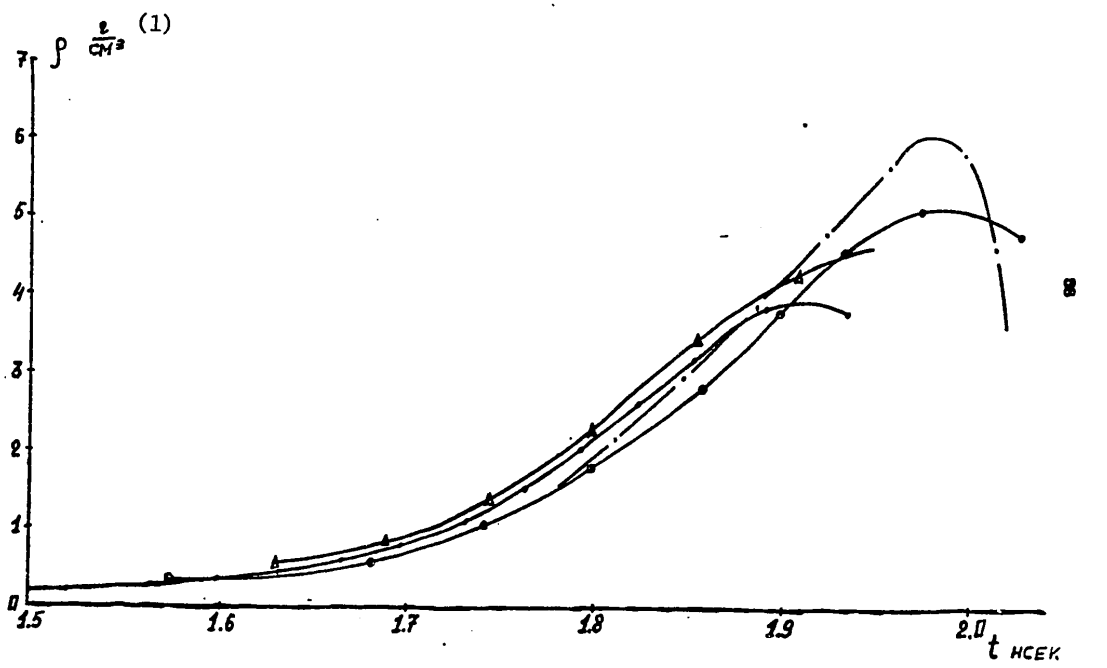

Figure 24

Key:
1. g/cm^3
2. nanoseconds

Defining the values in (6.5) from the calculation, it is possible to obtain that in the given case this ratio reaches 10%.

BIBLIOGRAPHY

1. Afanas'yev, Yu. V.; Basov, N. G.; Volosevich, P. P.; Gamaliy, Ye. G.; Krokhin, O. N.; Kurdyumov, S. P.; Levanov, Ye. I.; Rozanov, V. B.; Samarskiy, A. A.; Tikhonov, A. N. DOKLADY NA U KONFERENTSII PO FIZIKE PLAZMY I UPRAVLYAYEMOMU TERMOYADERNOMU SINTEZU [Reports at the 5th Conference on Plasma Physics and Controlled Nuclear Fusion], November 1974, Tokyo.

2. Afanas'yev, Yu. V.; Basov, N. G.; Volosevich, P. P.; Gamaliy, Ye. G.; Krokhin, O. N.; Kurdyumov, S. P.; Levanov, Ye. I.; Rozanov, V. B.; Samarskiy, A. A.; Tikhonov, A. N. PIS'MA V ZHETF [Letters to the Journal of Experimental and Theoretical Physics], No 21, 1975, p 150.

3. Afanas'yev, Yu. V.; Volosevich, P. P.; Gamaliy, Ye. G.; Krokhin, O. N.; Kurdyumov, S. P.; Levanov, Ye. I.; Rozanov, V. B. PIS'MA V ZHETF, No 23, 1976, p 470.

4. Afanas'yev, Yu. V.; Basov, N. G.; Gamaliy, Ye. G.; Krokhin, O. N.; Rozanov, V. B.; PIS'MA V ZHETF, No 23, 1976, p 617.

5. Afanas'yev, Yu. V.; Gamaliy, Ye. G.; Krokhin, O. N.; Rozanov, V. B.; KRATKIYE SOOBSHCHENIYA PO FIZIKE, FIAN [Brief Reports on Physics of the Physics Institute of the USSR Academy of Sciences], 1975.

6. Basov, N. G.; Kologrivov, A. A.; Krokhin, O. N.; Rupasov, A. A.; Sklikov, G. V.; Shikanov, A. S. PIS'MA V ZHETF, No 23, 1976, p 474.

7. Volosevich, N. P.; Gamaliy, Ye. G.; Gulin, A. V.; Rozanov, V. B.; Samarskiy, A. A.; Tyurina, N. N.; Favorskiy, A. P. PIS'MA V ZHETF, No 24, 1976, p 283.

8. Bunatyan, A. A.; Neuvazhayev, V. Ye.; Strontseva, L. G.; Frolov, V. L. PREPRINT IPM AN SSSR [Preprint of the Institute of Applied Mathematics of the USSR Academy of Sciences], No 71, 1975.

9. Afanas'yev, Yu. V.; Basov, N. G.; Gamaliy, V. G.; Gasilov, V. A.; Krokhin, O. N.; Lebo, I. G.; Rozanov, V. B.; Samarskiy, A. A.; Tishkin, V. F.; Favorskiy, A. P. PREPRINT FIAN SSSR [Preprint of the Physics Institute of the USSR Academy of Sciences], No 167, 1977.

10. Gamaliy, Ye. G.; Rozanov, V. B.; Samarskiy, A. A., et al. PREPRINT IPM AN SSSR, No 117, 1978.

11. Basov, N. G.; Krokhin, O. N. ZHETF, No 46, 1964, p 171.

12. Basov, N. G.; Krokhin, O. N. VESTNIK AN SSSR [Vestnik of the USSR Academy of Sciences], No 6, 1970, p 55.

13. Volosevich, P. P.; Kurdyumov, S. P.; Levanov, Ye. I. PMTF (Applied Mechanical-Thermal Physics) No 5, 1972, p 41.

14. Volosevich, P. P.; Kurdyumov, S. P.; Levanov, Ye. I. PREPRINT IPM AN SSSR, No 40, 1970.

15. Nuckolls, J.; Wood, L.; Thiessen, A.; Zimmerman, G. "Laser Compression of Matter to Superhigh Densities," PROCEEDINGS IEEE QUANTUM ELECTRONICS CONFERENCE, Montreal, 1972.

16. Zimmerman, G.; Wood, L.; Thiessen, A.; Nuckolls, J. "LASNIX, A General Purpose Laser-Fusion Simulation Code," PROCEEDINGS IEEE QUANTUM ELECTRONICS CONFERENCE, Montreal, 1972.

17. Thiessen, A.; Nuckolls, J.; Zimmerman, G.; Wood, L. "Computer Calculation of Laser Implosion of DT to Super-High Densities," PROCEEDINGS IEEE QUANTUM ELECTRONICS CONFERENCE, Montreal, 1972.

18. Wood, L.; Nuckolls, J.; Thiessen, A.; Zimmerman, G. "The Super-High Density Approach to Laser-Fusion CTR," PROCEEDINGS IEEE QUANTUM ELECTRONICS CONFERENCE, Montreal, 1972.

19. Volosevich, P. P.; Degtyarev, L. M.; Levanov, Ye. I.; Kurdyumov, S. P.; Popov, Yu. P.; Samarskiy, A. A.; Favorskiy, A. P. FIZIKA PLAZMY [Plasma Physics], Vol 2, No 6, 1976, p 883.

20. Book, D. L.; Ott, E.; Sutoh, A. L. PHYS. FLUIDS, No 19, 1974, p 676.

21. Ott, E. PHYS. REV. LETT., No 29, 1972, p 1429.

22. Bashilov, Yu. V.; Pokrovskiy, S. V. PIS'MA V ZHETF, Vol 23, No 8, p 462.

23. Taylor, G.I. PROC. R. SOC., London, A201, 1950, p 192.

24. Davies, R. M.; Taylor, G. I. PROC. R. SOC., London, A200, 1950, p 375.

25. Frieman, E. A. ASTROPHYS. J., No 8, 1954, p 120.

26. Layzer, D. ASTROPHYS. J., No 1, 1955, p 122.

27. Birkhoff, G.; Carter, D. J. MATH. MECH., No 6, 1957, p 769.

28. Chang, G. T. PHYS. FLUIDS, No 2, 1959, p 656.

29. Chandrecekhar, S. HYDRODYNAMIC AND HYDROMAGNETIC STABILITY, Clarendon Press, Oxford, 1961.

30. Gasilov, V. A.; Goloviznin, V. M.; Tishkin, V. F.; Favorskiy, A. P. PREPRINT IPM AN SSSR, No 119, 1977.

31. Mead, W. C.; Lindl, J. D. University of California. Preprint No UCRL-77057, 1975.

32. Volosevich, P. P.; Gamaliy, Ye. G.; Gasilov, V. A.; Tishkin, V. F. PREPRINT IPM AN SSSR, No 24, 1978.

33. Gamaliy, Ye. G. KRATKIYE SOOBSHCHENIYA PO FIZIKE, FIAN, No 5, 1976, p 23.

34. Landau, L. D.; Lifshits, Ye. M. MEKHANIKA SPLOSHNYKH SRED [Mechanics of Continuous Media], Costekhizdat, Moscow, 1954.

35. Belen'kiy, S. Z.; Fradkin, Ye. S. TRUDY FIAN [Works of the Physics Institute of the USSR Academy of Sciences], No 29, 1965.

36. Bokov, N. N.; Bunatyan, A. A.; Lykov, V. A.; Neuvazhayev, V. V.; Stroptseva, A. P.; Frolov, V. D. PIS'MA V ZHETF, Vol 26, No 9, 1977, p 630.

37. Goloviznin, V. M.; Tishkin, V. F.; Favorskiy, A. P. PREPRINT IPM AN SSSR, No 16, 1977.

38. Garabedian. PROC. R. SOC. LONDON, A241, 1957, p 423.

UDC 532.5; 519.6

MATHEMATICAL MODELS OF THE FORMATION OF TORNADOES AS A RESULT OF THE DEVELOPMENT OF GAS DYNAMIC INSTABILITIES

[N. M. Zuyeva, V. V. Paleychik, L. S. Solov'yev, pp 65-105]

A study is made of the development in time of axisymmetric convective and helical instabilities of an ideal gas. By numerical integration of the equations of hydrodynamics it was demonstrated that the development of the instability can serve as the mechanism of generation of high angular velocities of the gas. A study is made of the effect of the variation of the parameters of the initial steady-state on the specifics of the process dynamics.

Introduction

If it is assumed that the rotating formations of the atmosphere such as tornadoes arise as a result of the development of gas dynamic instabilities, then, in particular, convective instability caused by the growth of entropy in the vertical direction, Rayleigh instability connected with a decrease in the rotational moment with respect to radius and helical instability caused by a decrease in vertical velocity along the radius can be possible.

Each of these three problems can be formulated as the problem of development of an instability in the one-dimensional equilibrium configuration having axial symmetry. If we limit ourselves to the investigation of axisymmetric motions in the first two cases and helical motion in the third case, the problem of the development of instability reduces to a two-dimensional problem for all three cases.

In the investigated mathematical models it is assumed that during the development of the instability it is possible to neglect all of the dissipative processes and the thermal conductivity and consider the gas to be ideal. In the initial equilibrium state the investigated volume of the gas is assumed to be included within an impermeable cylindrical cavity. In this case the problem reduces to the solution of the equations of Euler motion with boundary conditions of vanishing of the normal velocity component. The time problem of the development of an instability is solved on a computer with assignment of the two-dimensional initial disturbance. As a result of the development of the instability, the initial equilibrium configuration becomes a "quasi-steady" configuration characterized by concentration of the rotational moment and the presence of meridional motion.

Chapter I. Axisymmetric Instability

§1. Statement of the Problem

Under the assumption of axial symmetry, the equations of motion of an ideal gas in the gravitational field $-g\vec{e}_z$ is described in the form [1]

$$\frac{\partial \rho}{\partial t}+\operatorname{div}\rho\vec{v}=0,\quad \frac{\partial N}{\partial t}+\vec{v}\nabla N=0,\quad \frac{\partial I}{\partial t}+\vec{v}\nabla I=0, \tag{1}$$

$$\frac{\partial v_r}{\partial t}+\vec{v}\nabla v_r=-\frac{1}{\rho}\frac{\partial p}{\partial r}+\frac{v_\varphi^2}{r},\quad \frac{\partial v_z}{\partial t}+\vec{v}\nabla v_z=-\frac{1}{\rho}\frac{\partial p}{\partial z}-g$$

where ρ is the density, p is pressure, $\vec{v}$ is velocity, $N=p\rho^{-\gamma}$, $I=rv_\varphi$,

$$\vec{v}\nabla=v_r\frac{\partial}{\partial r}+v_z\frac{\partial}{\partial z},\quad \operatorname{div}\rho\vec{v}=\frac{1}{r}\frac{\partial}{\partial r}\rho r v_r+\frac{\partial}{\partial z}\rho v_z$$

γ is the adiabatic exponent. Obviously, instead of N and I it is possible to use arbitrary functions for them which satisfy the same equations.

When investigating the development of a convective instability, we give the initial vertical equilibrium state, which depends on one constant parameter γ_0 in which the temperature $T=\frac{m}{k}p/\rho$ decreases linearly with respect to z:

$$\frac{\rho}{\rho_0}=\left(\frac{p}{p_0}\right)^{\frac{1}{\gamma_0}},\quad \frac{T}{T_0}=1-\frac{\gamma_0-1}{\gamma_0}\frac{\rho_0 g}{p_0}z,\quad \frac{p}{p_0}=\left(\frac{T}{T_0}\right)^{\frac{\gamma_0}{\gamma_0-1}} \tag{2}$$

This equilibrium is unstable if $\gamma_0>\gamma$. If we take the density ρ_0 as one and the speed of sound $c_0=\sqrt{\gamma p_0/\rho_0}$, then the initial density and pressure distributions will be

$$\rho=\left[1-\left(1-\frac{1}{\gamma_0}\right)\frac{\rho g}{p_0}z\right]^{\frac{1}{\gamma_0-1}},\quad p=\frac{\rho^{\gamma_0}}{\gamma} \tag{3}$$

As the boundary conditions let us take that v_n vanishes at the boundaries r=a and z=c; b, from which it follows that N=const for z=0, b, I=const for r=a.

For investigation of the development of the Rayleigh instability it is possible to give the rotational velocity in the form

$$v_\varphi=v_0 z\left[1+\alpha z^{2n}-(1+\alpha)z^{2n}\right] \tag{4}$$

In this case $v_\varphi=0$ for r=a=1, and for specially large n it is characterized by one parameter γ. If we neglect the gravitational force g and assume the entropy to be constant, that is, $p=\rho^{\gamma_0}/\gamma$, then the equilibrium density distribution corresponding to (4) will be

$$\rho^{\frac{1}{\gamma_0-1}}=\frac{\gamma_0-1}{\gamma}\frac{v_0^2 z^2}{2}\left[1+\alpha z^{2n}+\frac{\alpha^2 z^{4n}}{3}+(1+\alpha)^2\frac{z^{4n}}{2n+1}-2(1+\alpha)\left(\frac{z^{2n}}{n+1}+\alpha\frac{z^{4n}}{3n+1}\right)\right] \tag{5}$$

The initial velocity disturbance satisfying the boundary conditions $v_n=0$ and the equation div $\vec{v}=0$ will be given in the form

$$v_r=\frac{1}{r}\frac{\partial\psi}{\partial z},\quad v_z=-\frac{1}{r}\frac{\partial\psi}{\partial r},\quad \psi=\lambda r^2\left(1-\frac{r^2}{a^2}\right)\sin\frac{\pi z}{b}. \tag{6}$$

The parameter λ characterizes the velocity disturbance amplitude. The current lines Ψ=const are shown in Figure 5a.

In the problem of convective instability the initial rotation is considered as a disturbance. If we set $a_0=1$, then the problem will contain two dimensionless parameters $b=b_0/a_0$ and g. Here if we take the dimensionless values for the speed of sound $c_0=340$ m/sec and the gravitational acceleration $g_0=10$ m/sec, the dimensionless unit of time will correspond to the interval $\Delta t_0=34$ g sec, and the cylinder radius $a_0=11.6$ g km, where g is the dimensionless parameter of the problem.

§2. Conservation Laws and Energy of Instabilities

Under the adopted boundary condition the system of equations of motion (1) contains the laws of conservation of mass, energy, entropy and angular momentum

$$\langle\rho\rangle=\text{Const},\ \left\langle\frac{p}{\gamma-1}\right\rangle+\langle\rho g z\rangle+\left\langle\frac{\rho v^2}{2}\right\rangle=\text{Const},\ \langle\rho N\rangle=\text{Const},\ \langle\rho I\rangle=\text{Const} \tag{7}$$

The angular brackets indicate averaging with respect to the volume $V=\pi a^2 b$.

The development of the instabilities is characterized by the growth of the kinetic energy of the instability

$$W_\perp=\frac{V}{2}\langle\rho v_\perp^2\rangle=\frac{V}{2}\langle\rho(v_r^2+v_z^2)\rangle,$$

where, as the results of the numerical calculation show, the curve $W_\perp(t)$ has a maximum, that is, the growth of $W_\perp$ is limited. A contribution to the energy of the instability $W_\perp$ can be made by the thermal energy $W_T=V\left\langle\frac{p}{\gamma-1}\right\rangle$, gravitational energy $W_g=V\langle\rho gz\rangle$ and rotational energy $W_\varepsilon=V\langle\rho v^2\phi/2\rangle$.

Here we shall present some restrictions on the maximum possible consumptions of potential energy $W_m=W_T+W_g+W_\phi$ following from the conservation laws (7).

From the conservation of mass and entropy we have the conservation law $\langle p^{1/\gamma}\rangle$=const, by using which it is possible to obtain the limit on the thermal energy flow rate [2]

$$-\delta W_T\leq\frac{V}{\gamma-1}\left(\langle p\rangle-\langle p^{1/\gamma}\rangle^\gamma\right)_0, \tag{8}$$

defined by the initial distribution of the pressure p. Hence, for the equilibrium distribution (3) we obtain [3]

$$-\delta W_T \leq \frac{V}{\gamma-1}\frac{1}{\gamma}\left\{\frac{n}{8g}\frac{1-(1-4g/n)^{n+1}}{n+1}-\left[\frac{n}{8g}\frac{1-(1-4g/n)^{n+1/2}}{n+1/2}\right]^2\right\}, \tag{8a}$$

where $n=\gamma_0/(\gamma_0-1)$. For $V=\pi$, $\gamma=3/2$, $\gamma_0=2$, $g=1$ the inequality $-\delta W_T\leq 0.116$ is valid. For small g we have $-\delta W_T \approx Vg^2/24$. In order to obtain the dimensionless formula, the righthand side of the expression (8a) must be multiplied by $\rho_0 c_0^2$ and in it it is necessary to replace g by $g_0 b_0/c_0^2$.

If we neglect the variation of the density ρ, the gravitational energy does not change, but the law of conservation of angular momentum leads to the following restriction on the rotational energy consumption

$$-\delta W_\varphi \leq \frac{V}{2}\left(\langle\rho z v_\varphi^2\rangle - \frac{\langle\rho z v_\varphi\rangle^2}{\langle\rho z\rangle}\right)_0 \tag{9}$$

Hence, for the equilibrium distribution (4) when $n\gg 1$, in the case of $\rho=$const, we obtain

$$-\frac{\delta W_\phi}{W_{\phi_0}} \leq \frac{\alpha^2}{36}\Big/\left(\frac{\alpha^2}{4}+\frac{2\alpha}{3}+\frac{1}{2}\right) \tag{9a}$$

Consequently, for a parabolically decreasing angular rotational velocity $v_\phi=v_\phi/r$, ($\alpha=-1$): $-\delta W_\phi/W_{\phi 0}\leq 1/3$, and for parabolically increasing ($\alpha=1$): $-\delta W_\phi/W_{\phi 0}\leq 1/51$. In the case of uniform rotation $v_\phi=$const, the formula (9) gives $-\delta W_\phi\leq 0$, that is, in this case the rotational energy can only increase so that the uniform rotation is the stabilizing factor.

§3. Steady-State Axisymmetric Configuration

Under the assumption of axial symmetry $\partial/\partial\phi=0$, and under the condition of stationarity $\partial/\partial t=0$, the meridional velocity components are determined by the current function $\phi(r, z)$:

$$v_z = \frac{1}{\rho r}\frac{\partial\psi}{\partial r}, \quad v_r = \frac{1}{\rho r}\frac{\partial\psi}{\partial z}, \tag{10}$$

there are three integrals of motion

$$S=S(\psi), \quad rv_\varphi = I(\psi), \quad \frac{\gamma}{\gamma-1}\frac{p}{\rho}+\frac{v^2}{2}+gz = U(\psi), \tag{11}$$

expressing the constancy of the entropy, the angular momentum and the Bernoulli integral on the current lines $\psi=$const. The function ψ satisfies the equation [4]

$$\frac{\partial}{\partial r}\frac{1}{r^2}\frac{\partial\psi}{\partial r}+\frac{\partial}{\partial z}\frac{1}{r^2}\frac{\partial\psi}{\partial z}+\frac{1}{r^2}\frac{dI^2}{d\psi}=-\rho^{\gamma-1}\frac{dS}{d\psi} \tag{12}$$

[word illegible] arbitrary functions $x(\psi)$, $N(\psi)$ and $v(\psi)$.

Equation (12) is simplified significantly for an incombustible medium

$$[\text{illegible}] = \nu \qquad (12a)$$

It is possible to construct the exact solution of (12a) which satisfies the boundary condition $\phi=0$ for $r=a$ and $z=0$; b. actually setting [formula illegible], v=const, we obtain the linear equation with separated constants, the solution of which

$$[\text{illegible}]\, J_1\left(\frac{x_{11} r}{a}\right) \sin\frac{\pi z}{b}, \quad c^2 = \frac{x_{11}^2}{a^2} + \frac{\pi^2}{b^2}, \qquad (13)$$

[illegible formula] is the first root of the Bessel function $J_1(x)$, and v_2 is the peak value of $v_z = v_z(0, b/2)$. Here the azimuthal velocity and the pressure distribution are defined by the formulas

$$[\text{illegible}]\; p + \frac{\varepsilon^2 \psi'^2}{2 r^2} + \frac{(\nabla \psi')^2}{2 r^2} + gz = \mathrm{Const} \qquad (14)$$

The solution obtained is characterized by proportionality of the maximum values of the angular rotational velocity ν_0 and the vertical velocity v_0 at the point $\eta=0$, $z=b/2$:

$$\nu_0 = \frac{1}{2}\sqrt{\frac{x_{11}^2}{a^2} + \frac{\pi^2}{b^2}}\, v_0 \qquad (15)$$

The angular velocity distribution $\nu_\phi(r)$ and the pressure distribution $p(r)$ for z=b/2

$$\nu_\varphi = 2\nu_0 \frac{J_1(x_{11} r/a)}{x_{11} r/a}, \quad p = p_0 + \frac{v_0^2}{2}\left[[\text{illegible}] \right] \qquad (16)$$

are presented in Figure 1 for a=b=1, $v_0=1$, $p_0=5$.

§4. Linear Theory

In the simplest case a tornado is an axisymmetric steady-state configuration. Our problem is investigation of the process of formation of this configuration from the initial steady-state configuration without meridional velocity as a result of the development of the instability. The linear theory of the instability of the rotating configuration is a quite complex problem as a result of the two-dimensionality of the initial configuration. Here we shall discuss two limiting cases -- the problem of stability of the equilibrium configuration with dependence only on z and stability of the steady-state rotating configuration with dependence only on η. In the following section a study is also made of the stability of the two-dimensional steady-state rotating configuration within the framework of the variation problem.

The equations of motion linearized with respect to v_1 (1) [illegible section to the end of p 71 of source].

1. In the case of equilibrium configuration with $\partial/\partial r=0$, the solution of equation (17) has the form

$$\dots J_0(kz), \qquad v_z = F(z) J_1(kz), \tag{19}$$

where

$$\dots, \quad \mathcal{D} = -\frac{1}{\rho} \frac{k^2 \rho' f + \rho\omega^2 f'}{k^2 c^2 - \omega^2} J_0(kz), \tag{20}$$

and f(z) satisfies the equation

$$\dots - \left\{\rho + r\left(\frac{\rho}{k^2 c^2 - \omega^2}\right)' - \frac{k^2 g}{\omega^2} \frac{\rho^\gamma N'}{k^2 c^2 - \omega^2}\right\} f = 0, \tag{21}$$

where $c^2=\gamma p/\rho$, and the boundary conditions $f(0)=f(b)=0$.

Thus, the dependence of the eigenfunctions on r is defined by one parameter $k=\chi_{1\pi}/a$, where $\chi_{1\pi}$ are the roots of $J_1(x)$. From (21) we have the known condition of Schwartzschild stability $N^1>0$ (see [1]).

2. In the case of the rotational configuration with $\partial/\partial z=0$, the solution of (17) has the form

$$\dots v_r = f(r)\cos kz, \qquad v_z = F(z)\sin kz, \tag{22}$$

where

$$\dots, \quad \mathcal{D} = -\frac{1}{\rho z} \frac{k^2 \rho' f + \rho\omega^2 f'}{k^2 c^2 - \omega^2} \cos kz, \tag{23}$$

and f(r) satisfies the condition

$$\dots \left(\frac{\rho c^2}{r^2 c^2 - \omega^2} \frac{f'}{r}\right)' - \left\{\frac{\rho}{r} - \frac{1}{\omega^2}\left[\frac{4\rho V_\varphi^2}{r} + \left(\frac{k^2 c^2 \rho V_\varphi^2}{k^2 c^2 - \omega^2}\right)' \frac{k^2 r \rho V_\varphi^2}{k^2 c^2 - \omega^2}\right]\right\} f = 0 \tag{24}$$

with the boundary conditions $f(0)=f(a)=0$, the parameter $k=\pi m/b$, $m=1,2,3\dots$ From (24) we have the stability condition [4]

$$\dots \rho r^2 v_r^2)' - \rho r v_\varphi^4 / c^2 > 0, \tag{25}$$

which, considering the equilibrium equation it is possible, analogously to the preceding case, to write in terms of the "frozen functions" $I=rv_\phi$ and $K=N^{-1/\gamma}$ $=\rho p^{-1/\gamma}$ in the form $(I^2K)^1>0$. In the case of constant entropy $K=0$, and also for an incompressible liquid $\gamma\to\infty$, the stability condition becomes the Rayleigh number $(I^2)'>0$.

3. In conclusion, let us construct the class of stable rotating configurations localized in space. Let us represent the condition of stability (25) in the form

$$[z^3(\rho^{1-1/\gamma})']'>0 \tag{25a}$$

and let us set

$$z^4\frac{d}{dz^2}\rho^{1-1/\gamma}=\varepsilon\ln(1+z^2), \tag{26}$$

where $\varepsilon>0$ is the stability index equal to $\varepsilon=(1-1/\gamma)\rho_0 v_0^2/2$, where the characteristic scale of the pressure variation $p(r)$ is taken as the unit length. For $p_0=1$, $\rho_0=\gamma$, according to (26) and the equation of equilibrium $p'=\rho r v_\phi^2$, we obtain the distributions $v_\phi^2(r)$ and $p(r)$ in the form

$$v_\phi^2=v^2\frac{\gamma\rho^{1/\gamma}}{\rho}\frac{\ln(1+z^2)}{z^4}$$

$$\rho=\begin{cases}\left[1+\frac{\gamma-1}{2}v^2\left(2\operatorname{arctg}z^2-\frac{\ln(1+z^4)}{z^2}\right)\right]^{\frac{\gamma}{\gamma-1}}, & \gamma\neq 1,\\ \exp\left[\frac{v^2}{2}\left(2\operatorname{arctg}z^2-\frac{\ln(1+z^4)}{z^2}\right)\right], & \gamma=1,\end{cases} \tag{27}$$

where $\rho(r)$ is an arbitrary function. In the obtained class of one-dimensional configurations which depends on one dimensionless parameter v, with an increase in v, the stability increases, the depth of the hole increases $p(r)$, and its radial dimension decreases. If the characteristic radius of the configuration r_0 is dimensionless and R is dimensional, then the dimensional angular velocity of rotation in the center $v_0=vc_0r_0/R$, $c_0^2=\gamma p_0/\rho_0$.

In Figure 2 we have the stable equilibrium distributions of $v_\phi(r)$, $p(r)$ described by formulas (27) for $\rho=3/2$, $\gamma=3/2$, 1 for values of the parameters $v^2=1$, 2. The configurations more concentrated and with greater angular velocity of rotation are more stable.

§5. Variation Principle

For investigation of the stability of steady-state rotating axisymmetric configurations it is convenient to use the expression for the variation of the potential energy $\delta W=\frac{w^2}{2}\int\rho v^2{}_1 dv$. Multiplying equation (17) by $\rho\vec{v}_\phi$ and integrating over the volume V, we obtain

$$\delta W=\frac{1}{2}\int\left[\delta p\left(\frac{\delta\rho}{\gamma\rho}-\frac{\delta p}{\gamma p}\right)-\frac{\vec{F}_0}{\rho}\vec{\nabla}N+\frac{\rho v_\phi^2}{2r^2}(\vec{r}\nabla\xi)\right]dv \tag{28}$$

Minimization with respect to $\delta\rho$: $\delta\rho=\rho^2$ gives

$$\delta\rho=-(\xi\nabla\rho)/\gamma p,$$

$$\delta W=\frac{1}{2}\int\left[-\frac{\vec{F}_0}{\rho}\vec{\nabla}N+\frac{\rho v_\phi^2}{2r^2}(\vec{r}\nabla\xi)\right]dv \tag{30}$$

In the limiting cases of one-dimensional equilibrium $\partial/\partial r=0$ and $\partial/\partial z=0$ the dependence of the eigenfunctions on r and on z is known (see (19) and (22)) and equation (29) permits expression of v in terms of v_z or vice versa

$$\kappa F(z) = -\frac{(\rho_0 \gamma_0 p_0)'}{\rho_0 \gamma_0}; \qquad \kappa f(z) = -\frac{(\rho_0 \gamma_0 p_0)'}{2\rho \gamma p} \tag{31}$$

Substituting (31) in (30), we obtain the variation expressions for the minimum square frequency ω^2 for both limiting cases

$$\omega^2 = \frac{\int \rho_0 \gamma_0 p_0 f^2 dz}{\int \left\{ f^2 \left(\frac{\rho_0 \gamma_0 p_0}{\kappa^2 \rho_0 \gamma_0} \right)' \right\} dz}, \qquad \omega^2 = \frac{\int \rho_0 \gamma_0 p_0 \left(\frac{f^2}{r^2} \right)' r^3 dr}{\int \left\{ f^2 \left(\frac{\rho_0 \gamma_0 p_0}{\kappa^2 \rho_0 \gamma_0} \right)' \right\} r^2 dr} \tag{32}$$

Thus, in the limiting cases the increments in the development of the stability are expressed by the integrals of one function f(z) or f(r).

1. For equilibrium configuration $p=p_0(\rho/\rho_0)^{\gamma_0}$, substituting the first expression of (32) $f(z)=\sin m\pi z/b$, $k=x_{1n}/\alpha$ and for simplicity neglecting the variation of $\rho^{1/\gamma}$, we obtain

$$\omega^2 = \frac{a^2}{c^2} \frac{1-\gamma/\gamma_0}{1+\frac{a^2}{x_{1n}^2 m^2}\frac{a^2}{b^2}}; \tag{33}$$

where x_{1n} are the roots of the Bessel function $(J_1(x)$. The increment in the development of the stability for $\gamma_0>\gamma$ is maximal for the mode m=1 and increases by the dimension n. Thus, the eigenfunctions not having nodes in the "main" direction Z and having a large number of nodes in the secondary direction r have the maximum increments. With an increase in the ratio a/b the dependence of the increment on m and n is intensified.

2. In the case of a rotating configuration let us consider the distribution

$$f = v_0 z^2 (1 - z^2/a^2). \tag{34}$$

Inasmuch as in this case $I'<0$ only when $r^2>a^2/n$, the eigenfunction corresponding to the maximum increment must be localized primarily in the region $r>a\sqrt{2}$. Therefore we shall select the function

$$f(r) = r^{l+1}(1 - r^2/a^2), \qquad l > 1; \tag{35}$$

which corresponds to the basic mode with respect to r and find l from the condition of localization of ω^2. Neglecting $p^{1/\gamma}$ in the second expression of (32) we obtain

$$\omega^2 = \frac{\int (I^2)' \rho f^2 dz}{2\pi \int \left(\frac{I^2}{r^2} \right)' \rho f^2 dz}$$

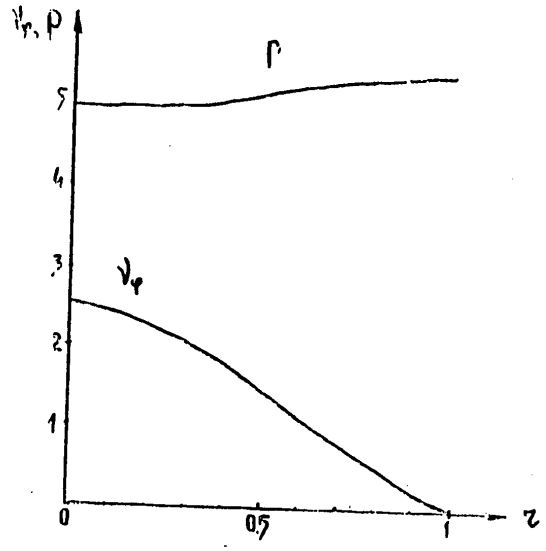

Figure 1

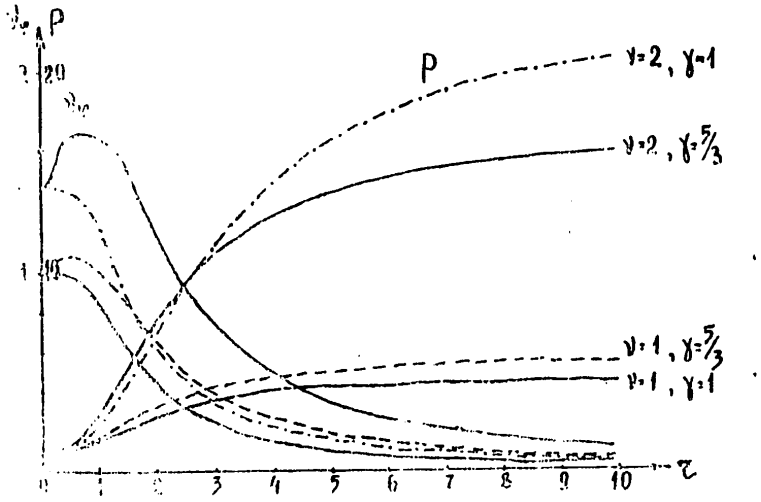

Figure 2

The determination of the integrals for f(r) defining in (35) leads to the following:

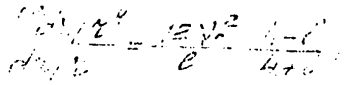

[three words illegible] ℓ gives $\ell=4(1+\sqrt{2})$ [letters illegible].
Thus, setting [formula illegible] and neglecting the variation of ρ, we obtain

$$-\omega^2=-\frac{\nu_0^2/2}{1+\frac{I^2k^2}{m^2q^2}}. \tag{36}$$

By complete analogy with the preceding case of (33), the increments of the basic mode not having nodes along the main direction r increase with an increase in the number of nodes m along the second direction z.

3. In the general case of two-dimensional equilibrium, assuming smallness of the derivatives with respect to z and with respect to r and selecting the dependence of $\vec{v}$ on z in the form of (22) and also setting $\rho\sim\rho^{\gamma_0}$, we obtain

$$-\omega^2=\frac{\frac{q^2}{k^2c^2}\left(1-\frac{\gamma}{\gamma_0}\right)\int f'^2\frac{dz}{z}-\int\frac{(I^2)'}{z^3}f^2dz}{\int\left(f^2+\frac{f'^2}{k^2}\right)\frac{dz}{z}} \tag{37}$$

where $k=m\pi/b$.

a) For the case of uniform rotation $I=\nu_0 r^2$, selecting the trial function $f(r)=rJ_1(x_{1n}r/a)$, we obtain

$$-\omega^2=\frac{\frac{q^2x_{1n}^2b^2}{c^2\pi^2m^2q^2}\left(1-\frac{\gamma}{\gamma_0}\right)-4\nu_0^2}{1+x_{1,1}^2b^2/\pi^2m^2a^2} \tag{38}$$

Thus, the uniform rotation is the stabilizing factor and leads to a sharper increase in the increment with an increase in x_{1n}/m.

b) In the case of destabilizing rotation (34), the use of the test function (35) with $\ell\approx10$ leads to the expression

$$-\omega^2=\frac{(1-\gamma/\gamma_0)q^2/c^2+(m\alpha/\pi b)^2\nu_0^2/2}{1+(m\alpha/\pi b)^2} \tag{39}$$

Consequently, if the convective increment of the development of the stability predominates $(1-\gamma/\gamma_0)g^2/c^2>\nu_0^2/2$, then $-\omega^2$ decreases with the mode number m, and otherwise, $-\omega^2$ increases with m.

§6. Results of the Numerical Calculation

In the simplest statement the problem of the development of a convective instability contains three parameters: the mismatch characteristic $\gamma_0-\gamma$, the size ratio b/a and the gravitational acceleration g.

In order to study the dynamics of the development of a convective instability, determine the role of the above-indicated parameters and also to discover the effect of the initial, uniform rotation on its development, the system of equations of ideal gas dynamics in the cylindrical coordinates (1)

$$\frac{\partial \rho}{\partial t} + \operatorname{div}\rho\vec{v} = 0, \quad \frac{\partial N}{\partial t} + \vec{v}\nabla N = 0, \quad \frac{\partial I}{\partial t} + \vec{v}\nabla I = 0,$$
$$\frac{\partial v_z}{\partial t} + \vec{v}\nabla v_z = -\frac{1}{\rho}\frac{\partial p}{\partial z} + \frac{I^2}{r^3}, \quad \frac{\partial v_r}{\partial t} + \vec{v}\nabla v_r = -\frac{1}{\rho}\frac{\partial p}{\partial r} - g$$

were integrated numerically in the region:

$$0 \le z \le a, \quad a \le r \le b,$$

with the following boundary conditions:

For $z = 0$: $v_z = 0$, $I = 0$, $\partial p/\partial z = 0$, $\partial N/\partial z = 0$
For $z = a$: $v_z = 0$, $I = Const$
For $r = a$: $v_r = 0$, $N = Const$
For $r = b$: $v_r = 0$, $N = Const$

The initial equilibrium state was described by the density and the pressure (3)

$$\rho = [1 - (1 - 1/\gamma_0)\gamma g z]^{\frac{1}{\gamma_0 - 1}}, \quad p = \rho^{\gamma_0},$$

depending only on the coordinate z, that is, the height. The initial velocity disturbance was given in the form $\psi = \lambda r^2(1 - r^2/a^2)\sin \pi z/a$:

$$v_r = -\frac{1}{r}\frac{\partial \psi}{\partial z} = \frac{\pi}{a}\lambda r^2\left(1 - \frac{r^2}{a^2}\right)\cos\frac{\pi z}{a},$$
$$v_z = \frac{1}{r}\frac{\partial \psi}{\partial r} = 2\lambda z\left(1 - \frac{2r^2}{a^2}\right)\sin\frac{\pi z}{a}, \qquad (40)$$
$$v_\varphi = r\omega.$$

the current lines of the meridional velocity Ψ=const are depicted in Figure 5a.

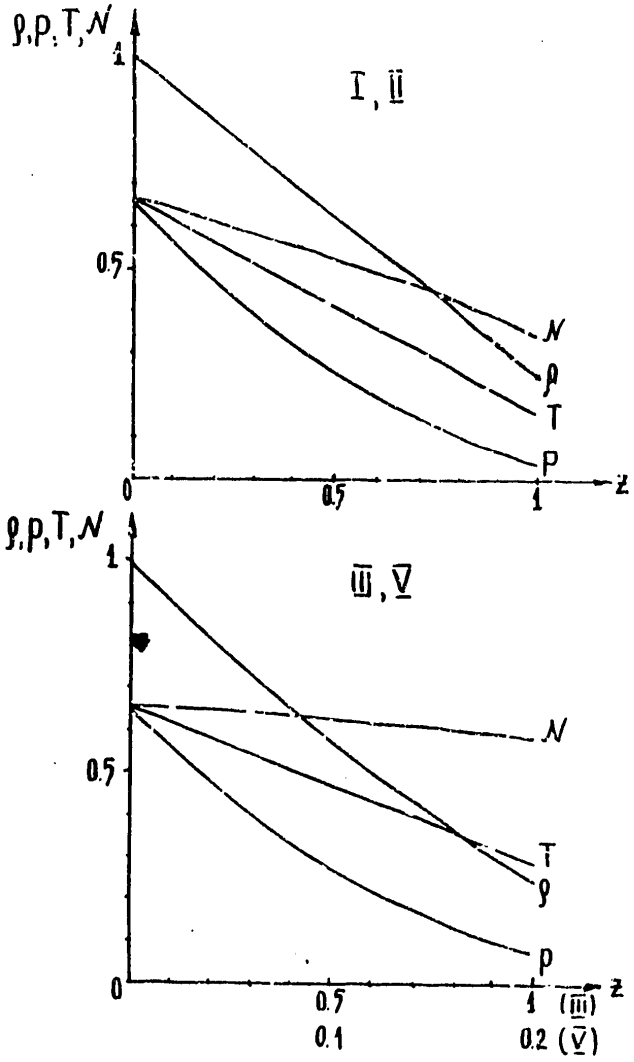

Figure 3

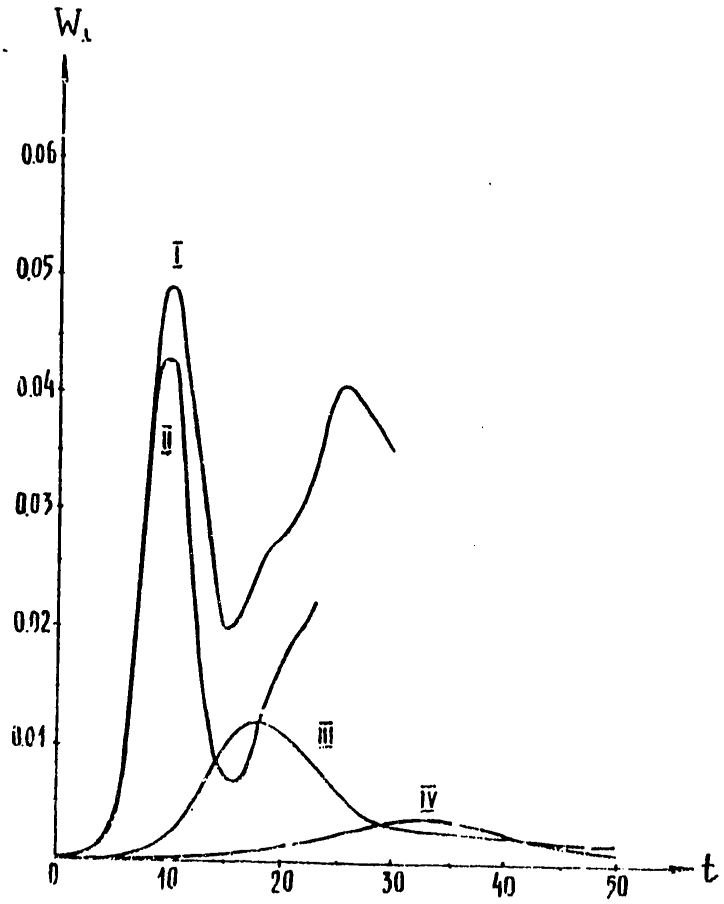

Figure 4a

A series of calculations were performed with the following initial conditions:

Version I $\gamma_0=2;\ \gamma=1.5;\ g=1;\ v_0=0;\ \lambda=-0,01;\ \alpha=1;\ \beta=1$

Version II $\gamma_0=2;\ \gamma=1.5;\ g=1;\ v_0=0,1;\ \lambda=-0,01;\ \alpha=1;\ \beta=1$

Version III $\gamma_0=1,6;\ \gamma=1.5;\ g=1;\ v_0=0.01;\ \lambda=-0,01;\ \alpha=1;\ \beta=1$

Version IV $\gamma_0=1,6;\ \gamma=1.5;\ g=0.5;\ v_0=0.01;\ \lambda=-0,01;\ \alpha=1;\ \beta=1$

Version V $\gamma_0=1,6;\ \gamma=1.5;\ g=5;\ v_0=0;\ \lambda=-0,01;\ \alpha=1;\ \beta=0,2$

The versions I and V were considered without nucleating rotation, and in the remaining versions, it was present.

Figure 3 shows the initial distribution of the values of p, ρ, T, n for versions I, II, III, V. Let us note that in all versions the entropy decreases with height. This indicates that the selected equilibrium state is unstable, for the known condition of absence of convection is reduced to the inequality $dN/dz>0$ (see [1]), that is, the entropy should increase with height.

The results of the calculations are presented in Figures 4-11. Figure 4a shows the variation with time of the kinetic energy of the instability, $W_\perp=(1/2)\int(v_r^2+v_z^2)dV$ for versions I-IV. For all versions an increase in the energy to some maximum value is characteristic, the value of which is determined by the parameters of equilibrium configuration. It is obvious that as $\gamma_0-\gamma$ (IIIc) and g(IVc) decrease, the maximum decreases, which indicates the development of the instability takes place with ever-decreasing rates.

From the energy graph $W_\perp$ for versions I and II it follows that the development of the instability takes place nonmonotonically and that the existence of new peaks with smaller amplitudes is possible.

In Figure 4b a graph is drawn of the variation of the kinetic energy $W_\perp$ for the versions V (b/a=0.2). It is distinguished from the preceding versions by the existence of the second peak, the magnitude of which is greater than the magnitude of the first. This is connected with the peculiarities of the development of the instability in a given version. This will be discussed later.

Figure 4c shows the dependence of the energy of rotation $W_\phi=(1/2)\int v_\theta^2 dV$ for the versions II, III, IV. This energy also increases by comparison with the initial value, just as the energy of the instability $W_\perp$ where their growth is related to each other. The potential energy of the equilibrium system outputs a defined quantity of energy for the development of the instability, which is distributed between $W_\perp$ and W_ϕ.

In Figure 4a I the graph pertains to version I in which there is no rotation, and graph II, to version II differing from I only by the magnitude of the rotation. It is obvious that in the latter case the maximum $W_\perp$ is less, but in this case the energy of rotation W_ϕ has increased (Figure 4a, II).

The growth of the kinetic energy $W_\perp=(1/2)\int(v_r^2+v_z^2)dV$ with development of convective instability indicates an increase in the meridional components v_r and v_z of the velocity. In order to present a picture of the motion of the gas as a whole, the current lines $\Psi(r,z)=$const were constructed where the current function $\Psi(r,z)$ was approximately defined by the formula

$$\Psi(z,z)=\int_0^z \rho z v_z dz, \tag{40}$$

which is valid on neglecting $\partial\rho/\partial t$.

Figure 5a shows the current lines for the initial disturbance, and Figure 5b,c,d the current lines for versions I, II, III at the time corresponding to the middle of the decrease in kinetic energy $W_\perp$. It is obvious that these families of lines are topologically equivalent to each other.

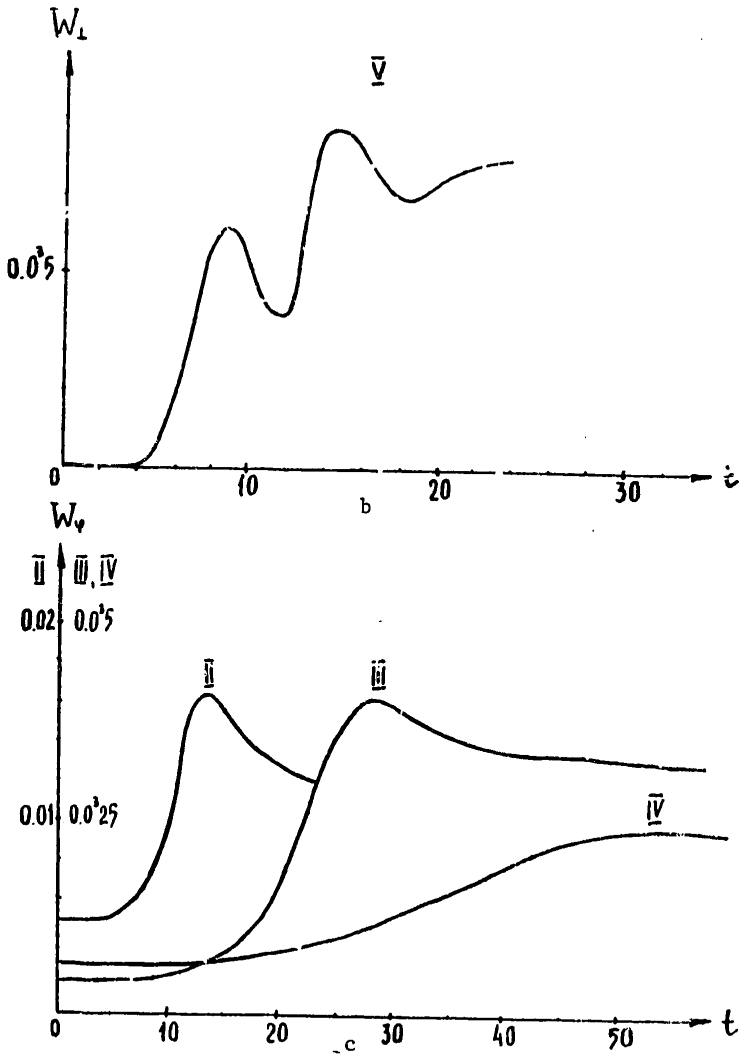

Figure 4 b, c

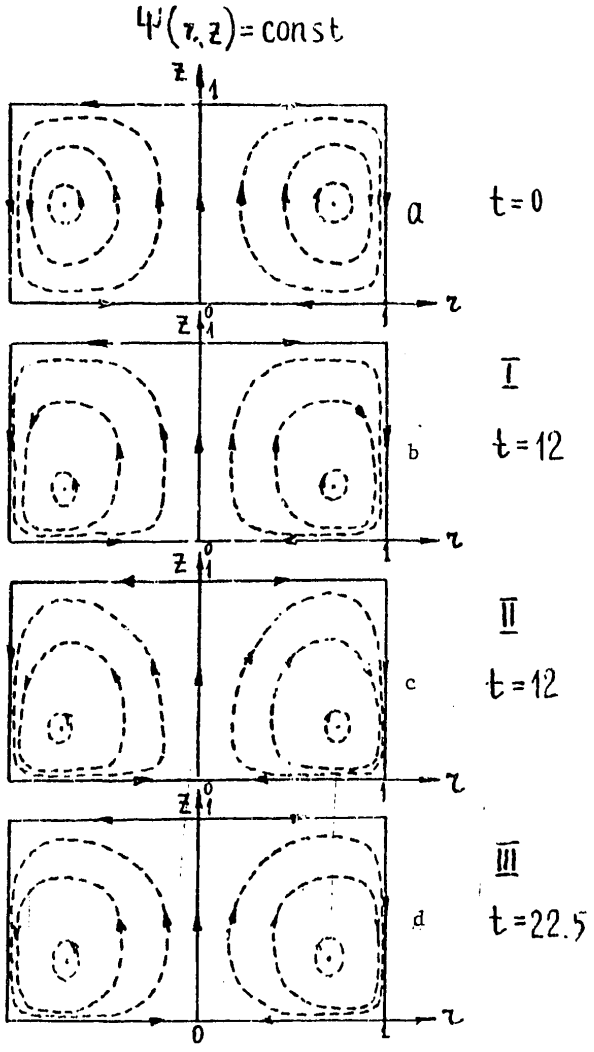

Figure 5 a,b,c,d

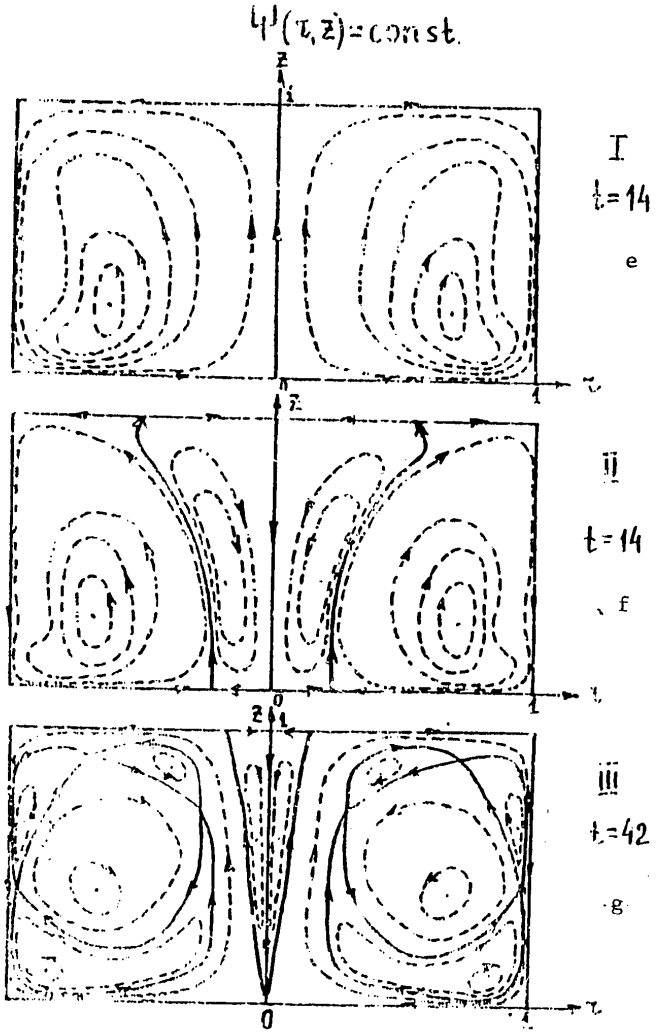

Figure 5 e,f,g

In Figure 5e, f, g, the current lines are constructed for the same versions, but at later points in time. Here the topology of the current lines is different. Difference 1 is manifested in the fact that in versions II and III, a new family of lines has appeared in the vicinity of the axis. This is the rotation effect, and it does not exist in version 1. This is related to the fact that the centrifugal force I^2/r^3 enters into the equation for the v_r velocity component as a term. With an increase in the rotational velocity in the vicinity of the axis this force can become defining, which leads to motion of the material from the axis.

The difference II is that in version III of the time t=41.7 instead of one large vortex, we see several smaller vortexes, which obviously is connected with the development of the higher modes.

The tendency toward formation of such a structure is also to be seen in Figure 5 e,f.

Figure 5a depicts the current lines for version V. In this case a multimodal pattern of the current line is developed in the radial direction in spite of the large-scale nature of the initial disturbance. The process of formation of this structure takes place in several steps, in connection with which the graph of the variationof the kinetic energy has the form differing from the other versions which was discussed (see Figure 4b). The peculiarities of the development of version V are connected with elongation of the investigated region in the radial direction b/a=0.2.

In Figure 5a,b,c,d it is obvious that in the development of convective instability over a sufficiently long time period, unidirectional motion of the substance occurs. Let us consider how the entropy N and the rotational moment I "frozen in the substance" behave in this case, dN/dt=0, dI/dt=0.

Figure 6 shows the evolution of the isentropic surfaces N=const or version II. For version I, III, IV the picture is analogous. Since unstable initial equilibrium configurations are considered, as was noted above, they are characterized by a decrease in entropy with an increase in altitude (Figure 6a).

During the development of the instability, the lower layers with high entropy rise upward and, on the contrary, the upper layers with lower entropy drop downward. A complex mixing process takes place, that is, the system strives to convert to the stable state characterized by an increase in entropy with height.

Figure 7 shows the evolution of the surfaces $I=rv_\phi$=const for version II which is characterized by elongation toward the z axis of the surfaces of the level of rotational moment, which leads to an increase in the rotation rate in its vicinity. This is clearly to be seen in Figure 8 where the profile of the azimuthal velocity v'_ϕ is depicted for z=0 for versions II, III, IV at the times corresponding to the greatest elongation. Let us note that in version III larger azimuthal velocities are achieved in the vicinity of the axis than in version II, in spite of the smaller nucleating rotation. Thus, at the point r=0.025 for version III this velocity is 0.26, and for version II, a total of 0.05.

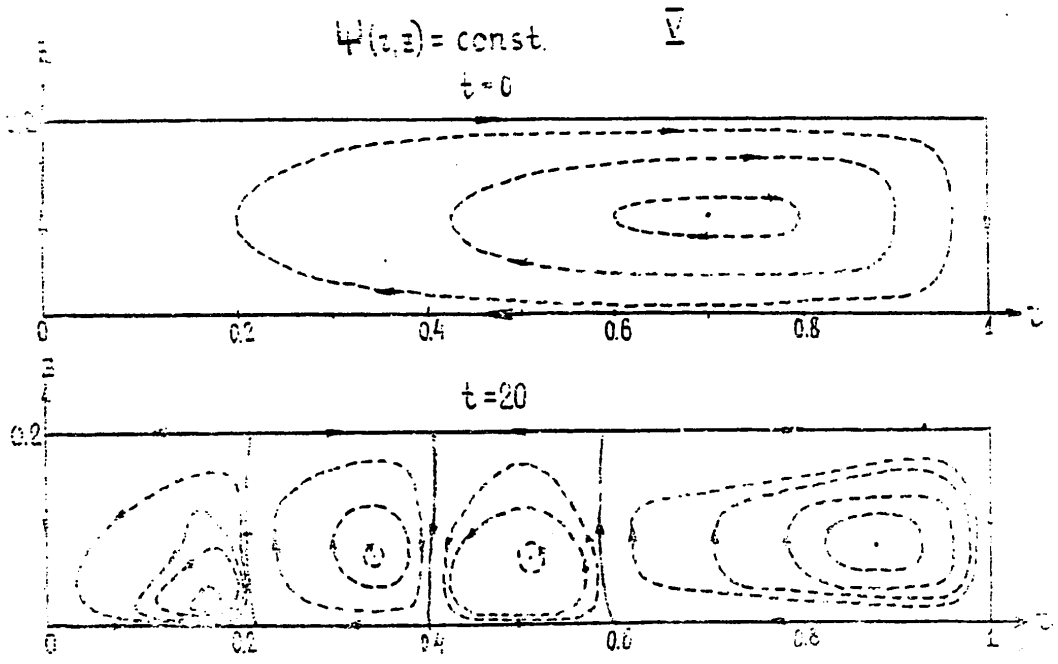

Figure 5h

Figure 9 shows the variation with time of the velocity v_ϕ for the versions II, III and IV at the point z=0, r=0.025.

For all three versions the initial increase in velocity to some value is initial, and then a difference appears in the behavior of v_ϕ.

Thus, in version II it decreases to zero and stays at this value at the same time as in version III it fluctuates near the value of 0.08.

Along with the azimuthal velocity v_ϕ, the behavior of the v_2-component of the velocity on the axis is also of interest. Figure 3 shows the variation of this velocity with time at the point r=0, z=0.5 for versions I-IV. In all versions initially this velocity is positive and increases with time, and then, just as in the case of azimuthal velocity, a difference appears. In version I, v_z remains positive; in versions II and III, it changes sign, and in version IV it fluctuates near zero.

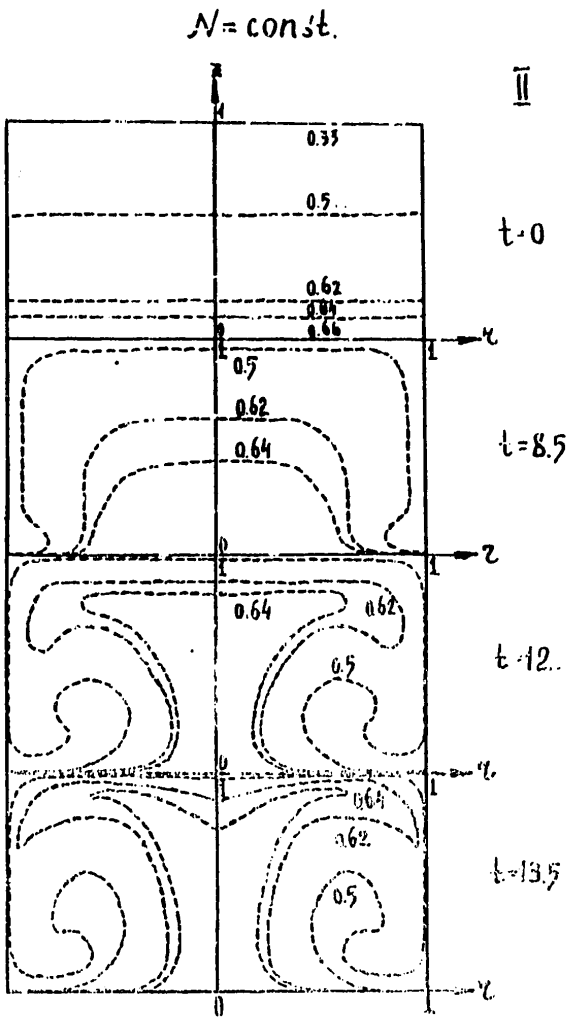

Figure 6

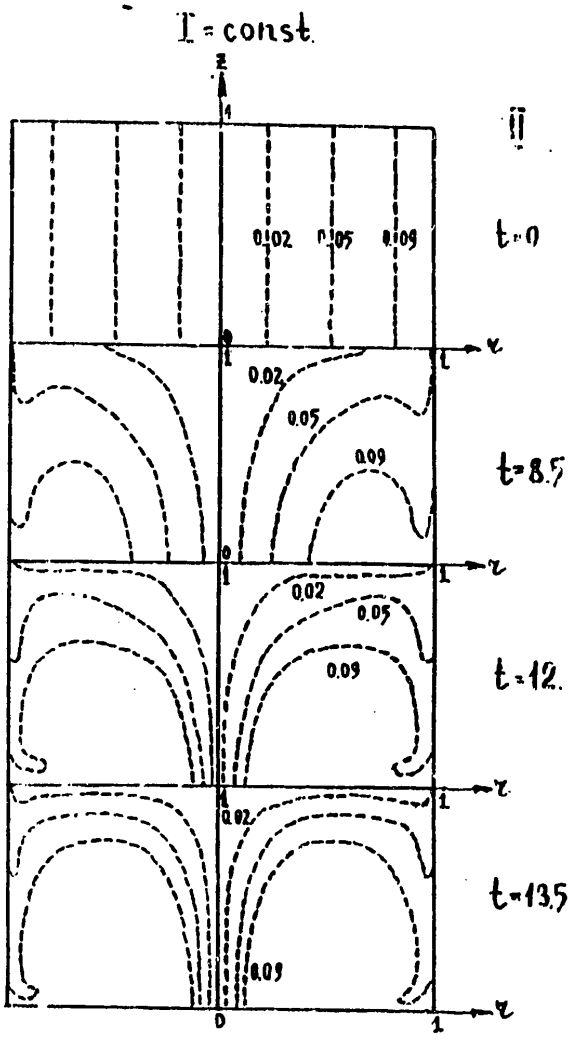

Figure 7

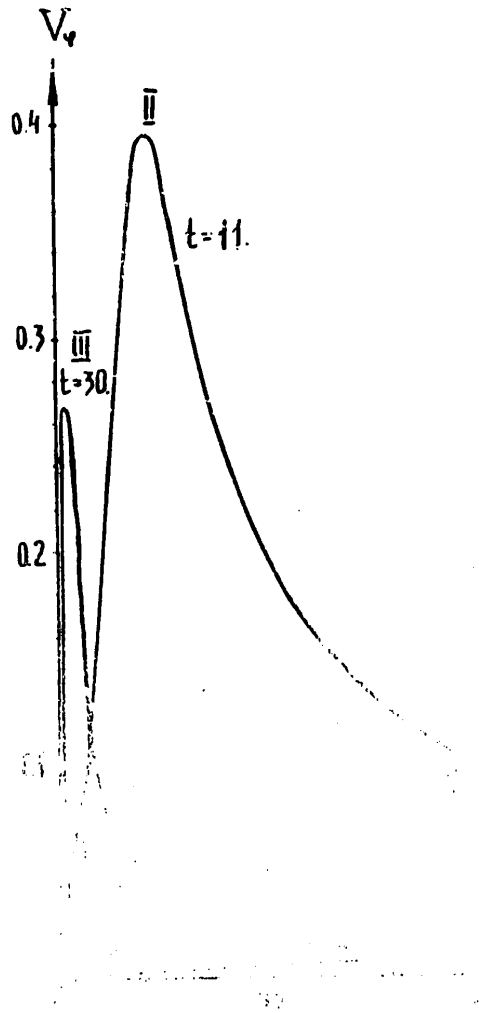

Figure 8

The density profiles of the pressure, temperature and entropy are presented in Figures 11a and 11b for version III at the time t=66.2 for values of z=0.2 and z=0.8, respectively. It is obvious that at z=0.2 the temperature and entropy have decreased, and at z=0.8 they have increased; for z=0.8 the entropy has become larger than for z=0.2. It is possible to note that the profile of all the variables, excluding the vicinity of 0, are almost constant.

Thus, the numerical solution of the nonlinear problem with given initial disturbance leads to the conclusion of the possibility of generation of large angular velocities of rotation as a result of the development of convective instability in the ideal gas. The investigated mechanism is based on the development of an instability of meridional motion which leads to scattering of the rotational moment rv_ϕ to the z-axis from the entire volume where the instability develops. For a sufficiently small ratio a/b in the nonlinear stage, roughly speaking, the main eigenfunction of the linear boundary problem develops, and for large a/b, higher radial modes develop.

The investigated mathematical model obviously permits qualitative explanation of the occurrence of tornadoes in the atmosphere as a result of the difference in convective instability.

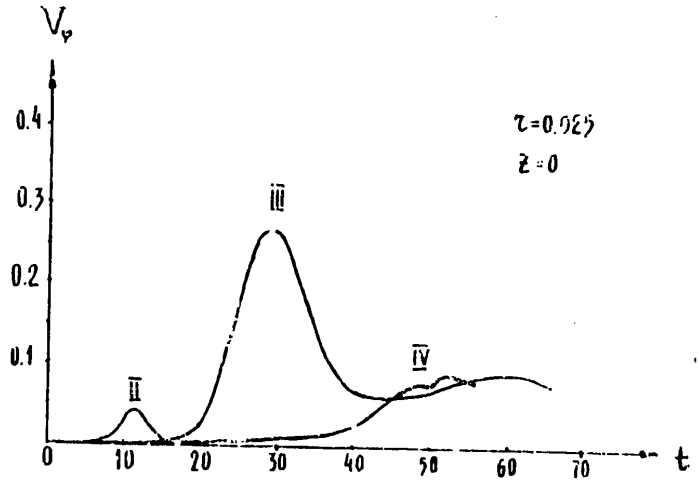

Figure 9

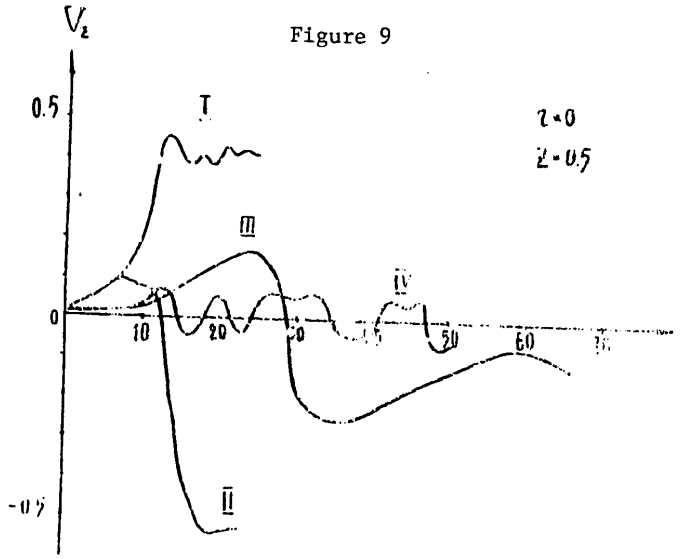

Figure 10

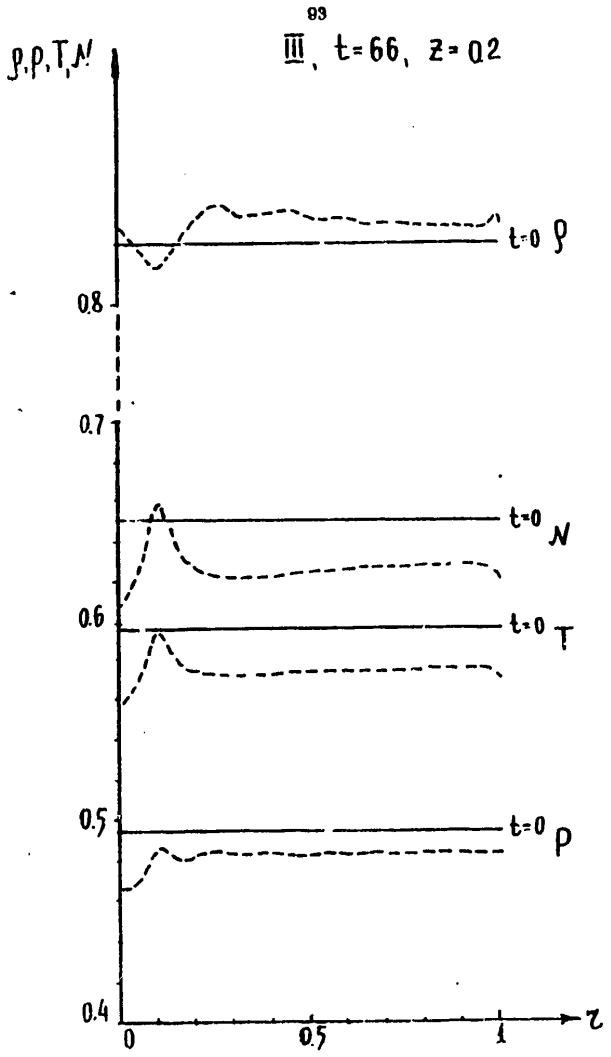

Figure 11a

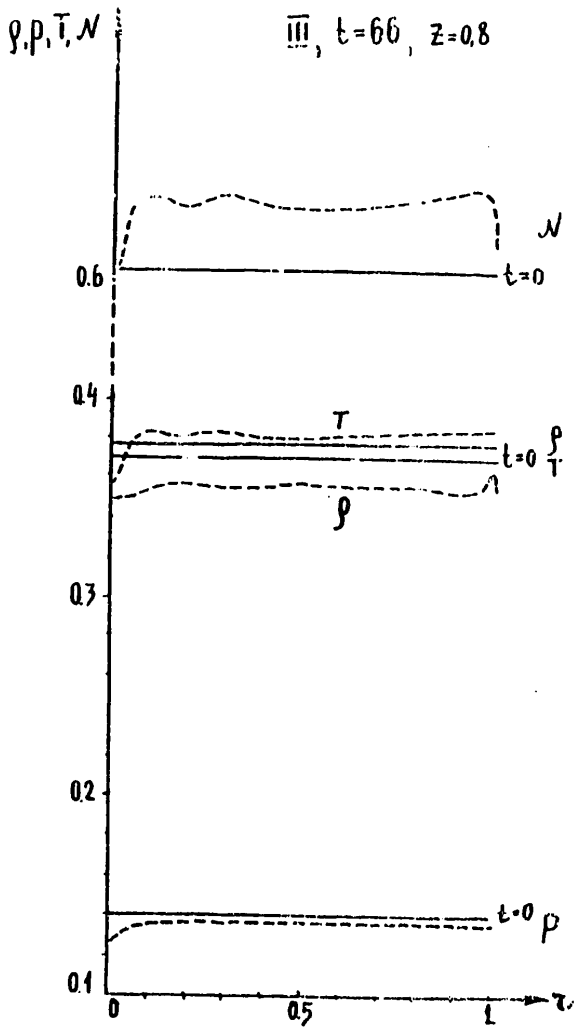

Figure 11b

Chapter II. Helical Instability of a Cylindrical Gas Jet

§1. Statement of the Problem

Under the assumption of helical symmetry, the equations of motion of an ideal gas can be represented in the form

$$\frac{\partial \rho}{\partial t}+\operatorname{div}\rho\vec{v}=0,\quad \frac{\partial N}{\partial t}+\vec{v}\nabla N=0,\quad \frac{\partial I}{\partial t}+\vec{v}\nabla I=0, \tag{41}$$

$$\frac{\partial v_z}{\partial t}+\vec{v}\nabla v_z=-\frac{1}{\rho}\frac{\partial p}{\partial z}+\frac{v_\varphi^2}{r},\quad \frac{\partial}{\partial t}v_\varphi+\vec{v}\nabla v_\varphi=-\frac{1}{\rho}\frac{\partial p}{\partial \varphi}$$

where

$$I=v_z+\alpha r v_\varphi,\quad \theta=\varphi-\alpha z,\quad \alpha=2\pi/L=\text{const},$$

$$\vec{v}\nabla=v_r\frac{\partial}{\partial r}+\left(\frac{v_\varphi}{r}-\alpha v_z\right)\frac{\partial}{\partial\theta},\quad \operatorname{div}\rho\vec{v}=\frac{1}{r}\frac{\partial}{\partial r}\rho r v_r+\frac{\partial}{\partial\theta}\rho\left(\frac{v_\varphi}{r}-\alpha v_z\right).$$

We shall consider that in the initial steady-state all values depend only on r, and the equation of equilibrium $p'=\rho v_\varphi^2/r$ is satisfied. As the initial disturbance let us use the velocity $\vec{v}$ satisfying the condition div $\vec{v}=0$ and described by the current function $\Psi=\lambda r^m(1-r^2)\sin m\theta$.

On satisfaction of the condition of periodicity in the length of the cylinder L and vanishing of the normal component of the velocity v_r for $r=\alpha$, from the equations (41) we have the laws of conservation of mass, energy, entropy and momentum:

$$\int\rho dV=\text{Const},\quad \int\left(\frac{p}{\gamma-1}+\frac{\rho v^2}{2}\right)dV=\text{Const},\quad \int pN dV=\text{Const},\quad \int\rho I dV=\text{Const}. \tag{42}$$

The presence in the initial steady-state motion of both velocities v_ϕ and v_z is a significant difference from the preceding problems which leads to the possibility of appearance of complex eigenvalues of the frequency ω.

§2. Linear Theory

The linearized equations (41) for cylindrically symmetric stationary configuration reduce to one equation [4] for $rv_r=f(r)\cos m\theta\cdot\cos\omega t$:

$$\left(\frac{\rho r y^2 c^2}{S}f'\right)'-\left\{\frac{m^2\rho y^2}{r}-\frac{4\alpha\rho v_\varphi^2}{\beta r}-\left(\frac{\beta\rho c^2 q}{S}\right)'+\frac{\beta\rho r^2 q^2}{S}\right\}f=0, \tag{43}$$

where

$$\beta=1+\alpha^2r^2,\quad y=\alpha v_z-v_\varphi/r,\quad S=\rho c^2-r^2y^2,\quad q=\left(\frac{2y}{\beta}-\frac{v_\varphi}{r}\right)\frac{v_\varphi}{r},\quad c^2=\frac{\gamma p}{\rho}.$$

We shall limit ourselves to the case $v_\phi=\alpha r v_z$ where the current lines are helical lines $\theta=\text{const}$ with constant pitch. Then at the limit $\omega\to 0$, equation (43) becomes

$$\left(\frac{\rho r}{\beta}f'\right)'-\left\{\frac{m^2\rho}{r}-\frac{m^2\rho v_\varphi^2}{\omega^2 r^2}\left[\frac{(v_z^2)'+(r^2v_\varphi^2)'/r^2}{v^2}-\frac{N'}{\gamma N}\right]\right\}f=0 \tag{43a}$$

Hence, we have the required stability condition of [5]

$$v_\varphi^2\left[\frac{(v_z^2)'+(r^2v_\varphi^2)'/r^2}{v^2}-\frac{N'}{\gamma N}\right]>0, \tag{44}$$

in which the term $\sim N'$ describes the stability condition with respect to the convective transport to the centrifugal force field, and it disappears for an incompressible liquid ($\gamma\to\infty$). The remaining terms are caused by instability as a result of $\vec{j}=\text{rot }\vec{v}\neq 0$. The stability condition (44) can also be represented in the form

$$(I^2N^{-1/\gamma})'>0, \tag{44a}$$

where it is expressed in terms of the frozen functions N and I.

For the steady-state configuration $\rho=\text{const}$.

$$v_z=1-r^2,\quad v_\varphi=\alpha r(1-r^2),\quad p=p_0+\frac{\rho\alpha^2}{6}[1-(1-r^2)^3] \tag{45}$$

we obtain the following expression for the stability criterion (44)

$$-1+\alpha^2\frac{1-r^2}{\beta}-\frac{\alpha^2}{4c^2}(1-r^2)^3>0. \tag{46}$$

Here the first term describes the destabilization as a result of the decreasing longitudinal velocity $v_z(r)$, the second term, stabilization caused by an increase in $rv_\phi(r)$, and the third, convective instability. If the inequality (46) is not satisfied in the entire interval $0<r<1$, then unstable eigenfunctions exist which encompass the entire cross section $0<r<1$.

Let us consider the equation (43a) for the case $v^2\ll c^2$; $\alpha^2r^2\ll 1$ and, limiting ourselves to weak instability, we set $v_z=1-\varepsilon r$, $v_\phi=\alpha r(1-\varepsilon r)$, where $|\varepsilon|\ll 1$. Here (43a) reduces to the equation

$$\frac{1}{r}(rf')'-\left\{\frac{m^2}{r^2}+\frac{4\alpha^2m^2}{\omega^2}\left(\varepsilon+\alpha^2-\frac{\omega\varepsilon}{m\alpha}\right)\right\}f=0. \tag{43b}$$

the solution of which is expressed by the Bessel function $J_m(kr)$. The natural values of the frequency ω for the boundary problem $f(0)=f(\alpha)=0$ are defined by the formula

$$\frac{\omega}{m}=\frac{2\alpha\varepsilon}{\chi_{mn}}\pm\frac{2\alpha i}{\chi_{mn}}\sqrt{\varepsilon+\alpha^2}, \tag{47}$$

where x_{mn} are the roots of $J_m(x)$. Since for $\varepsilon>0$ the frequency ω contains an imaginary part, there is an instability caused by a decrease in $v_z(r)$.

§3. Energy Limitations

The kinetic energy occurring on development of an instability has as its sources the consumption of thermal and kinetic energy of the initial stationary flow. Let us represent the kinetic energy in the form

$$W_k=\frac{V}{2}\langle\rho v^2\rangle=\frac{V}{2}\{\langle\rho v_z^2\rangle+\langle\rho v_\perp^2\rangle+\langle\rho v_\parallel^2\rangle\}, \tag{48}$$

where $v_\perp=(v_\phi-\alpha r v_z)/\sqrt{\beta}$, $v_\parallel=(v_z+\alpha r v_\phi)/\sqrt{\beta}=I/\sqrt{\beta}$, and the provisional brackets indicate averaging over the volume $V=\pi a^2 L$. If in the investigated steady-state $v_r=0$, $v_\perp=0$, obviously only the longitudinal energy can be expended $W_\parallel=(V/2)\langle\rho I^2/\beta\rangle$. Using the law of conservation of momentum (42) and assuming the density distribution ρ is invariant, we obtain the following restriction on the maximum possible consumption of the longitudinal energy

$$-\delta W_\parallel\le\frac{V}{2}\left(\left\langle\frac{\rho I^2}{\beta}\right\rangle-\frac{\langle\rho I\rangle^2}{\langle\beta\rho\rangle}\right)_0 \tag{49}$$

An analogous restriction on the consumption of the thermal energy caused by conservation of mass and entropy has the form [2]

$$-\delta W_T\le\frac{V}{\gamma-1}\left(\langle\rho\rangle-\langle\rho^{1/\gamma}\rangle^\gamma\right)_0 \tag{50}$$

For stationary configuration (45), assuming for simplicity that $\alpha^2a^2\ll1$, we obtain

$$-\delta W_\parallel\le\frac{\rho V}{24}v_{z0}^2,\quad -\delta W_T\le\frac{\rho V}{896}\frac{(\alpha a v_{z0})^4}{c^2}, \tag{51}$$

Thus, in the investigated case basically the kinetic energy of longitudinal motion is expended.

§4. Results of Solving the Nonlinear Problem

The system of equations (41) was solved by numerical methods in the region $0\le r\le1$, $0\le z\le2\pi/\alpha$ under the condition of periodicity with respect to z and vanishing of v_r for r=1. The initial stationary flow (45) for $p_0=\rho_0=\alpha=1$, $\gamma=5/3$. As the initial disturbance, an additional velocity $\tilde{\vec{v}}$ was used which satisfies the condition $\operatorname{div}\tilde{\vec{v}}=0$ and described by the current function $\tilde{\Psi}(r,\theta)$ of the second harmonic m=2

$$\tilde{v}_r=\frac{1}{r}\frac{\partial\tilde{\psi}}{\partial\theta},\quad \tilde{v}_\varphi-\alpha r\tilde{v}_z=-\frac{\partial\tilde{\psi}}{\partial r},\quad \tilde{\psi}=\lambda r^m(1-r^2)\sin m\theta, \tag{52}$$

for $\lambda=0.1$, $\tilde{v}_z=0$. Inasmuch as the steady-state velocities (45) are given so that their current function $\Psi=0$, at the initial point in time the transfer cross sections of the helical surfaces of the flow are defined by the equation $\tilde{\Psi}(r, \theta)=\text{const}$, and they are depicted in Figure 14a. For the investigated disturbance mode $m=2$ the flow surfaces for $t=0$ are 4 helical tubes. The kinetic energy of the instability is defined by the expression

$$W_\perp = \frac{1}{2}\int v_z^2 dV + \frac{1}{2}\int \frac{1}{\beta}(v_\varphi - \alpha z v_z)^2 dV \tag{53}$$

Figure 12 shows the variation in time of the radial energy W_r. The graph of W_r has the characteristic form of a curve with a maximum which coincides with respect to order of magnitude with the maximum possible consumption of longitudinal energy (51).

Figure 13 shows the evolution of helical surfaces $I(r, \theta)=\text{const}$ which for $t=0$ were cylinders. It is obvious that the instability circle encompasses the entire cross section $0<r<1$, and narrow layers are formed with large gradients [2].

Figure 14 shows the cross sections of the flow surfaces $\Psi(r,\theta)=\text{const}$ constructed by the approximate formula

$$\psi = \int_0^z \rho(\alpha z v_z - v_\varphi) dz, \tag{54}$$

obtained neglecting the variation of ρ. As is obvious from Figure 14b, as a result of evolution of the unstable disturbed flow basically two helical current tubes develop with opposite direction of rotation of the gas around the axes of these tubes.

Figure 15 shows the cross section of the surfaces of constant density $\rho(r,\theta)=\text{const}$ for different points in time t.

Thus, the possibility of nonlinear development of the helical instability caused by a decrease in the longitudinal velocity with respect to radius and leading to the formation of characteristic large-scale structures $I=\text{const}$ with narrow layers is demonstrated. During the process of the instability, helical current tubes are formed in which the gas rotates around the axes of these tubes.

As follows from the choice of the equilibrium parameters, the dimensionless unit of velocity is $c_0/\sqrt{\gamma}$, and length is the radius of the cylinder a. Consequently, the dimensionless unit of time corresponds to the interval $\Delta t_0=\sqrt{\gamma}a/c_0$.

Conclusion

In the above-investigated problems a study was made of the development of instability in the one-dimensional initial configurations. However, it is natural that in a more realistic model the formation of the tornado must be considered as the result of evolution of a two-dimensional steady-state configuration.

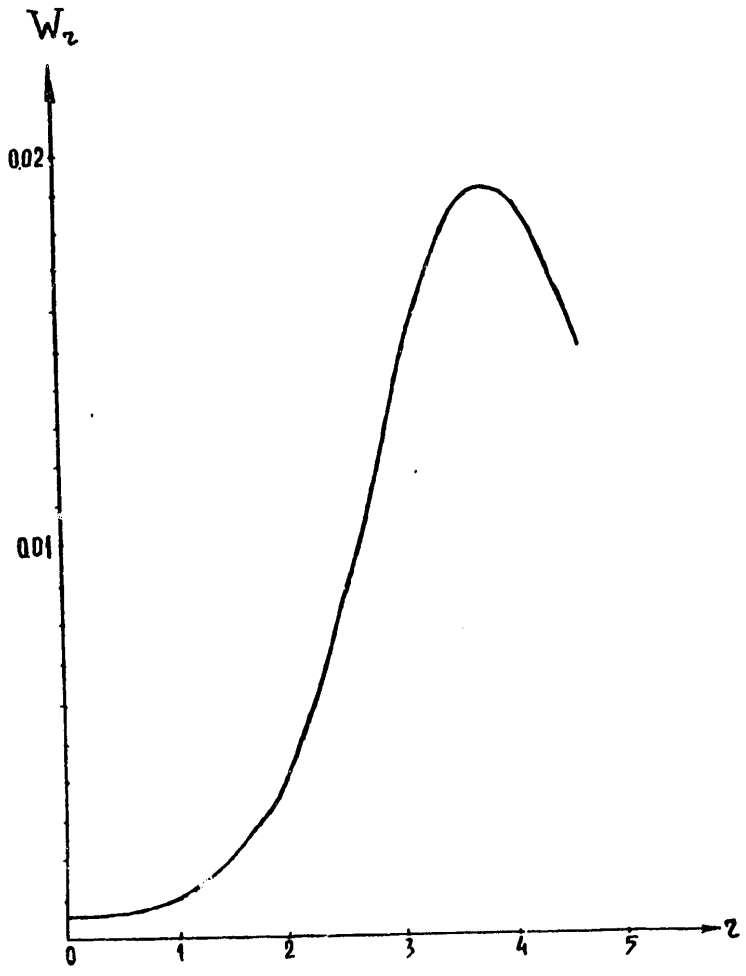

Figure 12

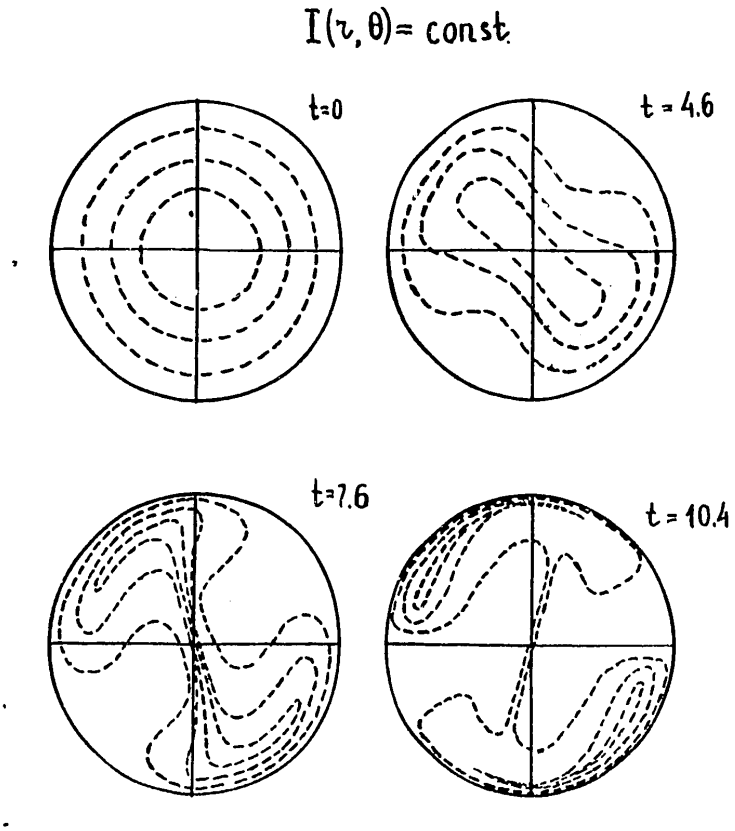

Figure 13

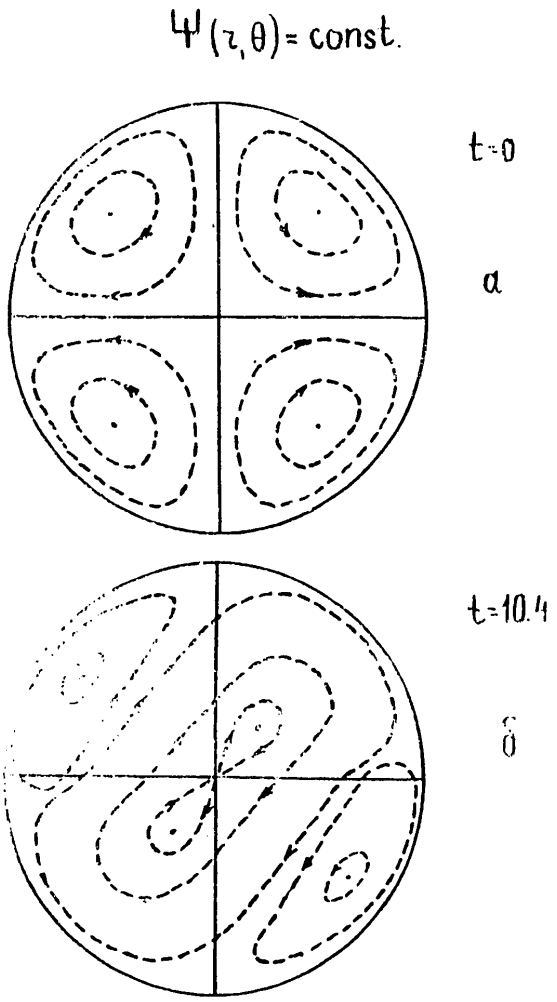

Figure 14

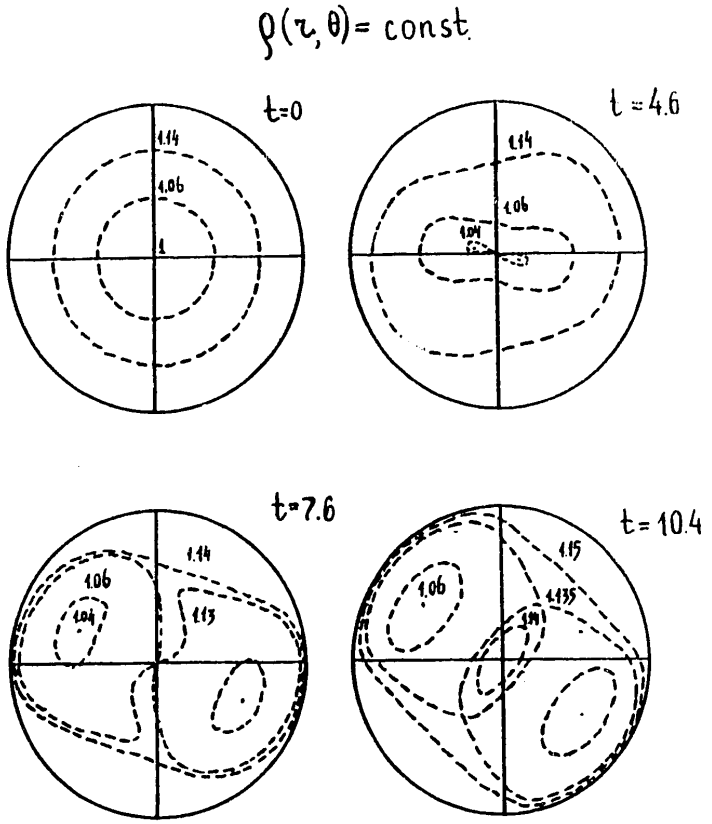

Figure 15

Actually, for example, the radial pressure gradient occurring as a result of local superheating leads if necessary to a current in the gas having radial velocity components. The two-dimensional flow that is formed, in turn, becomes an additional strong factor promoting concentration of the rotational moment in the vicinity of the axis of rotation.

In conclusion, the authors express their sincere appreciation to N. N. Chentsov for his interest in this paper and useful discussions.

BIBLIOGRAPHY

1. Landau, L. D.; Lifshits, Ye. M. MEKHANIKA SPLOSHNYKH SRED. [Mechanics of Continuous Media], Moscow, GITTL, 1954.

2. Zuyev, N. M.; Solov'yev, L. S. "Nonlinear Helical MHD-Instability," MAGNITNAYA GIDRODINAMIKA [Magnetohydrodynamics], No 3, 1977, pp 5-22.

3. Zuyev, N. M.; Paleychik, V. V.; Solov'yev, L. S. "Development of Convective Instability in a Rotating Gas," Preprint No 11, Institute of Applied Mechanics of the USSR Academy of Sciences, 1978, PIS'MA V ZHTF [Letters to the Technical Physics Journal], No 8, 1978, pp 436-440.

4. Solov'yev, L. S. VOPROSY TEORII PLAZMY [Problems of Plasma Theory], No 3, Gosatomizdat, 1963, pp 245-289.

5. Burshteyn, E. L.; Solov'yev, L. S. "Stability of a Rotating Liquid," DAN SSSR [Reports of the USSR Academy of Sciences], Vol 204, No 1, 1972, pp 56-59.

HYDRODYNAMIC DESCRIPTION OF THE SELF-FOCUSING OF LIGHT BEAMS IN A CUBIC MEDIUM

[L. M. Degtyarev, V. V. Krylov, pp 106-161]

Contents

Introduction

The self-focusing of light beams is one of the nonlinear optical effects, interest in which was manifested at the beginning of the 1960's in connection with building lasers. The essence of this phenomenon consists in the following. The light wave field changes the properties of the material, in particular, the index of refraction. The optical nonuniformity creating the lens effect appears. As a result, the path of the rays in such a nonlinear medium can change significantly by comparison with the linear medium, which leads to the formations of regions of localization of the light intensity -- the focal points [1]-[4]. For the study of light beams in nonlinear media, the quasioptical approximation was fruitful -- the equation of the Schroedinger type with nonlinear potentials for the complex amplitude of the electric field of the wave [2], [3].

In reference [5] it was demonstrated that a uniform beam is unstable with respect to disturbances in the plane normal to the direction of propagation. In the nonlinear stage of this instability the beam is broken down into filaments, in each of which self-focusing takes place. This instability is similar to the Rayleigh-Taylor instability in a liquid. The basis for such an analogy can be the hydrodynamic formulation of the nonstationary Schroedinger equation [6], [2].

This paper is on the hydrodynamic formulation of the quasioptical approximation and the study of the steady-state self-focusing of an axially cylindrical beam of light based on it. This approach turns out to be natural and fruitful in that, as a rule, the phenomenon with strong spatial deformations, which include self-focusing, are conveniently studied in Lagrange variables which are most simply introduced in hydrodynamics.

This paper is a survey of works by the authors [7]-[9].

In §1 the variation formulation of the steady-state quasioptical equations and hydrodynamic interpretation of the problem are given. In §2 the axisymmetric problem is formulated in hydrodynamic variables, the coordinates connected with the rays are introduced -- the optical analog of Lagrange mass coordinates [7]. This formulation of the problem permits the well-developed difference schemes for the equations of gas dynamics to be used for its numerical solution. In particular, in §3 the variation principle recently successfully used in hydrodynamics has been used to obtain difference systems in the problems of the propagation of light in nonlinear media [10], [11]. The difference schemes obtained, by analogy with hydrodynamics can in this case be called completely conservative [12]. This property of the difference schemes is theoretical in this case: as the numerical experiments have demonstrated, violation of it leads to incorrect determination of such self-focusing characteristics as the focal length and nature of the asymptotic behavior of the solution near the focal point. As a special case of the general approach, in §3 difference schemes are obtained for the axisymmetric problem [7]. As a result of using the Lagrange coordinates, the Euler net in the plane of normal propagation of the beam is moving and is automatically adjusts to the solution. In §4 the Lagrange hydrodynamic formulation is used to study the asymptotic behavior near the focal point of self-focusing in a cubic medium. By simple separation of variables the class of self-similar solutions was obtained [13]. It is proved that independently of the input data the solution near the focal point will become one of the self-similar solutions of [9]. In §5, a discussion is presented of the results of the numerical solution. Here it was found that only part of the beam with a power on the order of critical is focused. Near the focal point the solution goes to the self-similar regime. The solution of the problem is exhausted by studying the peripheral rays (aberrations). In §6, a simplified equation was obtained for the peripheral rays. The study of its solution and comparison with the numerical results are the subjects for §7 [9]. Good agreement of the approximate behavior of the peripheral rays with the results of the numerical solution to the focal region offers the possibility of obtaining a formula for the focal length for arbitrary monotonic intensity distributions in the input cross section.

As became known to us, the hydrodynamic approach to the numerical solution of the propagation of light in linear media is also developed in [14].

The authors express their appreciation to Academician A. A. Samarskiy for numerous useful discussions and T. A. Gorbushin for participating in the various stages of the work in the numerical calculations.

§1. Variation Statement of the Problem. Integrals of Motion. Hydrodynamic Analogy

Let us consider the problem of the steady-state propagation of a beam of light limited in the transverse direction in a nonlinear, nonabsorbing medium. We shall begin with the stationary wave equation in the quasioptical approximation of [15, 2-4]

$$2ik\frac{\partial A}{\partial z} = \Delta_1 A + k^2\frac{\overset{(1)}{\varepsilon_{n\ell}}(|A|^2)}{\varepsilon_0}A \tag{1.1}$$

Key: 1. nℓ

where A is the complex envelope of the electric field ("slowly varying amplitude" of the wave so that the field oscillating with respect to space

$$E_\sim = Ae^{ikz} + \text{k.c.}$$

k is the wave number, $\varepsilon_{n\ell}(|A|^2)$ is the nonlinear additive to the dielectric constant ε_0 of the linear medium

$$\overset{(1)}{\varepsilon} = \varepsilon_0 + \varepsilon_{n\ell}(|A|^2)$$

Key: 1. nℓ

Δ_1 is the Laplace operator in the plane transverse to the beam. At the boundary of the nonlinear medium z=0, a value of the amplitude is given

$$A(\vec{r}_1, 0) = A^{(0)}(\vec{r}_1), \quad \vec{r}_1 = (x, y) \tag{1.2}$$

The other boundary condition is a decrease in amplitude in the transverse direction

$$A(\vec{r}_1, z)_{|\vec{r}_1|\to\infty} \to 0 \tag{1.3}$$

The physical meaning of this condition consists in limiting the beam with respect to the transverse coordinates.

Let us consider the variation formulation of the problem. This formulation includes the selection of the dynamic variables (field functions), selection of the spatial coordinates, Lagrange function density recording, the condition of steady-state effect and, finally, the Lagrange-Euler equation [16]. In the given case the field is described by two dynamic variables F_1, F_2 (for example, the amplitude A [illegible word] the function A^* complex conjugate for it) and three coordinates ε_1, ε_2, ε_3, for example, ε_1=x, ε_2=y, ε_3=z. The density of the Lagrange function L depends on the field variables, and the first derivatives and, generally speaking, the coordinates

$$L = L\left(F_1, F_2, \frac{\partial F_1}{\partial \xi_1}, \frac{\partial F_1}{\partial \xi_2}, \frac{\partial F_1}{\partial \xi_3}, \frac{\partial F_2}{\partial \xi_1}, \frac{\partial F_2}{\partial \xi_2}, \frac{\partial F_2}{\partial \xi_3}, \ldots\right)$$

The effect of J is the integral of L with respect to the region of the given problem

$$J = \int_{\Xi} L\, d\xi_1 d\xi_2 d\xi_3$$

The variation formulation of the problem consists in requiring equality of the variation of the effect to zero on variation of the dynamic variables

$$\delta J = 0$$

This condition (with the variation of the variables vanishing at the boundary of the region) leads to the Lagrange-Euler equations

$$\sum_{\alpha=1}^{3} \frac{\partial}{\partial \xi_\alpha} \frac{\partial L}{\partial\left(\frac{\partial F_\ell}{\partial \xi_\alpha}\right)} = \frac{\partial L}{\partial F_\ell}, \quad \ell = 1, 2 \tag{1.4}$$

Setting $F_1 = A$, $F_2 = A^*$; $\xi_1 = x$, $\xi_2 = y$, $\xi_3 = z$

and considering the problem in the region

$$\Xi : x \in (-\infty, \infty),\ y \in (-\infty, \infty),\ z \in (0, \infty)$$

we find that the equation (1.1) and the one complex conjugate to it are Lagrange-Euler equations for the following L

$$L = \frac{1}{2}\left\{ik\left(A\frac{\partial A^*}{\partial z} - A^*\frac{\partial A}{\partial z}\right) - |\vec{\nabla}_1 A|^2 + \frac{k^2}{\varepsilon_0}\beta_{nn}(|A|^2)\right. \tag{1.5}$$

where $\beta_{nn}(|A|^2) = \int_0^{|A|^2} \varepsilon_{nn}(I)\, dI$.

It is possible to perform the time-space analogy, interpreting the longitudinal coordinate as time [17]. With this interpretation the Lagrange function naturally is the integral in the transverse density from the density

$$\mathcal{L} = \frac{1}{2\pi}\int_{\Sigma} L\, d\sigma_1$$

(the factor $1/2\pi$ is introduced for convenience of notation of subsequent formulas). Then let us consider the spatial analog of the Hamiltonian

$$\mathcal{H} = \frac{1}{2\pi}\int_{\Sigma} H\, d\sigma_1$$

where H is determined from the equality

$$H = \frac{\partial F_1}{\partial z}\frac{\partial L}{\partial\left(\frac{\partial F_1}{\partial z}\right)} + \frac{\partial F_2}{\partial z}\frac{\partial L}{\partial\left(\frac{\partial F_2}{\partial z}\right)} - L$$

and for $F_1 = A$, $F_2 = A^*$

$$\mathcal{H} = \frac{1}{4\pi}\int_{\Sigma}\left\{|\vec{\nabla}_1 A|^2 - \frac{k^2}{\varepsilon_0}\beta_{nn}(|A|^2)\right\} d\sigma_1 \tag{1.6}$$

Let us note that the Lagrange function density (1.5) does not explicitly depend on the coordinate z. By the corresponding theorem of variation calculus it follows directly from this that the value of the integral $\mathcal{H}$ (hereafter called the Hamiltonian) will be defined only by the boundary conditions [16]. In particular, for the condition (1.3) the integral $\mathcal{H}$ does not depend on z (it is invariant); its value is determined only by the condition (1.2).

Let us represent the complex amplitude $A(\vec{r}_\perp, z)$ in the form

$$A = A_0 \exp(-iks) \tag{1.7}$$

where A_0 is the real amplitude, s is the eikonal (the spatial phase). Selecting A_0 and s as the dynamic variables, we convert the Lagrangian (1.5)

$$L = -\frac{k^2}{2}\left\{2A_0^2\frac{\partial s}{\partial z} + A_0^2(\vec{\nabla}_\perp s)^2 + \frac{1}{k^2}(\vec{\nabla}_\perp A_0)^2 + \frac{\beta_{нл}(A_0^2)}{\varepsilon_0}\right\}$$

The Lagrange-Euler equations in this case (1.4) assume the form

$$\frac{\partial A_0^2}{\partial z} + \vec{\nabla}_\perp\cdot(A_0^2\vec{\nabla}_\perp s) = 0 \tag{1.8}$$

$$2\frac{\partial s}{\partial z} + (\vec{\nabla}_\perp s)^2 = \frac{\varepsilon_{нл}(A_0^2)}{\varepsilon_0} + \frac{1}{k^2}\frac{\Delta_\perp A_0}{A_0} \tag{1.9}$$

and form the system equivalent to the initial equation (1.1).

From the amplitude equation (1.8) and the condition (1.3) we have conservation with respect to z of the integral

$$\mathcal{M} = \frac{1}{2\pi}\int_\Sigma A_0^2\, d\sigma_\perp = \frac{1}{2\pi}\int_\Sigma |A|^2 d\sigma_\perp \tag{1.10}$$

which coincides with accuracy to the constant dimensional factor with the total beam power $P = cn\mathcal{M}/4$ (c is the speed of light, n is the index of refraction). The beam power is the value which essentially defines the nature of its propagation. Strictly speaking, the boundary conditions (1.2) only with a finite value of the integral $\mathcal{M}$ have meaning (finite-power beam). Hereafter, discussing the limited beams, in addition to the conditions (1.2), (1.3) we set

$$\int_\Sigma |A|^2 d\sigma_\perp < \infty \tag{1.11}$$

The concept of ray tubes is closely connected with the power integral. The ray trajectory is the line

$$\vec{r}_\perp(z) = \{x(z), y(z)\}$$

defined by the equation

$$\frac{d\vec{r}_\perp}{dz} = \vec{\nabla}_\perp s, \qquad \vec{r}_\perp(0) = \vec{r}_{\perp 0}$$

Applying the operator $\vec{\nabla}_1$ to the common parts of (1.9), we obtain the ray equation

$$\frac{d^2\vec{r}_1}{dz^2} = \frac{1}{2}\vec{\nabla}_1\left\{\frac{\varepsilon_m(A_0^2)}{\varepsilon_0} + \frac{1}{k^2}\frac{\Delta_1 A_0}{A_0}\right\} \tag{1.12}$$

where

$$\frac{d}{dz} = \frac{\partial}{\partial z} + (\vec{\nabla}_1 S)\vec{\nabla}_1 \tag{1.13}$$

[paragraph illegible]

$$A^2 = \rho, \quad \vec{\nabla}_1 S = \vec{v} \tag{1.14}$$

Then (1.8) corresponds to the continuity equation, (1.9)(or (1.12)) corresponds to the equation of motion. The power integral and the Hamiltonian are interpreted, respectively, as the total mass and the total energy of the liquid

$$M = \frac{1}{2\pi}\int_\Sigma \rho\, d\sigma_1, \quad \mathcal{H} = \frac{k^2}{2\pi}\int_\Sigma\left\{\frac{1}{2}\rho\vec{v}^2 + \frac{1}{8k^2}\frac{1}{\rho}(\vec{\nabla}_1\rho)^2 - \frac{\beta_m(\rho)}{\varepsilon_0}\right\} d\sigma_1 \tag{1.15}$$

It is possible to consider the ray tube as an element of constant mass consisting of liquid particles (the current tube). Finally, the derivative with respect to the ray direction is the analog of the total (Lagrange or substationary) derivative with respect to time.

The hydrodynamic analogy turns out to be useful primarily in procedural respects. In particular, for numerical simulation it turns out to be possible to use the ideas and methods of the well-developed theory of the difference schemes of gas dynamics [12].

§2. Coordinates Connected with the Rays (Optical Analog of the Lagrange Mass Coordinates)

The hydrodynamic analog of the coordinates connected with the rays is the Lagrange coordinates. In the general case these coordinates can be introduced in full correspondence to the hydrodynamics of two-dimensional flow. In the given section we shall consider the axisymmetric case in detail. Inasmuch as in the transverse direction there is only one coordinate, it turns out to be possible to introduce the analog of the Lagrange mass coordinates [7].

Let us introduce the cylindrical coordinate system (r, z) (Oz is the beam axis, r is the distance from the axis) and hereafter let us use the dimensionless variables (the system of units with scale of length 1/k)

$$r \to kr, \quad z \to kz, \quad s \to ks. \tag{2.1}$$

Then using the hydrodynamic notation

$$\rho = A^2, \quad v = \frac{\partial S}{\partial r}; \quad \varepsilon_m(\rho) = \frac{\varepsilon_m(A^2)}{\varepsilon_0} \tag{2.2}$$

The equations for the amplitude and the eikonal will be written in the form

$$\frac{\partial \rho}{\partial z} + \frac{1}{r}\frac{\partial}{\partial r} r\rho v = 0 \tag{2.3}$$

$$\frac{\partial S}{\partial z} + \frac{1}{2} v^2 = v_r \tag{2.4}$$

where

$$v_r = \frac{1}{2}\left[\varepsilon_\infty(\rho) + \frac{1}{A_0}\frac{1}{r}\frac{\partial}{\partial r} r \frac{\partial A_0}{\partial r}\right] \tag{2.5}$$

The problem for A_0, s is considered in the region

$$0 < r < \infty, \quad z > 0$$

with the boundary condition

$$\rho(r, 0) = \rho_0(r); \quad v(r, 0) = v_0(r) \tag{2.6}$$

(the input data are the conditions at the boundary of the nonlinear medium)

$$\frac{\partial \rho}{\partial r}(0, z) = 0, \quad v(0, z) = 0 \tag{2.7}$$

(the conditions on the beam axis following from the requirements of symmetry and smoothness of the distributions),

$$\rho(r, z) \xrightarrow[r \to \infty]{} 0, \quad v(r, z) \xrightarrow[r \to \infty]{} \lim_{\varepsilon_\infty(\rho) \to 0} v(r, z) \tag{2.8}$$

(the conditions of "transition to the shadow region") and also the condition of finite power of the beam

$$\int_0^\infty \rho_0 r\, dr < \infty \tag{2.9}$$

We shall find the solution of the problem (2.3)-(2.9) in the form

$$\rho = \rho(m, z'), \quad S = S(m, z'), \quad r = r(m, z') \tag{2.10}$$

where the transformation of the coordinates

$$(r, z) \to (m, z')$$

is given by the equalities

$$z = z' \tag{2.11}$$

$$m = \int_0^r \rho r\, dr \tag{2.12}$$

The value of m is the analog of the Lagrange mass coordinate and has the meaning of the power integral in the ray tube of radius r, and accordingly (m, z) can be called the coordinates of constant power ("m-coordinates") [7].

The formulas for transformation of the derivatives have the form:

$$\frac{\partial}{\partial r} = \rho r \frac{\partial}{\partial m} \tag{2.13}$$

$$\frac{\partial}{\partial z} + \rho r v \frac{\partial}{\partial m} = \frac{\partial}{\partial z} = \frac{d}{dz} \tag{2.14}$$

Substituting r in (2.13) and (2.14), we arrive, respectively, at the equations

$$\rho r \frac{\partial r}{\partial m} = 1 \tag{2.15}$$

$$v = \frac{dr}{dz} \tag{2.16}$$

from which by the beam trajectories r(m,z) the intensity ρ and the slope of the rays v are determined. The continuity equation (2.3) is converted to the form

$$\frac{d}{dz}\left(\frac{1}{\rho}\right) = \frac{\partial}{\partial m}(rv) \tag{2.17}$$

and it is a consequence of (2.15). Converting the derivatives entering into w (2.5), in the coordinates (m,z) we obtain the equation for the phase

$$\frac{ds}{dz} - \frac{v^2}{2} = w(m,z)$$

and, as a consequence, the equation of the ray trajectories

$$\frac{d^2 r}{dz^2} = \rho r \frac{\partial w}{\partial m} \tag{2.18}$$

Let us proceed to the formulation of the boundary conditions. First of all, let us note that by transformation of (2.12) the halfaxis $0<r<\infty$ is mapped one to one on the finite interval $0<m<M$, where

$$M = \int_0^\infty \rho r dr \tag{2.19}$$

is the integral of total power of the beam, finite with respect to the condition (2.9). Thus, in the new coordinates the region of the problem is given in the form

$$0<m<M \quad (M<\infty), \quad z>0 \tag{2.20}$$

The conditions (2.7)-(2.8) are now formed on the boundaries of the interval (0, M) (in the first of the conditions (2.7), instead of the equality sign it is necessary to substitute the sign of the limiting transition). Finally, the transformation of the input data (2.6) is realized by means of the relations

$$m(r) = \int_0^r \rho_0(r) r dr \Rightarrow r = r(m) \Rightarrow \rho_0(r(m)) = \rho_0(m),$$

$$v_0'(r(m)) = v_0'(m)$$

In conclusion, let us write the statement of the problem in the coordinates (m, z). Here the ray equation will be written in another form closer to the equation in hydrodynamics. It is most simply obtained using the variation principle.

Using the introduction of the notation (2.2), let us write the integral of effect in the coordinates (r,z)

$$J = \frac{1}{2}\int_0^z\int_0^\infty \left\{ -2\frac{\partial s}{\partial z} - v^2 - \frac{1}{4}\left(\frac{1}{\rho}\frac{\partial \rho}{\partial r}\right)^2 + \frac{\beta_n(\rho)}{\rho} \right\} \rho r\, dr\, dz,$$

where $\beta_n(\rho) = \int \varepsilon_n(\rho)\, d\rho$

Making the transition to the coordinates (m,z) we obtain

$$J = \int_0^z\int_0^M \left\{ r\left(\frac{dr}{dz}\right)^2 - \frac{1}{4} r^2 \left(\frac{\partial \rho}{\partial m}\right)^2 + \frac{1}{\rho}\beta_n(\rho) \right\} dm\, dz$$

Equating the variation J to zero

$$\delta J = 0$$

Calculating the variation of the expression under the integral sign and considering that on the basis of

$$\delta\left(\frac{dr}{dm}\right) = -\rho^2 \frac{\partial}{\partial m}(r\delta r)$$

δJ is integrable by parts; assuming that at the boundary of the region of variation the functions s, r and ρ vanish, we obtain

$$\int_0^z\int_0^M \left\{ -\frac{d^2 r}{dz^2} - \frac{1}{4} r\left(\frac{\partial \rho}{\partial m}\right)^2 + \frac{1}{4} r \frac{\partial}{\partial m}\rho^2 \left(\frac{\partial}{\partial m}\left(r^2 \frac{\partial \rho}{\partial m}\right)\right) + 2\frac{\partial}{\partial \rho}\frac{1}{\rho}\beta_n(\rho) \right\} \delta r\, dm\, dz = 0$$

Equating the expression under the integral sign in braces to zero, we obtain a new form of the equation of the ray trajectories.

The problem is now formulated as follows: Let us find the functions r(m,z), v(m,z) and $\rho(m,z)$ in the region $0<m<M$ ($M<\infty$), $z>0$
satisfying the system of equations (2.15), (2.16), (2.21)-(2.23):

$$\frac{dv}{dz} + r\frac{\partial \chi}{\partial m} + \frac{1}{4} r\left(\frac{\partial \rho}{\partial m}\right)^2 = 0 \tag{2.21}$$

$$\chi = -\frac{1}{4}\rho^2\left[\frac{\partial}{\partial m} r^2 \frac{\partial \rho}{\partial m} + \gamma_n(\rho)\right] \tag{2.22}$$

$$\gamma_n(\rho) = 2\frac{\partial}{\partial \rho}\frac{1}{\rho}\beta_n(\rho), \quad \beta_n(\rho) = \int \varepsilon_n(\rho)\, d\rho \tag{2.23}$$

and the boundary conditions

$$\rho(m,0)=\rho_0(m), \qquad v(m,0)=v_0(m) \tag{2.24}$$

$$r(0,z)=0, \quad \rho\frac{\partial\rho}{\partial m}\underset{m\to 0}{=}O\left(\frac{1}{r}\right); \quad v(0,z)=0 \tag{2.25}$$

$$\rho(M,z)=0; \quad v(m,z)\xrightarrow[m\to M]{}\lim_{\varepsilon(\rho)\to 0} v(m,z) \tag{2.26}$$

In this formulation of the problem $\chi(m,z)$ is the analog of the pressure for the equations of hydrodynamics. The integrals of motion here are 1) the total beam power integral M trivially maintained ("the length of the segment" in which the problem is stated), 2) the Hamiltonian in the coordinates (m,z) written in the form

$$\mathcal{H}=\int_0^M\left(\frac{v^2}{2}+\frac{1}{8}r^2\left(\frac{\partial\rho}{\partial m}\right)^2-\frac{1}{2}\frac{\beta_n(\rho)}{\rho}\right)dm=\text{const} \tag{2.27}$$

§3. Numerical Simulation of Self-Focusing. Conservativeness. Method of Moving Finite-Difference Nets

When developing the method of numerical solution of the problems of mathematical physics, some general principles of the construction of difference systems must be taken into account [18]. One of the basic requirements which must be imposed on the difference scheme is the requirement of conservativeness, that is, execution in a finite difference net for the system of the difference analogs of the integrals of motion [8]-[10]. Conservativeness is the general requirement on the theory of difference systems: the digital model of the medium should be able to transmit the properties of the continuous medium as completely as possible [12]. With respect to the above-stated problem we shall say that the system is conservative if the approximation of the finite-difference function of the power integral and the Hamiltonian maintained on transition to the next step with respect to z are indicated in advance. The nonconservativeness of the system indicates the presence of fictitious sources and discharges not having physical meaning, and it can significantly distort the representations of the solution. Thus, failure to maintain the total power integral on the finite-difference net indicator fictitious absorption (amplification) not having any bearing on the initial problem. The maintenance of the difference analog of the Hamiltonian for the dynamics of the process indicates the same thing as conservation of the energy integral in the problems of hydrodynamics. Nonconservation of this integral on the finite-difference net as numerical experiments have demonstrated, leads to distortion of such important characteristics as the focal length and the growth rate of the intensity near the focal point. However, in addition to the general requirements when constructing the difference schemes it is necessary to consider the specific nature of the solved problems. Self-focusing is the essentially nonlinear process which in a number of cases leads to strong spatial nonuniformity of the phase-amplitude distribution of the beam. It is natural to require that the characteristic spatial scale of the net (its step size) will remain much less than the characteristic scale of the nonuniformity. Here it is natural to use

the above-formulated hydrodynamic analogy. For numerical solution of the problems of hydrodynamics an effective method of studying the singularities and discontinuities is use of the Lagrange coordinates. For a number of problems of the propagation of light beams, including self-focusing, their optical analog -- the coordinates connected with the rays -- turns out to be the most natural. Here the Lagrange net is equivalent to the "moving" finite-difference net of the spatial (Euler) coordinates automatically rearranged in accordance with the development of the process. Beginning with what has been stated above and using the coordinates related to the rays, let us construct the difference system for the equation of ray trajectories which has the difference analog of the Hamiltonian. For this purpose we then arrive at the following:

1. Using the hydrodynamic analog, let us substitute the problem of the dynamics of the continuous medium.

2. Applying the variation method of the construction of difference schemes, let us proceed from the problem of the dynamics of a continuous medium to the problem of the dynamics of N particles [10].

3. Applying the difference analog of the Hamiltonian equations, we obtain the conservative difference scheme of the initial problem.

Beginning with (1.5) and using the notation (1.14) and (2.1) we write the Lagrange function. We have

$$\mathcal{L} = \mathcal{T} - \mathcal{U} \tag{3.1}$$

where

$$\mathcal{T} = \frac{1}{2\pi}\int_{\Sigma}\left\{\frac{\vec{v}^2}{2}\right\}\rho\, d\sigma_1, \quad \mathcal{U} = \frac{1}{2\pi}\int_{\Sigma}\left\{\frac{1}{8}\left(\frac{\vec{\nabla}\rho}{\rho}\right)^2 - \frac{1}{2}\frac{\mathcal{R}_n(\rho)}{\rho}\right\}\rho\, d\sigma_1 \tag{3.2}$$

Let the coordinates ξ,η be introduced into the transverse plane. We then shall discuss the dynamics of the continuous medium with the potential energy U and the kinetic energy $\mathcal{T}$. Its total energy $\mathcal{H} = \mathcal{T} + \mathcal{U}$ and total mass $\mathcal{M}$ are conserved (§1).

In the plane Σ let us introduce the difference net $\omega^{(n)}(\xi_{ij}(t), \eta_{ij}(t))$ (n is the layer number with respect to t), breaking down the plane into tetragonal cells with apexes at the nodes of the difference net. Then we shall number these cells with the same indexes i, j. Let us introduce the finite-difference density function ρ_{ij} pertaining to the cell with the number (i, j). Let σ_{ij} be the area of the cell; then for its mass we have

$$m_{ij} = \rho_{ij}\sigma_{ij}$$

Let us require that m_{ij} not depend on t and be determined only by the initial (for z=t=0) density ρ^0_{ij} and the initial "volume" σ^0_{ij}. Let us note that the "volume" $\sigma_{ij}(t)$ is a function of the coordinates of the cell apexes. Let us approximate the kinetic and the potential energy by the sums

$$\mathcal{T}_k = \frac{1}{2\pi i}\sum_{ij}\left[\frac{v^2}{2}\right]_{ij} m_{ij}\ , \qquad \mathcal{U}_k = \frac{1}{2\pi i}\sum_{ij}\left[\frac{1}{8}\left(\frac{\vec{\nabla}_k \rho}{\rho}\right)^2 - \frac{1}{2}\frac{\beta_n(\rho)}{\rho}\right]_{ij} m_{ij}$$

here the brackets $[\ ]_{ij}$ can denote the difference in the approximation of the corresponding functions reduced to the corresponding cells.

Then using a dot to denote differentiation with respect to time, we have

[display missing in source]

The approximation of $[\vec{v}^2/2]_{ij}$ thus includes the values of $\dot{\xi}$, $\dot{\eta}$, ξ, η defined at the apexes surrounding the given cell, and the kinetic energy $\mathcal{T}$ is approximated by the function

$$\mathcal{T}_k(\dot{\xi}_{ij}, \dot{\eta}_{ij}, \xi_{ij}, \eta_{ij}) \quad (1 \leq i \leq N_1,\ 1 \leq j \leq N_2)$$

On the other hand, as is easy to see, the approximation of the potential energy is expressed in terms of the finite-difference function of the density ρ_{ij} and the coordinates of the apexes; however, $\rho_{ij}=m_{ij}/\sigma_{ij}$, where σ_{ij} is expressed in terms of the coordinates; thus, $u_h=u_h(\xi_{ij},\eta_{ij})(1\leq i\leq N_1,\ 1\leq j\leq N_2)$. The masses of the cells contained in the approximations $\mathcal{T}_k$ and $\mathcal{U}_k$, play the role of the parameters.

Thus, we arrive at the problem of the system dynamics N of particles with generalized coordinates ξ_{ij}, η_{ij}, the generalization velocities $\dot{\xi}_{ij}$, $\dot{\eta}_{ij}$ $(1\leq i\leq N_1,\ 1\leq j\leq N_2;\ N_1N_2=N)$ and the Lagrange function

$$\mathcal{L}_k(\dot{\xi}_{ij}, \dot{\eta}_{ij}, \xi_{ij}, \eta_{ij}) = \mathcal{T}_k - \mathcal{U}_k \tag{3.3}$$

The requirement of steady-state effect $\delta\int_0^t \mathcal{L}_k\,dt = 0$ leads to the Lagrange equations

$$\frac{d}{dt}\frac{\partial \mathcal{L}_k}{\partial \dot{\xi}_{ij}} = \frac{\partial \mathcal{L}_k}{\partial \xi_{ij}}\ , \quad \frac{d}{dt}\frac{\partial \mathcal{L}_k}{\partial \dot{\eta}_{ij}} = \frac{\partial \mathcal{L}_k}{\partial \eta_{ij}} \tag{3.4}$$
$$(1 \leq i \leq N_1,\ 1 \leq j \leq N_2)$$

which is the differential-difference analog of the equation of motion of a continuous medium. Here the value of

$$\mathcal{M}_k = \frac{1}{2\pi i}\sum m_{ij}$$

(corresponding to total mass) is the obvious integral of motion.

Let us introduce the Hamiltonian corresponding to the Lagrange function (3.3)

$$\mathcal{H}_k = \sum_{ij}\dot{\xi}_{ij}p_i^{\xi} + \sum_{ij}\dot{\eta}_{ij}p^{\eta} - \mathcal{L}_k \tag{3.5}$$

where $p_{ij}^{k} = \partial \mathcal{L}_k / \partial \dot{\xi}_{ij}$, $p_j^{k} = \partial \mathcal{L}_k / \partial \dot{\eta}_j$ are the generalized pulses. The Hamiltonian (3.5) does not explicitly depend on time, it is the integral of motion and it is identified with the total energy of the system.

The system (3.4) of second-order Lagrange equations is equivalent to the system of first-order Hamiltonian equations. Let us formulate the difference analog of the Hamiltonian equations for which the analog of the conservation of energy is satisfied. Let

$$\mathcal{H} = \mathcal{H}(p_\alpha, q_\alpha) \quad (\alpha = 1, \ldots, N) \tag{3.6}$$

be the Hamiltonian of the mechanical system of N particles with generalized coordinates q_α and generalized pulses p_α, where $\mathcal{H}$ does not depend explicitly on time. Writing the differential of this function

$$d\mathcal{H} = \sum_\alpha \frac{\partial \mathcal{H}}{\partial p_\alpha} dp_\alpha + \sum_\alpha \frac{\partial \mathcal{H}}{\partial q_\alpha} dq_\alpha \tag{3.7}$$

on the basis of the Hamiltonian equations

$$\frac{dp_\alpha}{dt} = -\frac{\partial \mathcal{H}}{\partial q_\alpha}, \quad \frac{dq_\alpha}{dt} = \frac{\partial \mathcal{H}}{\partial p_\alpha} \quad (\alpha = 1, \ldots, N) \tag{3.8}$$

we find that $d\mathcal{H} = 0$. Conversely, beginning with $d\mathcal{H} = 0$, it is easy to write the Hamiltonian equations (3.8).

Now let the difference net with respect to time be introduced. Let us consider two arbitrary successive time layers -- lower and upper separated by the step τ. The symbol "^" will denote all the variables reduced to the upper layer. Let us write the Hamiltonian on the upper and lower layer

$$\hat{\mathcal{H}} = \hat{\mathcal{H}}(\hat{p}_\alpha, \hat{q}_\alpha); \quad \mathcal{H} = \mathcal{H}(p_\alpha, q_\alpha)$$

and let us rewrite the difference of these expressions in the form analogous to (3.7)

$$\hat{\mathcal{H}} - \mathcal{H} = \sum_\alpha \left(\frac{\Delta \mathcal{H}}{\Delta p}\right)_\alpha (\hat{p}_\alpha - p_\alpha) + \sum_\alpha \left(\frac{\Delta \mathcal{H}}{\Delta q}\right)_\alpha (\hat{q}_\alpha - q_\alpha) \tag{3.9}$$

Here $\left(\frac{\Delta \mathcal{H}}{\Delta p}\right)_\alpha$, $\left(\frac{\Delta \mathcal{H}}{\Delta q}\right)_\alpha$ are the coefficients, respectively, for $\Delta p = \hat{p}_\alpha - p_\alpha$ and $\Delta q = \hat{q}_\alpha - q_\alpha$; they approximate the partial derivatives of the Hamiltonian (3.7). Let us write the difference analog of the Hamiltonian equations (3.8)

$$\frac{\hat{p}_\alpha - p_\alpha}{\tau} = -\left(\frac{\Delta \mathcal{H}}{\Delta q}\right)_\alpha, \quad \frac{\hat{q}_\alpha - q_\alpha}{\tau} = \left(\frac{\Delta \mathcal{H}}{\Delta p}\right)_\alpha \tag{3.10}$$

These equations approximate the equations of the differential problem. The expression

$$\hat{\mathcal{H}} = \mathcal{H}.$$

is a corollary of (3.10) on the basis of (3.9).

The method of obtaining the difference schemes investigated above is applicable for the problems of stationary propagation of light beams in arbitrary coordinates and transverse to the cross section beam. Then in §§4-8, we discuss the results pertaining only to the self-focusing of the axisymmetric beams in the cubic medium. Accordingly, let us present the scheme obtained for the initial axisymmetric problem (2.21)-(2.27). Let us introduce two finite-differences nets:with "integral" and "semi-integral" nodes with respect to mass

$$\Omega = \omega_m \times \omega_t, \quad \Omega' = \omega'_m \times \omega_t.$$

here

$$\omega_m = \{M_0 = 0,\ M_{i+1} = M_i + m_i,\ i = 0,\dots,N,\ m_N = 0,\ M_{N+1} = M\}$$

$$\omega'_m = \{M'_i = M_i + 0.5 m_i,\ i = 0,\dots,N\}$$

$$\omega_t = \{t_0 = 0,\ t_{n+1} = t_n + \tau_n,\ n = 0, 1, \dots\}$$

The difference scheme for r_i^n, v_i^n defined in Ω and ρ_i^n defined in Ω' has the form

$$\rho_i [0.5 (r_{i+1} + r_i)] r_{m,i} = 1, \quad i = 0,\dots,N-1 \tag{3.11}$$

$$\frac{\hat{r}_i - r_i}{\tau} = \langle v_i \rangle, \quad i = 1,\dots,N \tag{3.12}$$

$$\frac{\hat{v}_i - v_i}{\tau} + \langle r_i \rangle \chi_{\bar{m},i} + \frac{1}{2} \langle r_i \rangle \langle (\rho_{\bar{m},i})^2 \rangle = 0, \quad i = 1,\dots,N \tag{3.13}$$

$$\chi_0 = -\frac{1}{2} \hat{\rho}_0 \rho_0 \left\{ \frac{1}{m_0} \langle r_1^2 \rangle \langle \rho_{\bar{m},1} \rangle + \gamma_0 \right\} \tag{3.14}$$

$$\chi_i = -\frac{1}{2} \hat{\rho}_i \rho_i \left\{ (\langle r^2 \rangle \langle \rho_{\bar{m}} \rangle)_{m,i} + \gamma_i \right\}, \quad i = 1,\dots,N-1 \tag{3.15}$$

$$\gamma_i = 2 \left(\frac{\beta_n(\hat{\rho}_i)}{\hat{\rho}_i} - \frac{\beta_n(\rho_i)}{\rho_i} \right) \Big/ (\hat{\rho}_i - \rho_i)$$

$$i = 0,\dots,N-1$$

$$\beta_n(\rho_i) = \left[\int_0^{\rho} \varepsilon_n(\rho)\, d\rho \right]_{\rho = \rho_i}$$

with the initial data

$$\begin{cases} \rho_i^0 = \rho_i(0), \\ i = 0,\dots,N-1; \end{cases} \quad \begin{cases} v_i^0 = v_i(0) \\ i = 1,\dots,N \end{cases} \tag{3.16}$$

and the boundary condition

$$p_N = 0, \quad \chi_N = 0 \tag{3.17}$$

Here the index-free notation is used:

$$f = f^n, \quad \hat{f} = f^{n+1}, \quad \langle f \rangle = 0.5(f + \hat{f})$$

$$f_{m,i} = (f_{i+1} - f_i)/m_i, \quad f_{\bar{m},i} = (f_i - f_{i-1})/\bar{m}_i, \quad \bar{m}_i = 0.5(m_{i-1} + m_i)$$

With randomly different analog of the Hamiltonian equations (3.12), (3.13) the integrals $\mathcal{T}$ and $\mathcal{U}$ were approximated by the sums

$$\mathcal{T}_h = \sum_{i=1}^{N} \frac{p_i^2}{2m_i} = \sum_{i=1}^{N} \frac{1}{2}$$

$$\mathcal{U}_h = \sum_{i=1}^{N} \left\{ 0.5 \left[r_i^2 (\rho_{\bar{m},i})^2 + r_{i-1}^2 (\rho_{\bar{m},i-1})^2 \right] - \frac{1}{2} \left[\frac{1}{\rho_i} \beta_N(\rho_i) \right] \right\} m_i$$

As follows from what has been stated, the law of conservation of the value of $\mathcal{H}_h$ is satisfied on the difference net

$$\mathcal{H}_h = \mathcal{T}_h + \mathcal{U}_h$$

which approximates the Hamiltonian $\mathcal{H}$ of the initial differential problem.

Let us note that the difference scheme gives the trajectory of the last beam $r_N(z)$ without the assumption of any previously given information on it. Thus, here the problem of the transition to the shadow region for numerical solution of the problems of optics with diffraction is eliminated.

§4. Asymptotic Behavior of the Solution of the Problem of Self-Focusing in the Vicinity of the Focal Point

When investigating the self-focusing and the nonlinear diffractin the first approximation is the optical system of a cubic medium [2], [3]

$$\varepsilon_{nl}(|A|^2) = \varepsilon_2 |A|^2 \tag{4.1}$$

In the first papers on the self-focusing theory [15, 20-22] various authors demonstrated that the behavior of the three-dimensional beam is determined by the nonlinearity and diffraction relation quantitatively characterized by the ratio of the total beam power P to some critical power P_k [2], [20], [23]. For classification by this parameter the following cases were isolated:

A. $P \lesssim P_k$ -- diffraction predominates; the beam blurs, but this occurs more slowly than in the linear medium;

B. $P \simeq P_k$ -- the mutual "extinguishing" of the diffraction and nonlinearity and the dimensions and shape of the beam do not vary or vary slowly;

C. $P \geq P_k$ -- self-focusing occurs -- deflection of the beams toward the axis caused by nonlinear refraction which in the quasioptical approximation by diffraction is not complicated.

The weakly nonlinear case of A is of interest from the point of view of the quantitative corrections to the linear theory, but it does not lead to any new physical effects.

Case B is in the framework of the more general problem of compensation of diffraction divergence by nonlinear effects, and then it is not considered.

Let us consider the "strongly nonlinear" case C. For the formulated prerequisites

$$\text{(quasioptical approximation)} + \text{(cubic nonlinearity)} + (P \geq P_k) \tag{4.2}$$

The self-focusing leads to the formation of a focal point on the axis with infinite intensity [15], [21], [23]. We shall take this fact as the initial fact for further discussion.

Within the framework of the quasioptical approximation let us substitute the problem of investigation of the structure of the focal region in the cubic medium (beam properties in the vicinity of the focal point). Here we shall not discuss the limits of applicability of the physical model (4.2), and we shall state the problem as the mathematical problem. Let us note that in many problems of optics the vicinity of the focal point is of significant interest, and here the quasi-optical system of the cubic medium gives good zero approximation for finer investigation (compare the ratio of the geometric optics to wave optics [24]).

For solution of the problem of the asymptotic behavior in the vicinity of the focal point, let us use the transformation of the equations to the beam coordinates (m, z) (§2). Below these coordinates we obtain a family of special solutions of the initial equations important for the future. Let us first more precisely define the concept of critical power.

Let us introduce the coordinates (m,z), writing the initial problem (1.1)-(1.3) in the form (2.15), (2.16), (2.21)-(2.26). In these equations r and z are dimensionless (k=1). For the investigated case of cubic nonlinearity let us also introduce the dimensionless amplitude

$$A \to \sqrt{\frac{\varepsilon_2}{\varepsilon_0}} A \qquad \left(\rho \to \frac{\varepsilon_2}{\varepsilon_0}\rho\right) \tag{4.3}$$

From (2.23) we have

$$\varepsilon_m(\rho) = \rho, \quad \beta_m(\rho) = \frac{1}{2}\rho^2, \quad \gamma_m(\rho) = 1 \tag{4.4}$$

The power integral

$$M = \int_0^\infty \rho r\, dr \tag{4.5}$$

in the adopted notation is a dimensionless variable, and it is related to the dimensionless power P by the expression

$$P = \frac{c\,(\varepsilon_0)^{1/2}}{4k^2\varepsilon_2} M \tag{4.6}$$

Hereafter the integral M will be simply called the power for brevity, considering the corresponding dimensionless factor in (4.6).

Let us proceed to the definition of the critical power. For the amplitude distribution of the given form the critical power will be the power defined from the condition of equality of the integral $\mathcal{H}$ to zero (1.6) or (2.27).

$$\mathcal{H} = 0 \tag{4.7}$$

The power defined in this way is minimal for the so-called waveguide profile ("first waveguide mode" [20], [23], [25]) -- the solution in the cubic medium having invariant intensity distribution with respect to z (see the case B). In the adopted dimensionless variables for this profile

$$M_c \simeq 1.83 \tag{4.8}$$

The critical power of the collimated gaussian beam $A^{(0)}(r) = E_0 \exp(-r^2/2a^2)$ is close to M_k [23]

$$M_k = 2 \simeq 1.09\, M_c \tag{4.9}$$

In general, the definition of the critical power from the expression (4.7) for unimodal beams with smooth amplitude distribution gives the results distinguished from each other only by a factor on the order of one. Actually, let us write the condition (4.7) (for determinacy we set v≡0: the beams with flat phase front)

$$\mathcal{H} = \int_0^{M_k'} \left\{ \frac{1}{8} r^2 \left(\frac{\partial \rho}{\partial m}\right)^2 - \frac{1}{4}\rho \right\} dm = 0 \tag{4.10}$$

For unimodal beams with smooth profile we have

$$r^2\Big|_{m=\frac{M_k'}{2}} \simeq a^2, \quad \rho\Big|_{m=\frac{M_k'}{2}} \simeq \frac{1}{2}E_0^2, \quad M_k' = \frac{1}{2}E_0^2 a^2 \tag{4.11}$$

where E_0^2 is the intensity on the axis, a is the beam radius. Then

$$\frac{\partial \rho}{\partial m} \simeq \frac{\rho(0) - \rho(M_k')}{M_k'} = \frac{E_0^2}{M_k'}$$

consequently,

$$\mathcal{H} \simeq \frac{1}{8}\left(\frac{E_0^2}{M_k'}\right)^2 \int_0^{M_k'} r^2 dm - \frac{1}{4}\int_0^{M_k'} \rho\, dm \simeq \frac{1}{8}\left(\frac{E_0^2}{M_k'}\right)^2 a^2 M_k' -$$

$$- \frac{1}{4}\left(\frac{1}{2}E_0^2 M_k'\right) = \frac{1}{8}E_0^2\left(\frac{E_0^2 a^2}{M_k'} - M_k'\right) = \frac{1}{8}E_0^2(2 - M_k')$$

Therefore from (4.10) and (4.11) we have

$$M_{\kappa}' \simeq 2.$$

Hereafter, speaking of the power "on the order of critical," we consider expression (4.9). Let us show that the structure of the focal region in the cubic medium is defined by the partial solution of the parabolic equation from a family. It is natural that in the coordinates (m,z) these solutions are obtained by simple separation of variables. Substituting the function r(m,z) in the form

$$r(m,z) = a(z)R(m) \tag{4.12}$$

in the equations (2.15), (2.16) and also using the beam equation in the form (2.18), we obtain:

$$\rho = \frac{1}{a^2}\frac{1}{RR'} \tag{4.13}$$

$$v = a'R \tag{4.14}$$

$$u_r = \frac{1}{a^2}W(m) \tag{4.15}$$

$$a''R = \frac{1}{a^3}u^2RW' \tag{4.16}$$

where

$$W(m) = \frac{1}{2}\left[u^2 + u\frac{d}{dm}u^2R^2\frac{du}{dm}\right]$$

$$l^2(R(m)) = \frac{1}{RR'} \tag{4.17}$$

Separating the variables in (4.16), we obtain

$$a''a^3 = -\nu_1 \tag{4.18}$$

$$-\nu_1 = u^2W' \tag{4.19}$$

Dividing both sides of equation (4.19) by u^2, using (4.17) and integrating with respect to m, we have

$$u^2 + u\frac{d}{dm}u^2R^2\frac{du}{dm} = -\nu_1R^2 + 2\nu_2 \qquad *$$

where ν^2 is the integration constant. Finally, taking R as the independent variable, we obtain the equation for the function u(R)

$$\frac{1}{R}\frac{d}{dR}R\frac{du}{dR} + (\nu_1R^2 - 2\nu_2 + u^2)u = 0 \tag{4.20}$$

This equation defines the amplitude structure of the solution

$$A_0(r,z) = \frac{1}{a}u\left(\frac{r}{a}\right) \tag{4.21}$$

Then, from (4.12), (4.14), we have

$$v = \frac{a'}{a} r \tag{4.22}$$

and, consequently, comparing the *, (2.4), (2.5) it is possible to define the phase in the form

$$S(r, z) = \frac{a'}{a} \frac{r^2}{2} + \int_0^z \frac{\nu_z}{a^2} dz + \text{const} \tag{4.23}$$

Thus, the class of partial solutions represented in the coordinates (m, z) by separation of variables is determined from (4.21), (4.23) where u(R) and a(z) satisfy the equations (4.20) and (4.18). By analogy with hydrodynamics these solutions will be called self-similar [13]; in essence, these solutions describe the spherical waves with variable radius of curvature [2], [21].

For self-focusing in a cubic medium when $z=z_\phi$ let the focal point be formed on the axis. We shall assume that generally speaking, not the entire beam is focused on the point, but only some part of it, containing the power m_k. In the coordinates (m,z) the propagation of focusing part of the beam is written in the form

$$r(m,z) \xrightarrow[z \to z_\phi]{} 0 \tag{4.24}$$

for all m from the interval $0<m<m_k$ ($m_k<M$). Let us demonstrate that the solution of the initial problem for $z \to z_\phi$ asymptotically approaches one of the self-similar solutions (4.21), (4.23). Let us use the equation for intensity and beam trajectories

$$\rho = \frac{1}{\frac{\partial}{\partial m}\left(\frac{r^2}{2}\right)} \tag{4.25}$$

$$\frac{d^2 r}{dz^2} = \rho r \frac{\partial u}{\partial m} \tag{4.26}$$

where

$$u_r = \frac{1}{2}\left[\rho + \frac{1}{2}\rho \frac{\partial}{\partial m} r^2 \frac{\partial \rho}{\partial m} + \frac{1}{4}\left(r \frac{\partial \rho}{\partial m}\right)^2\right] \tag{4.27}$$

The solution $r^2(m,z)$ will be found in the form of the series with respect to powers of $\zeta = z_\phi - z$

$$r^2(m,z) = \zeta^{1+\alpha}\left(R^2(m) + \mathcal{O}(\zeta)\right) \tag{4.28}$$

where, generally speaking, $\alpha=\alpha(m)$, that is, for each fixed m from the interval $(0,m_k)$ the expansion of the function $r^2(m,z)$ is carried out with respect to integral or nonintegral powers of ζ.

From the equation (4.25) we obtain:

$$\rho(m,z) = \zeta^{-(1+\alpha)} \frac{1}{RR' + \alpha' \frac{R^2}{2} \ln \zeta} + \mathcal{O}(\zeta^{-\alpha}) \tag{4.29}$$

Substituting r^2 and ρ from (4.28), (4.29) in the righthand side of equation (4.26), we obtain

$$\rho r \frac{\partial u}{\partial m} = O\left(\zeta^{-\frac{1}{2}-\frac{1}{2}\alpha}\right) \tag{4.30}$$

On the other hand, it is easy to see that

$$\frac{d^2 r}{dz^2} = O\left(\zeta^{-\frac{1}{2}+\frac{\alpha}{2}}\right) \tag{4.31}$$

and, consequently, if $\alpha \neq 0$ for $0<m<m_k$, then the equation (4.26) cannot be satisfied for sufficiently small ζ. Thus, for the axial part of the beam containing the power m_k $(0<m<m_k)$ representation of the function $r^2(m,z)$ in the form of the series with respect to powers of ζ has the form

$$r^2(m,z) = \zeta R^2(m) + O(\zeta^2) \tag{4.32}$$

Substituting $r^2(m,z)$ from (4.32) in equations (4.25), (4.26) and isolating the terms of the same order of smallness, we find that the first term of the expansion of (4.32) $r^2(m,z)=\zeta R^2$ is the solution. At the same time r^2 is the function with separated variables; therefore it is one of the self-similar solutions, where in this case

$$a(z) = \sqrt{z_* - z}\ ; \quad R(m) = \frac{r}{\sqrt{z_* - z}}\ ; \quad \nu_1 = -a''a^3 = \frac{1}{4} \tag{4.33}$$

Equation (4.20) for the amplitude distribution has the form

$$\frac{1}{R}\frac{d}{dR}R\frac{du}{dR} + \left(\frac{1}{4}R^2 - 2\nu_2 + u^2\right)u = 0 \tag{4.34}$$

and the phase is defined by the expression

$$S = -\frac{1}{4}\frac{r^2}{z_* - z} - \nu_2 \ln(z_* - z) \tag{4.35}$$

Thus, we obtain the following basic result: independently of the data at the input to the nonlinear medium (for z=0) the part of the beam focused on the point assumes the shape of a converging spherical wave

$$A \xrightarrow[z \to z_*]{} \frac{1}{\sqrt{z_* - z}}\, u\left(\frac{r}{\sqrt{z_* - z}}\right) \exp i\left\{-\frac{1}{4}\frac{r^2}{z_* - z} - \nu_2 \ln(z_* - z)\right\} \tag{4.36}$$

the beams in the vicinity of the focal point have the shape of parabolas

$$r^2(m,z) \xrightarrow[z \to z_*]{} (z_* - z)R^2(m) \tag{4.37}$$

For the intensity $\rho \equiv A_0^2$ and the slope of the rays $v \equiv dr/dz$, correspondingly, we have

$$\rho \longrightarrow \frac{1}{z_\phi - z} u^2\left(\frac{r}{\sqrt{z_\phi - z}}\right), \quad v \longrightarrow -\frac{1}{2}\frac{r}{z_\phi - z} \tag{4.38}$$

In (4.36) the function is a solution of the equation (4.34) in the segment $0<R<R_k$, where

$$R_\kappa = \lim_{\zeta \to 0} \frac{r(m_\kappa, z)}{\sqrt{z_\phi - z}} \tag{4.39}$$

$$\int_0^{R_\kappa} u^2(R) R\,dR \tag{4.40}$$

Let us note that the result for the intensity (4.38) coincides with the result of reference [32] to the logarithmic factor $\sim \ln|z_\phi - z|$.

§5. Results of the Numerical Integration

Let us present the results of numerical integration of the problem. The application of the procedure described in §3 made it possible numerically to simulate the formation of the focal region and perform the calculation to high intensities where the asymptotic behavior is manifested quite clearly.

Let us present the results of the calculations for the input intensity data represented in Figure 1 (i-iii). The phase front for $z=0$ is planar for all three beams. Beam (i) is gaussian; the profile (ii) simulates the part of the beam cut off by the iris; the beam (iii) represents the profile, differing from gaussian, the power of which greatly exceeds critical. In Figure 2 (i)-(iii) the same intensity distributions are given, but as a function of the coordinate m.

The numerical calculations permitted, first of all, confirmation of the assumption (4.24), according to which during self-focusing of the beam of "supercritical" power, part of the beam is focused on the point.

Figure 3 shows the lines $(1/2)r^2(m,z)$ for $z \to z_\phi$ for the beam (i) (exactly the same picture is valid for [words missing in the original]. This graph illustrates the expression (4.37) according to which r^2 approaches zero by a linear law. The numerical solution approaches the self-similar solution. The position of the focal point (the value of z_ϕ) is determined by extrapolation of these lines to the z-axis.

Then, as the numerical calculations demonstrated, the function v(r) of the tangent of the slope angle of the beams for small ζ has a maximum (see Figure 4) corresponding to the boundary R_k (4.39), (4.40) in the sense that

$$r(v_{max}) \xrightarrow[z \to z_\phi]{} r_\kappa = r(m_\kappa, z) \tag{5.1}$$

Inside the interval $(0, m_k)$ in accordance with (4.38), the function v(r) is linear with respect to r.

The value of m_k determined by the ray of maximum slope has the same value for all three beams

$$m_k \simeq 2.0 = M_k \tag{5.2}$$

that is, part of the beam with a power on the order of critical is focused on the point.

The intensity distributions $\rho(m,z)$ with the factor ζ

$$\varphi(m,z) = (z_+ - z)\rho(m,z)$$

for the beams (i)-(iii) for small ζ are shown in Figure 5. Comparison with Figure 2 clearly illustrates the independence of the structure of these distributions with respect to the input data (let us note that these graphs always confirm the expression (5.2)). Now let us show that $\phi(m,z)$ for small ζ satisfies equation (4.34) with good accuracy. Let us replace the equation equivalent to it

$$L(\varphi) \equiv \frac{R^2}{2}\left[\varphi\varphi_{mm} + \frac{1}{2}(\varphi_m)^2 + \frac{1}{2}\right] + \varphi_m + \varphi = 2\nu_2 \quad (\varphi = u^2)$$

by the difference scheme and let us substitute the numerical values of ϕ and $R^2=r^2/$ in it. The results are presented in Table 1. Within the limits of accuracy of the system the lefthand side of the equation remains constant with respect to m to the boundary $m_k \simeq 2$ of the interval $(0,m_k)$. An estimate is obtained simultaneously for ν_2

$$\nu_2 \simeq 1.0 \tag{5.3}$$

From the results of the numerical calculations (in particular, presented in Figure 5), the estimate is obtained for $u_0^2=u^2(0)$

$$u_0^2 \simeq 9.0 \tag{5.4}$$

Figure 6 shows the function

$$\varphi(R,\zeta) = \zeta\rho\left(\frac{r}{\sqrt{\zeta}},\zeta\right) \xrightarrow[z\to z_+]{} u^2(R)$$

which gives the intensity distribution with respect to the radius and for small ζ asymptotically approaches $u^2(R)$ (the graph is presented for the gaussian beam (i); the results from all three beams (i)-(iii) for $\zeta \simeq 0$ coincide graphically).

The results of all of the presented numerical calculations indicate that the asymptotic behavior of (4.37), (4.38) is valid in the finite segment $0<R<R_k$. The processing of the numerical results gives (see (4.39))

$$R_k \simeq 2.5 \tag{5.5}$$

Figures 5 and 6 illustrate expresion (see (4.40)):

$$\int_0^{R_k} u^2(R) R\,dR = m_k \simeq 2.0 \tag{5.6}$$

Let us note, finally, the following conclusion from the result of the numerical integration: the transition from the vicinity of the focal point $0<m<m_k$ to the regular variations of the solution for $m>m_k$ is not discontinuous, there is a transition region between the singular and regular parts.

Thus, the numerical integration of the problem permits both illustration of expressions (5.25)-(5.27) and obtaining of important additional information about the behavior of the solution for $z \to z_\phi$.

§6. Ray Equation and Its Simplification

In the quasioptical approximation let us consider the problem of axisymmetric self-focusing in a medium with cubic nonlinearity on the whole, not limiting ourselves to the focusing part of the solution. Its basic complexity consists in nonlinearity of the equation (1.1), its exact analytical solution at the present time is unavailable. At the same time, combination of the analytical and numerical methods permits us to obtain quite complete information about the solution.

In §§4-5 a study was made of the problem of the structure of the focal region. It was demonstrated, in particular, that for self-focusing in a cubic medium the beam of "supercritical" power, generally speaking, only part of the beam is focused on the point (namely, including the power on the order of critical). The numerical integration of the problem with different input data permits the general conclusion of aberration nature of self-focusing to be drawn: the peripheral rays are focused more slowly than the axial rays; the self-focusing of the beam as a whole, generally speaking, does not occur. The aberrations are taken here as the errors in the lens formed by the beam on passage through a nonlinear medium. The calculation of the aberrations means in essence investigation of the behavior of the peripheral rays.

Attention was attracted to the aberrations by various authors as early as the first theoretical and experimental papers on self-focusing [15], [20], [21] and [26]. It was emphasized that the aberration self-focusing is the most typical of real beams [21]. It was noted that the aberrations must be considered, in particular, when using a nonlinear medium as the lens [26, 27]. Thus, the calculation of the aberration pattern is an important part of the problem of steady-state self-focusing in a cubic medium. In this section a study is made of the behavior of the beam during self-focusing inside the focal region, in particular, in the region of the peripheral rays. Thus, the statement of §4 and the given section mutually complement each other, completely exhausting the problem of self-focusing in a cubic medium. As was demonstrated in §§1, 3, the initial problem for the parabolic equation (1.1)-(1.3) is equivalent to the problem of determining the ray trajectories. In dimensionless variables

$$(r,z) \longrightarrow (kr, kz), \qquad A \longrightarrow \sqrt{\frac{\varepsilon_1}{\varepsilon_0}} A \tag{6.1}$$

in Lagrange coordinates (m,z) the problem can be formulated (see §2) in the form

$$\rho r \frac{\partial r}{\partial m} = 1 \tag{6.2}$$

$$\frac{d^2r}{dz^2} = \rho r \frac{\partial w}{\partial m} \tag{6.3}$$

where

$$\rho = A_0^2, \quad w = \frac{1}{2}\left[\rho + \frac{1}{2}\rho \frac{\partial}{\partial m} r^2 \frac{\partial \rho}{\partial m} + \frac{1}{4}\left(r\frac{\partial \rho}{\partial m}\right)^2\right] \tag{6.4}$$

For z=0, the following conditions must be given

$$r(m,0) = r_0(m), \quad \frac{dr}{dz}(m,0) = v_0(m); \quad \rho(m,0) = \rho_0(m) \tag{6.5}$$

where $\rho_0(m)$, $r_0(m)$ are related by the equation (6.2).

In the righthand side of the equation of the rays (6.3) the term $(1/2)\rho r(\partial\rho/\partial m)$ corresponds to the nonlinear refraction; the diffraction effects are taken into account by the remaining terms in the quasioptical approximation. The relations between them define the total "strength" acting on the given ray. However, this expression can vary sharply in transition from the axis to the periphery of the beam which is easy to be convinced of in the simplest example of the gaussian distribution of the intensity

$$\rho_0(r) = E_0^2 \exp\left(-\frac{r^2}{a^2}\right)$$

or, what amounts to the same thing

$$\rho_0(m) = E_0^2\left(1 - \frac{m}{M}\right) \tag{6.6}$$

($M=(1/2)E_0^2a^2$ is the total beam power). As is easy to see, in this case

$$\rho r \frac{\partial w}{\partial m} = r\frac{E_0^4}{2M^2}\left[m - \left(M - \frac{1}{2}\right)\right] \tag{6.7}$$

and if $M' \equiv M-(1/2)>0$, then $d^2r/dz^2<0$ for $m<M'$ and $d^2r/dz^2>0$ for $m>M'$. If for z=0 the phase front is plane ($v_0(m)=0$), then for $m<M'$ the rays are focused (deflected toward the axis, nonlinear refraction predominates); for $m>M'$ they are defocused (diffraction predominates); for $m=M'$ the beam is in "equilibrium": $d^2r/dz^2=0$.

Thus, the relation between diffraction and nonlinearity generally speaking has a local nature which depends on the coordinate of the ray. Giving the ray by the coordinate m, it is possible to talk about the dependence of the self-focusing rate on this transverse coordinate. For description of this relation it is necessary to have the solution to the problem (6.2)-(6.5).

The exact solution of problem (6.2)-(6.5) of calculating the ray trajectories for arbitrarily given conditions $r_0(m)$ and $v_0(m)$ is no less difficult than the solution of the initial problem (1.1)-(1.3) inasmuch as the system (6.2) (6.3) is equivalent to the fourth-order nonlinear equation for r(m,z). However, isolating the defined class of input distributions of intensity and phase, on the basis of the qualitative picture of the phenomenon it turns out to be possible to simplify the equations, reducing their order, and to obtain the problems solved analytically. Let us discuss these problems in more detail.

Let us consider self-focusing of the beam with arbitrary intensity distribution monotonically decreasing from the axis and smooth phase front (the standard example is a gaussian beam with plane phase front or focused or defocused by a lens). If the beam power M exceeds the critical power M_k, then for zome $z=z_\phi$, a focal point is formed on the axis. As was demonstrated in §5, the focal region in this case includes part of the beam of power $\sim M_k$, that is, in the coordinates (m,z) the focal region is $0<m<M_k$, $z\sim z_\phi$. Here for $z\sim z_\phi$ the rays are axial. Assuming that the total power M exceeds the critical by several times ($M/M_k \geq 2$), part of the beam $0<m<M_k$ will also be called axial. For $m>M_k$ and $z\sim z_\phi$ the beams do not reach the focal point and are peripheral. Hereafter this part of the beam will also be called peripheral (see Figure 7) on the entire self-focusing length.

For the formulated assumption let us substitute the problem of calculating the operations based on equations (6.2)-(6.4). Let us introduce the function of the deflection of the rays f(m,z)

$$r(m,z) = r_0(m) f(m,z) \tag{6.8}$$

The factor f is the compression coefficient (f<1) or the tension coefficient (f>1) of the transverse coordinate of the given ray. Substituting f(m,z) from (6.8) in (6.2)-(6.5), we obtain the following problem. The equations (6.2)-(6.4) reduce (after exclusion of ρ from (6.2)) to one nonlinear, fourth-order equation

$$\frac{d^2 f}{dz^2} = F\left(f, \frac{\partial f}{\partial m}, \ldots, \frac{\partial^4 f}{\partial m^4}, m\right) \tag{6.9}$$

with the boundary conditions

$$f(m,0) = 1 \tag{6.10}$$

$$\frac{df}{dz}(m,0) = \frac{v_0(m)}{r_0(m)} \tag{6.11}$$

In this form the problem is much simpler than the initial (6.2)-(6.5). However, let us turn attention to the fact that the boundary condition for f (6.10) does not depend on the specific form of the beam for z=0, and it has an especially simple form. Let us consider the variation of the function f for z>0. Its derivatives with respect to z obviously characterize the focusing or defocusing rate of the given part of the beam. At the same time its transverse derivatives (with respect to m) characterize the transverse nonuniformity of the self-focusing process, that is, the dependence of f on m describes the aberrations themselves.

The special case of the aberration-free self-focusing corresponds to independence of f with respect to m

$$f(m,z) \equiv f(z) \tag{6.12}$$

In this special case the ray trajectories r(m,z) are represented by the function with separated variables (are "similar"), and the solution of the initial problem is self-similar (§5). Near the boundary of the nonlinear medium on the basis of

the condition (6.10) with monotonic phase distribution uniform with respect to radius, it is possible approximately to consider the self-focusing aberrationless. The approximation by the condition (6.12) of the process on the whole leads to aberration-free approximation [23].

The above-substituted problem of aberrations, however, requires a more detailed picture and consideration of the variation of the function across the beam. The nonuniformities of f, small for z~0, are accumulated during the self-focusing process, noticeably distorting the shape of both the amplitude profile and the phase front.

The problem of calculating the beam trajectories can be simplified significantly if we consider the nature of the process. Let us estimate the transverse derivatives, entering into the righthand side of equation (6.9). We have

$$\frac{\partial f}{\partial m} \sim \frac{(\Delta f)_{max}}{M}, \ldots, \frac{\partial^4 f}{\partial m^4} \sim \frac{(\Delta f)_{max}}{M^4} \tag{6.13}$$

where

$$\Delta f = |f(m,z) - f(m,0)| = |f-1|; \quad (\Delta f)_{max} = \max_{0<m<M} |\Delta f|$$

In (6.13) estimates are presented for the derivatives with respect to the cross section of the entire beam as a whole. However, the beam experiences the greatest distortion for formation of the focal region and the derivative of f with respect to m are larger here than in (6.13). At the same time, on the periphery of the beam the transverse variations are smoother; correspondingly, the derivatives of f with respect to m are smaller here than from the estimates of (6.13).

Then we proceed as follows. In the region of peripheral rays we estimate the derivatives $\partial f/\partial m$, ..., $\partial^4 f/\partial m^4$ by relations analogous to (6.13), assigning them, however, a defined order of smallness μ

$$\frac{\partial f}{\partial m} \sim \mu \frac{(\Delta f)_{max}}{M}, \ldots, \frac{\partial^4 f}{\partial m^4} \sim \mu \frac{(\Delta f)_{max}}{M^4} \tag{6.14}$$

Then let us substitute these derivatives in the equations for f and let us drop the terms of higher order of smallness. Thus, we obtain the truncated equation describing the trajectories of the peripheral rays.

From equations (6.8) and (6.2) we have

$$\rho = \frac{1}{f^2 \frac{\partial}{\partial m} \frac{r_0^2}{2} + \frac{1}{2} r_0^2 \frac{\partial f^2}{\partial m}} = \frac{\rho_0}{g}$$

where

$$g = f^2 + \frac{1}{2} \rho_0 r_0^2 \frac{\partial f^2}{\partial m}$$

In the last equality we estimate the term $\frac{1}{2}\rho_0 r_0^2 \frac{\partial f^2}{\partial m}$. For beams of monotonic smooth profile (in particular, for the gaussian beams) the functions $(1/2)\rho_0(m)r_0^2(m)$ has a unique maximum at a distance on the order of the radius of the beam a from the axis, and it reaches the values of

$$\left(\frac{1}{2}\rho_0 r_0^2\right)_{max} \simeq \frac{1}{4} E_0^2 a^2 = \frac{1}{2} M$$

(E_0^2 is the intensity on the axis). On the other hand, setting $(\Delta f^2)_{max} \sim f^2$, we have

$$\frac{\partial f^2}{\partial m} \sim M \frac{f^2}{M}$$

Thus,

$$g = f^2 + \frac{1}{2}\rho_0 r_0^2 \frac{\partial f^2}{\partial m} \simeq f^2 + \frac{1}{2} M M \frac{f^2}{M} \simeq f^2$$

and

$$\rho \simeq \frac{\rho_0}{g} \tag{6.15}$$

Now let us consider the derivative $\partial\rho/\partial m$

$$\frac{\partial \rho}{\partial m} = \frac{1}{g}\frac{\partial \rho_0}{\partial m} - \frac{\rho_0}{g^2}\frac{\partial g}{\partial m}$$

Let us estimate $\partial g/\partial m$. We have

$$\frac{\partial g}{\partial m} = \frac{\partial f^2}{\partial m}\left(1 + \frac{\partial}{\partial m}\left(\frac{1}{2}\rho_0 r_0^2\right)\right) + \frac{1}{2}\rho_0 r_0^2 \frac{\partial^2 f^2}{\partial m^2}$$

Inasmuch as

$$\frac{\partial \rho_0}{\partial m} \simeq -\frac{E_0^2}{M}$$

we obtain

$$1 + \frac{\partial}{\partial m}\left(\frac{1}{2}\rho_0 r_0^2\right) = 2 + \frac{1}{2} r_0^2 \frac{\partial \rho_0}{\partial m} \simeq 2 - \frac{1}{2} r_0^2 \frac{E_0^2}{M}$$

The initial quasicoptical approximation is valid if r_0 exceeds the radius a by no more than a few times ($r_0 << ka^2$). Consequently,

$$2 - \frac{1}{2} r_0^2 \frac{E_0^2}{M} \simeq 2 - \frac{1}{2} a^2 E_0^2 \frac{1}{M} \simeq 1$$

Thus,

$$\frac{\partial g}{\partial m} \simeq \frac{\partial f^2}{\partial m} + \frac{1}{2}\rho_0 r_0^2 \frac{\partial^2 f}{\partial m^2} \simeq \frac{M}{M} f^2$$

Comparing the terms in the expression for $\partial\rho/\partial m$, we have (inasmuch as $g \simeq f^2$)

$$\frac{1}{g}\frac{\partial \rho_0}{\partial m} \simeq -\frac{1}{f^2}\frac{E_0^2}{M}; \quad \left(\frac{\rho_0}{g^2}\frac{\partial g}{\partial m}\right)_{max} \simeq \frac{E_0^2}{f^4}\frac{M}{M}f^2 \simeq M\frac{E_0^2}{M}\frac{1}{f^2}$$

and for the derivative $\partial\rho/\partial m$ we obtain

$$\frac{\partial \rho}{\partial m} \simeq \frac{1}{f^2}\frac{\partial \rho_0}{\partial m} \tag{6.16}$$

As a result, the first term in the righthand side of the beam equation (6.3) corresponding to nonlinear refraction assumes the form

$$\frac{1}{2}\rho r\frac{\partial \rho}{\partial m} \simeq \frac{1}{2}\frac{\rho_0 r_0}{f^3}\frac{\partial \rho_0}{\partial m}$$

Analogously, it is possible to obtain the approximation for the diffraction "force"

$$\frac{1}{4}\rho r\frac{\partial}{\partial m}\left[\rho\frac{\partial}{\partial m}r^2\frac{\partial \rho}{\partial m} + \frac{1}{2}\left(r\frac{\partial \rho}{\partial m}\right)^2\right]$$

For this purpose it is necessary to estimate the derivatives $\partial^2\rho/\partial m^2$ and $\partial^3\rho/\partial m^3$ entering into it similarly to how this was done for the first derivative $\partial\rho/\partial m$. As a result, we obtain

$$\frac{\partial^2 \rho}{\partial m^2} \simeq \frac{1}{f^2}\frac{\partial^2 \rho_0}{\partial m^2}, \quad \frac{\partial^3 \rho}{\partial m^3} \simeq \frac{1}{f^2}\frac{\partial^3 \rho_0}{\partial m^3}$$

and, consequently,

$$\rho r\frac{\partial u_r}{\partial m} \simeq \frac{\rho_0 r_0}{f^3}\frac{\partial u_{r0}}{\partial m} \tag{6.17}$$

where

$$u_{r0} = u_r(m,0) = \frac{1}{2}\left[\rho_0 + \frac{1}{2}\rho_0\frac{\partial}{\partial m}r_0^2\frac{\partial \rho_0}{\partial m} + \frac{1}{4}\left(r_0\frac{\partial \rho_0}{\partial m}\right)^2\right]$$

The approximate equation for f assumes the form

$$\frac{d^2 f}{dz^2} = \frac{1}{f^3}\rho_0\frac{\partial u_{r0}}{\partial m} \tag{6.18}$$

The truncated beam equation will be obtained, returning from f to $r(m,z)=r_0(m)f(m,z)$ in (6.18).

§7. General Solution of the Simplified Equation. Aberrations During Self-Focusing of Gaussian Beams. Results of Numerical Integration

The simplification of the equation (6.3) of the ray trajectory performed in the preceding section consisted in replacing the differential dependence on m entering into the equation by the parametric function (6.18). Returning from f to the ray trajectories and denoting them as before by r(m,z), let us write the truncated equation of the ray trajectories

$$\frac{d^2r}{dz^2} = -\frac{G(m)}{r^3} \tag{7.1}$$

where

$$G(m) = -r_0^4 \rho_0 \frac{\partial W_0}{\partial m} \tag{7.2}$$

The first approximation of (6.5) was written for the intensity $\rho(m,z)$. We obtain the next approximation, solving (7.1) and defining from equation (6.2)

$$\rho(m,z) = \frac{1}{r \frac{\partial r}{\partial m}} \tag{7.3}$$

Equation (7.1) is an ordinary differential equation (m plays the role of the parameter). The initial conditions (for z=0) for it will be obtained from (6.5)

$$r(m,0) = r_0(m) \tag{7.4}$$

$$\frac{dr}{dz}(m,0) = v_0(m) \tag{7.5}$$

On the basis of (7.3), r_0 and ρ_0 are related by the expression

$$\frac{1}{2} r_0^2(m) = \int_0^m \frac{dm}{\rho_0(m)} \tag{7.6}$$

therefore it is sufficient to give any of these functions.

Let us write the general solution to the problem (7.1)-(7.5). The general solution of the equation (7.1) has the form

$$r^2 = \alpha z^2 + \beta z + \gamma$$

where

$$\alpha\gamma - \beta^2 = -G$$

Considering the conditions (7.4)-(7.5), we obtain

$$\alpha = v_0^2 - \frac{G}{r_0^2}, \quad \beta = v_0 r_0, \quad \gamma = r_0^2$$

Thus, the general solution to the problem (7.1)-(7.5) has the form

$$r(m,z)=\left[\left(v_0^2+\rho_0 r_0^2\frac{\partial U_0}{\partial r_1}\right)z^2+2v_0 r_0 z+r_0^2\right]^{1/2} \tag{7.7}$$

Thus, the ray trajectories are represented by a single-parametric family of second-order curves; their type, location in the plane (r, z) and the distribution with respect to the parameter m are defined by the boundary conditions of the initial problem (7.4)-(7.5).

In accordance with the conclusions of the preceding section, the solution (7.7) of the problem (7.1)-(7.5) describes the self-focusing aberrations of a beam of power $m>M_k$ for small $M>M_k$ with arbitrary smooth amplitude and phase distribution on the boundary of the nonlinear medium.

As an example, let us consider the aberrations for self-focusing of the gaussian beam with plane phase front

$$A(r,0)=E_0\exp\left(-\frac{r^2}{2a^2}\right)$$

In the coordinates (m,z) we have

$$\left.\begin{aligned}&\rho_0(m)=E_0^2\left(1-\frac{m}{M}\right),\quad M=\tfrac{1}{2}E_0^2a^2>M_k\\&\tfrac{1}{2}r_0^2(m)=-\frac{a^2}{2}\ln\left(1-\frac{m}{M}\right)\\&v_0(m)=0\end{aligned}\right\} \tag{7.8}$$

The solution of (7.7) is written in the form

$$r(m,z)=r_0(m,z)\left[\frac{2}{a^4}(m-M')z^2+1\right]^{1/2} \tag{7.9}$$

where $M'=M-\frac{1}{2}$ (see (6.7), (7.2)).

For $0<z<z_\phi$, $m<M'$ the ray trajectories are the rays of ellipses having a common center (0,0) and the halfaxes r_0, $a^4/2(M'-m)$. For $m=M'$ the ray trajectory is a straight line $r=r_0$. Finally, for $m>M'$ the rays are deflected from the axis and are represented by arcs of hyperbolas with the halfaxes r_0, $a^4/2(m-M')$.

For the intensity profile $\rho(m,z)$ from the equation (7.3) we obtain

$$\rho(m,z)=\frac{\rho_0}{\left[(m-M')+\frac{1}{2}\rho_0 r_0^2\right]\frac{2z^2}{a^4}+1} \tag{7.10}$$

For the tangent to the slope angle of the rays to the z axis (the transverse derivative of the phase) $dr/dz=\partial s/\partial r$, from (7.9) we have

$$\frac{dr}{dz}(m,z) = \frac{2r_0^2}{a^4 r}(m-M')z \tag{7.11}$$

that is, $dr/dz>0$ for $m>M'$ and $dr/dz<0$ for $m<M'$.

Let us emphasize that here we are talking about the peripheral self-focusing rays; therefore the solution of (7.9)-(7.11) is acceptable, strictly speaking, only for $m \geq M_k$.

Let us compare the solution to the problem (7.1)-(7.5) with the results of numerical integration of the initial problem (6.2)-(6.5).

Let us consider the self-focusing of the beams with plane phase front $v_0(m)=0$ for the following input distribution of the intensity

$$\text{(i)}\ \rho_0(r) = E_0^2 \exp\left(-\frac{r^2}{a^2}\right) \tag{7.12}$$

$$\text{(ii)}\ \rho_0(r) = \frac{E_0^2}{1+(r/a)^4} \tag{7.13}$$

The distribution (i) is gaussian; the conditions (7.4), (7.5) and the solution to the problem (7.1)-(7.5) for it were written out above (7.8)-(7.11).

The profile (ii) is presented as an example of distribution differing from gaussian. Here

$$m(r) = \int_0^r \rho_0(r) r dr = \frac{1}{2} E_0^2 a^2 \operatorname{arctg} \frac{r^2}{a^2}, \quad M = \frac{\pi}{4} E_0^2 a^2$$
$$\rho_0(m) = E_0^2 \cos^2 \frac{\pi}{2} \frac{m}{M}, \quad r_0^2(m) = a^2 \operatorname{tg} \frac{\pi}{2} \frac{m}{M} \tag{7.14}$$

Let us note that the critical power M'_k of this distribution is exactly equal to M_k (in this regard, see §4): $M'_k=2.0$. Using formulas (6.17) and (7.7) and equation (7.3), it is easy to write the approximate analytical solution similarly to how this was done above for a gaussian beam.

Figure 7 shows the typical path of the rays for self-focusing of a beam of "supercritical" power; the focal and peripheral regions are noted as well as the axial region including part of the beam with a power on the order of critical.

Figure 8 shows the path of the rays during self-focusing of the gaussian beam (i) for $m>M_k$ obtained: (a) as a result of numerical integraion and (b) as a result of analytical calculation. In essence, in the region of the peripheral rays $M_k \leq m < M$ the results coincide graphically. Analogously, the conclusion of good quantitative correspondence can be drawn, comparing the results of the analytical and numerical calculations for the beam (ii) (Figure 9). Let us emphasize that the analytical picture is valid to the boundary of the focal region $m=M_k$.

Figure 10 gives the intensity distributions $\rho(r,z)$ for $z \sim z_\phi$ obtained from the numerical and the analytical calculation. Just as for the ray trajectories,

it is possible to draw the conclusion of satisfactory quantitative agrement. The results analogous to those presented are obtained for the beams (i)-(ii) of other powers (see Tables 2, 3).

Analyzing the results of the numerical and the analytical calculations, it is possible to draw the general conclusion of good quantitative agreement of the results of the numerical calculation and approximate solution of the analytical problem.

§8. Formula for the Focal Length

As was demonstrated above in §§ 6-7, the developed method permits sufficiently exact calculation of the self-focusing aberrations of the beams from a broad, in practice, important class of input data (monotonic data for the intensity and phase distribution). This method in essence gives a quantitative description of the behavior of the beam everywhere in the peripheral region $m>M_k$.

A comparison of the analytical and numerical results of solving the problem for the entire beam as a whole, including the axial region, is of interest. Such a comparison shows that the difference in the numerical solution of the problem (6.2)-(6.5) from the analytical solution of the approximate problem (7.1)-(7.5) does not exceed a few percentages for $z\leq 0.5z_\phi$ (see Tables 2, 3). Let us note that in this region good results are provided by the axial approximation [21]. On the whole it is possible to say of the solution to problem (7.1)-(7.5) that in addition to describing the behavior of the peripheral rays it gives, in any case, a semiquantitative picture of the formation of the focal region and the formation of the focal point on it. For example, let us consider the self-focusing of the gaussian beam with plane phase front. For $m<M_k<M$ the ray trajectories in the solution to the analytical problem represent a family of arcs of ellipses which f or $m\to 0$ contract to a segment of length

$$z_\phi = \frac{a^2}{\sqrt{\frac{M}{M_k^*}-1}}, \qquad M_k^* = \frac{1}{2}$$

or, in dimensional variables (6.1)

$$z_\phi = \frac{ka^2}{\sqrt{\frac{P}{P_k^*}-1}} \tag{8.1}$$

which coincides with results of the axial approximation. In the formula (8.1) P_k^* is the critical power defined in the axial approximation (in the adopted dimensionless variables it corresponds to $M_k^*=1/2$).

As was demonstrated in §7, the solution to the approximate problem in practice coincides with the numerical solution for $m>M_k$ to a value of $m=M_k$. This is explained by the fact that the approximation of §6 (smooth variation of the function f with respect to m) is violated only in the narrow interval $(M_k-\delta m, M_k+\delta m)$. Thus, the "boundary ray" $r(M_k,z)$ is well described by the solution of (7.7). At the same time this beam cuts off the region in which the beam is

focused on the point. This fact permits us to obtain the general formula of the focal length for beams of arbitrary, monotonic smooth profile. Setting $m=M_k=2$ in (7.7), from the condition $r(M_k,z)=0$ we find

$$(v_k^2+\rho_k r_k^2\frac{\partial w_k}{\partial m})z_\phi^2+2v_k r_k z_\phi+r_k^2=0 \tag{8.2}$$

where

$$r_k=r_0(M_k),\quad v_k=v_0(M_k),\quad \rho_k=\rho_0(M_k),\quad w_k=w_0(M_k)$$

and z_ϕ is determined from (8.2). As an example let us again consider the self-focusing of the gaussian beam by a plane phase front. In this case (8.2) has the form (see 7.9).

$$\frac{2}{a^4}((M_k+M_k^*)-M)z_\phi^2+1=0$$

and for the focal length we have

$$z_\phi=\frac{a^2}{2\sqrt{\frac{M}{M_k}-1.25}} \tag{8.3}$$

In Table 4a the values of z_ϕ obtained by formula (8.3) and from the numerical calculations for gaussian beams of different power are presented. In Table 4b an analogous comparison is made for the focal length of the beam (7.13). The numerical values and the values obtained from (8.2) are compared. The formula for z_ϕ is the following here

$$z_\phi=a^2\frac{1+y^2}{2\sqrt{\frac{2M}{\pi}y+\frac{y^4-9y^2+2}{1+y^2}}} \tag{8.4}$$

where

$$y=\left(\frac{r_k}{a}\right)^2=\operatorname{tg}\frac{\pi}{2}\frac{M_k}{M} \tag{8.5}$$

Setting for $M/M_k\simeq 2$–10

$$y\simeq\frac{\pi}{2}\frac{M_k}{M}$$

from (8.4) we have

$$z_\phi\simeq\frac{a^2}{4}(1+y^2)\sqrt{\frac{1+y^2}{1-\frac{7}{4}y^2}} \tag{8.6}$$

The results of the comparison indicate that in the range of powers of practical interest $M/M_k\simeq 2$ to 10, formulas (8.3) and (8.4) or (8.6) give values which are equal to the numerical values with very good accuracy. The calculations for the axial beams of power significantly exceeding critical, do not appear to be of great practical interest inasmuch as the disturbances of such a beam lead to

breakdown of it into "filaments" each of which contains a power on the order of critical [28-30]. Comparing formulas (8.3) and (8.4), it is possible to draw the following conclusion: the focal length is determined as a function of the power to a great extent by the form of the amplitude profile.

The formula for the focal length (the self-focusing length) is of unconditional interest for applied problems inasmuch as it includes the values experimentally known or subject to determination (the power P, the distance to the focal region z_ϕ, the nonlinearity coefficient ε_2, the beam radius a).

A study was made above of the beams with monotonic smooth distributions of intensity and phase. The nonmonotonic profiles correspond to annular structures which can also be generated by diffraction on the edge of the "clipped" smooth amplitude distribution. In these cases the behavior of the beam differs, generally speaking, from the above-investigated case of "monotonic" self-focusing [31]. Using the solution to problem (6.1)-(6.5) here, we find that the defined beam trajectories (7.7) for some z' begin to intersect, which corresponds to going beyond the framework of the approximation adopted in §6. For $z<z'$ the solution to the problem (7.1)-(7.5) is applicable in any case for the description of the initial phase of development of the nonmonotonicities.

BIBLIOGRAPHY

1. Askar'yan, G. A. "Effect of the Intense Electromagnetic Radiation Field Gradient on the Electrons and Atoms," ZHETF [Journal of Experimental and Theoretical Physics], Vol 42, No 6, 1962, pp 1567-1570.

2. Akhmanov, S. A.; Sukhorukov, A. P.; Khokhlov, R. V. "Self-Focusing and Diffraction of Light in a Nonlinear Medium," UFN [Progress in the Physical Sciences], Vol 93, No 1, 1967, pp 19-70.

3. Lugovoy, V. N.; Prokhorov, A. M. "Theory of the Propagation of Powerful Laser Radiation in a Nonlinear Medium," UFN, Vol 111, No 2, 1973, pp 203-247.

4. Svelto, O. "Self-Focusing, Self-Trapping and Self-Phase Modulation on Laser Beam," PROGRL OPTICS 12, Amsterdam-London, 1974, pp 1-51.

5. Bespalov, V. I.; Talanov, V. I. "Filamentary Structure of Light Beams in Nonlinear Liquids," PIS'MA V REDAKTSIYU ZHETF [Letters to the Editors of the Journal of Experimental and Theoretical Physics], Vol 3, No 12, 1966, pp 471-476.

6. Dirak, P. A. M. PRINTSIPY KVANTOVOY MEKHANIKI [Principles of Quantum Mechanics], Fizmatgiz, Moscow, 1960.

7. Degtyarev, L. M.; Krylov, V. V. "Method of Numerical Solution of the Problems of Dynamics of Wave Fields with Singularities," ZH. VYCHISL. MATEM. I MATEM. FIZ. [Journal of Computational Mathematics and Mathematical Physics], Vol 17, No 6, 1977, pp 1523-1530.
Gorbushina, T. A.; Degtyarev, L. M; Krylov, V. V. PREPRINT IPM AN SSSR [Preprint of the Institute of Applied Mathematics of the USSR Academy of Sciences, No 51, 1976.

8. Degtyarev, L. M.; Krylov, V. V. "Asymptotic Behavior of the Solution of the Problem of Self-Focusing of Light in a Cubic Medium," DAN SSSR [Reports of the USSR Academy of Sciences], Vol 241, No 1, 1978, pp 64-67. Gorbushina, T. A.; Degtyarev, L. M.; Krylov, V. V. PREPRINT IPM AN SSSR, No 122, 1977.

9. Degtyarev, L. M.; Krylov, V. V. "Approximate Description of the Self-Focusing of Light in a Cubic Medium," PREPRINT IPM AN SSSR, No 75, 1978.

10. Goloviznin, V. M.; Samarskiy, A. A.; Favorskiy, A. P. "Variation Approach to the Construction of Finite-Difference Mathematical Models in Hydrodynamics," DAN SSSR, Vol 235, No 6, 1977, pp 1285-1287.

11. Favorskiy, A. P. "Variation-Discrete Models of the Equations of Hydrodynamics," PREPRINT I. PRIKL. MATEM. IM. M. V. KELD'SHA AN SSSR [Preprint of the Institute of Applied Mathematics imeni M. V. Keldysh of the USSR Academy of Sciences, No 159, 1979.

12. Samarskiy, A. A.; Popov, Yu. P. RAZNOSTNIYE SKHEMY GAZOVOY DINAMIKI [Difference Systems of Gas Dynamics], Nauka, 1975.

13. Talanov, V. I. "Self-Similar Wave Beams in Nonlinear Dielectric," IZV. VUZOV (RADIOFIZIKA) [News of the Institutions of Higher Learning, Radiophysics], Vol 9, No 2, 1966, pp 410-412.

14. Mattar, F. P. "A Fluid Approach to Nonlinear Optics Propagation, PROCEEDINGS OF THE EIGHTH CONFERENCE ON NUMERICAL SIMULATION OF PLASMAS, 1978, USA.

15. Kelley, P. L. "Self-Focusing of Optical Beams," PHYS. REV. LETTERS, Vol 15, No 26, 1965, pp 1005-1008.

16. Morse, F. M.; Fishbach, G. METODY TEORETICHESKOY FIZIKI [Methods of Theoretical Physics], Vol 1, IIL, Moscow, 1958.

17. Malyuzhinets, G. D. "Development of the Representations of Diffraction Phenomena," UFN, Vol 59, No 2, pp 321-334.

18. Samarskiy, A. A. VVEDENIYE V TEORIYU RAZNOSTNYKH SKHEM. [Introduction to the Theory of Difference Systems], Nauka, 1973.

19. Karamzin, Yu. N. "Difference Systems for Calculating the Three-Frequency Interactions of Quasimonochromatic Waves Considering Diffraction," ZH.VYCHISL. MATEM. I MATEM. FIZ, Vol 15, 1975, pp 429-435.

20. Chiao, R. Y.; Garmire, E.; Towns, C. H. "Self-Trapping of Optical Beams," PHYS. REV. LETT., Vol 13, No 5, 1964, pp 479-482.

21. Akhmanov, S. A.; Sukhorukov, A. P.; Khokhlov, R. V. "Self-Focusing and Self-Channeling of Intense Light Beams in a Nonlinear Medium," ZHETF, Vol 50, No 6, 1966, pp 1537-1549.

22. Talanov, V. I. "Self-Focusing of Wave Beams in Nonlinear Media," PIS'MA V REDAKTSIYU ZHETF, Vol 2, No 5, 1965, pp 218-222.

23. Vlasov, S. N.; Talanov, V. I.; Petrishchev, V. A. "Average Description of Wave Beams in Linear and Nonlinear Media (Method of Moments)," IZV. VUZOV (RADIOFIZIKA), Vol 14, No 9, 1971, pp 1353-1363.

24. Born, M.; Wolf, E. OSNOVY OPTIKI [Fundamentals of Optics], Nauka, 1973.

25. Yankauskas, Z. K. "Radial Field Distributions in a Self-Focused Light Beam," IZV. VUZOV (RADIOFIZIKA), Vol 9, No 2, 1966, pp 413-415.

26. McWane, P. D. "Variable Focal Length Lenses Using Materials with Intensity-Dependent Refractive Indexes," NATURE, Vol 241, No 5053, 1966, pp 1081-1082.

27. Kaplan, A. Ye. "External Self-Focusing of Light by a Nonlinear Layer," IZV. VUZOV (RADIOFIZIKA), Vol 12, No 6, 1969, pp 669-674.

28. Suadam, B. R. "Self-Focusing of Very Powerful Laser Beams," II IEEE J. QUANT. ELECTRON., Vol 10, No 11, 1974, pp 837-843.

29. Rozanov, N. N.; Smirnov, V. A. "Decay of Limited Laser Beams in a Nonlinear Medium," ZHETF, Vol 70, No 6, 1976, pp 2060-2073.

30. Lyakhov, G. A. "Stratification of a Gaussian Laser Beam in a Cubic Medium," OPTIKA I SPEKTROSKOPIYA [Optics and Spectroscopy], Vol 33, No 5, 1972, pp 969-974.

31. Baranova, N. B.; Zel'dovich, B. Ya.; Senatskiy, Yu. V. "Diffraction Phenomena in Powerful Light Pulse Amplifiers and Their Effect on the Self-Focusing of a Laser Beam," PREPRINT FIAN SSSR [Preprint of the Physics Institute of the USSR Academy of Sciences], No 24, 1974.

32. Vlasov, S. N.; Piskunova, L. V.; Talanov, V. I. "Field Structure Near a Singularity Arising During Self-Focusing in a Cubic Medium," ZHETF, Vol 75, No 5(11), 1978, pp 1602-1609.

$\zeta = 3,43 \cdot 10^{-4}$ $\gamma_\varphi = 0,291208$		$\zeta = 2,29 \cdot 10^{-4}$ $\gamma_\varphi = 0,180549$		$\zeta = 4,0 \cdot 10^{-5}$ $\gamma_\varphi = 0,284004$	
m	$\frac{1}{2} L(\varphi)$	m	$\frac{1}{2} L(\varphi)$	m	$\frac{1}{2} L(\varphi)$
0,07	I,076	0,07	I,077	0,2I	I,042
0,25	I,070	0,25	I,07I	0,38	I,044
0,44	I,08I	0,44	I,083	0,55	I,039
0,63	I,065	0,63	I,034	0,7I	I,040
0,8I	I,040	0,8I	I,042	0,88	I,04I
I,00	I,087	I,00	I,089	I,05	I,040
I,I9	I,085	I,I9	I,086	I,22	I,042
I,38	I,062	I,38	I,022	I,38	I,050
I,56	I,065	I,56	I,086	I,55	I,052
I,75	I,087	I,75	I,088	I,72	I,06I
I,94	I,09I	I,94	I,090	I,89	I,073

Table 1

z \ m	0,373	0,773	I,I73	I,573	I,973	2,373	2,773	3,I73	3,573	3,973
		(1)	Результаты численного интегрирования							
0,000	0,22I3	0,3278	0,4I67	0,4999	0,583I	0,6707	0,7688	0,8879	I,0578	I,577I
0,096	0,I962	0,2950	0,3809	0,464I	0,5497	0,6420	0,747I	0,8759	I,0595	I,60I8
0,I73	0,I467	0,226I	0,3007	0,3793	0,4674	0,5695	0,69I2	0,8432	I,0585	I,6502
0,228	0,I008	0,I674	0,2I38	0,2786	0,3609	0,47I2	0,6I70	0,802I	I,0540	I,6939
0,264	0,06I7	0,0972	0,I339	0,I793	0,2462	0,36II	0,54I8	0,7654	I,0498	I,7248
0,279	0,0380	0,060I	0,0835	0,II40	0,I650	0,2846	0,5006	0,7475	I,0478	I,7389
0,288	0,0I92	0,0304	0,0423	0,0583	0,0889	0,22II	0,4754	0,7370	I,0462	I,7466
		(2)	Результаты аналитического расчета							
0,000	0,22I3	0,3278	0,4I67	0,4999	0,583I	0,6707	0,7688	0,8879	I,0578	I,577I
0,096	0,I940	0,2928	0,3790	0,4628	0,549I	0,642I	0,7478	0,877I	I,0607	I,6I03
0,I73	0,II04	0,I925	0,2767	0,3664	0,4640	0,5728	0,6985	0,8523	I,067I	I,6704
0,228	*	*	0,0745	0,2227	0,3522	0,4889	0,642I	0,8253	I,0739	I,73I7
0,264	*	*	*	*	0,2254	0,4093	0,593I	0,8030	I,0792	I,7793
0,279	*	*	*	*	0,I256	0,365I	0,568I	0,792I	I,08I8	I,80I7
0,288	*	*	*	*	*	0,3386	0,5540	0,786I	I,0832	I,8I37

Table 2. Trajectories of rays r(m,z) during self-focusing of a gaussian beam ($M/M_k=2$, $a^2=1/2$)

Key:
1. Results of numerical integration
2. Results of analytical calculation

$\frac{m}{z}$	2,011	4,189	6,367	8,545	10,72	12,90	15,08	17,26	19,44	21,61	Координаты лучей в приосевой области (z =0,146)
(2) Результаты численного интегрирования											
0,000	0,355	0,518	0,648	0,769	0,890	1.021	1,173	1,366	1,640	2,115	m числ. аналит.
0,050	0,349	0,505	0,632	0,751	0,872	1,005	1,161	1,357	1,635	2,113	0,168 0,091 0,092
0,099	0,326	0,464	0,580	0,694	0,817	0,956	1,123	1,331	1,620	2,107	0,503 0,153 0,157
0,146	0,281	0,390	0,486	0,591	0,718	0,873	1,061	1,291	1,599	2,099	0,838 0,192 0,200
0,186	0,196	0,276	0,350	0,442	0,577	0,768	0,950	1,247	1,575	2,089	1,173 0,223 0,233
0,210	0,014	0,096	0,178	0,279	0,443	0,681	0,939	1,216	1,559	2,082	1,508 0,248 0,260
(3) Результаты аналитического расчета											1,843 0,271 0,283
0,000	0,355	0,518	0,648	0,769	0,890	1,021	1,173	1,366	1;640	2,115	2,178 0,291 0,303
0,050	0,349	0,505	0,632	0,751	0,872	1,005	1,161	1,357	1,635	2,113	2,513 0,310 0,322
0,099	0,328	0,466	0,580	0,693	0,817	0,957	1,123	1,331	1,620	2,107	2,848 0,327 0,339
0,146	0,294	0,397	0,486	0,592	0,721	0,876	1,060	1,288	1,596	2,098	3,183 0,344 0,354
0,186	0,248	0,299	0,351	0,449	0,593	0,772	0,983	1,237	1,569	2,088	3,519 0,360 0,369
0,210	"	"	0,193	0,298	0,474	0,684	0,921	1,198	1,547	2,080	3,854 0,375 0,383
											4,189 0,390 0,397

Table 3. Trajectories of rays during self-focusing of a beam (ii) of "bell-shaped' profile. ($M/M_k=8\pi$, a=1)

Key:
1. Coordinates of the rays in the axial region (z=0.146)
2. Results of numerical integration
3. Results of analytical calculation

	$z_ф$ \ $M_1/M_к$	1,5	2	3	4	5	7	9	I2
(1)	Численное значение	0,4342	0,29I2	0,I898	0,I473	0,I232	0,0960	0,0804	0,0665
(2)	Формула (8.3)	0,5000	0,2887	0,I890	0,I503	0,I29I	0,I043	0,0898	0,0782
(3)	Формула (4.I5) из работы 23.	0,5079	0,3249	0,2055	0,I575	0,I307	0,I0I0	0,0844	0,0695

(4) а) Фокусные расстояния гауссовых пучков (i) ($a^2 = I/2$).

	$z_ф$ \ $M/M_к$	π	$3/2\pi$	2π	3π	4π
(5)	Численное значение	0,4933	0,3452	0,2839	0,2304	0,2I09
(6)	Формула (8.4)	0,4942	0,328I	0,2900	0,2667	0,2592
(7)	Формула (8.6)	0,4658	0,3262	0,290I	0,267I	0,2592

(8) (б) Фокусные расстояния пучков (ii) "колокообразного" профиля ($a^2 = I$).

Table 4. Values of the focal lengths (self-focusing lengths) obtained from numerical calculations and by analytical formulas

Key:
1. Numerical value
2. Formula (8.3)
3. Formula (4.15) from reference [23]
4. a) focal lengths of gaussian beams (i) ($a^2=1/2$)
5. Numerical value
6. Formula (8.4)
7. Formula (8.6)
8. b) focal lengths of beams (ii) of "bell-shaped profile" ($a^2=1$)

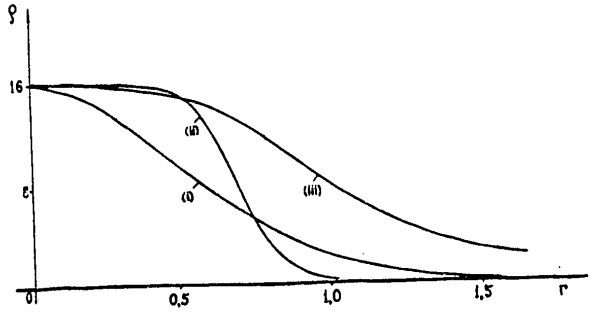

(i) $\rho(r) = E_0^2 \exp(-\frac{r^2}{a^2})$ $M = \frac{1}{2}E_0^2 a^2$ ($E_0=4$, $a^2=\frac{1}{2}$; $M=4$)

(ii) $\frac{r^2}{2} = \frac{a^2}{2}\int_{\rho}^{E_0^2} \frac{E_0^{2N}\, d\rho}{2\rho(E_0^2-\rho)^{1/2}}$ $M = E_0^2 a^2$ ($E_0=4$, $a=1/2$; $M=4$)

(iii) $\rho(r) = \frac{E_0^2}{1+(\frac{r}{a})^2}$ $M = \frac{\pi}{2}E_0^2 a^2$ ($E_0=4$, $a=1$; $M=4\pi$)

Figure 1. Input intensity data (as a function of r)

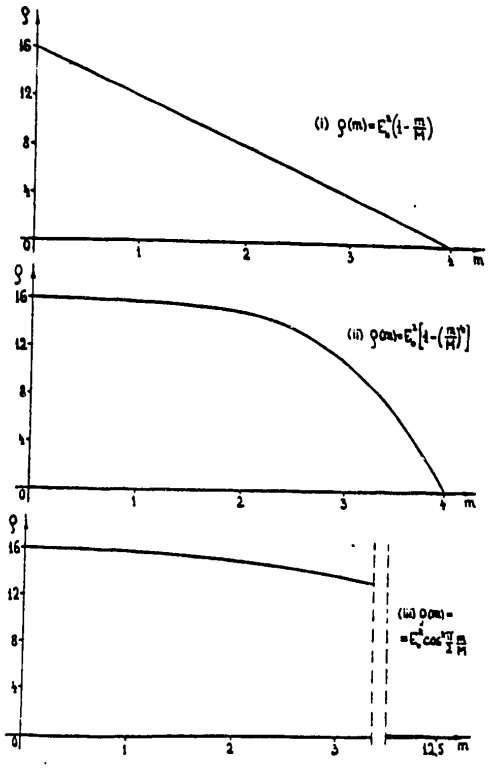

Figure 2. Input intensity data (as a function of m)

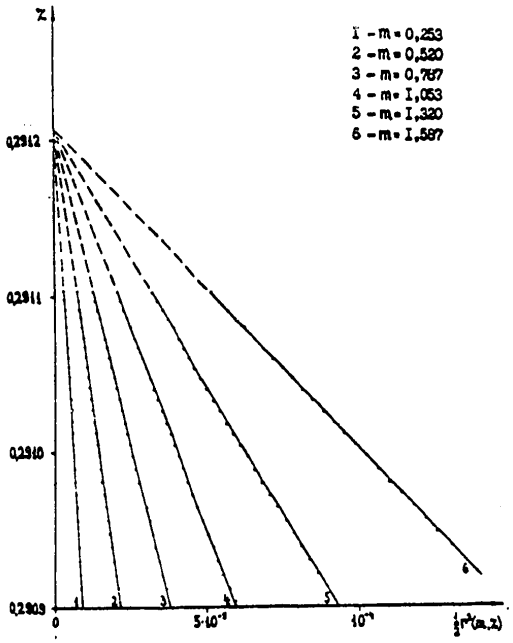

Figure 3. (i). Asymptotic behavior in the vicinity of the focal point: lines $(1/2)r^2(m,z)$, beams (i)

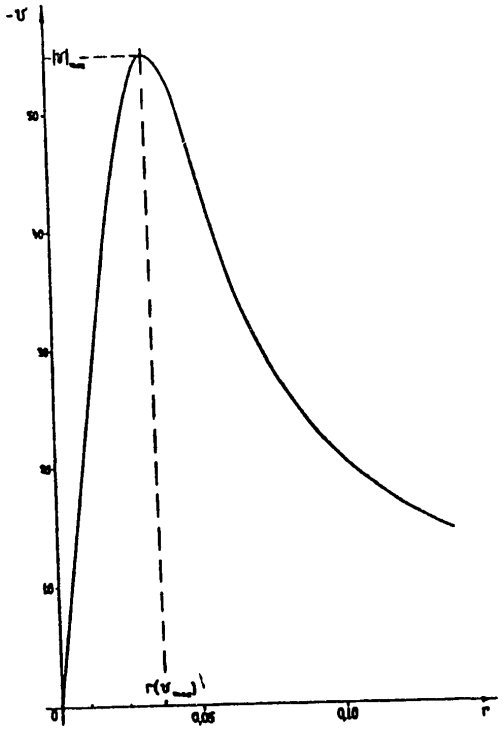

Figure 4. Slope of the rays $v(r)=\partial s/\partial r$ for $z \sim z_\phi$ (beam (i); $\zeta=2.51\cdot10^{-4}$)

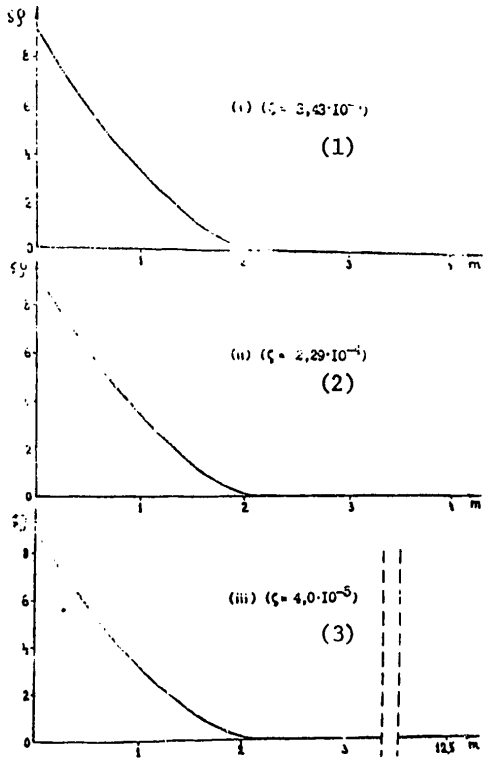

Figure 5. Intensity distribution as a function of the coordinate m.

Key:
1. (i) ($\varsigma=3.43\cdot10^{-4}$)
2. (ii) ($\varsigma=2.29\cdot10^{-4}$)
3. (iii) ($\varsigma=4.0\cdot10^{-5}$)

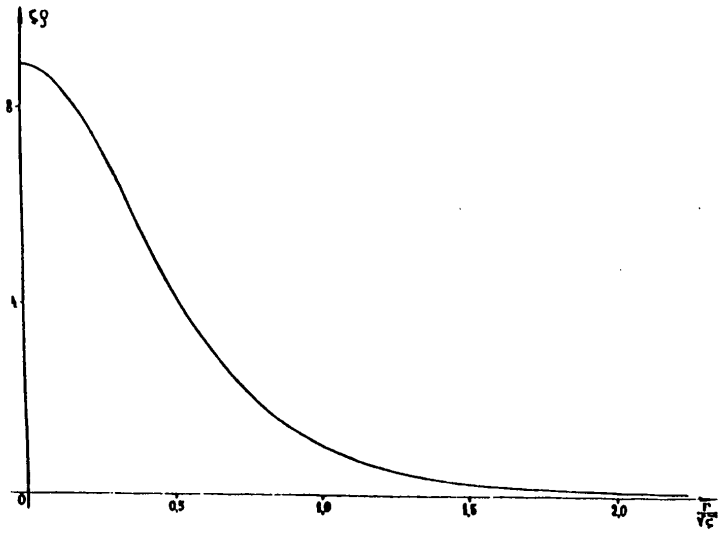

Figure 6. Intensity in the vicinity of the focal point: distribution with respect to radius

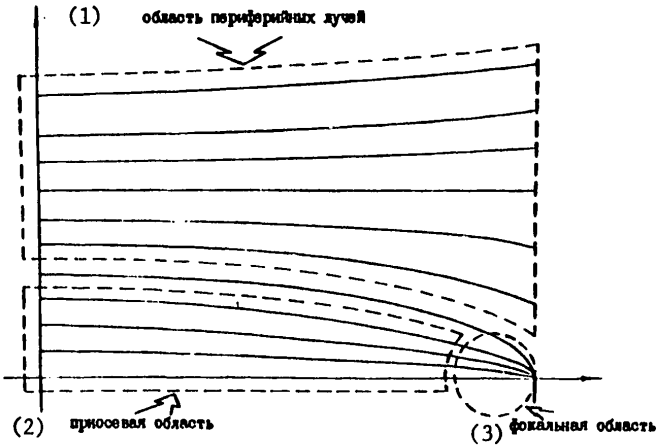

Figure 7. Behavior of the rays during self-focusing: axial, focal and peripheral regions

Key:
1. region of peripheral rays
2. axial region
3. focal region

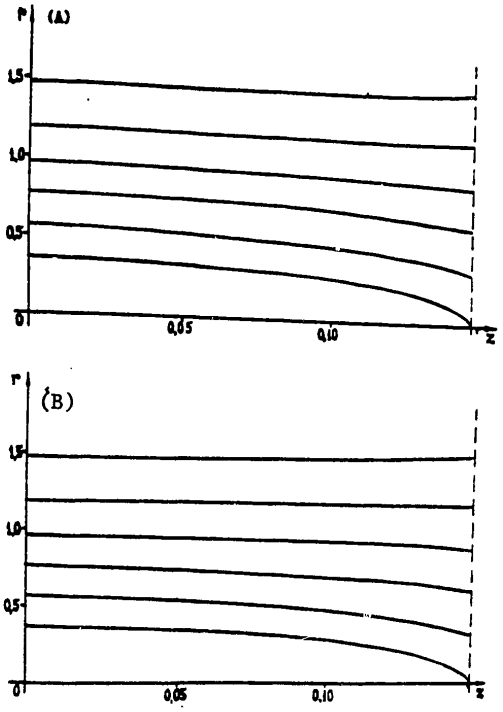

Figure 8. Aberrations (peripheral rays) during self-focusing of a gaussian beam of "supercritical" power ($M/M_k=4$): numerical integration (A) and analytical calculation (B)

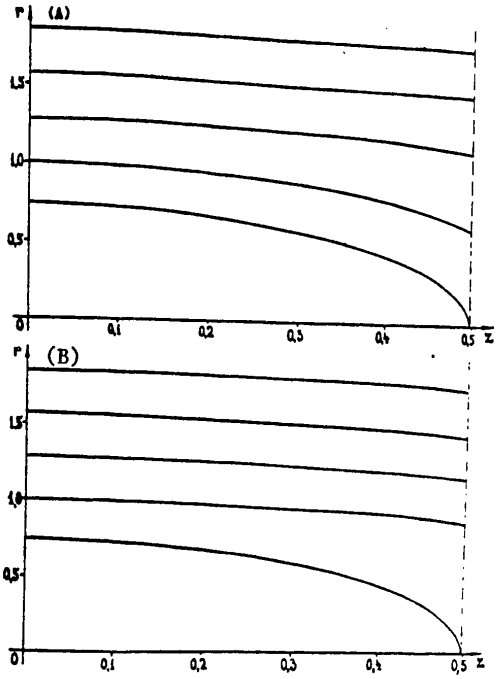

Figure 9. Aberrations (peripheral rays) during self-focusing of a beam of "bell-shaped" profile of intensity (ii) ($M/M_k=\pi$: numerical integration (A) and analytical calculation (B)

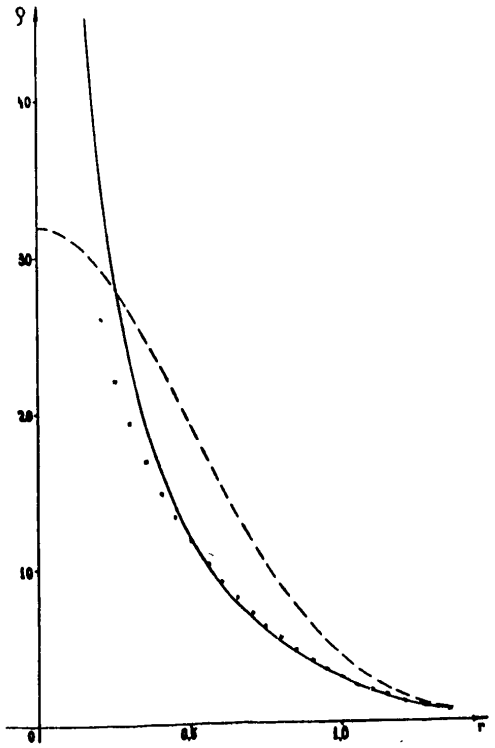

Figure 10. Intensity distribution with respect to radius for $z \sim z_0$ in the region of peripheral radius (gaussian beam, $M/M_k=4$). The results of the analytical calculations (the solid line) and numerical integration. The dotted line -- distribution for z=0.

VARIATION SYSTEMS OF MAGNETOHYDRODYNAMICS IN AN ARBITRARY COORDINATE SYSTEM

[V. M. Goloviznin, T. K. Korshiya, A. A. Samarskiy, V. F. Tishkin, A. P. Favorskiy, pp 162-185]

Introduction

One of the basic concepts used for numerical solution of the applied problems of mathematical physics consists in the fact that the difference scheme is considered as a digital analog of the used physical model. According to this principle, the quality of the system can be determined not only by the canonical categories of the theory of numerical methods, but also by how completely the corresponding discrete model carries over the basic features of the real process.

Thus, for example, for description of physical system the primary role is played by the conservation laws. The satisfaction of difference analogs of these laws must be considered the most important requirement imposed on the discrete model of the medium. The successive application of this principle has made it possible to isolate a class of conservative [1] and then also completely conservative difference systems for the equations of hydrodynamics and magnetohydrodynamics [2]-[4]. Here it turned out that one and the same difference scheme corresponds to qualitatively different mathematical forms of writing the initial equations.

In this paper the completely conservative difference schemes for three-dimensional equations of magnetohydrodynamics written in an arbitrary system of coordinates are constructed beginning with the generalized principle of the least Hamiltonian effect [5]. The use of the variation approach permits automatic obtaining of difference analogs of the conservation laws as a direct consequence of the absence of explicit dependence of the Lagrangian on the spatial coordinates in time.

A significant disadvantage of the variation principle is its invariance with respect to the choice of the specific system of coordinates and form of representation of the vector and tensor fields. The use of the apparatus of tensor calculus permits constructive formalization and simplification of the construction procedure and the procedure for realizing the difference schemes. Here the difference equations are written in a unique form in different coordinate systems.

It must be noted that in the case of two spatial variables for Cartesian, cylindrical and spherical coordinates, the obtained systems coincide with those presented in references [6]-[10].

In this paper a study is made of the properties of the constructed difference schemes. It is demonstrated that the three-dimensional variation schemes of magnetohydrodynamics have the property of complete conservativeness, and they have second order approximation. The results of the test calculations and comparison with the exact solutions are presented.

In conclusion, the authors express their appreciation to M. Yu. Shashkov and V. A. Gasilov and also B. Ya. Lyubimov who participated in the discussion of the differential equations and made a number of important suggestions.

§1. Differential Equations

1. During numerical simulation of the motion of a continuous medium it turns out to be convenient to use the formalism based on the introduction of the Lagrange function [3]. In the absence of dissipative processes the Lagrangian of the continuous medium submerged in a magnetic field can be represented in the form

$$\mathcal{I} = \int_{\Omega} \left(\frac{v_i v^i}{2} - \varepsilon - \frac{H_i H^i}{8\pi\rho} \right) \rho \sqrt{g}\, d\Omega \tag{1.1}$$

Here the arbitrary stationary curvilinear coordinate system x^i, $i=1,2,3$ is used as the Euler coordinate system; ρ is the density, ε is the specific internal energy, v_i, v^i are the covariant and contravariant components of the velocity vector, H_i, H^i are the covariant and contravariant components of the magnetic field intensity vector $\vec{H}$, Ω is the region occupied by the medium, $d\Omega = dx^1 dx^2 dx^3$, g is the determinant of the metric tensor g_{ik}. Hereafter it is proposed that the Latin indexes assume values from 1 to 3; the repeating index indicates summation.

Proceeding to the Lagrangian coordinates q^i, that is, setting $x^i = x^i(q^1, q^2, q^3, t)$, $\partial x^i/\partial t = v^i(q^1, q^2, q^3, t)$. It is possible to rewrite the Lagrangian (1.1) in the form

$$\mathcal{I} = \int_{\Omega_q} \left(\frac{v_i v^i}{2} - \varepsilon - \frac{H_i H^i}{8\pi\rho} \right) \rho J \sqrt{g}\, d\Omega_q \tag{1.1'}$$

where $\Omega_q = \Omega(x(q))$, $d\Omega = dq^1 dq^2 dq^3 \cdot \partial(x^1, x^2, x^3)/\partial(q^1, q^2, q^3)$.

The assignment of the Lagrangian together with the auxiliary relations reflecting the characteristic features of the flow completely describes the magnetohydrodynamic system. In the investigated case the role of such relations is played by the continuity conditions, the conditions of conservation of the magnetic current and adiabatic nature.

2. The continuity condition follows from the law of conservation of mass of arbitrary liquid volume $\Omega' \subset \Omega$

$$\frac{d}{dt} M_{\Omega'} = \frac{d}{dt} \int_{\Omega'} \rho \sqrt{g}\, d\Omega = \frac{d}{dt} \int_{\Omega'_q} \rho J \sqrt{g}\, d\Omega_q = 0$$

or

$$\rho J \sqrt{g} = \rho_0(\vec{q}) \tag{1.2}$$

If we take the coordinates of the particles of the medium at the initial point in time as q^i, then ρ_0 has the meaning of density for t=0. Differentiating (1.2) with respect to time, we obtain the relation

$$\frac{d\rho}{dt} + \rho \frac{1}{\sqrt{g}} \frac{\partial \sqrt{g} v^i}{\partial x^i} = 0 \tag{1.2}$$

which are the continuity equation in the curvilinear coordinate system [11].

3. The condition of conservation of the magnetic flux through an arbitrary liquid surface Σ (the conditions of freezing for an infinitely electrically conducting medium) is expressed in the form

$$\frac{d}{dt} \int_{\Sigma} H^i \sqrt{g}\, dS_i = 0 \tag{1.3}$$

here dS_i are the components of the pseudovector of the elementary area [11]. The values of $\sqrt{g}\, dS_i$ are components of the vector directed along the model to the element of the surface and equal with respect to absolute magnitude to its area. Using the rules of conversion of the pseudovectors [12], we find that

$$\frac{d}{dt} \int_{\Sigma_q} H^i J \sqrt{g} \frac{\partial q^k}{\partial x^i} dS_{qk} = 0 \tag{1.4}$$

Here dS_{qk} are the components of $\vec{dS}$ in the Lagrangian coordinate system. From (1.4) it is easy to obtain the freezing conditions in the form

$$\sqrt{g}\, J_i^k H^i = \Phi^k(\vec{q}) \tag{1.5}$$

where the following notation is introduced

$$J_i^k = J \frac{\partial q^k}{\partial x^i} = \frac{1}{2} e^{kmn} \varepsilon_{ike} \frac{\partial x^k}{\partial q^m} \frac{\partial x^\ell}{\partial q^n}$$

ℓ^{kmn}, $\ell_{ik\ell}$ are absolutely antisymmetric tensors [12]. Considering the properties J_i^k

$$J_i^k \frac{\partial x^m}{\partial q^k} = \delta_i^m J; \quad \frac{\partial J_i^m}{\partial q^m} = 0 \tag{1.6}$$

it is easy to resolve the equalities (1.5) with respect to H^i

$$J \sqrt{g} H^i = \Phi^k \frac{\partial x^i}{\partial q^k} \tag{1.7}$$

From (1.7) the equations follow directly for the induction and variation of the energy of the magnetic field in the Lagrangian variables:

$$J\sqrt{g}\,\frac{dH^i}{dt} = -H^i\frac{d\,J\sqrt{g}}{dt} + \varphi^\kappa\frac{\partial v^i}{\partial q^\kappa} \tag{1.8}$$

$$\frac{d}{dt}\left\{J\sqrt{g}\,\frac{H_i H^i}{8\pi}\right\} = -\frac{H_i H^i}{8\pi}\frac{d\,J\sqrt{g}}{dt} + \tag{1.9}$$

$$+\frac{H_i\varphi^\kappa}{4\pi}\frac{\partial v^i}{\partial q^\kappa} + \frac{J\sqrt{g}\,H^m H^n}{8\pi}\frac{d\,g_{mn}}{dt}$$

The transition from Lagrangian variables q^i to the variables x^i permits the equations (1.8) and (1.9) to be reduced to the ordinary Euler form of notation. Omitting the intermediate calculations, for example, let us convert the equation of magnetic field induction:

$$\frac{dH_i}{dt} + v^\kappa H^\ell\Gamma^i_{\ell\kappa} = -\frac{H^i}{\sqrt{g}}\frac{\partial\sqrt{g}\,v^\kappa}{\partial x^\kappa} + H^\kappa v^{\ i}_{;\,\kappa} \tag{1.8}$$

where $v^{\ i}_{;\kappa} = \frac{\partial v^i}{\partial x^\kappa} + v^\ell\Gamma^i_{\ell\kappa}$, $\Gamma^i_{\ell\kappa}$ are the second-type Christoffel symbols (see, for example [11]).

4. The conditions of adiabatic flow are expressed by the equality:

$$d\varepsilon = -p\,d\left(\frac{1}{\rho}\right) \tag{1.10}$$

Jointly with the continuity equation (1.2) condition (1.10) defines the law of variation of ε

$$\rho\frac{d\varepsilon}{dt} = -p\frac{d}{dt}\left[J\sqrt{g}\right] \tag{1.11}$$

5. According to the principle of least effect according to Hamilton, the motion of the medium takes place in such a way that the functional of the effect $F = \int_{t_0}^{t_1}\mathcal{L}\,dt$ assumes a stationary value [5], that is,

$$\delta F = \int_{t_0}^{t_1}\int_{\Omega_q}\left\{\rho_0\left[g_{ie}\,v^\ell\,\delta v^i + \frac{v^i v^\ell}{2}\frac{\partial g_{ie}}{\partial x^\kappa}\delta x^\kappa - \right.\right. \tag{1.12}$$

$$\left. - \delta\varepsilon\right] - \delta(J\sqrt{g})\frac{H_i H^i}{8\pi} - \frac{J\sqrt{g}}{4\pi}g_{ie}H^\ell\delta H^i -$$

$$\left. - \frac{J\sqrt{g}}{4\pi}H^\ell H^i\frac{\partial g_{i\ell}}{\partial x^\kappa}\delta x^\kappa\right\}d\Omega_q\,dt = 0$$

Using the additional conditions (1.2), (1.7), (1.10) from (1.12) it is possible to exclude the versions $\delta\varepsilon$, δv^i, δH^i, $\delta(J\sqrt{g})$, expressing them in terms of the variation δx^i.

Equating the factors to zero for independent variations, we arrive at the equation of motion of magnetohydrodynamics:

$$\rho_0\left(\frac{dv_i}{dt}-\frac{v^\kappa v^\varepsilon}{2}\frac{\partial g_{\kappa\varepsilon}}{\partial x^i}\right)=-\sqrt{g}\frac{\partial}{\partial q^j}(p^*)_i+$$
$$+\frac{\partial}{\partial q^\varepsilon}\frac{H^i q^\varepsilon}{4\pi}-\frac{H^\kappa H^\varepsilon}{8\pi}\frac{\partial g_{\kappa\varepsilon}}{\partial x^i}\,J\sqrt{g}. \tag{1.13}$$

where $p^*=p+\frac{H_iH^i}{8\pi}$.

The equations (1.2), (1.7) or (1.8), (1.11) and (1.2) agree with the kinematic relations $dx^i/dt=v^i$ and the equation of state $p=p(\rho, \varepsilon)$ completely define the behavior of the dissipativeless MHD-medium for the corresponding initial and boundary conditions.

For distribution of the initial magnetic field it is necessary to satisfy observation of the condition of solenoidality

$$\operatorname{div}\vec{H}=H^i_{;i}=\frac{1}{\sqrt{g}}\frac{\partial}{\partial x^i}(\sqrt{g}H^i)=0 \tag{1.14}$$

which can be expressed in terms of the fluxes ϕ^i as follows

$$\frac{\partial\Phi^i}{\partial q^i}=0 \tag{1.15}$$

§2. Discrete Model

1. We shall assume that Ω_q is a unit cube in the space of the Lagrangian variables q^i. In Ω_q let us introduce the rectangular difference net with the steps $\Delta q^i=h_i$. We shall index the finite-difference values by the Greek letters. Let us place a triplet of natural numbers in correspondence to each node:

$$(\alpha,\beta,\gamma)\in\omega_h=\{(\alpha,\beta,\gamma):\ \alpha=0,1,\ldots,N,\ \beta=0,1,\ldots,M,$$
$$\gamma=0,1,\ldots,P\}.$$

The set of all nodes defining the finite-difference cell (elementary parallelepiped) will be denoted by W_1, considering that the index of the cell is equal to the nodal index $(\alpha,\beta,\gamma)\in W_1$, in which min $(\alpha+\beta+\gamma)$ is reached. The set of all cells containing the given node (α,β,γ) as the apex will be called $W_2(\alpha,\beta,\gamma)$. Let us introduce the set of cells ω_h and all the internal nodes $\overset{\circ}{\omega}_h$, and also the space of the finite-difference functions R_h and $\overset{\circ}{R}_h$ defined in ω_h and $\overset{\circ}{\omega}_h$, respectively.

The values of x^i, v^i, v_i and g_{ik} belong to the nodes of the difference net, denoting them, respectively $\{(x^i)_{\alpha\beta\gamma}\}$ and so on. Then the relation between the covariant and contravariant components $\vec{v}$ will be written in the usual way for each node:

$$v_i=g_{i\kappa}v^\kappa \qquad \text{for} \quad (\alpha,\beta,\gamma)\in\omega_h \tag{2.1}$$

(for simplification of the notation the index (α,β,γ) is omitted in the formula).

The thermodynamic values and also H_i, H^i, J and J_n^m will be referred to the centers of the Lagrangian cell and marked by the cell index. Since $\{(g_{ik})_{\alpha\beta\gamma}\} \in R_h$, the relation between $(H_i)_{\alpha\beta\gamma}$ and $(H^i)_{\alpha\beta\gamma}$ will be established by the expression

$$(H_i)_{\alpha\beta\gamma} = \langle g_{ik} \rangle_{\alpha\beta\gamma} (H^k)_{\alpha\beta\gamma} \tag{2.2}$$

where $\{\langle g_{ik} \rangle_{\alpha\beta\gamma}\} \in \bar{R}_h$ is an approximation of g_{ik} at the center of the cell, for example, of the type

$$\langle g_{ik} \rangle_{\alpha\beta\gamma} = \frac{1}{8} \sum_{\nu \in \Pi_1(\alpha\beta\gamma)} (g_{ik})_\nu \tag{2.3}$$

2. Let us define the difference analogs for the partial derivatives $\partial f/\partial q^i$. For the Lagrangian cell (α,β,γ) let us introduce the expressions:

$$\begin{aligned} \partial_{\bar{1}} f &= \frac{1}{4h_1} \sum_{\alpha_1,\beta_1,\gamma_1=0,1} f_{\alpha+\alpha_1,\beta+\beta_1,\gamma+\gamma_1} (-1)^{\alpha_1+1} \\ \partial_{\bar{2}} f &= \frac{1}{4h_2} \sum_{\alpha_1,\beta_1,\gamma_1=0,1} f_{\alpha+\alpha_1,\beta+\beta_1,\gamma+\gamma_1} (-1)^{\beta_1+1} \\ \partial_{\bar{3}} f &= \frac{1}{4h_3} \sum_{\alpha_1,\beta_1,\gamma_1=0,1} f_{\alpha+\alpha_1,\beta+\beta_1,\gamma+\gamma_1} (-1)^{\gamma_1+1} \end{aligned} \tag{2.4}$$

where $\{f_{\alpha\beta\gamma}\} \in R_h$. Expression (2.4) approximates $\partial f/\partial q^i$ at the center of the cell. For sufficiently smooth f:

$$\partial_{\bar{i}} f = \frac{\partial f}{\partial q^i}\Big|_{\overline{\alpha\beta\gamma}} + O(h^2) \tag{2.4}$$

here the bar over the index indicates that the approximation is made in the center of the cell, $h^2=h_1^2+h_2^2+h_3^2$.

Let us note that for $\partial_{\bar{i}} f$ the formula that follows is valid:

$$\partial_{\bar{i}} f = \frac{1}{3} \sum_{\nu \in \Pi_1(\alpha\beta\gamma)} f_\nu \frac{\partial}{\partial (x^k)_\nu} (\partial_{\bar{i}} x^k) \tag{2.5}$$

The difference analog of the derivative $\partial f/\partial q^i$ defined at the node of the difference net will be introduced as follows:

$$(\partial_i f)_{\alpha\beta\gamma} = -\frac{1}{3} \sum_{\nu \in \Pi_2(\alpha\beta\gamma)} f_\nu \frac{\partial}{\partial (x^k)_{\alpha\beta\gamma}} (\partial_{\bar{i}} x^k)_\nu \tag{2.6}$$

It is easy to see that $\partial_i f$ $(f \in \bar{R}_h)$ is an approximation of $\partial f/\partial q^i$ at the node with second order.

3. Using $\partial_{\bar{i}}$, let us carry out the digitalization of the variables J_j^i and J_i. In accordance with J_i^i and J let us substitute the difference expressions S^i and S obtained by formal replacement of the derivative $\partial/\partial q^i$ by $\partial_{\bar{i}}$:

$$S_j^i = \frac{1}{2} e^{imn} e_{j\kappa\ell} \partial_{\bar{m}} x^\kappa \partial_{\bar{n}} x^\ell$$

$$S = \frac{1}{6} e^{imn} e_{j\kappa\ell} \partial_{\bar{m}} x^\kappa \partial_{\bar{n}} x^\ell \partial_{\bar{i}} x^j \tag{2.8}$$

Here $S_j^i = J_j^i\big|_{\overline{\alpha\beta\gamma}} + o(h^2)$; $S = J\big|_{\overline{\alpha\beta\gamma}} + o(h^2)$ and the difference analogs of the identities (1.6) occurring in the differential case can be satisfied

$$S_j^i \partial_{\bar{i}} x^m = \delta_j^m S \tag{2.9}$$

in addition, let us note the equality

$$\sum_{\nu \in W_1(\alpha\beta\gamma)} \frac{\partial S_{\alpha\beta\gamma}}{\partial (x^m)_\nu} = 0$$

Using (2.9) and (2.4), it is possible to demonstrate that $f \in R_h$ and $\phi \in \overline{R}_h$, then

$$\sum_{\nu \in W_1(\alpha\beta\gamma)} f_\nu \frac{\partial S_{\alpha\beta\gamma}}{\partial (x^\kappa)_\nu} = S_\kappa^i \partial_{\bar{i}} f = J \frac{\partial f}{\partial x^\kappa}\bigg|_{\overline{\alpha\beta\gamma}} + o(h^2)$$

$$\sum_{\nu \in W_2(\alpha\beta\gamma)} \varphi_\nu \frac{\partial S_\nu}{\partial (x^\kappa)_{\alpha\beta\gamma}} = [\partial_{\bar{i}} (\varphi S_\kappa^i)]_{\alpha\beta\gamma} = -J \frac{\partial \varphi}{\partial x^\kappa}\bigg|_{\alpha\beta\gamma} + o(h^2) \tag{2.10}$$

Consequently, the expressions $\sum_{W_1} f_\nu \frac{\partial S}{\partial (x^\kappa)_\nu}$ and $\sum_{W_2} \varphi_\nu \frac{\partial S_\nu}{\partial (x^\kappa)_{\alpha\beta\gamma}}$ can be considered as difference analogs of the partial derivatives $\partial/\partial x^k$ reduced, correspondingly, to the cell and the node of the finite-difference net.

4. Let us discuss the problem of approximation of the expression $\sqrt{g}$ in the cell. Inasmuch as g_{ik} pertains to the nodes, the value of $\sqrt{g}$ at the center of the cell can be defined, for example, as follows

$$\ll \sqrt{g} \gg = \frac{1}{8} \sum_{\nu \in W_1(\alpha\beta\gamma)} (\sqrt{g})_\nu \tag{2.11}$$

where $(\sqrt{g})_\nu = \sqrt{\det (g_{ik})_\nu}$, here $\ll g \gg = \sqrt{g}\big|_{\overline{\alpha\beta\gamma}} + o(h^2)$

On the other hand, if the difference expression is known for $V = J\sqrt{g}$ (see, for example, [7]), it is possible to define the mean value for $\sqrt{g}$ as

$$\langle \sqrt{g} \rangle_{\alpha\beta\gamma} = \frac{V_{\alpha\beta\gamma}}{S_{\alpha\beta\gamma}} \tag{2.12}$$

It is obvious that $\langle\sqrt{g'}\rangle = \sqrt{g}\,|_{\overline{\alpha\beta\gamma}} + o(h^2)$ under the condition that $V_{\alpha\beta\gamma}$ approximates $(\sqrt{g}J)|_{\overline{\alpha\beta\gamma}}$ with second order.

§3. Differential-Difference Equations of Magnetohydrodynamics

1. The set of Lagrangian cells $\overline{\omega}_h$ can be considered as a discrete model of a continuous medium. The state of each cell is determined by the values of $P_{\alpha\beta\gamma}$, $\rho_{\alpha\beta\gamma}$, $V_{\alpha\beta\gamma}$, $H^i_{\alpha\beta\gamma}$, $\varepsilon_{\alpha\beta\gamma}$ and $(v^i)_\nu$, $\nu \in W_i(\alpha\beta\gamma)$. The variation approach permits construction of the class of differential-difference equations giving match to variation of all of the MHD values.

For the discrete system of $\overline{w}_h$ the Lagrangian is defined as the difference of the kinetic and potential energy:

$$\mathcal{L}_h = \sum_{\alpha\beta\gamma \in \overline{\omega}_h} \rho_{\alpha\beta\gamma} V_{\alpha\beta\gamma} \left(K_{\alpha\beta\gamma} - \Pi_{\alpha\beta\gamma}\right) \tag{3.1}$$

here $K_{\alpha\beta\gamma}$, $\Pi_{\alpha\beta\gamma}$ denote the specific kinetic and potential energies of the cell, respectively

$$K_{\alpha\beta\gamma} = \frac{1}{8} \sum_{\nu \in W_i(\alpha\beta\gamma)} \frac{(v^k v_k)_\nu}{2}$$
$$\Pi_{\alpha\beta\gamma} = \varepsilon_{\alpha\beta\gamma} + \frac{(H^k H_k)_{\alpha\beta\gamma}}{8\pi\rho_{\alpha\beta\gamma}} \tag{3.2}$$

It is obvious that $\mathcal{L}^h = \mathcal{L} + o(h^2)$. Let us note that the approximations of the kinetic energy of the cell can be made also by other methods.

For the difference Lagrangian, the influence functional according to the Hamiltonian $F_h = \int_{t_1}^{t_2} \mathcal{L}^h(t)\,dt$ is introduced.

In order to obtain the additional conditions imposed on the variation of the functions entering into $\mathcal{L}^h$, let us consider the difference analog of the continuity conditions and freezing of the magnetic field.

2. Using the expression for V introduced in §2, it is possible to write

$$V_{\alpha\beta\gamma}\,\rho_{\alpha\beta\gamma} = m_{\alpha\beta\gamma} = \sqrt{g}\,J\,\rho\,|_{\overline{\alpha\beta\gamma}} + O(h^2) \tag{3.3}$$

here m has the meaning of the mass of the Lagrangian cell which is invariant in time (it is assumed that the mass exchange between the cells does not take place). From (3.3) we have the differential-difference equation of continuity in the form

$$V\frac{d\rho}{dt} + \rho\frac{dV}{dt} = 0 \tag{3.4}$$

The derivative of V with respect to time can be approximated dually:

a) If the expression for the volume is considered as a function of the coordinates $V_{\alpha\beta\gamma} = V_{\alpha\beta\gamma}(x^i_\nu : \nu \in \mathcal{U}_1(\alpha\beta\gamma))$, then it is necessary to set

$$\frac{dV}{dt} = \sum_{\nu \in \mathcal{U}_1(\alpha\beta\gamma)} \frac{\partial V}{\partial (x^k)_\nu} \frac{d(x^k)_\nu}{dt} = \sum_{\nu \in \mathcal{U}_1(\alpha\beta\gamma)} \frac{\partial V}{\partial (x^k)_\nu} (v^k)_\nu \tag{3.5}$$

Inasmuch as V is a known algebraic function, $\partial V/\partial (x^k)_\nu$ is calculated explicitly.

b) On the other hand, the equality $dV/dt = J \frac{\partial \sqrt{g} v^\kappa}{\partial x^\kappa}$ can be approximated with the help of (2.10) by the expression

$$\frac{dV}{dt} = S^i_\kappa \partial_{\bar{i}} (v^\kappa \sqrt{g}) = \sum_{\nu \in \mathcal{U}_1(\alpha\beta\gamma)} \frac{\partial S}{\partial (x^\kappa)_\nu} (v^\kappa \sqrt{g})_\nu \tag{3.6}$$

We see that equation (3.4) approximates the differential equation of continuity (1.2) in the center of the cell if we use (3.6) or (3.5) for dV/dt. In the first case this is obvious, for from (2.7) we have

$$\frac{dV}{dt} = S^i_\kappa \partial_{\bar{i}} (v^\kappa \sqrt{g}) = J \frac{\partial v^\kappa \sqrt{g}}{\partial x^\kappa}\Big|_{\overline{\alpha\beta\gamma}} + O(h^2)$$

For (3.5), using (2.10)-(2.12), it is possible to write

$$\sum_{\nu \in \mathcal{U}_1(\alpha\beta\gamma)} \frac{\partial V}{\partial (x^\kappa)_\nu} (v^\kappa)_\nu = \sum_{\nu \in \mathcal{U}_1(\alpha\beta\gamma)} \Big\{ \langle \sqrt{g} \rangle \frac{\partial S}{\partial (x^\kappa)_\nu} v^\kappa_\nu + \tag{3.7}$$

$$+ S v^\kappa_\nu \frac{\partial \langle \sqrt{g} \rangle}{\partial (x^\kappa)_\nu} \Big\} = J \sqrt{g} \frac{\partial v^\kappa}{\partial x^\kappa}\Big|_{\overline{\alpha\beta\gamma}} + O(h^2) +$$

$$+ \frac{S}{8} \sum_{\nu \in \mathcal{U}_1(\alpha\beta\gamma)} (v^\kappa)_\nu \frac{\partial (\sqrt{g})_\nu}{\partial (x^\kappa)_\nu} = J \Big(\sqrt{g} \frac{\partial v^\kappa}{\partial x^\kappa} + v^\kappa \frac{\partial \sqrt{g}}{\partial x^\kappa} \Big)\Big|_{\overline{\alpha\beta\gamma}} + O(h^2)$$

3. Let us digitalize the freezing equation for the magnetic field. The difference expression

$$\langle \sqrt{g} \rangle H^\kappa S^i_\kappa = \Phi^i \tag{3.8}$$

on the basis of (2.8), (2.12) approximates the freezing condition (1.5) at the center of the cell with accuracy $O(h^2)$. It is possible to show that ϕ^i is the "difference" fluxes through the planes passing through the center of the cell perpendicular to q^i. Performing the convolution of $\phi^i \partial_{\bar{I}} x^k$ considering (2.9) we convert equations (3.8) to the difference analog of equation (1.7)

$$VH^{\kappa} = \varphi^{i}\partial_{\bar{i}} x^{\kappa} \tag{3.8'}$$

Differentiation of (3.8) with respect to time leads to the difference equation of induction corresponding to (1.9)

$$V\frac{dH^{\kappa}}{dt} = -H^{\kappa}\frac{dV}{dt} + \varphi^{i}\partial_{\bar{i}} v^{\kappa} \tag{3.9}$$

here by dV/dt we mean one of the expressions (3.5) or (3.6).

From (3.9) and from the induction equation written for the covariant components H^k by standard transformations we have the equation for the energy of the magnetic field of the cell in the form

$$\frac{d}{dt}\left(\frac{H^{\kappa}H_{\kappa}}{8\pi}V\right) = -\frac{H^{\kappa}H_{\kappa}}{8\pi}\frac{dV}{dt} + \frac{H_{\kappa}\varphi^{i}\partial_{\bar{i}}v^{\kappa}}{4\pi} + \frac{VH^{n}H^{\kappa}}{8\pi}\frac{d\langle g_{n\kappa}\rangle}{dt} \tag{3.10}$$

As is easily seen, (3.10) approximates (1.10) with accuracy $o(h^2)$. For $d\langle g_{nk}\rangle/dt$, just as for the derivative dV/dt, different approximations are permissible. In the general case, obviously

$$\frac{d\langle g_{ik}\rangle}{dt} = \sum_{\nu\in W_1(\alpha\beta\gamma)} \frac{\partial\langle g_{ik}\rangle}{\partial(x^{\ell})_{\nu}}(v^{\ell})_{\nu} \tag{3.11}$$

If $\langle g_{ik}\rangle$ is calculated by formula (2.3), then (3.11) becomes

$$\frac{d\langle g_{ik}\rangle}{dt} = \frac{1}{8}\sum_{\nu\in W_1(\alpha\beta\gamma)}\left(\frac{\partial g_{ik}}{\partial x^{\ell}}v^{\ell}\right)_{\nu} \tag{3.12}$$

In conclusion, let us consider the problem of satisfaction of the condition of solenoidality of the magnetic field. The differential expression for the divergence H looks like the following

$$div\,\vec{H} = H^{\kappa}_{;\kappa} = \frac{1}{\sqrt{g}}\frac{\partial\sqrt{g}H^{\kappa}}{\partial x^{\kappa}}$$

Using the formula of difference differential (2.10) and expression (3.8) let us approximate the given expression by the equality:

$$\frac{1}{\hat{V}}\partial_{i}\left(\langle\sqrt{g}\rangle H^{\kappa}S^{i}_{\kappa}\right) = \frac{1}{\hat{V}}\partial_{i}\varphi^{i} = 0 \tag{3.13}$$

However, on the basis of (2.10) the lefthand side of (3.13) is none other than the approximation of H^{k}_{ik}. Consequently, the condition

$$\partial_{i}\varphi^{i} = 0 \tag{3.14}$$

can be considered the condition of solenoidality of the magnetic field. Thus, just as in the differential case, if at the time $t=t_0$ (3.14) is satisfied, the magnetic field remains solenoidal also during the subsequent points in time.

4. Let us find the conditions of equality of the first version of the influence function F_n to zero

$$\delta F_h = \int_{t_0}^{t_1} \Big\{ \sum_{(\alpha\beta\gamma)\in\overline{\omega}_h} \Big\{ m_{\alpha\beta\gamma} \Big[\sum_{\nu\in \mathrm{III}_1(\alpha\beta\gamma)} (v^\kappa)_\nu (\delta v^\kappa)_\nu + \\ + \Big(\frac{v^i v^\kappa}{2} \delta g_{i\kappa}\Big)_\nu - \delta\varepsilon_{\alpha\beta\gamma} \Big] - \delta V_{\alpha\beta\gamma} \Big(\frac{H^\kappa H_\kappa}{8\pi}\Big)_{\alpha\beta\gamma} - \\ - V_{\alpha\beta\gamma} \frac{(H_\kappa \delta H^\kappa)_{\alpha\beta\gamma}}{4\pi} - \frac{(\nabla H^\kappa H^\ell)_{\alpha\beta\gamma} \delta \langle g_{\kappa\ell}\rangle_{\alpha\beta\gamma}}{8\pi} \Big\} \Big\} h_1 h_2 h_3 \, dt \tag{3.15}$$

Let us take $\partial x^i{}_{\alpha\beta\gamma}$ as the independent versions, and let us define their relation to the versions of the remaining variables entering into (3.15). They are established by the expressions:

$$\begin{aligned} \delta v^i &= \delta \frac{dx^i}{dt} = \frac{d}{dt} \delta x^i \\ \delta g_{ik} &= \frac{\partial g_{ik}}{\partial x^n} \delta x^n \\ \nabla \delta H^\kappa &= -H^\kappa \delta V + \Phi^i \partial_i \delta x^\kappa \\ \delta\varepsilon &= -\frac{p}{m} \delta V \end{aligned} \tag{3.16}$$

For ∂V and $\partial\langle g_{ik}\rangle$, we use two types of expressions corresponding to (3.5), (3.11) or (3.6), (3.12). They look like the following

$$\begin{aligned} \delta V &= \sum_{\nu\in \mathrm{III}_1(\alpha\beta\gamma)} \frac{\partial V}{\partial (x^\kappa)_\nu} \delta x^\kappa_\nu \\ \delta\langle g_{ik}\rangle &= \sum_{\nu\in \mathrm{III}_1(\alpha\beta\gamma)} \frac{\partial \langle g_{\kappa\ell}\rangle}{\partial (x^\eta)_\nu} \delta (x^\eta)_\nu \end{aligned} \tag{3.17}$$

$$\delta V = S^i_\kappa \partial_i (\delta x^\kappa \sqrt{g}) = \sum_{\nu\in \mathrm{III}_1(\alpha\beta\gamma)} (\sqrt{g})_\nu \frac{\partial S^i}{\partial (x^\eta)_\nu} \delta (x^\eta)_\nu \tag{3.18}$$

$$\delta\langle g_{k\ell}\rangle = \frac{1}{8} \sum_{\nu\in \mathrm{III}_1(\alpha\beta\gamma)} \delta (g_{\kappa\ell})_\nu = \frac{1}{8} \sum_{\nu\in \mathrm{III}_1(\alpha\beta\gamma)} \frac{\partial (g_{\kappa\ell})_\nu}{\partial (x^\eta)_\nu} \delta (x^\eta)_\nu$$

As is easy to note, the presence of different approximations of ∂V and $\partial\langle g_{k\ell}\rangle$ leads to different dynamic equations, for the obtaining of which it is necessary to substitute (3.16) and (3.17) or (3.18) in (3.15) and carry out the corresponding transformation. Let us write these equations in final form:

$$M\left(\frac{dv_i}{dt} - \frac{v^\kappa v^\ell}{2}\frac{\partial g_{\kappa\ell}}{\partial x^i}\right) = \sum_{\nu\in\omega_2(\alpha\beta\gamma)}\left\{p + \frac{H^\kappa H_\kappa}{8\pi}\right\}_\nu \frac{\partial V_\nu}{\partial x^i} - \\ - \partial_n \frac{H_i \Phi^n}{4\pi} + \sum_{\nu\in\omega_2(\alpha\beta\gamma)} \frac{\partial \langle g_{\ell\kappa}\rangle_\nu}{\partial x^i} V_\nu \frac{(H^\ell H^\kappa)_\nu}{8\pi} \qquad (3.19)$$

(it corresponds to the case where (3.17)).

$$M\left(\frac{dv_i}{dt} - \frac{v^\kappa v^\ell}{2}\frac{\partial g_{\kappa\ell}}{\partial x^i}\right) = \sqrt{g}\sum_{\nu\in\omega_2(\alpha\beta\gamma)} P^*_\nu \frac{\partial S_\nu}{\partial x^i} - \\ - \partial_n \frac{H_i \Phi^n}{4\pi} + \frac{1}{8}\frac{\partial g_{\ell\kappa}}{\partial x^i}\sum_{\nu\in\omega_2(\alpha\beta\gamma)} \frac{(VH^\kappa H^\ell)_\nu}{8\pi} \qquad (3.20)$$

(corresponds to the case where (3.18))

Here

$$M = \rho_{\alpha\beta\gamma} = \frac{1}{8}\sum_{\nu\in\omega_2(\alpha\beta\gamma)} m_\nu, \quad P^* = p + \frac{H_\kappa H^\kappa}{8\pi}$$

Since $H = p^{ik} g_{ik}|_{\alpha\beta\gamma} + O(h^2)$, the second-order approximation for equations (3.20) is easily established on the basis of the formulas for §2. In equation (3.19) it is necessary to estimate the order of the approximation of the expression

$$\sum_{\nu\in\omega_2(\alpha\beta\gamma)} P^*_\nu \frac{\partial V_\nu}{\partial x_i} = \sum_{\nu\in\omega_2(\alpha\beta\gamma)}\left\{P^*_\nu \langle\sqrt{g}\rangle_\nu \frac{\partial S_\nu}{\partial x^i} + P^*_\nu S_\nu \frac{\partial \langle\sqrt{g}\rangle_\nu}{\partial x^i}\right\}$$

Using (2.10) and the fact that $\langle\sqrt{g}\rangle_{\alpha\beta\gamma} = \frac{1}{8}\sum_{\nu\in\omega_1(\alpha\beta\gamma)} (\sqrt{g})_\nu + o(h^2)$

we obtain

$$\sum_{\nu\in\omega_2} P^*_\nu \frac{\partial V_\nu}{\partial x^i_\nu} = \frac{1}{8}\frac{\partial\sqrt{g}}{\partial x^i}\sum P^*_\nu S_\nu - J\frac{\partial p^\kappa\sqrt{g}}{\partial x^i}\Big|_{\alpha\beta\gamma} + o(h^2) = \\ = \left\{p^\kappa J\frac{\partial\sqrt{g}}{\partial x^i} - J\frac{\partial p^\kappa\sqrt{g}}{\partial x^i}\right\}_{\alpha\beta\gamma} + o(h^2) = -\sqrt{g}\frac{\partial p^\kappa J^\eta}{\partial q^\eta}\Big|_{\alpha\beta\gamma} + o(h^2)$$

Thus, the approximation of the dynamic equations (3.19), (3.20) is demonstrated.

3. The equation for the specific internal energy can be obtained analogously to how this is done in reference [6]:

$$m\frac{d\varepsilon}{dt} = -p\frac{dV}{dt} = \frac{m}{\rho^2}\frac{d\rho}{dt} \tag{3.21}$$

Equation (3.21) has entropy form; for dV/dt it is possible to use any of the expressions (3.5), (3.6).

For calculation of the currents with shock waves accompanied by an increase in entropy, it is necessary to introduce artificial dissipative processes. This can be done by the recommendations proposed in references [13], [14]. We shall not discuss this problem, for it is a subject of special study.

The digitalization technique with respect to time does not differ in any way from the one developed in [6], [7].

§4. Some Properties of the Differential-Difference Equations of Magnetohydrodynamics

In this section a study is made of the properties of the difference system of MHD equations for cases where the dynamic equation (3.19) is used, and the expression for dV/dt is given from (3.5). All of the results obtained are extended without difficulty to the case with equations (3.20) and (3.6).

1. Let us write the complete system of differential-difference equations of magnetohydrodynamics:

$$M\left(\frac{dv_i}{dt} - \frac{v^k v^\ell}{2}\frac{\partial g_{k\ell}}{\partial x^i}\right) =$$

$$= \sum_{\nu\in\omega_1(\alpha\beta\gamma)}\left(p^*_\nu\frac{\partial V_\nu}{\partial x^i} - \frac{\partial\langle g_{k\ell}\rangle_\nu}{\partial x^i}\frac{(VH^kH^\ell)_\nu}{8\pi}\right) - \partial_k\frac{H_i\Phi_k}{4\pi} \tag{4.1}$$

$$\rho V\frac{d\varepsilon}{dt} = -p\frac{dV}{dt} = -p\sum_{\nu\in\omega_2(\alpha\beta\gamma)}\frac{\partial V}{\partial(x^k)_\nu}(v^k)_\nu \tag{4.2}$$

$$\begin{cases} VH^k = \Phi^i\partial_{\bar i}x_k \\ V\frac{dH^i}{dt} = -H^i\frac{dV}{dt} + \Phi^k\partial_{\bar k}v^i \end{cases} \tag{4.3}$$

$$\frac{d}{dt}\left(\frac{H^kH_k}{8\pi}V\right) = -\frac{H_kH^k}{8\pi}\frac{dV}{dt} + \frac{H_k\Phi^i}{4\pi}\partial_{\bar i}v^k - \frac{VH^kH^\ell}{8\pi}\frac{d\langle g_{k\ell}\rangle}{dt} \tag{4.4}$$

$$m = V\rho \tag{4.5}$$

$$\frac{dx^i}{dt} = v^i \quad \therefore \quad p = p(\rho,\varepsilon) \tag{4.6}$$

Let us note that the system of equations uses the mixed components of the velocity vectors and the magnetic field intensity vectors which complicates their notation. However, it is easy to reduce these equations to the form of notation in which

only the covariant or contravariant components were used; for this purpose it is necessary to resort to the transformation formulas (2.1) and (2.1').

2. Let us consider the problem of the conservation laws for the system (4.1)-(4.6). As follows from the differential dynamic equation (1.13), the law of variation of the pulse of isolated volume of the liquid $\Omega' \subseteq \Omega$ has the form:

$$\frac{d}{dt}\int_{\Omega_q'} \rho_* v_i \, d\Omega_q = \int_{\Omega_q'} \rho_* \frac{\partial g_{ik}}{\partial x^i}\left(\frac{v^k v^l}{2} + \frac{H^k H^l}{8\pi}\right) d\Omega_q - \int_{-L_q'} p^* \frac{\partial \sqrt{g}}{\partial x^i} J \, d\Omega_q - \oint_{S_q'} \left(p^* \delta_i^k - \frac{H_i H^k}{8\pi}\right) dS_k \tag{4.7}$$

Let Ω' in the difference case correspond to the set $\omega_h' = \{\alpha_1 \le \alpha \le \alpha_2;\ \beta_1 \le \beta \le \beta_2;\ \gamma_1 \le \gamma \le \gamma_2\} \subset \omega_h$. The dynamic equations (4.1) define the pulse variation of the set. Let us sum (4.1) with respect to all $(\alpha\beta\gamma) \in \omega_h'$, and let use the expression

$$\sum_{\nu \in \mathrm{III}_1(\alpha\beta\gamma)} \frac{\partial V_{\alpha\beta\gamma}}{\partial (x^i)_\nu} = S_{\alpha\beta\gamma} \sum_{\nu \in \mathrm{III}_1(\alpha\beta\gamma)} \frac{\partial \langle \sqrt{g} \rangle_{\alpha\beta\gamma}}{\partial (x^i)_\nu}$$

As a result, we obtain the difference analog (4.7)

$$\frac{d}{dt}\sum_{(\alpha\beta\gamma)\in\omega_h'} M_{\alpha\beta\gamma}(v_i)_{\alpha\beta\gamma} = \sum_{(\alpha\beta\gamma)\in\omega_h'} \left\{ M_{\alpha\beta\gamma}\left(\frac{v^k v^l}{2}\frac{\partial g_{kl}}{\partial x^i}\right)_{\alpha\beta\gamma} + \sum_{\nu \in \mathrm{III}_2(\alpha\beta\gamma)} \frac{\partial \langle g_{kl}\rangle_\nu}{\partial (x^i)_{\alpha\beta\gamma}} \frac{V H^l H^k}{8\pi} \right\} + \sum_{(\alpha\beta\gamma)\in\overline{\omega}_h'} p^*_{\alpha\beta\gamma} S_{\alpha\beta\gamma} \sum_{\nu \in \mathrm{III}_1(\alpha\beta\gamma)} \frac{\partial \langle \sqrt{g}\rangle_{\alpha\beta\gamma}}{\partial (x^i)_\nu} + F_{bH} \tag{4.8}$$

where F_{bH} represents the difference analog of the surface integral in (4.7). Thus, the difference equations (4.1) are conservative with respect to pulses.

Using equations (4.2) and (4.4), analogously it is possible to obtain the expressions for the variation of the specific internal and magnetic energy of the discrete set ω_h' in the form

$$\frac{d}{dt}\sum_{(\alpha\beta\gamma)\in\overline{\omega}_h'} m_{\alpha\beta\gamma}\varepsilon_{\alpha\beta\gamma} = -\sum_{(\alpha\beta\gamma)\in\omega_h'} p_{\alpha\beta\gamma}\frac{dV_{\alpha\beta\gamma}}{dt} \tag{4.9}$$

$$\frac{d}{dt}\sum_{(\alpha\beta\gamma)\in\overline{\omega}_h'}\left(V\frac{H^k H_k}{8\pi}\right)_{\alpha\beta\gamma} = -\sum_{\alpha\beta\gamma\in\overline{\omega}_h'}\left(\frac{H^k H_k}{8\pi}\right)_{\alpha\beta\gamma}\frac{dV_{\alpha\beta\gamma}}{dt} + \left(\frac{H_k \Phi^i \partial_i v^k}{4\pi}\right)_{\alpha\beta\gamma} - \left(\frac{V H^l H^k}{8\pi}\right)_{\alpha\beta\gamma}\frac{d\langle g_{kl}\rangle_{\alpha\beta\gamma}}{dt} \tag{4.10}$$

These equations express the balance of the individual forms of energy.

3. Let us show that for the differential-difference system (4.1)-(4.6) the analog of the conservation law of total energy is satisfied

$$\frac{d}{dt}\int_{\Omega'_h}\rho_0\left(\frac{v_k v^k}{2}+\varepsilon+\frac{H^k H_k}{8\pi\rho}\right)d\Omega_q=\oint\left(p^k\delta_i^k-\frac{H_i H^k}{8\pi}\right)v^i\sqrt{g}\,dS_k \tag{4.11}$$

We obtain in advance the expression defining the variation of the kinetic energy ω'_h. For this purpose let us write the equation of motion using the contravariant component v':

$$M\left(\frac{dv^i}{dt}+\Gamma^i_{ke}v^k v^e\right)=g^{ik}\sum_{\nu\in\omega_h(\alpha\beta\gamma)}\left\{p_\nu\frac{\partial V_\nu}{\partial(x^k)_{\alpha\beta\gamma}}+\right.$$
$$\left.+\frac{\partial\langle g_{ke}\rangle_\nu}{\partial(x^k)_{\alpha\beta\gamma}}\left(\frac{VH^k H^e}{8\pi}\right)_\nu-g_{ik}\frac{\partial\bar{\varepsilon}}{\partial x^k}\frac{H_k\Phi^e}{4\pi}\right. \tag{4.12}$$

Performing convolution of (4.1) with $v^i/2$, and (4.11) with $v_i/2$ and summing with respect to all $(\alpha\beta\gamma)\in\omega'_h$, we obtain the expression for the variation of the kinetic energy of the nodes

$$\frac{d}{dt}\sum_{(\alpha\beta\gamma)\in\omega'_h}\left(M\frac{v_i v^i}{2}\right)_{\alpha\beta\gamma}=\sum_{\nu\in\omega_h(\alpha\beta\gamma)}\left\{p^*_{\alpha\beta\gamma}\frac{\partial\bar{V}_{\alpha\beta\gamma}}{\partial(x^k)_\nu}(v^k)_\nu+\right.$$
$$\left.+\frac{(VH^k H^e)_{\alpha\beta\gamma}}{8\pi}\frac{\partial\langle g_{ke}\rangle_\nu}{\partial(x^k)_\nu}(v^k)_\nu\right\}-\left(\frac{H_k\Phi^e\partial\bar{\varepsilon}}{4\pi}v^k\right)_{\alpha\beta\gamma}\Bigg\}+ \tag{4.13}$$
$$+A_{\rho H}$$

Here A_{bH} is the work of the pressure and magnetic field from the direction of the cells bordering ω'_h.

Then adding the equations (4.9), (4.10) and (4.13), we obtain the desired expression:

$$\frac{d}{dt}\left\{\sum_{(\alpha\beta\gamma)\in\omega'_h}\left(M\frac{v_i v^i}{2}\right)_{\alpha\beta\gamma}+\sum_{(\alpha\beta\gamma)\in\bar{\omega}'_h}m_{\alpha\beta\gamma}\left\{\varepsilon+\frac{H_\varepsilon H^k}{8\pi\rho}\right\}_{\alpha\beta\gamma}\right\}=A_{\rho H} \tag{4.14}$$

As a result of 2^0 and 3^0 and also on the basis of the self-consistency of the equation for the magnetic field and the entropic form of the equation for the specific internal energy (4.2) the system of differential-difference equations (4.1)-(4.6) has the property of complete conservativeness [3].

§5. Example of Numerical Calculation

Let us consider the motion of an ideal infinitely conducting gas where all of the values depend on the variables t, x^1. Let at the initial point in time $\rho=\rho_0=\text{const}$, $p=p_0=\text{const}$, $v_x=v^1=0$. The initial values of the velocity components $v_y=v^2$, $v_z=v^3$ will be selected as follows:

$$v_y = \begin{cases} 0 & \text{for} \quad x < 0 \\ W_0 \sin \frac{\pi x}{\ell} & \text{for} \quad 0 \le x \le \ell \\ 0 & \text{for} \quad x > \ell \end{cases}$$

$$v_z = \begin{cases} W_0 & \text{for} \quad x < 0 \\ \frac{W_0}{2}\left(1 + \cos \frac{\pi x}{\ell}\right) & \text{for} \quad 0 \le x \le \ell \\ 0 & \text{for} \quad x > \ell \end{cases} \qquad (5.1)$$

The initial magnetic field will be given by the expressions:

$$H_x = H^1 = H_{x0}$$

$$H_y = H^2 = \begin{cases} 0 & \text{for} \quad x < 0 \\ H_0 \sin \frac{\pi x}{\ell} & \text{for} \quad 0 < x \le \ell \\ 0 & \text{for} \quad x > \ell \end{cases}$$

$$H_z = H^3 = \begin{cases} -H_0 & \text{for} \quad x < 0 \\ -H_0 \cos \frac{\pi x}{\ell} & \text{for} \quad 0 < x \le \ell \\ H_0 & \text{for} \quad x > \ell \end{cases}$$

Let

$$W_0 = \frac{2H_0}{\sqrt{4\pi\rho_0}}$$

As is easy to see, in the coordinate system moving with respect to the laboratory system at a velocity $V_{rel}=(a_A, 0, W_{0/2})$ where $a_A=H_{x0}/\sqrt{4\pi\rho}$,

the following expressions are satisfied

$$H_\tau^2 = H_x^2 + H_y^2 = \text{const}$$
$$v_\tau^2 = v_x^2 + v_y^2 = \text{const} \qquad (5.3)$$
$$\vec{V} = -\frac{\vec{H}}{\sqrt{4\pi\rho}}$$

The initial conditions given in this way define the well-known [15] steady-state motion of a gas which is called the rotational or Alfven simple wave. In such a wave

the transverse components of the vectors $\overline{V}$ and $\overline{H}$ are rotated, without changing their magnitudes. It is possible to show that in the investigated case all of the wave phases are shifted with constant velocity, and the wave profile does not deform. Let us note that for $\ell=0$ the simple Alfven wave becomes a rotational discontinuity.

Figures 1-4 illustrate the results of the numerical calculation of a simple Alfven wave. In the figures graphs are presented for the values of H_z, H_y, V, W as a function of the Euler coordinate x at different points in time. The calculation was performed for the following values of the parameters

$$H_0 = 1, \quad \rho_0 = 1, \quad \rho_\infty = 0{,}01, \quad H_{x0} = 2, \quad \ell = 1.$$

The adiabatic exponent $\gamma=2$.

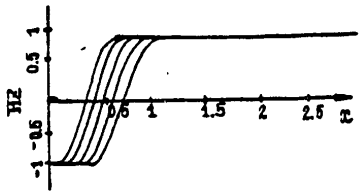

Figure 1

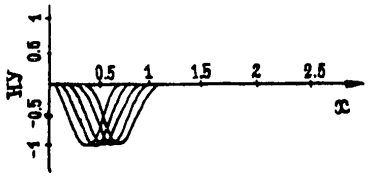

Figure 2

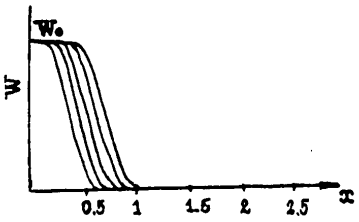

Figure 3

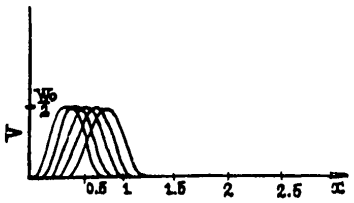

Figure 4

BIBLIOGRAPHY

1. Samarskiy, A. A. TEORIYA RAZNOSTNYKH SKHEM. [Theory of Difference Systems], Moscow, Nauka, 1977.

2. Popov, Yu. P.; Samarskiy, A. A. "Completely Conservative Difference Systems," ZHVM I MF [Journal of Computational Mathematics and Mathematical Physics], No 9, 1969, p 853.

3. Goloviznin, V. M.; Samarskiy, A. A.; Favorskiy, A. P. "Variation Approach to the Construction of Finite-Difference Models in Hydrodynamics," DAN SSSR [Reports of the USSR Academy of Sciences], Vol 235, No 6, 1977.

4. Goloviznin, V. M.; Korshia, T. K.; Samarskiy, A. A.; Favorskiy, A. P. "International Conference on Numerical Methods in Fluid Dynamics," 6th, Tbilisi, 1978, PROCEEDINGS OF THE CONFERENCE, Berlin, Heidelberg, New York, Springer-Verlag, 1979.

5. Seleger, R. L.; Whitham, G. B. "Variational Principles in Continuum Mechanics," PROC. ROY. SOC., A305, 1-25, 1968.

6. Goloviznin, V. M.; Samarskiy, A. A.; Favorskiy, A. P. "Variation Method of Constructing the Difference Systems of Magnetohydrodynamics," PREPRINT IPM AN SSSR [Preprint of the Institute of Applied Mathematics of the USSR Academy of Sciences], No 65, 1976.

7. Goloviznin, V. M.; Korshiya, T. K.; Samarskiy, A. A.; Favorskiy, A. P. "Variation-Difference Systems of Magnetohydrodynamics," PREPRINT IPM AN SSSR, No 57, 1977.

8. Favorskiy, A. P.; Tishkin, V. F.; Tyurina, N. N. "Difference Systems for Calculating the Hydrodynamic Currents in Cylindrical Coordinates," PREPRINT IPM AN SSSR, No 23, 1978.

9. Goloviznin, V. M.; Tishkin, V. F. Favorskiy, A. P. "Variation Method of Constructing the Difference Systems of Hydrodynamics in Spherical Coordinates," PREPRINT IPM AN SSSR, No 16, 1977.

10. Khert, S. "Arbitrary Lagrange-Euler Method," CHISLENNYYE METODY V MEKHANIKE ZHIDKOSTI [Numerical Methods in Fluid Mechanics], Mir, 1973.

11. Landau, L. D.; Lifshits, Ye. M. TEORIYA POLYA [Field Theory], izd. Nauka, Moscow, 1973.

12. Rashevskiy, P. K. RIMANOVA GEOMETRIYA I TENZORNYY ANALIZ [Riemann Geometry and Tensor Analysis], Moscow, Nauka, 1964.

13. Goloviznin, V. M.; Samarskiy, A. A.; Favorskiy, A. P. "Artificial Viscosity and Stability of Difference Equations of Gas Dynamics," PREPRINT IPM AN SSSR, No 70, 1977.

14. Goloviznin, V. M.; Korshiya, T. K.; Samarskiy, A. A.; Favorskiy, A. P. "Two-dimensional Variation-Difference Systems of Magnetohydrodynamics with Three Velocity and Magnetic Field Components," PREPRINT IPM AN SSSR, No 41, 1978.

15. Kulikovskiy, A. G.; Lyubimov, G. A. MAGNITNAYA GIDRODINAMIKA [Magnetohydrodynamics], Moscow, Nauka, 1963.

COMPLETELY NEUTRAL DIFFERENCE SCHEME FOR THE NAVIER-STOKES EQUATIONS

[B. D. Moiseyenko, I. V. Fryazinov, pp 186-209]

In this paper a study is made of the problems of the finite-difference approximation of the Navier-Stokes equations for an incompressible liquid in the variables ψ, ω (ψ is the current function, ω is the vortex) in a rectangle. At the boundary of the rectangle the velocities u and v are given in the directions of the coordinate axes Ox and Oy.

During the numerical solution of the problems of gas dynamic and hydrodynamics, it is highly significant to construct the difference schemes so that in them the analogs of the conservation laws set down in the initial differential equations will be satisfied. The schemes of this type were called conservative [1]. Further development of the principle of conservativeness has led to the concept of complete conservativeness of the difference schemes in which additional characteristics expressing the balance of the individual types of energy are reflected [1, 2].

In the paper by Arakawa [3] when investigating the transport equations [several lines illegible], reflecting the properties of the initial equations for zero velocities and the boundary of the region. These schemes will be called energy neutral and entropy neutral. The scheme having both properties will be called completely neutral. The energy neutral schemes for the equations of hydrodynamics based on the application of the Galerkin method were proposed earlier in [4].

In this paper the energy and entropy neutral schemes are proposed for the systems of equations of hydrodynamics of a viscous incompressible liquid on nonuniform (with respect to x and y) difference nets. The completely neutral scheme has also been constructed.

The investigation of these problems has required the study of the approximation of the boundary conditions in the variables ψ, ω. Here it turned out that the known approximation of the vortex at the boundary nodes according to the Tom formula (see, for example, [4]) permits construction of neutral implicit schemes equivalent to the schemes with nonlocal boundary conditions. Here the finite-difference operators retain important properties of the differential operators of the initial problem, and the scheme is uniform. For solution of the system of equations for ψ and ω for each $t=t_j$ iteration methods are required.

Paying tribute to the generally accepted methods of solving the Navier-Stokes equations in this paper, a procedure is proposed for calculating the votex at the boundary of the region generalizing the method of V. I. Polezhayev [8] to the case of an arbitrary region.

§1. Statement of the Initial Problem

In the rectangle $G=\{0<x<a,\ 0<y<b\}$ with the boundary Γ we shall consider the system of Navier-Stokes equations for an incompressible liquid with density $\rho=1$ for $0<t\leq T$ written in the variables ψ, ω, Q, where Q is the head, $Q=p+(u^2+v^2)/2$, p is pressure.

The system of equations will be written in the form

$$\omega_t = W_2 x - W_1 y\ ,\ W_{1x}+W_{2y}=0\ ,\ \Delta\psi=-\omega \tag{1.1}$$

Here the "flows" W_1 and W_2 have the form

$$W_1=-(\nu\omega_y-\mathfrak{A}_2+Q_x),\ \mathfrak{A}_2=v\omega\ ,\ v=-\psi_x,$$
$$W_2=(\nu\omega_x-\mathfrak{A}_1-Q_y),\ \mathfrak{A}_1=u\omega\ ,\ u=\psi_y$$

Let us add the boundary in the initial conditions to the system (1.1). In Γ we give the velocity

$$u=u_0(x,y,t)\ ,\ v=v_0(x,y,t)\ ,\ (x,y)\in\Gamma,$$
$$\oint u_0\,dy+v_0\,dx=0,\quad 0\leq t\leq T. \tag{1.2}$$

The boundary conditions for the system (1.1) in this case have the form

$$W_1=u_{0t}\ ,\ W_2=v_{0t}\ ,\ \psi=\psi_0(x,y,t),\ (x,y)\in\Gamma, \tag{1.3}$$
$$0<t\leq T.$$

Here ψ_0 is determined from the equation

$$-\frac{\partial\psi_0}{\partial s}=u_0\cos(n,x)+v_0\cos(n,y)=u_{0n}\ ,\ \psi_0(0,0)=0$$

s is the vector that is tangent to Γ in the direction of the positive course of Γ, n is the internal normal to Γ.

The initial values of ψ^0 and ω^0 will be calculated by the initial values of u^0 and v^0 of the velocities u and v. We shall assume that

$$u^0_x+v^0_y=0,\ (x,y)\in G,\ u^0=u_0, v^0=v_0\ ,\ (x,y)\in\Gamma.$$

Then

$$\omega^0=v^0_x-u^0_y\ ,\ \psi^0_y=u^0,\ \psi^0_x=-v^0,\ \psi^0(0,0)=0. \tag{1.4}$$

Let us note that the derivative is also known with respect to the normal n to Γ of the function ψ,

$$\frac{\partial \psi}{\partial n} = u_0 \cos(s,x) + v_0 \cos(s,y) = u_{0s}, \quad (x,y) \in \Gamma. \tag{1.5}$$

Let us assume that a unique solution to the stated problem exists. The equations (1.1) follow from the system of Navier-Stokes equations written in standard form.

§2. Finite-Difference Nets and Functions

In the segments $0 \leq x \leq a$, $0 \leq y \leq b$ let us introduce points $x_0=0$, x_1, $-x_M=a$, $y_0=0$, y_1, y_2, ..., $y_N=b$. The spacings between adjacent points will be denoted by $h^{(1)}_{i+1/2}=x_{i+1}-x_i$, $h^{(2)}_{k+1/2}=y_{k+1}-y_k$. Let us also introduce the average steps with respect to directions x and y:

$$h^{(1)}_0 = 0.5\, h^{(1)}_{1/2}, \quad h^{(1)}_i = (h^{(1)}_{i+1/2} + h^{(1)}_{i-1/2})/2, \quad 0<i<M, \quad h^{(1)}_M = 0.5\, h^{(1)}_{M-1/2},$$
$$h^{(2)}_0 = 0.5\, h^{(2)}_{1/2}, \quad h^{(2)}_k = (h^{(2)}_{k+1/2} + h^{(2)}_{k-1/2})/2, \quad 0<k<N, \quad h^{(2)}_N = 0.5\, h^{(2)}_{N-1/2}.$$

In the rectangle $\bar{G} = G \cup \Gamma$ let us introduce the difference net $\bar{\Omega}_h = \Omega_h \cup \Gamma_h$ of the nodes $X = (x_i, y_k)$, $i = 0,1,\ldots M$, $k = 0,1,\ldots N$, $\Omega_h = \Omega_h \cap G$, $\Gamma_h = \bar{\Omega}_h \cap \Gamma$

Let us place the rectangle $H_{ik} \subset G$ bounded by the segments of straight lines $x = x_{i\pm1/2} = (x_i + x_{i\pm1})/2$, $y = y_{k\pm1/2} = (y_k + y_{k\pm1})/2$ and the boundary Γ if $(x_i, y_k) \in \Gamma_h$ in correspondence to each node $(x_i, y_k) \in \Omega_h$.

The cell of the difference net and its area and also the segment and its length will be designated by the same letters so that $H_{ik} = h^{(1)}_i h^{(2)}_k$. The same finite-difference functions and the functions of the initial problem corresponding to them will be denoted by the same values. At the nodes of the difference net $\bar{\Omega}_h$ we shall define the finite difference values ψ_{ik} and ω_{ik}.

The finite-difference functions $Q = Q_{i+1/2k+1/2}$ will be reduced to the intermediate nodes $X_0 = (x_{i+1/2}, y_{k+1/2})$ [one formula illegible] and also the boundary nodes $(x_{i+1/2}, y_k)$, $k=0, N$ and $(x_i, y_{k+1/2})$, $i=0, M$ ($Q_{i+1/2k}$, $k=0, N$, $Q_{ik+1/2}$, $i=0,M$), the set of which will be denoted by Γ_{h0}, $\bar{\Omega}_{h0} = \Omega_{h0} \cup \Gamma_{h0}$, $H_{0i+1/2k+1/2}$ is a cell of the difference net Ω_{h0} is a rectangle bounded by the segments of straight lines $x=x_i$, $x=x_{i+1}$ and $y=y_k$, $y=y_{k+1}$, its area $H_{0i+1/2k+1/2} = h^{(1)}_{i+1/2} h^{(2)}_{k+1/2}$.

Let us introduce, finally, the sets Ω_{h1} and Ω_{h2} of the flow nodes $X_1 = (x_{i+1/2}, y_k) \in \bar{G}$ and $X_2 = (x_i, y_{k+1/2}) \in G$ and also the sets Γ_{h1} and Γ_{h2} of the flow boundary nodes (x_i, y_k), $i=0, M$, $(x_i y_k)$, $k=0, N$, $\bar{\Omega}_{hs} = \Omega_{hs} \cup \Gamma_{hs}$, $s=1,2$, $H_{1i+1/2k} = h^{(1)}_{i+1/2} h^{(2)}_k$,

$H_{2\ ik+1/2}=h_i^{(1)}h_{k+1/2}^{(2)}$, ... In the nodes Ω_{h1} and Ω_{h2} we define the finite-difference functions $v_{i+1/2k}$, $W_{2i+1/2k}$ and $U_{ik+1/2}$, $W_{1ik+1/2}$. Below sometimes we shall omit the indexes and write $\psi=\psi_{ik}$, $Q=Q_{i+1/2k+1/2}$, $u=u_{ik+1/2}$, and so on.

Let us introduce the spaces H_h, H_{h0}, H_{hs}, s=1,2 of the finite-difference functions defined, respectively, by Ω_h, Ω_{h0}, Ω_{hs}, s=1,2 with the scalar products and norms

$$(\psi,\omega)=\sum_{\Omega_h}\psi\omega H,\quad \|\omega\|=(\omega,\omega)^{1/2},\quad \psi,\omega\in H_h,$$

$$(Q,P)=\sum_{\Omega_{h0}}Q\cdot P\cdot H_0,\quad \|Q\|=(Q,Q)^{1/2},\quad Q,P\in H_{h0},$$

$$(v,W_2)_1=\sum_{\Omega_{h1}}vW_2H_1,\quad \|v\|_1=(v,v)_1^{1/2},\quad v,W_2\in H_{h1},$$

$$(u,W_1)_2=\sum_{\Omega_{h2}}uW_1H_2,\quad \|u\|_2=(u,u)_2^{1/2},\quad u,W_1\in H_{h2}.$$

Let us introduce the notation for the finite-difference analogs of the derivatives with respect to x and y. For the finite-difference functions

$z_{is}=z(x_i,y_s)$, $s=k,k+1/2$, $z_{sk}=z(x_s,y_k)$, $s=i,i+1/2$ correspondingly, we determine

$$z_{x\,i+1/2\,s}=(z_{i+1\,s}-z_{is})/h_{i+1/2}^{(1)},\quad s=k,k+1/2,$$

$$z_{y\,s\,k+1/2}=(z_{s\,k+1}-z_{sk})/h_{k+1/2}^{(2)},\quad s=i,i+1/2.$$

For the functions $z_{i+1/2\,s}=z(x_{i+1/2},y_s)$, $s=k,k+1/2$

and $z_{s\,k+1/2}=z(x_s,y_{k+1/2})$, $s=i,i+1/2$ let us introduce the differences

$$z_{\hat{x}\,is}=\begin{cases}(z_{1/2\,s}-z_{0s})/h_0^{(1)}, & i=0,\\ (z_{i+1/2\,s}-z_{i-1/2\,s})/h_i^{(1)}, & 0<i<M,\\ (z_{Ms}-z_{M-1/2\,s})/h_M^{(1)}, & i=M,\end{cases}\quad s=k,k+1/2,$$

and

$$z\hat{y}_{sk} = \begin{cases} (z_{s\,1/2} - z_{s0})/h^{(2)}_0, & k=0, \\ (z_{sk+1/2} - z_{s\,k-1/2})/h^{(2)}_k, & 0<k<N, \\ (z_{sN} - z_{s\,N-1/2})/h^{(2)}_N, & k=N, \quad s=i, i+1/2. \end{cases}$$

The difference ratios

$$z\hat{x}_{ik},\ z\hat{y}_{ik} \in \mathcal{H}_h,\quad z_{x\,i+1/2\,k+1/2},$$
$$z_{y\,i+1/2\,k+1/2} \in \mathcal{H}_{h0},\ z_{x\,i+1/2\,k}, z\hat{y}_{i+1/2\,k} \in \mathcal{H}_{h1},\ z\hat{x}_{ik+1/2}, z_{y\,ik+1/2} \in \mathcal{H}_{h2}.$$

Let us introduce the difference net with respect to time with the step size τ

$$\Omega_\tau = \{t_j = j\cdot\tau,\ t_{j+1/2} = (j+1/2)\tau,\ j=0,1,\ldots j_0 = T/\tau\}.$$

We shall consider the function $Q_{i+1/2k+1/2}$ in the intermediate time layers

$$Q^{j+1/2}_{i+1/2\,k+1/2} = Q_{i+1/2\,k+1/2}(t_{j+1/2}),$$ the functions ψ, u, v, ω, in the integral layers t_j: t_j: $\psi^j_{ik} = \psi_{ik}(t_j)$, $u^j_{ik+1/2} = u_{ik+1/2}(t_j)$ and so on,

$$\omega^{j+1}_{\xi ik} = (\omega^{j+1}_{ik} - \omega^j_{ik})/\tau,$$
$$\psi^{j+1/2}_{ik} \equiv (\psi^{j+1}_{ik} + \psi^j_{ik})/2,\quad u^{j+1/2}_{ik+1/2} = (u^{j+1}_{ik+1/2} + u^j_{ik+1/2})/2 \qquad (2.1)$$

and so on.

§3. Balance Equation. Approximation of Flows

Let us integrate the first and second equations of (1.1) over the area H_{ik} and $H_{0i+1/2k+1/2}$ and with respect to time from t_j to t_{j+1}. The third equation (1.1) will be integrated for $t=t_{j+1}$ over the area H_{ik}, $(x_i, y_k) \in \Omega h$. We obtain

$$\omega^{j+1}_{\xi ik} = (\overline{W}_2^{j+1/2})\hat{x}_{ik} - (\overline{W}_1^{j+1/2})\hat{y}_{ik},\ (x_i, y_k) \in \overline{\Omega}_h, \qquad (3.1)$$

$$(\overline{W}_1^{j+1/2})_{x\,i+1/2\,k+1/2} + (\overline{W}_2^{j+1/2})_{y\,i+1/2\,k+1/2} = 0,\ (x_{i+1/2}, y_{k+1/2}) \in \Omega_{h0}, \qquad (3.2)$$

$$\left(\frac{\overline{\partial\psi}}{\partial x}^{j+1}\right)_{\hat{x}ik} + \left(\frac{\overline{\partial\psi}}{\partial y}^{j+1}\right)_{\hat{y}ik} = -\overline{\omega}^{j+1}_{ik},\quad (x_i, y_k) \in \Omega_h. \qquad (3.3)$$

In (3.1) the values of $\overline{W}_{1\,sk}^{j+1/2}$, $\overline{W}_{2\,is}^{j+1/2}$ are the means from

$W_1(x_s, y, t)$, $s = 0, 1/2, 3/2, \ldots M-1/2, M$, $W_2(x, y_s, t)$

$s = 0, 1/2, 3/2, \ldots N-1/2, N$ by the integral $\tau = t_{j+1} - t$; and in accordance with the segments $h_k^{(2)}$ and $h_i^{(1)}$. In (3.2) the flows $W_1(x_i, y, t)$ and $W_2(x, y_k, t)$ are averaged with respect to the interval $\tau = t_{j+1} - t_j$ and in accordance with the segments $h^{(2)}_{k+1/2}$ and $h^{(1)}_{i+1/2}$. In (3.3) the values of $\partial\psi^{i+1}/\partial x$ and $\partial\psi^{i+1}/\partial y$ are averaged with respect to the same segments as W_1 and W_2 in (3.1), ω^j_{ik} is the mean with respect to H_{ik} from the function $\omega(x,y,t_j)$.

Let us approximate $W_1^{j+1/2}$, $W_2^{j+1/2}$ in (3.1) and in (3.2) using the same finite-difference expressions. Let us first introduce the average velocities

$$u_{i\,k+1/2} \equiv \overline{u}_{0\,i\,k+1/2} = \left(h^{(2)}_{k+1/2}\right)^{-1} \int_{y_k}^{y_{k+1}} u_0 \Big|_{x=x_i} dy, \quad i = 0, M,$$
$$v_{i+1/2\,k} \equiv \overline{v}_{0\,i+1/2\,k} = \left(h^{(1)}_{i+1/2}\right)^{-1} \int_{x_i}^{x_{i+1}} v_0 \Big|_{y=y_k} dx, \quad k = 0, N. \tag{3.4}$$

Let us also set

$$u_{ik} = u_{0\,ik} \equiv (\overline{u}_0)_{ik}, \; k = 0, N, \; v_{ik} = v_{0\,ik} \equiv (\overline{v}_0)_{ik}, \; i = 0, M. \tag{3.5}$$

The finite-difference analogs of the flows $\overline{W}_1^{j+1/2}$, $\overline{W}_2^{j+1/2}$ in Γ will be given by the formulas

$$W_{1\,i\,k+1/2}^{j+1/2} = \overline{u}_{0\,\tau\,i\,k+1/2}^{\,j+1}, \; W_{2\,ik}^{j+1/2} = \overline{v}_{0\,\tau\,ik}^{\,j+1}, \; i = 0, M,$$
$$W_{2\,i+1/2\,k}^{j+1/2} = \overline{v}_{0\,\tau\,i+1/2\,k}^{\,j+1}, \; W_{1\,ik}^{j+1/2} = \overline{u}_{0\,\tau\,ik}^{\,j+1}, \; k = 0, N. \tag{3.6}$$

Let us set

$$u_{i\,k+1/2} = \psi_{y\,i\,k+1/2}, \; v_{i+1/2\,k} = -\psi_{x\,i+1/2\,k}. \tag{3.7}$$

From (3.4), (3.7), that is, from

$$\overline{u}_0^{\,j+1}{}_{i\,k+1/2} = \psi_y^{\,j+1}{}_{i\,k+1/2}, \; i = 0, M, \; \overline{v}_{0\,i+1/2\,k}^{\,j+1} =$$
$$= -\psi_x^{\,j+1}{}_{i+1/2\,k}, \; k = 0, N, \; \psi_{00}^{j+1} = 0 \tag{3.8}$$

Let us define the finite-difference values of the function

$$\psi_{ik}^{j+1} = \overline{\psi}_0^{j+1}{}_{ik}, \quad (x_i, y_k) \in \Gamma_h, \tag{3.9}$$

The means of $\nu\partial\omega/\partial x$, $\partial Q/\partial x$, $\nu\partial\omega/\partial y$, $\partial Q/\partial y$ in $\overline{W}_1^{j+1/2}$, $\overline{W}_2^{j+1/2}$ we shall naturally approximate by the values of

$$\nu\omega_x^{j+1/2}{}_{i+1/2\,k} \equiv \nu\left(\frac{\omega^{j+1}+\omega^{j}}{2}\right)_{x\,i+1/2\,k}, \quad Q\hat{x}^{j+1/2}{}_{i\,k+1/2}$$

and so on, the means from $\partial\psi^{j+1}/\partial x$, $\partial\psi^{j+1}/\partial y$, ω^{j+1}, $\omega_{\mp}^{j+1}$ will be approximated by the values of $\psi_x^{j+1}{}_{i+1/2\,k}$, $\psi_y^{j+1}{}_{i\,k+1/2}$, ω_{ik}^{j+1}, $\omega_{\mp}^{j+1}{}_{ik}$.

The approximation of the means of $u\omega$ and $v\omega$ by the finite-difference analogs $\mathcal{D}_1^{j+1/2}$ and $\mathcal{D}_2^{j+1/2}$ will be indicated below.

At all of the nodes Ω_{h1} and Ω_{h2} (including the nodes at Γ) the values of $\overline{W}_1^{j+1/2}$, $\overline{W}_2^{j+1/2}$ will be approximated as follows

$$\begin{aligned} W_1^{j+1/2}{}_{i\,k+1/2} &= -\left(\nu\omega_y^{j+1/2}{}_{i\,k+1/2} - \mathcal{D}_2^{j+1/2}{}_{i\,k+1/2} + Q\hat{x}^{j+1/2}{}_{i\,k+1/2}\right), (x_i, y_{k+1/2}) \in \Omega_{h1} \\ W_2^{j+1/2}{}_{i+1/2\,k} &= \left(\nu\omega_x^{j+1/2}{}_{i+1/2\,k} - \mathcal{D}_1^{j+1/2}{}_{i+1/2\,k} - Q\hat{y}^{j+1/2}{}_{i+1/2\,k}\right), (x_{i+1/2\,k}) \in \Omega_{h2} \end{aligned} \tag{3.10}$$

Let us note that since $W_1^{j+1/2}{}_{i\,k+1/2}, i=0,M$, $W_2^{j+1/2}{}_{i+1/2\,k}, k=0,N$ are given with respect to (3.6), hereafter from (3.6), (3.10) it will be possible to define the functions $Q^{j+1/2}{}_{i\,k+1/2}, i=0,M$ and $Q^{j+1/2}{}_{i+1/2\,k}, k=0,N$ by the calculation functions

$$\omega_{ik}^{j+1/2}, \psi_{ik}^{j+1/2}, Q^{j+1/2}{}_{i+1/2\,k+1/2}.$$

Let us introduce the notation

$$\alpha_i^{(1)} = h_{i+1/2}^{(1)}/(2h_i^{(1)}), \quad \alpha_k^{(2)} = h_{k+1/2}^{(2)}/(2h_k^{(2)}),$$

then

$$h_{i-1/2}^{(1)}/(2h_i^{(1)}) = 1-\alpha_i^{(1)}, \quad h_{k-1/2}^{(2)}/(2h_k^{(2)}) = 1-\alpha_k^{(2)}.$$

The values of $\mathcal{A}_1 = u\omega$ and $\mathcal{A}_2 = v\omega$ will be approximated by different methods. Let us indicate three methods of approximation leading to the schemes in the nine-point standard for the functions ω, ψ (the index j+1/2 on the functions ω, ψ, u, v will be omitted):

$$1)\quad \mathcal{A}_{1\,i+1/2\,k}^{(1)} = (\bar{u}_{i+1k}\omega_{i+1k} + \bar{u}_{ik}\omega_{ik})/2,$$
$$\mathcal{A}_{2\,ik+1/2}^{(1)} = (\bar{v}_{ik+1}\omega_{ik+1} + \bar{v}_{ik}\omega_{ik})/2. \qquad (3.11)$$

$$\bar{u}_{i0} = u_{i\,1/2},\ \bar{u}_{ik} = \alpha_k^{(2)} u_{ik+1/2} + (1-\alpha_k^{(2)})\, u_{ik-1/2},\ 0<k<N,$$
$$\bar{u}_{iN} = u_{iN-1/2},\ \bar{v}_{0k} = v_{1/2\,k},\ \bar{v}_{ik} = \alpha_i^{(1)} v_{i+1/2\,k} +$$
$$+ (1-\alpha_i^{(1)})\, v_{i-1/2\,k},\ 0<i<M,\ \bar{v}_{Mk} = v_{M-1/2\,k},$$

$$2)\quad \mathcal{A}_{1\,i+1/2\,0}^{(2)} = \bar{u}_{i+1/2\,1/2}\,\bar{\omega}_{i+1/2\,1/2},\ \mathcal{A}_{1\,i+1/2\,k}^{(2)} =$$
$$= \alpha_k^{(2)} \bar{u}_{i+1/2\,k+1/2}\,\bar{\omega}_{i+1/2\,k+1/2} + (1-\alpha_k^{(2)})\,\bar{u}_{i+1/2\,k-1/2}\bar{\omega}_{i+1/2,\,k-1/2},$$
$$0<k<N,\ \mathcal{A}_{1\,i+1/2\,N}^{(2)} = \bar{u}_{i+1/2\,N-1/2}\,\bar{\omega}_{i+1/2\,N-1/2},$$

$$\mathcal{A}_{2\,0\,k+1/2}^{(2)} = \bar{v}_{1/2\,k+1/2}\,\bar{\omega}_{1/2\,k+1/2},\ \mathcal{A}_{2\,ik+1/2}^{(2)} = \alpha_i^{(1)}\bar{v}_{i+1/2\,k+1/2}\bar{\omega}_{i+1/2\,k+1/2} \qquad (3.12)$$
$$+ (1-\alpha_i^{(1)})\,\bar{v}_{i-1/2\,k+1/2}\,\bar{\omega}_{i-1/2\,k+1/2},\ 0<i<M,\ \mathcal{A}_{2\,Mk+1/2}^{(2)} =$$
$$= \bar{v}_{M-1/2\,k+1/2}\,\bar{\omega}_{M-1/2\,k+1/2}.$$

Here

$$\bar{u}_{i+1/2\,k+1/2} = (u_{i+1k+1/2} + u_{ik+1/2})/2,\ \bar{v}_{i+1/2\,k+1/2} = (v_{i+1/2\,k+1} +$$
$$+ v_{i+1/2\,k})/2,\ \bar{\omega}_{i+1/2\,k+1/2} = 0.25\left(\omega_{i+1k+1} + \omega_{i+1k} + \omega_{ik+1} + \omega_{ik}\right),$$
$$3)\quad \mathcal{A}_{1\,i+1/2\,k}^{(3)} = \bar{u}_{i+1/2\,k}\,(\omega_{i+1k} + \omega_{ik})/2,\ \mathcal{A}_{2\,ik+1/2}^{(3)} = \qquad (3.13)$$
$$= \bar{v}_{ik+1/2}(\omega_{ik+1} + \omega_{ik})/2,\ \bar{u}_{i+1/2\,0} = \bar{u}_{i+1/2\,1/2},\ \bar{u}_{i+1/2}$$
$$= \alpha_k^{(2)}\bar{u}_{i+1/2\,k+1/2} + (1-\alpha_k^{(2)})\,\bar{u}_{i+1/2\,k-1/2},\ 0<k<N,\ \bar{u}_{i+1/2\,N} = \bar{u}_{i+1/2\,N-1/2},$$
$$\bar{v}_{0\,k+1/2} = \bar{v}_{1/2\,k+1/2},\ \bar{v}_{ik+1/2} = \alpha_i^{(1)}\bar{v}_{i+1/2\,k+1/2} + (1-\alpha_i^{(1)})\,\bar{v}_{i-1/2\,k+1/2},$$
$$0<i<M,\ \bar{v}_{Mk+1/2} = \bar{v}_{M-1/2\,k+1/2}.$$

The values of $\bar{u}$, $\bar{v}$ are expressed in terms of $u_{ik+1/2}$, $v_{i+1/2k}$, and the latter, with the help of (3.5), in terms of ψ_{ik}. Therefore

$$\mathcal{A}_s^{j+1/2} = \mathcal{A}_s^{(n)}(\psi^{j+1/2}, \omega^{j+1/2}), \quad s=1,2, \quad n=1,2,3. \tag{3.14}$$

The expressions for the flows $W_1^{1/2}$, $W_2^{1/2}$ (j=0) enter into the values of ω_{ik}^0, ψ_{ik}^0. Let us define them. Let us introduce the initial velocities

$$\begin{aligned} \overline{u^0}_{ik+1/2} &= (h^{(2)}_{k+1/2})^{-1} \int_{y_k}^{y_{k+1}} u^0\big|_{x=x_i} dy, \quad (x_i, y_{k+1/2}) \in \Omega_{h2}, \\ \overline{v^0}_{i+1/2k} &= (h^{(1)}_{i+1/2})^{-1} \int_{x_i}^{x_{i+1}} v^0\big|_{y=y_k} dx, \quad (x_{i+1/2}, y_k) \in \Omega_{h1}, \\ \overline{u^0}_{ik} &= \overline{u_0}_{ik}\big|_{t=0}, \; k=0,N, \; \overline{v^0}_{ik} = \overline{v_0}_{ik}\big|_{t=0}, \; i=0,M. \end{aligned} \tag{3.15}$$

Let us set

$$\psi^0_{ik} = \overline{\psi^0}_{ik}, \quad (x_i, y_k) \in \bar{\Omega}_h \tag{3.16}$$

where the function $\overline{\psi^0}_{ik}$ is determined from the equalities

$$\overline{\psi^0}_{x\,i+1/2\,k} = -\overline{v^0}_{i+1/2\,k}, \; \overline{\psi^0}_{y\,i\,k+1/2} = \overline{u^0}_{i\,k+1/2}, \; \overline{\psi^0}_{s} = 0 \tag{3.17}$$

The function ω^0_{ik} will be defined by the formula

$$\omega^0_{ik} = \overline{\omega^0_{ik}} \equiv (\overline{v^0})_{\hat{x}\,ik} - (\overline{u^0})_{\hat{y}\,ik}, \quad (x_i, y_k) \in \bar{\Omega}_h \tag{3.18}$$

Let us introduce the operators

$$\Lambda_{h1}(v), \Lambda_{h2}(u), \Lambda_h(u,v) = \Lambda_{h1}(v) + \Lambda_{h2}(u),$$

$$(\Lambda_{h1}(v)\psi)_{0k} = \frac{1}{h_0^{(1)}}(\psi_{x\,1/2\,k} + v_{0k}), \; (\Lambda_{h1}(v)\psi)_{Mk} = \frac{1}{h_M^{(1)}}(-v_{Mk} - \psi_{x\,M-1/2\,k}),$$

$k \neq 0,N$, $(\Lambda_{h2}(u)\psi)_{i0} = \frac{1}{h_0^{(2)}}(\psi_{y\,i\,1/2} - u_{i0})$. $(\Lambda_{h2}(u)\psi)_{iN} =$

$= \frac{1}{h_N^{(2)}}(u_{iN} - \psi_{y\,i\,N-1/2})$, $i \neq 0,M$, $(\Lambda_{h1}(v)\psi)_{ik} = -v_{\hat{x}\,ik}$,

$k=0,N$, $(\Lambda_{h2}(u)\psi)_{ik} = u_{\hat{y}\,ik}$, $i=0,M$.

At the other nodes

$$(\Lambda_{h1}(v)\psi)_{ik} = (\psi_x)\hat{x}_{ik}, (\Lambda_{h2}(u)\psi)_{ik} = (\psi_y)\hat{y}_{ik}, (x_i, y_k)\in\Omega_h$$

so that

$$(\Lambda_h(u,v)\psi)_{ik} = (\psi_x)\hat{x}_{ik} + (\psi_y)\hat{y}_{ik} = (\Delta_h\psi)_{ik}, \quad (x_i, y_k)\in\Omega_h.$$

The equality (3.18) can now be written in the form

$$\omega^0_{ik} = (\Lambda_h(\bar{u}^0\bar{v})\psi^0)_{ik}, \quad (x_i, y_k)\in\bar{\Omega}_h. \tag{3.19}$$

The approximation of ω^0_{ik} by Γ_h is the known Tom approximation.

§4. Difference Problem in the Variables ψ, ω, Q

In (3.1)-(3.3) let us replace the average values by their finite-difference analogs. We arrive at the following difference problem for the equations

$$\omega^{j+1}_{\tau ik} = (W_2)^{j+1/2}\hat{x}_{ik} - (W_1)^{j+1/2}\hat{y}_{ik}, \quad (x_i, y_k)\in\bar{\Omega}_h, \tag{4.1}$$

$$(W_1)^{j+1/2}_{x\, i+1/2\, k+1/2} + (W_2)^{j+1/2}_{y\, i+1/2\, k+1/2} = 0, \quad (x_{i+1/2}, y_{k+1/2})\in\Omega_{h0}, \tag{4.2}$$

$$(\Delta_h\psi^{j+1})_{ik} = -\omega^{j+1}_{ik}, \quad (x_i, y_k)\in\Omega_h \tag{4.3}$$

Under the boundary conditions at the nodes on Γ

$$W_{1\, i\,k+1/2}^{j+1/2} = \overline{u_0}^{j+1}_{\tau\, i\,k+1/2}, W_{1\, ik}^{j+1/2} = \overline{u_0}^{j+1}_{ik}, \quad i=0,M, \tag{4.4}$$

$$W_{2\, i+1/2\, k}^{j+1/2} = \overline{v_0}^{j+1}_{\tau\, i+1/2\, k}, W_{2\, ik}^{j+1/2} = \overline{v_0}^{j+1}_{\tau\, ik}, \quad k=0,N,$$

$$\psi^{j+1}_{ik} = \overline{\psi_0}^{j+1}_{ik}, \quad (x_i, y_k)\in\Gamma_h, \tag{4.5}$$

$$j = 0, 1, \ldots j_0,$$

in the initial data

$$\psi^0_{ik} = \overline{\psi^0_{ik}}, \quad \omega^0_{ik} = \overline{\omega^0_{ik}}, \quad (x_i, y_k)\in\overline{\Omega_h}. \tag{4.6}$$

Here $W_1^{j+1/2}$, $W_2^{j+1/2}$ will be defined by (3.10), (3.6), $\overline{\psi}_{ik}^{0}$, $\overline{\omega}_{ik}^{0}$, by the formulas (3.15)-(3.18), $\overline{\psi}_{0ik}^{j}$ by (3.4), (3.8), $\overline{u}_{0ik}^{j}$ $\overline{v}_{0ik}^{j}$, by (3.5). The values of $\mathfrak{D}_1^{j+1/2}$, $\mathfrak{D}_2^{j+1/2}$ will be defined by one of the formulas (3.11)-(3.13).

Let us note that for resolvability of the equations (4.2) with respect to the function $Q^{j+1/2}_{i+1/2k+1/2}$ it is necessary that the value of

$$S=\sum_{K=0}^{N-1} h^{(2)}_{K+1/2}\left(W_{1MK+1/2}^{j+1/2}-W_{10K+1/2}^{j+1/2}\right)+\sum_{i=0}^{M-1} h^{(1)}_{i+1/2}\left(W_{2i+1/2N}^{j+1/2}-W_{2i+1/20}^{j+1/2}\right)$$

vanish.

Let us substitute $W_1^{j+1/2}$, $W_2^{j+1/2}$ from (3.6), $\overline{u}_0{}^{j+1}_{ik+1/2}$, $\overline{v}_0{}^{j+1/2}_{i+1/2k}$ from (3.4) here; let us use (1.2). We find that

$$S=\left(\oint_\Gamma u_0^{j+1}dy+v_0^{j+1}dx\right)\bar{\tau}=0.$$

Let the problem (4.1)-(4.6) be resolvable. Then on the basis of (4.2) it is possible to introduce

$$W_{1\,iK+1/2}^{j+1/2}=\varphi_{y\bar{\tau}\,iK+1/2}^{j+1},\quad W_{2\,i+1/2\,K}^{j+1/2}=-\varphi_{x\bar{\tau}\,i+1/2\,K}^{j+1}.$$
$$\varphi^{0}_{iK}=\overline{\psi}^{0}_{iK},\ (x_i,y_K)\in\overline{\Omega}_h,\quad \varphi_{00}^{j+1}=0 \tag{4.7}$$

Then from (4.1) we find that

$$\left(\omega^{j+1}+\Lambda_h(\overline{u}_0^{j+1},\overline{v}_0^{j+1})\varphi^{j+1}\right)_{\bar{\tau}\,iK}=0,\ (x_i,y_K)\in\overline{\Omega}_h,$$

Hence also from (4.6), (4.7) $\left(\varphi_{iK}^{j+1}=\overline{\psi}_0^{j+1}{}_{iK},\ (x_i,y_K)\in\Gamma_h\right)$

it follows that $\varphi_{iK}^{j+1}\equiv\psi_{iK}^{j+1}$, $(x_i,y_K)\in\overline{\Omega}_h$

and the following equality occurs

$$\omega_{iK}^{j+1}=-\left(\Lambda_h(\overline{u}_0^{j+1},\overline{v}_0^{j+1})\psi^{j+1}\right)_{iK},(x_i,y_K)\in\Gamma_h. \tag{4.8}$$

Thus, from (4.1)-(4.6) it follows that the Tom approximation of the condition (1.5) occurs for all $t_j\in\Omega_\tau$. On derivation of (4.8) essentially the Tom approximation was used for t=0, $(x_i, y_k)\in\Gamma_h$.

Now let us consider the problem (4.1), (4.2), (4.4), (4.6) and (4.3), (4.5) will be replaced by the equation

$$\left(\Lambda_h(\bar{u}_0^{j+1}, \bar{v}_0^{j+1})\psi^{j+1}\right)_{ik} = -\omega_{ik}^{j+1}, \quad (x_i, y_k) \in \bar{\Omega}_h, \psi_{00}^{j+1} = 0. \tag{4.9}$$

For resolvability of (4.9) with respect to the function ψ_{ik}^{j+1} the following condition must be satisfied:

$$\sum_{\bar{\Omega}_h} \omega_{ik}^{j+1} H_{ik} = \sum_{k=0}^{N'} (v_{Mk}^{j+1} - v_{0k}^{j+1}) h_k^{(2)} + \sum_{i=0}^{M} (u_{iN}^{j+1} - u_{i0}^{j+1}) h_0^{(1)} = 0 \tag{4.10}$$

where

$$v_{ik}^{j+1} = \bar{v}_{0\,ik}^{j+1}, \quad i = 0, M, \quad u_{ik}^{j+1} = \bar{u}_{0\,ik}^{j+1}, \quad k = 0, N.$$

The equality (4.10) follows from (4.1), (4.4), (4.6).

Let the problem (4.1), (4.2), (4.4), (4.6), (4.9) be resolvable. Then $\psi_{ik}^{j+1} = \bar{\psi}_{0\,ik}^{j+1}$, $(x_i, y_k) \in \Gamma_h$. Let us demonstrate this. Let us introduce the function φ_{ik}^{j+1}, $\varphi_{ik}^{j+1} = \bar{\psi}_{0\,ik}^{j+1}$, $(x_i, y_k) \in \Gamma_h$ with respect to (4.7). Just as above we find $\psi_{ik}^{j+1} = \phi_{ik}^{j+1}$, $(x_i, y_k) \in \bar{\Omega}_h$. Thus, it is possible to consider instead of (4.3), (4.5), the equation (4.9).

Using the equation (4.8), we exclude the function $Q^{j+1/2}_{i+1/2k+1/2}$ from the investigation -- we break up the problem (4.1)-(4.6) into two problems -- the problem for determining the functions ψ_{ik}^{j+1}, ω_{ik}^{j+1} and the problem for determining the function $Q^{j+1/2}_{i+1/2k+1/2}$.

For the system (4.1)-(4.6) the energy estimate will be obtained below.

§5. Equivalent Difference Scheme in Variables ψ, ω

The equations (4.1) contain the desired function $Q^{j+1/2}_{i+1/2k+1/2}$ only for $i=0$, M and $k=0$, N (in the Γ_h nodes). We shall consider the equations (4.1) only at the nodes Ω_h, and at the nodes Γ_h we shall add equation (4.8) to the system (4.1)-(4.6). Let us consider the problem

$$\omega_{\bar{t}\,ik}^{j+1} = (W_2^{j+1/2})\hat{x}_{ik} - (W_1^{j+1/2})\hat{y}_{ik}, \quad (x_i, y_k) \in \Omega_h,$$

$$(\Lambda_h(\bar{u}_0^{j+1}, \bar{v}_0^{j+1})\psi^{j+1})_{ik} = -\omega_{ik}^{j+1}, \quad (x_i, y_k) \in \overline{\Omega}_h,$$

$$W_{1\,is}^{j+1/2} = \bar{u}_{0\,\bar{t}\,is}^{j+1}, \quad i=0,M, \; s=k, k+1/2, \; W_{2\,sk}^{j+1/2} =$$

$$= \bar{v}_{0\,\bar{t}\,sk}^{j+1}, \quad k=0,N, \; s=i, i+1/2. \tag{5.1}$$

$$\psi_{ik}^{j+1} = \psi_{0\,ik}^{j+1}, \quad (x_i, y_k) \in \Gamma_h, \quad j=0,1,\ldots j_0,$$

$$\psi_{ik}^{0} = \bar{\psi}_{ik}^{0}, \; \omega_{ik}^{0} = \bar{\omega}_{ik}^{0}, \quad (x_i, y_k) \in \overline{\Omega}_h.$$

Let the problem (5.1) be resolvable. By the functions ψ_{ik}^{j+1}, ω_{ik}^{j+1} found from (5.1), from (4.2) we find $Q^{j+1/2}{}_{i+1/2k+1/2}$ (with accuracy to the constant). By (4.7) let us introduce the function ϕ_{ik}^{j+1}. Just as before, $\phi_{ik}^{j+1} \equiv \psi_{ik}^{j+1}$ and

$$W_{1\,ik+1/2}^{j+1/2} = \psi_{y\bar{t}\,ik+1/2}^{j+1}, \quad W_{2\,i+1/2k}^{j+1/2} = -\psi_{x\bar{t}\,i+1/2k}^{j+1}.$$

Hence also from the equality

$$\omega_{\bar{t}\,ik}^{j+1} = -\left(\Lambda_h(\bar{u}_0^{j+1}, \bar{v}_0^{j+1})\psi^{j+1}\right)_{\bar{t}\,ik}, \quad (x_i, y_k) \in \Gamma_h$$

it follows that the equation (4.1) is satisfied on Γ_h. The problems (4.1)-(4.6) are equivalent.

Let us discuss the results obtained. For this purpose let us consider the linear problem with $\vartheta_1 = \vartheta_2 = 0$ (or we shall consider that ϑ_1, ϑ_2 are known, they are calculated with respect to ψ_{ik} and ω_{ik} from the preceding time layer). In this case the function $Q^{j+1/2}{}_{i+1/2k+1/2}$ can be expressed from (4.2) using the generalized Green finite-difference function in terms of the values of the desired function $\omega_{ik}^{j+1/2}$ (ω_{ik}^{j+1}) on Γ_h. Substituting $Q^{j+1/2}{}_{i+1/2k+1/2}$ in equations (4.1) for $(x_i, y_k) \in \Gamma_h$ we arrive at the nonlocal boundary conditions (compare [5]) for the function ω_{ik}^{j+1}:

$$\omega_{\bar{t}\,ik}^{j+1} = \pm\frac{\nu}{h_i^{(1)}}\omega_{x\,i+1/2k}^{j+1/2} + \sum_{(x_n,y_m)\in\Gamma_h} \mathcal{K}_{ik}(x_n,y_m)\omega_{nm}^{j+1/2} + g_{ik}^{j+1/2}, \quad i=0,M,$$

$$\omega_{\bar{t}\,ik}^{j+1} = \pm\frac{\nu}{h_k^{(2)}}\omega_{y\,ik+1/2}^{j+1/2} + \sum_{(x_n,y_m)} \mathcal{K}_{ik}(x_n,y_m)\omega_{nm}^{j+1/2} + g_{ik}^{j+1/2}, \quad k=0,N. \tag{5.2}$$

Here $K_{ik}(x_n, y_m)$, $g_{iu}^{j+1/2}$ are known functions. The problem with the condition (5.2) corresponds to the solution of the system of equations for ω_{ik}^{j+1}, $Q^{j+1/2}{}_{i+1/2k+1/2}$ (perhaps, with the help of the Green function) and it is equivalent to the problem (5.1) for the system of functions ω_{ik}^{j+1} and ψ_{ik}^{j+1}, the success of the solution of which is defined for each t_{j+1} by using a suitable iteration process. In the problem (4.1)-(4.6) the Tom conditions are satisfied automatically, the operator $\Lambda_h = \Lambda_h(0,0)$ ($u_0 = v_0 = 0$) in the functions $\psi_{ik} = \text{Const}$, $(x_i, y_k) \in \Gamma_h$ is nonpositive and self-conjugate: $\Lambda_h = \Lambda_h^* \leq 0$.

Equation (4.1) is written in the form

$$\omega_{\xi\, ik}^{j+1} = L_h(\omega^{j+1/2}, Q^{j+1/2})_{ik} + \mathfrak{N}_{ik}^{j+1/2}. \tag{5.3}$$

Here $\mathfrak{N}_{ik}^{j+1/2}$ are the nonlinear terms approximating the transport terms, $L_h(\omega^{j+1/2}, Q^{j+1/2})$ is the linear part containing the operators acting on the functions $\omega_{ik}{}^{j+1/2}$ and $Q^{j+1/2}{}_{i+1/2k+1/2}$.

For $\psi_{ik}=\psi_{0ik}=\text{const}$, $(x_i, y_k)\in\Gamma_h$, $u_0=v_0=0$ the following identities are correct

$$(\omega_\xi^{j+1}, \psi^{j+1/2}) = (E^{j+1})_\xi, \quad (L_h(\omega^{j+1/2}, Q^{j+1/2}), \psi^{j+1/2}) =$$
$$= \nu \|\omega^{j+1/2}\|^2, \quad E^{j+1} = 0.5\left(\|\psi_x^{j+1}\|_1^2 + \right. \tag{5.4}$$
$$\left. + \|\psi_y^{j+1}\|_2^2\right) = 0.5\left(\|v^{j+1}\|_1^2 + \|u^{j+1}\|_2^2\right).$$

For other methods of approximating (1.5) than the Tom formula, it is also necessary that the equalities (5.4) exist. The Tom approximation also reflects the uniformity of the difference scheme everywhere (in Γ_h and in Ω_h). The same equation is used for approximation of the balance. In all

$$(x_i, y_k)\in\overline{\Omega}_h, \quad \omega_{ik}^{j+1} = v_{\hat{x}}^{j+1}{}_{ik} - u_{\hat{y}}^{j+1}{}_{ik}.$$

In the case of the steady-state problem ($\omega_\xi^{j+1} = u_{0\xi}^{j+1} = v_{0\xi}^{j+1} = 0$)

it is necessary to add the following condition to (4.1)-(4.5):

$$(\Lambda_h(u_0, v_0)\psi)_{ik} = -\omega_{0k}, \quad (x_i, y_k)\in\Gamma_h, \tag{5.4}$$

§6. Families of Neutral Systems. Entirely Neutral System

Let us study the properties of the scheme (4.1)-(4.6) for various approximations of the values of $\mathfrak{N}_1$ and $\mathfrak{N}_2$ by the formulas (3.11)-(3.13) under uniform boundary conditions

$$u_0^j = v_0^j = 0, \quad \psi_0^j = \text{const}, \quad (x, y)\in\Gamma \tag{6.1}$$

In the equation (4.1) written in the form of (5.3),

$$\mathfrak{N}_{ik}^{j+1/2} = \mathfrak{N}_{ik}^{(n)} = -(\mathfrak{N}_1^{(n)})_{\hat{x}ik} - (\mathfrak{N}_2^{(n)})_{\hat{y}ik}, (x_i, y_k)\in\overline{\Omega}_h, \tag{6.2}$$
$$n = 1, 2, 3.$$

Inasmuch as $W_{ik}^{j+1/2}=0$, $i=0,M$, $W_{1\,ik}^{j+1/2}=0$, $k=0,N$, in (6.2) it is necessary to set $\mathfrak{N}_{1\,ik}^{j+1/2}=0$, $i=0,M$, $\mathfrak{N}_{2ik}^{j+1/2}=0$, $k=0,N$. At the nodes

$$(x_{i+1/2}, y_k),\ k=0,N, \quad (x_i, y_{k+1/2}),\ i=0,M, \quad W_1^{j+1/2}, W_2^{j+1/2}$$

will be defined by the formulas of (3.10). Accordingly, both $\mathfrak{D}_1^{j+1/2}{}_{i+1/2\,k}$, $k=0,N$ and $\mathfrak{D}_2^{j+1/2}{}_{i\,k+1/2}$, $i=0,M$ will be calculated by the formulas (3.11)-(3.13) (under the conditions (6.1)).

For the initial problem (1.1)-(1.4) under uniform boundary conditions we have the identity

$$\frac{\partial E}{\partial t} + \nu \int_G \omega^2 dxdy = 0, \quad \int_G \mathfrak{D}\psi \, dxdy = 0, \tag{6.3}$$

where

$$\mathfrak{D} = -\frac{\partial \mathfrak{D}_1}{\partial x} - \frac{\partial \mathfrak{D}_2}{\partial y}, \quad \mathfrak{D}_1 = u\omega, \quad \mathfrak{D}_2 = v\omega.$$

For uniform boundary conditions

$$\int_G \mathfrak{D}\omega \, dxdy = 0. \tag{6.4}$$

The equalities (6.3), (6.4) indicate that the transport terms do not make a contribution to the energy and entropy balance.

We shall state that the difference scheme is energywise neutral and entropy neutral if the finite difference analogs of the transport terms

$\mathfrak{D}^{j+1/2} = -(\mathfrak{D}_1^{j+1/2})_{\bar{x}} - (\mathfrak{D}_2^{j+1/2})_{\bar{y}}$ do not make a contribution to the energy balance $(\mathfrak{D}^{j+1/2}, \psi^{j+1/2}) = 0$ and the entropy balance $(\mathfrak{D}^{j+1/2}, \omega^{j+1/2}) = 0$.

If both of these equalities exist, then we shall call the difference scheme entirely neutral.

In order to discover the family of energy neutral schemes, it is necessary under the condition of (6.1) to calculate the scalar product $(\mathfrak{D}^{(n)\,j+1/2}, \psi^{j+1/2})$, $n=1,2,3$.

For the calculation we find that

$$(\mathfrak{D}^{(1)\,j+1/2}, \psi^{j+1/2}) = 0, \quad (\mathfrak{D}^{(2)\,j+1/2}, \psi^{j+1/2}) = 0 \tag{6.5}$$

that is, the schemes with $\mathfrak{D}^{j+1/2} = \mathfrak{D}^{(1)\,j+1/2}$, $\mathfrak{D}^{j+1/2} = \mathfrak{D}^{(2)\,j+1/2}$ (formulas (3.11), (3.12)) are energy neutral. For the schemes with $\mathfrak{D}^{j+1/2} = \mathfrak{D}^{(3)\,j+1/2}$ we have entropy neutrality

$$(\mathfrak{D}^{(3)\,j+1/2}, \omega^{j+1/2}) = 0. \tag{6.6}$$

For energy neutral schemes on the basis of (6.5), (5.4), (5.3), we have the analog of (6.3)

$$E_t^{j+1} + \nu \| \omega^{j+1/2} \|^2 = 0 \tag{6.7}$$

Let us consider the single-parametric family schemes (4.1)-(4.6) with the parameter β

$$\mathcal{D}_1{}^{j+1/2}_{i+1/2\,k} = \beta \mathcal{D}_1{}^{(1)\,j+1/2}_{i+1/2\,k} + (1-\beta)\,\mathcal{D}_1{}^{(2)\,j+1/2}_{i+1/2\,k},$$
$$\mathcal{D}_2{}^{j+1/2}_{i\,k+1/2} = \beta \mathcal{D}_2{}^{(1)\,j+1/2}_{i\,k+1/2} + (1-\beta)\,\mathcal{D}_2{}^{(2)\,j+1/2}_{i\,k+1/2}. \qquad (6.8)$$

It is obvious that this is the family of energy neutral schemes. Let us calculate the scalar products from $\omega_{ik}^{j+1/2}$ times $\mathcal{D}_{ik}^{j+1/2}$ for

$$\mathcal{D}_{ik}^{j+1/2} = \mathcal{D}^{(1)\,j+1/2}_{ik} \quad \text{and} \quad \mathcal{D}_{ik}^{j+1/2} = \mathcal{D}^{(2)\,j+1/2}_{ik}$$

We obtain

$$(\mathcal{D}^{(1)\,j+1/2},\ \omega^{j+1/2}) = \sum_{i=0}^{M-1}\sum_{k=0}^{N} H_{1\,i+1/2\,k}\,\bar{u}_{i+1/2\,k}^{j+1/2}\,\omega_{i+1\,k}^{j+1/2}\,\omega_{ik}^{j+1/2} +$$
$$+ \sum_{i=0}^{M-1}\sum_{k=0}^{N-1} H_{2\,i\,k+1/2}\,\bar{v}_{i\,k+1/2}^{j+1/2}\,\omega_{i\,k+1}^{j+1/2}\,\omega_{ik}^{j+1/2} \equiv F^{j+1/2},$$
$$(\mathcal{D}^{(2)\,j+1/2},\ \omega^{j+1/2}) = -0.5\,F^{j+1/2}.$$

Comparing the last two equalities, let us note that the energy neutral scheme (4.1)-(4.6) from the family (6.8) with $\beta=1/3$ is also entropy neutral. Thus, the scheme (4.1)-(4.6) with

$$\mathcal{D}_1{}^{j+1/2}_{i+1/2\,k} = \frac{1}{3}\mathcal{D}_1{}^{(1)\,j+1/2}_{i+1/2\,k} + \frac{2}{3}\mathcal{D}_1{}^{(2)\,j+1/2}_{i+1/2\,k} \equiv \bar{\mathcal{D}}_1{}^{j+1/2}_{i+1/2\,k},$$
$$\mathcal{D}_2{}^{j+1/2}_{i\,k+1/2} = \frac{1}{3}\mathcal{D}_2{}^{(1)\,j+1/2}_{i\,k+1/2} + \frac{2}{3}\mathcal{D}_2{}^{(2)\,j+1/2}_{i\,k+1/2} \equiv \bar{\mathcal{D}}_2{}^{j+1/2}_{i\,k+1/2}.$$

is completely neutral. The single-parametric family of entropy neutral schemes is constructed by $\mathcal{D}_1^{(3)}$, $\mathcal{D}_2^{(3)}$ and $\bar{\mathcal{D}}_1$, $\bar{\mathcal{D}}_2$. Similar approximations in a quadratic network were previously found in [3].

Notes. 1) Instead of (2.1) it is possible to introduce

$$\omega_{ik}^{j+1/2} = \sigma\,\omega_{ik}^{j+1} + (1-\sigma)\,\omega_{ik}^{j},\quad \psi_{ik}^{j+1/2} = \sigma\,\psi_{ik}^{j+1} + (1-\sigma)\,\psi_{ik}^{j} \qquad (6.9)$$

In this case it is necessary to add the term

$$\tau(\sigma-0.5)\,(\|\psi_{\bar{x}}^{j+1}\|_1^2 + \|\psi_{\bar{y}}^{j+1}\|_2^2),\quad E^{j+1} \to 0 \text{ for } t_{j+1} \to +\infty,$$

if $\sigma \geq 0.5$ to the lefthand side of (6.7). The preceding statements remain valid.

2) The scheme (4.1)-(4.6) with $\mathcal{D} = \mathcal{D}^{(1)}$ and $\mathcal{D} = \mathcal{D}^{(2)}$ remain energy neutral if $\mathcal{D}^{(1)}$ and $\mathcal{D}^{(2)}$ are calculated by $\psi_{ik}^{j+1/2}$ from (6.9) ($\sigma \geq 0.5$) and ψj_{ik}. The

schemes with $\mathfrak{A}=\vec{\mathfrak{A}}=-(\vec{\mathfrak{A}}_1)\hat{x}-(\vec{\mathfrak{A}}_2)\hat{y}$, $\mathfrak{A}=\mathfrak{A}^{(3)}$ are also entropy neutral if $\vec{\mathfrak{D}}$ and $\mathfrak{D}^{(3)}$ are calculated with respect to $\omega_{ik}^{j+1/2}$ from (6.9) ($\sigma\geq 0.5$) and ψ_{ik}^{j}. In these cases for ω_{ik}^{j+1}, ψ_{ik}^{j+1} the linear system of equations is obtained.

3) Let us present the two multipoint approximations of the values of $\mathfrak{A}_1$ and $\mathfrak{A}_2$ leading to entropy neutral schemes (4.1)-(4.6):

a) $$\mathfrak{A}_{1\,i+1/2\,k}=\mathfrak{A}^{(2)}_{1\,i+1/2\,k},\quad \mathfrak{A}_{2\,ik+1/2}=\frac{1}{2}(\overline{\omega}_{ik+1}\overline{v}_{ik+1}+\overline{\omega}_{ik}\overline{v}_{ik})$$
$$\overline{\omega}_{i0}=\omega_{i\,1/2},\quad \overline{\omega}_{ik}=(\omega_{i\,k+1/2}+\omega_{i\,k-1/2})/2,\ 0<k<N,$$
$$\overline{\omega}_{iN}=\omega_{i\,N-1/2},\quad \omega_{i\,k+1/2}=(\omega_{i\,k+1}+\omega_{ik})/2,$$

b) $$\mathfrak{A}_{1\,i+1/2\,k}=(\overline{\omega}_{i+1\,k}\overline{u}_{i+1\,k}+\overline{\omega}_{ik}\overline{u}_{ik})/2,\quad \mathfrak{A}_{2\,ik+1/2}=\mathfrak{A}^{(2)}_{2\,i\,k+1/2},$$

Here, in contrast to a) $\overline{\omega}_{0k}=\omega_{1/2\,k}$, $\overline{\omega}_{ik}=(\omega_{i+1/2\,k}+\omega_{i-1/2\,k})/2$, $0<i<M$, $\overline{\omega}_{Mk}=\omega_{M-1/2\,k}$, $\overline{\omega}_{i+1/2\,k}=(\omega_{i+1\,k}+\omega_{ik})/2$.

Using a), b) of the approximation $\mathfrak{A}^{(3)}$, $\vec{\mathfrak{A}}$ it is possible to construct the three-parametric family of entropy neutral schemes.

§7. Supplement

1) Monotonization. The expressions for $\mathfrak{A}_1^{(3)}$ and $\mathfrak{A}_2^{(3)}$ correspond to the central-difference approximation of the transport terms, which for small ν leads to nonmonotic systems. The methods of monotonization of the finite-difference equations (approximation of the transport terms by one-way spacings, monotonization with respect to [1], [6]) corresponds to the introduction of additional fictitious viscosities, that is, replacement in W_1, W_2 of the variables $\nu\omega_{ki+1/2k}$ and $\nu\omega_{yik+1/2}$ by $\nu(1+\rho_{1\,i+1/2k})\,\omega_{xi+1/2k}$, and $\nu(1+\rho_{2\,ik+1/2})\,\omega_{yik+1/2}$, $\rho_{1\,i+1/2\,k}$, $\rho_{2\,ik+1/2}\geq 0$.

Monotonization using the one-way differences corresponds to the selection of

$$\rho_{1\,i+1/2\,k}=|R_{1\,i+1/2\,k}|=\frac{h^{(1)}_{i+1/2}}{2\nu}|\overline{u}_{i+1/2\,k}|,\quad \rho_{2\,ik+1/2}=|R_{2\,ik+1/2}|=\frac{h^{(2)}_{k+1/2}}{2\nu}|\overline{v}_{i\,k+1/2}|$$

For monotonization with respect to [1], [6]

$$\rho_{1\,i+1/2\,k}=\frac{R^2_{1\,i+1/2\,k}}{1+|R_{1\,i+1/2\,k}|},\quad \rho_{2\,ik+1/2}=\frac{R^2_{2\,ik+1/2}}{1+|R_{2\,ik+1/2}|}.$$

We shall consider the monotonized schemes (4.1)-(4.6) with $\mathcal{A}_1 = \mathcal{A}_1^{(3)}$, $\mathcal{A}_2 = \mathcal{A}_2^{(3)}$ for the steady-state problem. The equation (4.1) for $\omega_t = 0$ using the finite-difference equation of continuity $\bar{u}\hat{x}_{ik} + \bar{v}\hat{y}_{ik} = 0$, $(x_i, y_k) \in \bar{\Omega}_h$ following from (3.13), (3.7), can be converted to the nondivergence form

$$(\bar{L}_h^{(1)}(\psi)\omega)_{ik} + (\bar{L}_h^{(2)}(\psi)\omega)_{ik} + (M_h Q)_{ik} = 0, \tag{7.1}$$

$L_h^{(1)}(\psi)\omega$, $L_h^{(2)}(\psi)\omega$ are the finite-difference analogs of the expressions $\nu\partial^2\omega/\partial x^2 - u\partial\omega/\partial x$, $\nu\partial^2\omega/\partial y^2 - v\partial\omega/\partial y$. Here it turns out that $\bar{L}_h^{(1)}(\psi)$, $\bar{L}_h^{(2)}(\psi)$ are the operators with diagonal predominance (the comparison theorem and the principle of the maximum are valid for (7.1) for $(M_h Q)_{ik} = 0$) (see also [6]). At the nodes $(x_i, y_k) \in \Omega_h$

$$\begin{aligned}
&(\bar{L}_h^{(1)}(\psi)\omega)_{ik} = (L_u^{(1)}\omega)_{ik} - (\alpha_i^{(1)}\bar{u}_{i+1/2,k}\omega_{\bar{x}i+1/2,k} + (1-\alpha_i^{(1)})\bar{u}_{i-1/2,k}\omega_{\bar{x}i-1/2,k}),\\
&(\bar{L}_h^{(2)}(\psi)\omega)_{ik} = (L_v^{(2)}\omega)_{ik} - (\alpha_k^{(2)}\bar{v}_{i,k+1/2}\omega_{\bar{y}i,k+1/2} + (1-\alpha_k^{(2)})\bar{v}_{i,k-1/2}\omega_{\bar{y}i,k-1/2})\\
&(L_u^{(1)}\omega)_{ik} = u((1+\rho_1)\omega_x)\hat{x}_{ik}, (L_v^{(2)}\omega)_{ik} = v((1+\rho_2)\omega_y)\hat{y}_{ik},\\
&(M_h Q)_{ik} = 0
\end{aligned} \tag{7.3}$$

The schemes $\mathcal{A} = \mathcal{A}^{(n)}$, $n = 1, 2$, $\mathcal{A} = \bar{\mathcal{A}}$ are distinguished from the scheme with $\mathcal{A} = \mathcal{A}^{(3)}$ by the terms $(\mu_1)\hat{x} + (\mu_2)\hat{y}$, $\mu_\alpha = O(h^2)$, $\alpha = 1, 2$ in the smooth functions.

2) Approximation of the boundary conditions for ω and ψ.

In the above-investigated schemes it is necessary to solve the system of algebraic equations for the functions ω_{ik}^{j+1}, $\omega^{j+1/2}{}_{i+1/2,k+1/2}$ or $\omega^{j+1}{}_{ik}$, ψ_{ik}^{j+1}. However, this is complicated. Usually it is proposed that the schemes be used in which the functions ψ_{ik}^{j+1} and ω_{ik}^{j+1} are calculated successively. Here the question arises of determining the function ω_{ik}^{j+1} at the boundary (the near-boundary [8]) nodes. Here let us present the procedure for "finish calculation" of the functions ω_{ik}^{j+1} in the near-boundary nodes generalizing the method of V. I. Polezhayev from [8] to the case of an arbitrary region G.

Let us draw the straight lines $x = x_i$, $i = 0, \pm1, \pm2, \ldots$, $y = y_k$, $k = 0, \pm1, \pm2, \ldots$. Let us denote by Ω_h the set of points $(x_i, y_k) \in G$ and by Γ_h the set of points of intersection of the indicated straight lines with the boundary Γ, $\bar{\Omega}_h = \Omega_h \cup \Gamma_h$. The node $(x_i, y_k) \in \Omega_h$ will be called the boundary node ($(x_i, y_k) \in \Gamma_h'$) if at least one of the nodes adjacent to it with respect to the directions $0x$ or $0y$ belongs to Γ_h, $\Omega_h' = \Omega_h \Gamma_h'$. From each node $(x_i, y_k) \in \Gamma_h'$ let us draw the segment Δn_{ik} orthogonal to Γ to the point $(\bar{x}_i, \bar{y}_k) \in \Gamma$. On Γ $\psi = \psi_0$, $\partial\psi/\partial n = \psi_{0n}$, $\partial^2\psi/\partial s^2 = \psi_{0ss}$ are given. Let $(x_i, y_k) \in \Gamma_h'$, $(\bar{x}_i, \bar{y}_k) \in \Gamma$ be the ends of Δn. Let us use the Taylor formula. We obtain

$$\psi(x_i, y_k, t) = \Phi_{ik}(t) + \frac{\Delta h^2_{ik}}{2} \Delta\psi\,(x_i, y_k, t) + O\left(\Delta h^3_{ik}\right), \qquad (7.4)$$
$$\Phi_{ik}(t) = \overline{\psi}_0(\overline{x}_i, \overline{y}_k, t) + \Delta n_{ik}\overline{\psi}_{0n}(\overline{x}_i, \overline{y}_k, t) - \frac{\Delta n^2_{ik}}{2}\overline{\psi}_{0ss}(\overline{x}_i, \overline{y}_k, t).$$

The values of $\omega_{ik}^{j+1/2}$, $\omega_{ik}^{j+1/1}$ in Γ'_h just as in [8] will be determined from

$$\omega_{ik}^{j+1/2} = \omega_{ik}^{j+1} = -(\Delta_h\psi^j)_{ik}, \quad (x_i, y_k) \in \Gamma'_h. \qquad (7.5)$$

Here and below the value of $\Delta\psi$ at the boundary node will be approximated by the value of $(\Delta_h\psi)_{ik}$ from [7].

At the nodes $(x_i, y_k) \in \Omega'_h$ the functions $\omega_{ik}^{j+1/2}$, ω_{ik}^{j+1} can be defined by using the method of variable directions (just as in [8]):

$$\frac{\omega_{ik}^{j+1/2} - \omega_{ik}^{j}}{0{,}5\tau} = \left(\Lambda_h^{(1)}(\psi^j)\,\omega^{j+1/2}\right)_{ik} + \left(\Lambda_h^{(2)}(\psi^j)\,\omega^j\right)_{ik}, \qquad (7.6)$$

$$\frac{\omega_{ik}^{j+1} - \omega_{ik}^{j+1/2}}{0{,}5\tau} = \left(\Lambda_h^{(1)}(\psi^j)\,\omega^{j+1/2}\right)_{ik} + \left(\Lambda_h^{(2)}(\psi^{j+1})\,\omega^{j+1}\right)_{ik}, \quad (x_i, y_k) \in \Omega'_h.$$

On the basis of (7.4), (4.3) for determination of ψ_{ik}^{j+1} we have

$$(\Delta_h\psi^{j+1})_{ik} - \frac{2}{\Delta n^2_{ik}}\psi_{ik}^{j+1} = -\frac{2}{\Delta n^2_{ik}}\Phi_{ik}^{j+1}, \quad (x_i, y_k) \in \Gamma'_h, \qquad (7.7)$$
$$(\Delta_h\psi^{j+1})_{ik} = -\omega_{ik}^{j+1}, (x_i, y_k) \in \Omega'_h, \quad \psi_{ik}^{j+1} = \psi_0^{j+1}(x_i, y_k) \in \Gamma_h.$$

$j=0, 1, \ldots, j_0$. At the initial point in time ψ_{ik}^0 and ω_{ik}^0 ($\omega_{ik}^0 = (\Delta_h\psi^0)_{ik}$) are the given functions.

In the vicinity of the angular points Γ at the nodes Γ'_h where the pair of segments Δn_1, Δn_2 and the pair of functions Φ_1 and Φ_2 are defined instead of the first equation of (7.7) it is necessary to write

$$(\Lambda_h\psi)_{ik}^{j+1} - \psi_{ik}^{j+1}\left(\frac{1}{\Delta n_1^2} + \frac{1}{\Delta n_2^2}\right) = -\left(\frac{\Phi_1^{j+1}}{\Delta n_1^2} + \frac{\Phi_2^{j+1}}{\Delta n_2^2}\right).$$

In conclusion the authors express their appreciation to A. A. Samarskiy and B. P. Rozhdestvenskiy for their useful discussion.

BIBLIOGRAPHY

1. Samarskiy, A. A. TEORIYA RAZNOSTNYKH SKHEM. [Theory of Difference Schemes], Nauka, Moscow, 1977.

2. Samarskiy, A. A.; Popov, Yu. P. RAZNOSTNYYE SKHEMY GAZOVOY DINAMIKI [Difference Schemes of Gas Dynamics], Nauka, Moscow, 1976.

3. Arakawa, A. "Computational Design for Long-Term Numerical Integration of the Equations of Fluid Motion: Two-Dimensional Incompressible Flow," Part 1, JOURNAL OF COMPUTATIONAL PHYSICS, No 1, 1966, pp 119-143.

4. Rozhdestvenskiy, B. L.; Levitan, Yu. L.; Mozhseyenko, B. D.; Priymak, V. G.; Sidorov, V. K. "Methods of Numerical Simulation of Turbulent Flows of an Incompressible Viscous Liquid," PREPRINT IPM AN SSSR [Preprint of the Institute of Applied Mathematics of the USSR Academy of Sciences], No 14, 1979.

5. Babenko, K. I.; Vvedenskaya, N. D. "Numerical Solution of the Boundary Problems for the Navier-Stokes Equations," ZH. VYCHISL. MATEM. I MATEM. FIZ. [Journal of Computational Mathematics and Mathematical Physics], Vol 12, No 5, 1972, pp 1343-1349.

6. Gadant, Ye. I. "Conjugate Families of Difference Schemes for Equations of the Parabolic Type with Low-Order Term," ZH. VYCHISL. MATEM. I MATEM. FIZ., Vol 18, No 8, 1978, pp 1162-1169.

7. Samarskiy, A. A.; Fryazinov, I. V. "Difference Schemes for the Solution of the Dirichlet Problem in an Arbitrary Region for Elliptic Equations with Variable Coefficients," ZH. VYCHISL. MATEM. I MATEM. FIZ., Vol 11, No 2, 1971, pp 385-410.

8. Gryaznov, V. L.; Polezhyayev, V. I. "Study of Some of the Difference Schemes and Approximations of Boundary Conditions for Numerical Solution of the Equations of Thermal Convection," PREPRINT INSTITUTA PROBLEM MEKHANIKI [Preprint of the Institute of Problems of Mechanics], No 40, 1974.

NUMERICAL SIMULATION OF THERMAL AND CONCENTRATION CONVECTION IN CHEMICAL REACTORS

[B. P. Gerasimov, I. S. Kalachinskaya, pp 210-227]

Introduction

In the processes of heat and mass exchange in some chemical reactors the convective transport capable of faster and more efficient course of the reaction has great significance. The purpose of this paper is numerical investigation of the thermal and concentration convection of a multicomponent gas mixture in a cylindrical reactor of circular cross section. In this paper a study is made of the structure of the flow of the gas mixture as a function of the reactor dimensions and the nature of injection of the mixture, and a study is also made for the model reaction of the reaction rate as a function of the flow structure.

I. Statement of the Problem

Let us consider mixed convection of the multicomponent gas mixture in a cylindrical cavity of height ℓ_1 and radius R, on the axis of which a rod of radius a_1 is located (see Figure 1). The rod temperature T_1 exceeds the wall temperature T_0, where both temperatures T_0, T_1 are constant in time. The injection and the discharge of the gas mixture are steady-state and take place through the ends of the reactor. The injection rate is uniform with respect to cross section.

Inasmuch as the pressure gradient and the flow velocity are comparatively small, the convective motion of the multicomponent gas mixture in the reactor can be described by a system of two-dimensional nonsteady-state Navier-Stokes equations for an incompressible liquid in the Boussinesq approximation [1] jointly with the equations for the concentrations of each of the components. In the cylindrical coordinate systems the initial system of equations can be written in the following dimensionless form

$$\frac{\partial \omega}{\partial t} + \frac{\partial (u\omega)}{\partial z} + \frac{\partial (v\omega)}{\partial r} = \frac{1}{Re}\Delta_{r,z}(\nu(T)\omega) - G\frac{\partial T}{\partial r} - \sum_{i=1}^{n} G_i \frac{\partial c_i}{\partial r}$$

$$\frac{\partial T}{\partial t} + \frac{\partial (uT)}{\partial z} + \frac{1}{r}\frac{\partial (rvT)}{\partial r} = \frac{1}{Pe}\operatorname{div}(\varkappa(T)\operatorname{grad} T) + q_i$$

$$\frac{\partial c_i}{\partial t} + \frac{\partial (uc_i)}{\partial z} + \frac{1}{r}\frac{\partial (rvc_i)}{\partial r} = \frac{1}{Pe_i}\operatorname{div}(\varphi(T)\operatorname{grad} c_i) \pm F_i(c_1,\ldots,c_n), \quad i = 1 \ldots n$$

$$\frac{1}{r}\frac{\partial^2\psi}{\partial z^2} + \frac{\partial}{\partial r}\left(\frac{1}{r}\frac{\partial\psi}{\partial r}\right) = -\omega$$

$$u = \frac{1}{r}\frac{\partial\psi}{\partial r}, \qquad v = -\frac{1}{r}\frac{\partial\psi}{\partial z}, \quad \omega = \frac{\partial v}{\partial z} - \frac{\partial u}{\partial r}$$

Here ψ is the current function, ω is the vortex, $G=Gr/Re^2$, Gr is the Grashoff number, $G_i=Gr_i/Re^2$, Gr_i is the concentration Grashoff number, Re is the Reynolds number, Pe is the Peclet number, Pe_i is the concentration Peclet number, q is the density of the heat sources, q(T), $\phi(T)$, $\mathcal{L}(T)$ are the dimensionless coefficients of kinematic viscosity, diffusion and thermal diffusivity, respectively, which are functions of the temperature, Fi are the sources and discharges defined by the rate constants of the chemical reaction. During dimensionalization, as the basic dimensional variables we selected R -- the reactor radius, u_0 -- the gas mixture injection rate, $\Delta T=T_1-T_0$ -- the temperature gradient in the reactor and e_0 -- the mole concentration of one of the substances during injection. The dimensionless variables entering into equations (1) (the tilde is omitted there) are expressed in terms of the dimensional ones as follows:

$$\tilde{z} = z/R, \quad \tilde{r} = r/R, \quad \tilde{v} = v/u_0, \quad \tilde{t} = t\cdot u_0/R,$$
$$\tilde{\psi} = \psi/u_0 R, \quad \tilde{\nu} = \nu/u_0 R, \quad \tilde{\mathcal{L}} = \mathcal{L}/u_0 R, \quad \tilde{T} = \frac{T-T_0}{T_1-T_0},$$
$$\tilde{\psi} = \psi/u_0 R^2, \quad \tilde{\omega} = R\omega/u_0, \quad \tilde{c}_i = c_i/c_0$$

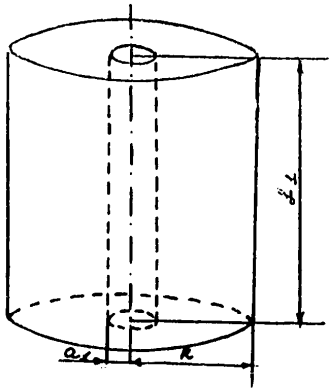

Figure 1

For the system of equations (1) a study is made of the internal boundary problem in the rectangle $a_1 \le r \le 1$, $0 \le z \le \chi_1$ (half the vertical cross section of the reactor in Figure 2).

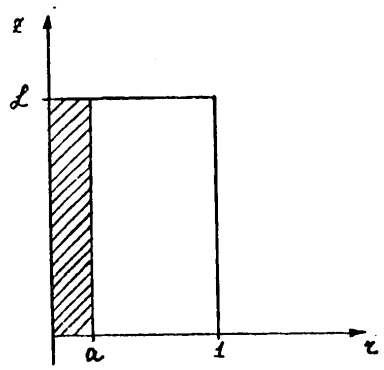

Figure 2

The desired solution must satisfy the following initial and boundary conditions

$$t=0\begin{cases}\psi=\dfrac{v_0}{2}(r^2-a^2),\ c_i=c_{0i};\ \omega=0, & a\le r\le 1;\ 0\le z\le l\\ T=1 & r=a,\ 0\le z\le l\\ T=0 & r=1,\ 0\le z\le l\\ T=1-z/\delta & a\le r\le 1,\ z=0;\ l\end{cases}$$

$$t>0\begin{cases}\psi=\dfrac{v_0}{2}(r^2-a^2),\ \dfrac{\partial\psi}{\partial z}=0;\ \dfrac{\partial c_i}{\partial z}=0; & a\le r\le 1;\ z=l\\ \psi=\dfrac{v_0}{2}(r^2-a^2);\ \dfrac{\partial\psi}{\partial z}=0;\ c_i=c_{0i}; & a\le r\le 1;\ z=0\\ \psi=0=\dfrac{\partial\psi}{\partial r};\ \varphi(T)\dfrac{\partial c_i}{\partial r}=\pm\Gamma_i,\ T=1 & r=a;\ 0\le z\le l\\ \psi=\dfrac{v_0}{2}(1-a^2);\ \dfrac{\partial\psi}{\partial r}=0;\ \dfrac{\partial c_i}{\partial r}=0;\ T=0 & r=1;\ 0\le z\le l\\ T=1-z/\delta & a\le r\le 1;\ z=0;\ l\end{cases}$$

where Γ_i (i=1,..., n) are defined by the rate constants of the chemical reaction. The boundary conditions for ω are found approximately in the finite-difference statement.

II. Solution Procedure

In order to solve the system of equations (1), the method based on using the monotonic approximation of the convective terms by directional difference in the longitudinal-transverse scheme [2] was used.

A rectangle $\{0\le r\le \mathcal{L}_1;\ a_1\le z\le 1\}$ will be covered by a nonuniform network

$$\bar{\Omega}_h=\{z_i,\ i=0,\ N;\ \bar{r}_j,\ j=0,\ M\}$$

h_i is the variable step size with respect to z

h_j is the variable step size with respect to r

and let us introduce the step size with respect to time τ, $t^n=m\tau$. On the network $\hat{\omega}_h$ the system of equations (1) is approximated by the following finite-difference system of variable directions

$$\frac{\bar{\omega}-\omega}{\tau/2} = \mathcal{K}_1(v,\omega)+\mathcal{K}_2(u,\bar{\omega})+\mathcal{D}_1(\nu,\omega,\bar{\omega})+G\cdot\hat{T}_x \tag{2}$$

$$\frac{\hat{\omega}-\bar{\omega}}{\tau/2} = \mathcal{K}_1(v,\hat{\omega})+\mathcal{K}_2(u,\bar{\omega})+\mathcal{D}_1(\nu,\hat{\omega},\omega)+G\hat{T}_x \tag{3}$$

$$\frac{\bar{T}-T}{\tau/2} = \tilde{\mathcal{K}}_1(v,T)+\mathcal{K}_2(u,\bar{T})+\mathcal{D}_2(\varkappa,T,\bar{T}) \tag{4}$$

$$\frac{\hat{T}-\bar{T}}{\tau/2} = \tilde{\mathcal{K}}_1(v,\hat{T})+\mathcal{K}_2(u,\bar{T})+\mathcal{D}_2(\varkappa,\hat{T},T) \tag{5}$$

$$\frac{\bar{c}_i-c_i}{\tau/2} = \tilde{\mathcal{K}}_1(v,c_i)+\mathcal{K}_2(u,\tilde{c}_i)+\mathcal{D}_2(\varphi,c_i,\bar{c}_i)+F_i(c_1,\dots,c_n) \tag{6}$$

$$\frac{\hat{c}_i-\bar{c}_i}{\tau/2} = \tilde{\mathcal{K}}_1(v,\hat{c})+\mathcal{K}_2(v,\bar{c}_i)+\mathcal{D}_2(\varphi,\hat{c},\bar{c}_i)+F_i(c_1,\dots,c_n) \tag{7}$$

$$\frac{\bar{\psi}-\psi^s}{\tau_s/2} = L_2\psi^s+L_1\bar{\psi}+\hat{\omega} \tag{8}$$

$$\frac{\psi^{s+1}-\bar{\psi}}{\tau_s/2} = L_2\psi^{s+1}+L_1\bar{\psi}+\hat{\omega} \tag{9}$$

Here $\mathcal{K}_i, \tilde{\mathcal{K}}_1, \mathcal{K}_2, \mathcal{D}_1, \mathcal{D}_2, L_2, L_1$ are difference operators of the type

$$\mathcal{K}_1(v,\omega) = \frac{1}{h_j}\left[\left(\frac{v_i-|v_i|}{2}-\frac{v_2+|v_2|}{2}\right)\omega_{i,j}+\frac{v_i+|v_i|}{2}\omega_{i,j+1}-\frac{v_2-|v_2|}{2}\omega_{i,j-1}\right]$$

$$\tilde{\mathcal{K}}_1(v,T) = \frac{1}{\gamma_j h_j}\left[\left(\gamma_{j+.5}\frac{v_2-|v_2|}{2}-\gamma_{j-.5}\frac{v_2+|v_2|}{2}\right)T_{i,j}+\gamma_{j+.5}\frac{v_i+|v_i|}{2}T_{i,j+1}\right.$$
$$\left.-\gamma_{j-.5}\frac{v_2+|v_2|}{2}T_{i,j-1}\right]$$

$$\mathcal{K}_2(u,\bar{\omega}) = \frac{1}{h_i}\left[\left(\frac{u_i+|u_i|}{2}-\frac{u_2-|u_2|}{2}\right)\bar{\omega}_{i,j}+\frac{u_i-|u_i|}{2}\bar{\omega}_{i+1,j}-\frac{u_2+|u_2|}{2}\bar{\omega}_{i-1,j}\right]$$

$$\mathcal{D}_1(\nu,\omega,\bar{\omega}) = \left(\gamma_{j+.5}\frac{\nu_{i,j+1}\omega_{i,j+1}-\nu_{i,j}\omega_{i,j}}{h_{j+1}}-\gamma_{j-.5}\frac{\nu_{i,j}\omega_{i,j}-\nu_{i,j-1}\omega_{i,j-1}}{h_j}\right)/$$
$$\gamma_j h_j+\frac{1}{h_i}\left(\frac{\nu_{i+1,j}\bar{\omega}_{i+1,j}-\nu_{i,j}\bar{\omega}_{i,j}}{h_{i+1}}-\frac{\nu_{i,j}\bar{\omega}_{i,j}-\nu_{i-1,j}\omega_{i-1,j}}{h_i}\right)$$

$$\mathcal{D}_2(\varkappa,T,\bar{T}) = \frac{1}{\gamma_j h_j}\left(\varkappa_{i,j+.5}\gamma_{j+.5}\frac{T_{i,j+1}-T_{i,j}}{h_{j+1}}-\varkappa_{i,j-.5}\gamma_{j-.5}\frac{T_{i,j}-T_{i,j-1}}{h_j}\right)$$

$$+\frac{1}{h_i}\left(\varkappa_{i+.5,j}\,\frac{\bar{T}_{i+1,j}-\bar{T}_{ij}}{h_{i+1}}-\varkappa_{i-.5,j}\,\frac{\bar{T}_{ij}-\bar{T}_{i-1,j}}{h_i}\right)$$

$$L_2\,\psi^s=\frac{1}{h_j}\left(\frac{1}{r_{j+.5}}\,\frac{\psi^s_{i,j+1}-\psi^s_{ij}}{h_{j+1}}-\frac{1}{r_{j-.5}}\,\frac{\psi^s_{ij}-\psi^s_{ij-1}}{h_j}\right)$$

$$L_2\,\bar{\psi}=\frac{1}{r_j h_i}\left(\frac{\bar{\psi}_{i+1,j}-\bar{\psi}_{ij}}{h_{i+1}}-\frac{\bar{\psi}_{ij}-\bar{\psi}_{i-1,j}}{h_i}\right)$$

Here $\omega_{ij}=\omega^n_{ij}$, $\bar{\omega}_{ij}=\omega_{ij}^{n+1/2}$, $\hat{\omega}_{ij}=\omega_{ij}^{n+1}$

s is the number of the iteration ψ; τ_s', τ'' are the iteration parameters

$$T_i=\frac{T_{i,j+1}-T_{ij}}{h_j+h_{j+1}},\quad h_i=\frac{h_i+h_{i+1}}{2}$$

u_1, u_2, v_1, v_2 are the difference approximations of the vertical and radial velocities, respectively at the obtained nodes of the finite-difference net

$$u_1=\frac{1}{2}\left[(\psi_2)_{ij}+(\psi_2)_{i+1,j}\right]/r_j$$

$$u_2=\frac{1}{2}\left[(\psi_2)_{ij}+(\psi_2)_{i-1,j}\right]/r_j$$

$$v_1=-\frac{1}{2}\left[\left(\frac{1}{r}\psi_1^s\right)_{ij}+\left(\frac{1}{r}\psi_1^s\right)_{i,j+1}\right]$$

$$v_2=-\frac{1}{2}\left[\left(\frac{1}{r}\psi_1^s\right)_{ij}+\left(\frac{1}{r}\psi_1^s\right)_{i,j-1}\right]$$

The boundary conditions for the vorticity ω on the walls are obtained from the approximation at the boundary of the equation for the current function ψ [2].

The system of equations (2-7) is solved by successive passes. First, by the known values of the current function and the vorticity from equations (4-5) a new value of the temperature is determined. Then by the known temperature field and the current function, the concentration distribution and the distribution of the vorticity ω in the new layer are calculated, and, finally, using the new value of $\hat{\omega}$, the current function is calculated. In each time step the equations for ψ are iterated to convergence. The iteration parameters are selected according to Jordan on the basis of estimates of the difference operator spectrum

$$L = (L_1 + L_2)$$

For determination of the operator spectrum, standard programs were used. The boundaries of the operator spectra L_1, L_2 for the different nets used in the problem are presented in Table 1.

The indicated choice of the iteration parameters insures convergence of the iteration process in 4-8 iterations. As the convergence criterion of the iteration process, smallness of the error in the norm L_2 is taken

$$\left[\sum_{i,j} \left(L\psi^{s+1} + \vec{\omega}\right)^2 \tau k_i k_j\right]^{1/2} < \varepsilon_\psi; \quad \varepsilon_\psi = 0.05$$

III. Results of the Numerical Experiments

A program was written in ALGOL to implement the above-described method. The calculations were performed on the BESM-6 computer.

1. The first step of the investigation of heat and mass exchange in the reactor is study of the flow structure of the gas mixture without considering the multicomponent nature of it. The flows with circulation of the gas mixture are of interest. In this case, the time the gas spends in the reactor increases, and the reactions take place more efficiently. As the circulation characteristic let us take the ratio of the maximum value of the current function inside the region ψ_{max} to the value on the side surface ψ_{bound}. Let us denote the circulation coefficient $I=\psi_{max}/\psi_{bound}$ (for I=1 the circulation is absent).

The numerical solutions were obtained for the values

$$\mathcal{L} = 1,6;\ 3,6;\ 8,6;\ 10;$$
$$\alpha = 0,1;\ 0,4;$$
$$Re = 200;\ 1000;\ 2000$$

The results of the calculations are presented in Table 2. Some of the characteristic versions are presented graphically in Figure (2-5). Isotherms, current lines and graphs of the distribution of the vertical velocity component of the gas mixture near the surface of the rod are constructed for each version. All level lines are numbered, and the values of the functions corresponding to these numbers are presented under the figures.

The numerical investigation led, in particular, to the following results.

a) $\mathcal{L}$=1.6 (Figure 3-4).

For different values, the absolute values of the current velocity of the gas mixture along the rod differ little from each other. I decreases with an increase in the injection velocity. For Re=1000 the circulation is absent. A characteristic feature of the flow in the reactor is a shift of the center of the vortex to

the chamber walls. For Re=200 the appearance of a secondary vortex on the upper wall is observed (see Figure 2). In all of the temperature field patterns there is a clearly expressed thermal boundary layer. For large numbers (see Figure 3) it is obvious that the heat from the rod is carried away by the flow of cold gas, and it clearly penetrates into the reactor. For Re=200 (Figure 2), as a result of the development of free-convective motion, the reactor is better heated.

b) $\mathcal{L}=3.6$ (Figure 5).

By comparison with the preceding case, the circulation and the flow velocity increase. The remaining qualitative characteristics of the flow vary little.

c) $\mathcal{L}=8.6$ (Figure 6)

With an increase in the rod length the circulation coefficient increases (the circulation exists even for Re=2000), where with an increase in the rod diameter I decreases somewhat.

2. In the next step let us consider the convective motion of a four-component gas mixture. Let a mixture of gases M_2 and M_4 be injected into the reactor. As a result of a number of reactions, a crystalline substance M_5 precipitates out on the rod, which is an electrode. Such processes are characteristic, in particular, for obtaining substances without impurities [4]. Let us propose that there are two basic reactions in the reactor:

Homogeneous

$$M_1 + M_4 \rightleftharpoons M_3 + M_2$$

and heterogeneous, running to the surface of the rod

$$M_2 \rightarrow (1-\beta)M_5 + \beta M_1 + M_3 \quad \text{where } \beta < 1.$$

Let the rate of formation of M_2 as a result of the homogeneous reaction have the form

$$\frac{dC_2}{dt} = \kappa_1 C_1 C_4^{\alpha}$$

and the rate of formation of M_5 be the following

$$\frac{dC_5}{dt} = \kappa_2 C_2 - \kappa_3^{\beta} C_3$$

It is of interest to investigate the precipitation rate of M_5 as a function of the flow structure. For this purpose it is necessary to solve the complete system of equations (1). Let us assume that the precipitation of the solid phase be expressed very slowly by comparison with the time of establishment of the flow, and the calculations can be performed for fixed values of the rod radius. For our model problem

$$n = 4; \quad F_1 = F_4 = -F_2 = -F_3 = \kappa_1 C_1 C_4^{\alpha}$$

$$\Gamma_2 = -\Gamma_3 = -\frac{1}{\beta}\Gamma_1 = -\frac{1}{1-\beta}\left(\kappa_2 C_2 - \kappa_3 C_1^{\beta} C_3\right)$$

$$\Gamma_4 = 0;$$

A numerical study was made of the precipitation rate M_5 as a function of the Reynolds number and the rod radius for $\mathcal{L}=5$. Graphs of these relations are presented in Figures 7-8, respectively. Figure 9 shows the lines of the concentration levels of the reacting substances under steady-state conditions and the distribution of the precipitation rate M_5 along the rod for a=4, Re=200.

BIBLIOGRAPHY

1. Landau, L. D.; Lifshits, Ye. M. MEKHANIKA OPLOSHNYKH SRED. [The Mechanics of Continuous Media], GITL, Moscow, 1953.

2. Samarskiy, A. A. VVEDENIYE V TEORIYU RAZNOSTNYKH SKHEM. [Introduction to the Theory of Difference Schemes], Nauka, Moscow, 1971.

3. Torrance, K. E.; Rockett, J. H. "Numerical Study of Natural Convection in Enclosures," J. FLUID MECH., Vol 36, No 1, 1969, pp 33-54.

4. Lapidus, I. I., et al. METALLURGIYA POLIKRISTALLICHESKOGO KREMNIYA VYSOKOY CHASTOTY [Metallurgy of Highly Pure Polycrystalline Silicon], METALLURGIYA, Moscow, 1971.

Table 1

A	0.1	0.4	0.6
Δ_2	30653	68917	155000
δ_2	15.29	28.62	62.075

Table 2

	A=0.1						A=0.4					
L	1.6		3.6		8.6		1.6		3.6		8.6	
RE	U'	I	U'	I	U'	I	U'	I	U'	I	U'	I
200	119	5	174	10	240	35	114	6	149	17	268	30
1000	22	1	30	1	43	3	23	1	26	1.4	42	3
2000	14	1	20	1	27	1.9	13	1	19	1	27	1.7

$U' = U_{max}/U_0$

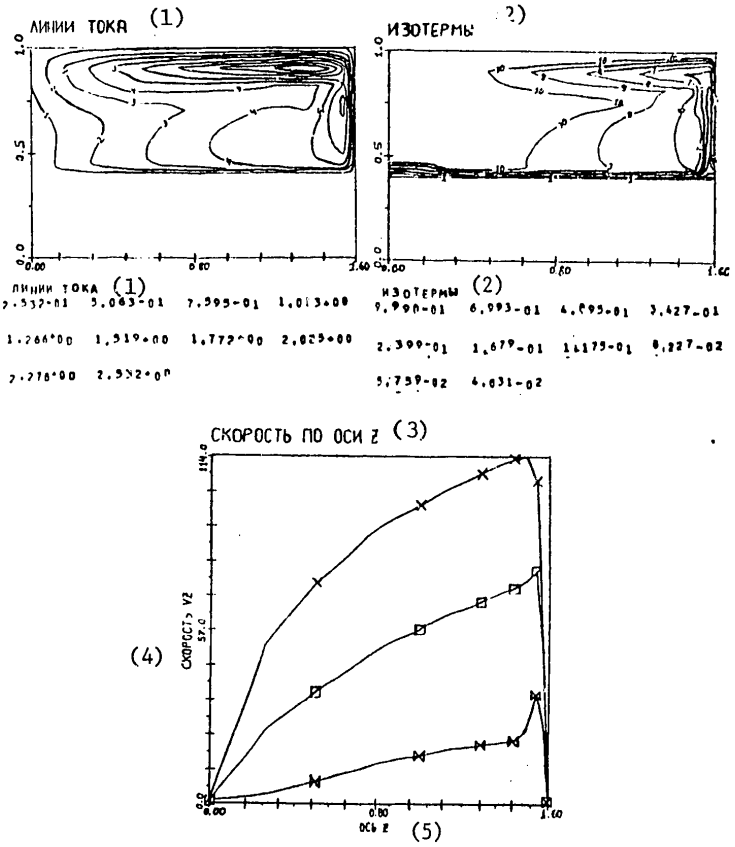

Figure 3

Key:
1. Current lines
2. Isotherms
3. Velocity along the z axis
4. Velocity
5. z axis

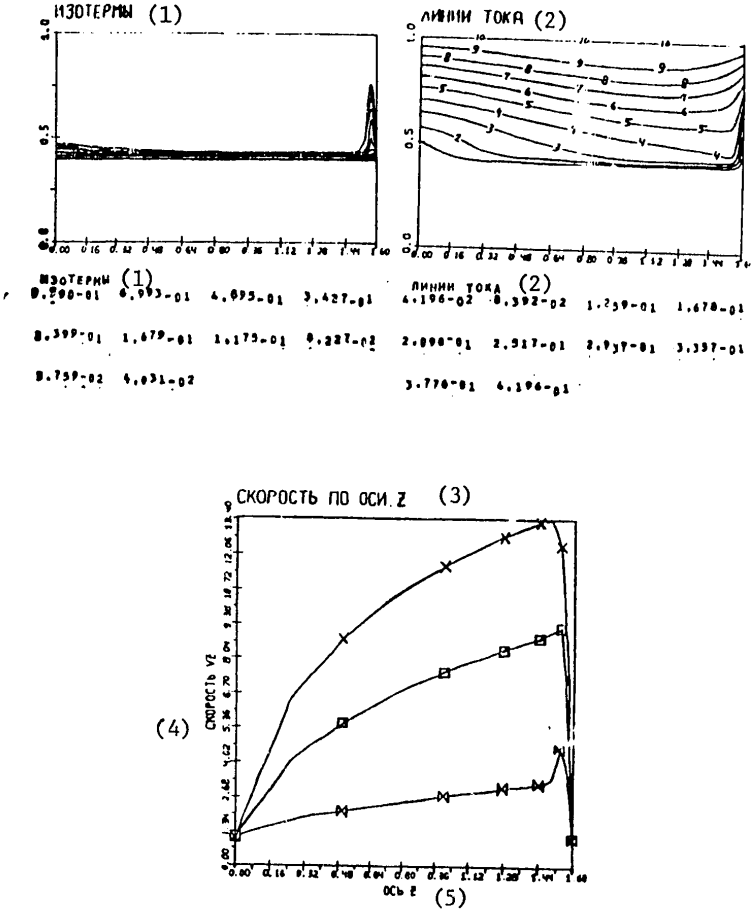

Figure 4

Key:

1. Isotherms
2. Current lines
3. Velocity along the z axis
4. Velocity
5. z axis

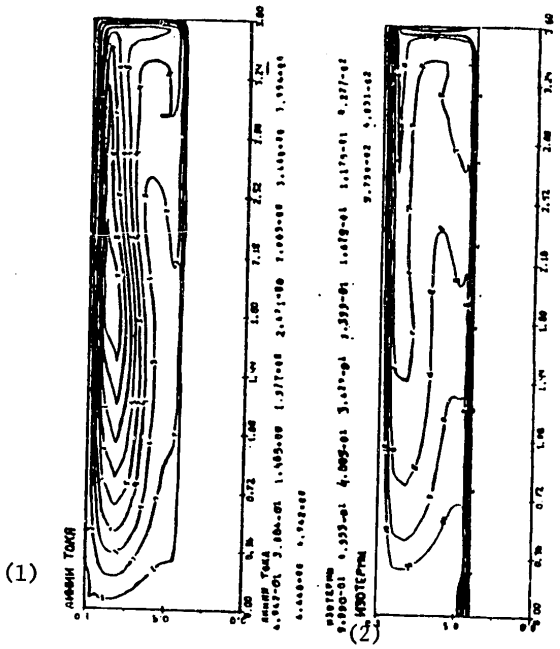

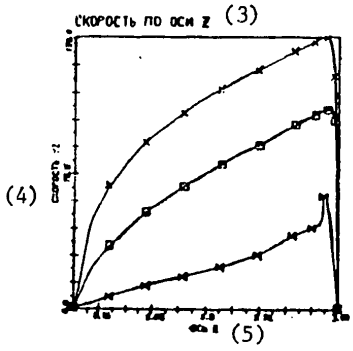

Figure 5

Key:
1. Current lines
2. Isotherms
3. Velocity along the z axis
4. Velocity
5. z axis

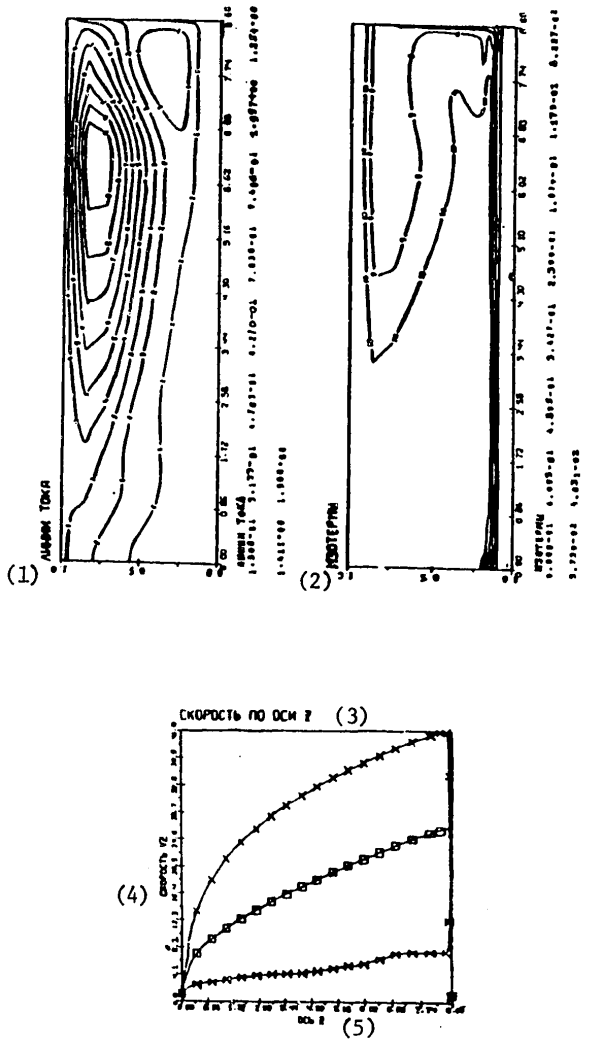

Figure 6

Key:
1. Current lines
2. Isotherms
3. Velocity along the z axis
4. Velocity
5. z axis

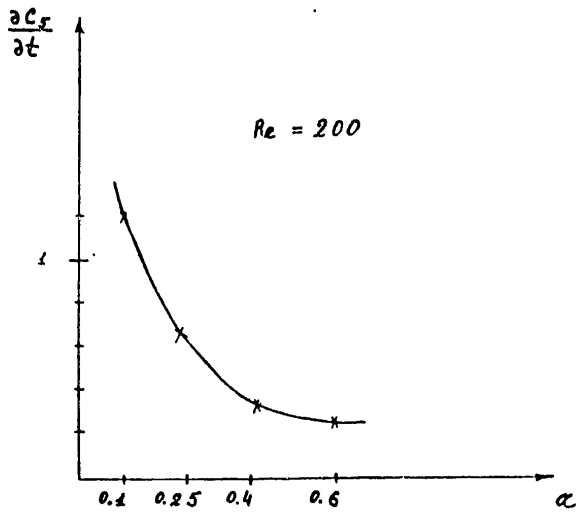

Figure 7

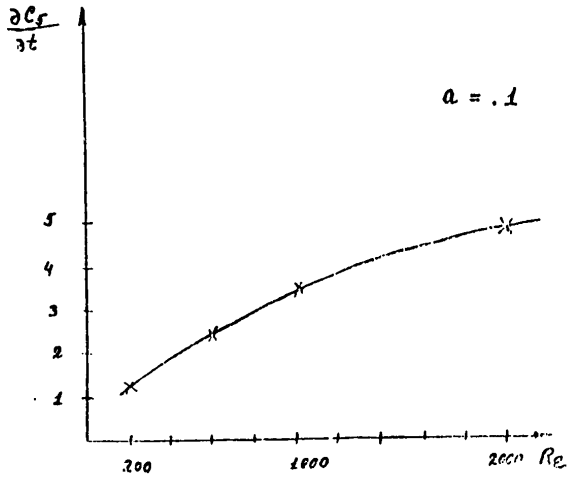

Figure 8

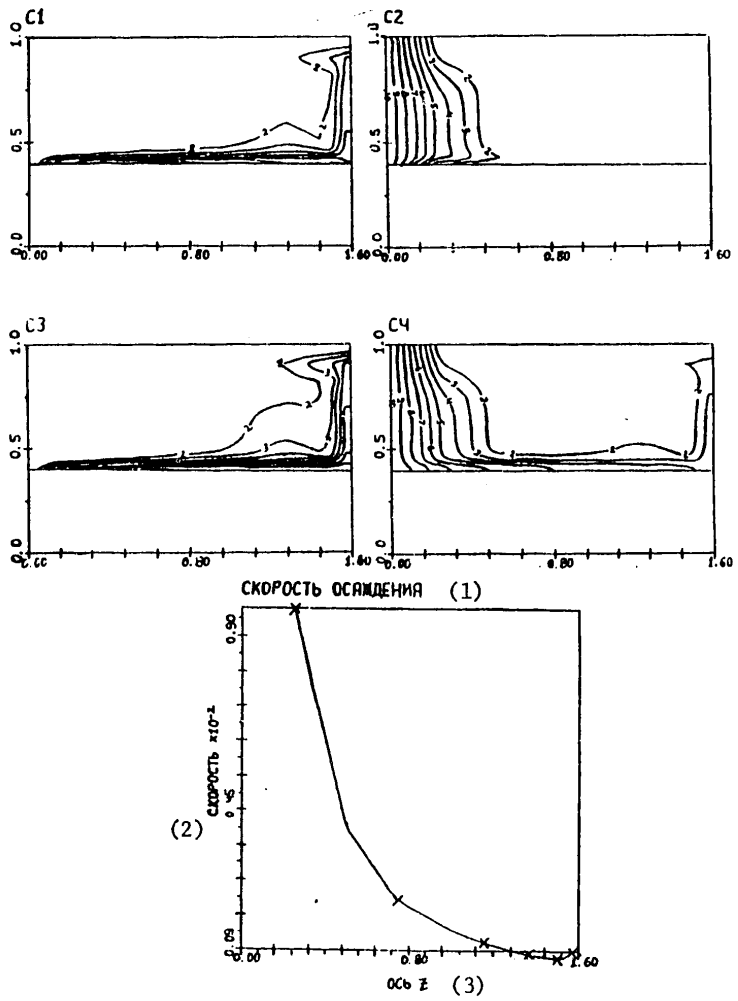

Figure 9

Key:
1. Precipitation rate
2. Velocity
3. z-axis

10845
CSO: 8144/0580

- END -